

**Search for novel antimicrobials against
Neisseria gonorrhoeae and *Chlamydia trachomatis***



DISSERTATION

zur Erlangung des akademischen Grades

doctor rerum naturalium

(Dr. rer. nat.)

im Fach Biologie

eingereicht an der Fakultät für Biologie

der Julius-Maximilians-Universität Würzburg

vorgelegt von

M.Sc. Biol.

Anastasija Reimer

geboren am 01.12.1988 in Katschar

Würzburg, Januar 2017

Eingereicht am:

Mitglieder der Prüfungskommission:

Vorsitzender:

Erstgutachter: PD Dr. Vera Kozjak-Pavlovic

Zweitgutachter: Prof. Dr. Georg Krohne

Tag des Promotionskolloquiums:

Doktorurkunde ausgehändigt am:

TABLE OF CONTENTS

ABSTRACT	6
ZUSAMMENFASSUNG	8
1 INTRODUCTION	10
1.1 <i>Neisseria gonorrhoeae</i>	10
1.1.1 The genus <i>Neisseria</i>	10
1.1.2 Gonorrhoea	10
1.1.3 Virulence factors.....	13
1.1.4 Interaction of <i>N. gonorrhoeae</i> with neutrophils.....	19
1.2 <i>Chlamydia trachomatis</i>	21
1.2.1 The order of Chlamydiales.....	21
1.2.2 <i>C. trachomatis</i> infection diseases.....	21
1.2.3 Developmental cycle of <i>C. trachomatis</i>	23
1.2.4 Host-pathogen interaction	25
1.2.5 Chlamydial macrophage infectivity potentiator (Ctr-MIP).....	27
1.3 Antimicrobials.....	29
1.3.1 Plant-derived compounds	29
1.3.2 Pípecolic acid derivatives	29
1.3.3 Antimicrobials derived from marine sponges or sponge-associated bacteria.....	30
1.4 Aim of the work.....	32
2 MATERIAL AND METHODS	33
2.1 Material	33
2.1.1 Bacterial strains	33
2.1.2 Cell lines.....	34
2.1.3 Plasmids.....	34
2.1.4 Oligonucleotides.....	35
2.1.5 Antibodies.....	37
2.1.6 Kits	38
2.1.7 Buffers, solutions and media	39
2.1.8 Chemicals.....	43
2.1.9 Technical equipment	45
2.1.10 Software	47
2.2 Methods	48
2.2.1 DNA methods	48

2.2.2 Gel electrophoresis and western blot	51
2.2.3 Cell culture methods	52
2.2.4 Bacterial culture techniques.....	55
2.2.4.1 <i>E. coli</i>	55
2.2.4.2 <i>S. aureus</i>	56
2.2.4.3 <i>N. gonorrhoeae</i>	56
2.2.4.4 <i>C. trachomatis</i>	59
2.2.4.5 ATP measurements	61
2.2.5 Bioactivity testing of compounds.....	62
2.2.6 Mitochondria techniques	63
2.2.7 Purification of native and recombinant proteins and antibodies	65
2.2.8 Co-immunoprecipitation (co-IP) and pull-down assays	68
2.2.9 Surface plasmon resonance (SPR) measurements.....	69
2.2.10 PPlase Assay	70
2.2.11 Statistical analysis.....	70
3 RESULTS.....	71
3.1 Analysis of the interaction between SREC-I and PorB _{IA}	71
3.1.1 Co-IP of neisserial PorB _{IA}	71
3.1.2 Pull-down of PorB _{IA} interaction partners with PorB _{IA} -FLAG coated neisserial blebs	72
3.1.3 Binding of soluble GFP-tagged SREC-I to PorB _{IA} -expressing <i>Neisseria</i>	75
3.1.4 Interaction analysis of SREC-I and PorB _{IA} by SPR.....	77
3.1.5 Generation of antibodies against Omp85, PorB _{IA} and PorB _{IB}	78
3.2 Screening for inhibitors of <i>N. gonorrhoeae</i> and <i>C. trachomatis</i>	79
3.3 Inhibitors of neisserial and chlamydial MIP	84
3.3.1 PipN3 and PipN4 inhibit the PPlase activity of Ng-MIP and Ctr-MIP	84
3.3.2 PipN3 and PipN4 decrease chlamydial infection in a dose-dependent manner.....	87
3.3.3 PipN3 and PipN4 affect chlamydial developmental cycle.....	88
3.3.4 PipN3 and PipN4 decrease the survival of <i>N. gonorrhoeae</i> in neutrophils.....	92
3.3.5 Site-specific mutation of Ng-MIP inhibits PPlase activity.....	94
3.4 Analysis of the bioactive compound SF2446A2	95
3.4.1 Gellusterol E and SF2446A2 inhibit chlamydial inclusion formation	95
3.4.2 Properties of SF2446A2	97
3.4.2.1 SF2446A2 affects fusion of chlamydial inclusions.....	97
3.4.2.2 Antichlamydial effect of SF2446A2 is partially reversible	98
3.4.2.3 SF2446A2 exhibit antioxidant potential	99

3.4.3 SF2446A2 inhibits mitochondrial respiration and enhances glycolysis	101
3.4.4. SF2446A2 impaires the mitochondrial ATP production	104
3.4.5. <i>C. trachomatis</i> is affected by the knockdown of F ₀ F ₁ -ATPase and detracton of glucose	106
3.4.6 Depletion of glucose and glutamine reduces chlamydial infection	108
3.4.7 SF2446A2 affects the growth of <i>N. gonorrhoeae</i> and <i>S. aureus</i>	112
4 DISCUSSION	115
4.1 The interaction of cellular SREC-I with neisserial PorB _{IA}	115
4.2 Search for novel antimicrobials	118
4.3 Inhibitors of the macrophage infectivity potentiator	120
4.3.1 The role of chlamydial MIP during bacterial developmental cycle	121
4.3.2 Neisserial MIP and relation to bacterial survival in PMNs	124
4.4 Mode of action of antichlamydial compound SF2446A2	128
4.4.1 Antioxidant property and antibacterial activity of SF2446A2	128
4.4.2 Inhibition of mitochondrial respiration by SF2446A2	129
4.4.3 Blockage of mitochondrial respiration and the antichlamydial effect	133
4.4.4 SF2446A2 and a direct effect on <i>C. trachomatis</i>	135
4.5 Conclusion and outlook	137
5 REFERENCES	140
6 APPENDIX	157
6.1 Abbreviations	157
6.2 Publications and presentations	160
6.3 Danksagung	161
6.4 Selbstständigkeitserklärung	163

ABSTRACT

The obligate human pathogen *Neisseria gonorrhoeae* is responsible for the widespread sexually transmitted disease gonorrhoea, which in rare cases also leads to the development of disseminated gonococcal infection (DGI). DGI is mediated by PorB_{IA}-expressing bacteria that invade host cells under low phosphate condition by interaction with the scavenger receptor-1 (SREC-I) expressed on the surface of endothelial cells. The interaction of PorB_{IA} and SREC-I was analysed using different *in vitro* approaches, including surface plasmon resonance experiments that revealed a direct phosphate-independent high affinity interaction of SREC-I to PorB_{IA}. However, the same binding affinity was also found for the other allele PorB_{IB}, which indicates unspecific binding and suggests that the applied methods were unsuitable for this interaction analysis.

Since *N. gonorrhoeae* was recently classified as a “super-bug” due to a rising number of antibiotic-resistant strains, this study aimed to discover inhibitors against the PorB_{IA}-mediated invasion of *N. gonorrhoeae*. Additionally, inhibitors were searched against the human pathogen *Chlamydia trachomatis*, which causes sexually transmitted infections as well as infections of the upper inner eyelid. 68 compounds, including plant-derived small molecules, extracts or pure compounds of marine sponges or sponge-associated bacteria and pipercolic acid derivatives, were screened using an automated microscopy based approach. No active substances against *N. gonorrhoeae* could be identified, while seven highly antichlamydial compounds were detected.

The pipercolic acid derivatives were synthesized as potential inhibitors of the virulence-associated “macrophage infectivity potentiator” (MIP), which exhibits a peptidyl prolyl *cis-trans* isomerase (PPIase) enzyme activity. This study investigated the role of *C. trachomatis* and *N. gonorrhoeae* MIP during infection. The two inhibitors PipN3 and PipN4 decreased the PPIase activity of recombinant chlamydial and neisserial MIP in a dose-dependent manner. Both compounds affected the chlamydial growth and development in epithelial cells. Furthermore, this work demonstrated the contribution of MIP to a prolonged survival of *N. gonorrhoeae* in the presence of neutrophils, which was significantly reduced in the presence of PipN3 and PipN4.

SF2446A2 was one of the compounds that had a severe effect on the growth and development of *C. trachomatis*. The analysis of the mode of action of SF2446A2 revealed an inhibitory effect of the compound on the mitochondrial respiration and mitochondrial ATP

production of the host cell. However, the chlamydial development was independent of proper functional mitochondria, which excluded the connection of the antichlamydial properties of SF2446A2 with its inhibition of the respiratory chain. Only the depletion of cellular ATP by blocking glycolysis and mitochondrial respiratory chain inhibited the chlamydial growth. A direct effect of SF2446A2 on *C. trachomatis* was assumed, since the growth of the bacteria *N. gonorrhoeae* and *Staphylococcus aureus* was also affected by the compound.

In summary, this study identified the severe antichlamydial activity of plant-derived naphthoquinones and the compounds derived from marine sponges or sponge-associated bacteria SF2446A2, ageloline A and gelliusterol E. Furthermore, the work points out the importance of the MIP proteins during infection and presents pipercolic acid derivatives as novel antimicrobials against *N. gonorrhoeae* and *C. trachomatis*.

ZUSAMMENFASSUNG

Neisseria gonorrhoeae ist ein obligat humanpathogenes Bakterium, das für die weltweit verbreitete sexuell übertragbare Krankheit Gonorrhoe verantwortlich ist. In seltenen Fällen kann es auch zur Ausbildung der Disseminierten Gonokokken-Infektion (DGI) kommen, die mit der Expression des Gonokokken Oberflächenproteins PorB_{IA} assoziiert ist. PorB_{IA}-exprimierende Bakterien invadieren in die Wirtszelle unter phosphatfreien Bedingungen, was durch eine Interaktion mit dem zellulären Oberflächenrezeptor scavenger receptor-1 (SREC-I) vermittelt wird. Die direkte Interaktion zwischen PorB_{IA} und SREC-I wurde mittels verschiedenster Methoden analysiert, einschließlich einer Oberflächenplasmonresonanzanalyse, die eine direkte Bindung von PorB_{IA} zu SREC-I in einem phosphatunabhängigen Schritt aufzeigte. Allerdings wurde dieselbe Affinität auch zu PorB_{IB} gefunden, was auf eine unspezifische Bindung hindeutet und dafür spricht, dass die verwendeten Methoden für diese Interaktionsanalyse ungeeignet sind.

N. gonorrhoeae wurde vor kurzem wegen der stetig steigenden Anzahl antibiotikaresistenter Stämme als „Superkeim“ bezeichnet. Aufgrund dessen wurden Inhibitoren gegen die PorB_{IA}-vermittelte Invasion von *N. gonorrhoeae*, aber auch gegen *Chlamydia trachomatis*, den humanpathogenen Erreger von sexuell übertragbaren Infektionen und chronisch-follikulärer Bindehautentzündung, gesucht. 68 niedermolekulare Substanzen wurden mittels eines automatisierten Fluoreszenzmikroskopieverfahrens auf ihre inhibitorische Wirkung hin analysiert. Zu den getesteten Substanzen zählten pflanzenabstammende Stoffe, Isolate aus marinen Schwämmen oder Schwamm-assoziierten Bakterien, sowie Pipecolinsäure-Derivate. Gegen *N. gonorrhoeae* konnten keine Substanzen identifiziert werden, während sieben antichlamydiale Inhibitoren detektiert wurden.

Pipecolinsäurederivate wurden synthetisiert als potentielle Inhibitoren des virulenz-assoziierten Proteins „macrophage infectivity potentiator“ (MIP), das eine Peptidyl-Prolyl-*cis-trans*-Isomerase Aktivität besitzt. Diese Arbeit untersuchte die Rolle des MIP Proteins von *N. gonorrhoeae* und *C. trachomatis* während einer Infektion. Die zwei Inhibitoren PipN3 und PipN4 senkten die PPIase Aktivität des rekombinanten Chlamydien und Neisserien MIPs. Beide Substanzen beeinträchtigten das chlamydiale Wachstum und die Entwicklung in Epithelzellen. Ebenso konnte eine tragende Rolle des *N. gonorrhoeae* MIPs für das Überleben der Bakterien in Gegenwart von Neutrophilen aufgezeigt werden, das durch PipN3 und PipN4 inhibiert wurde.

SF2446A2 war einer der Inhibitoren, der einen erheblichen Effekt auf das Wachstum und die Entwicklung von *C. trachomatis* aufgewiesen hat. Während der Analyse des Wirkmechanismus von SF2446A2 konnte eine Hemmung der mitochondrialen Atmungskette und eine Abnahme der mitochondrialen ATP Produktion in der Wirtszelle festgestellt werden. Allerdings war die Entwicklung von *C. trachomatis* unabhängig von der Funktionsfähigkeit der Mitochondrien. Eine Verbindung zwischen der antichlamydialen Wirkung von SF2446A2 und der Inhibierung der Mitochondrienatmungskette konnte damit ausgeschlossen werden. Nur das Reduzieren von zellulärem ATP durch Blockieren der Glykolyse und mitochondrialen Atmungskette verursachte eine Beeinträchtigung des Chlamydienwachstums. Eine direkte Auswirkung von SF2446A2 auf *C. trachomatis* wurde angenommen, da die Substanz auch das Wachstum von anderen Bakterien wie *N. gonorrhoeae* und *Staphylococcus aureus* inhibierte.

Zusammengefasst identifizierte diese Studie die antichlamydiale Aktivität pflanzenabstammender Naphthochinone und der Isolate aus marinen Schwämmen oder Schwamm-assoziierten Bakterien SF2446A2, ageloline A und gelliusterol E. Ebenso verdeutlicht die Arbeit die Bedeutung der MIP Proteine während der Infektion und legt Pipecolinsäurederivate als mögliche neue Antibiotika gegen *N. gonorrhoeae* und *C. trachomatis* nahe.

1 INTRODUCTION

1.1 *Neisseria gonorrhoeae*

1.1.1 The genus *Neisseria*

The genus *Neisseria* is a member of the Neisseriaceae family within the class of β -proteobacteria. It was named after the German physician Albert Neisser, who for the first time in 1879 observed and described diplococci within cells isolated from patients with gonorrhoea and conjunctivitis (Neisser, 1879). *Neisseria* are Gram-negative, strictly aerobic bacteria with a diameter of 0.6 to 1 μm . Most of the classified *Neisseria* are commensal bacteria such as *N. lactamica*, *N. mucosa* and *N. sicca*, which colonize the mucosal surface of the upper respiratory tract and are part of the healthy 'core microbiome' of the human oral cavity (Zaura *et al.*, 2009). The genus includes also the two clinically relevant human pathogens *N. gonorrhoeae* and *N. meningitidis*. *N. lactamica* is closely related to *N. meningitidis*, which makes it an interesting organism to point out the differences between non-pathogenic and pathogenic *Neisseria* (Hollis *et al.*, 1969). These bacteria share not only the respiratory niche, but *N. lactamica* was also found to protect against *N. meningitidis* infection (Bennett *et al.*, 2005). Although 10 - 35 % of the adult population in Europe and the United States carries *N. meningitidis* asymptotically, the bacteria can also cross the mucosal barrier and enter the bloodstream, which leads to epidemic septicaemia, meningitis and in 5 - 20 % of the cases to death (Stephens *et al.*, 2007, Caugant & Maiden, 2009).

1.1.2 Gonorrhoea

The diplococcus *N. gonorrhoeae* is the causative agent of the second most prevalent sexually transmitted disease gonorrhoea, with worldwide more than 106 million cases per year (WHO, 2012). The disease is transmitted by human to human contact during sexual intercourse through mucosa of the urogenital tract, rectum or the oropharynx. The gonococcal infection is mostly a local mucosal infection, which can manifest in an uncomplicated and treatable urethritis in men and cervicitis in women. Furthermore, infection of the rectum and pharynx are largely asymptomatic in men and women. The number of females carrying the urogenital infection asymptotically is estimated at 50 % (10 % of males). The risk of an unrecognized and therefore untreated infection can lead to

serious complications for women such as pelvic inflammatory disease, ectopic pregnancy, foetal loss and infertility. The consequences of untreated urethral infection comprise epididymitis, urethral stricture and also infertility. Besides men and women, also neonates can be infected during delivery by women with urogenital gonorrhoea. Infants are infected when passing through the birth canal, resulting in neonatal conjunctivitis that can lead to corneal scarring and blindness if untreated (WHO, 2016b, Unemo *et al.*, 2016).

In rare cases, untreated gonorrhoea can also cause a disseminated gonococcal infection (DGI), in which the pathogen enters the bloodstream and spreads within the body. Among 700 000 Americans with gonorrhoea, 0.5 to 3 % developed a DGI, which can result in arthritis, meningitis and endocarditis (Kerle *et al.*, 1992).

Gonococcal infections are often accompanied by other STIs due to the way of transmission. In approximately 50 % of the cases the patients are diagnosed with *Chlamydia trachomatis* (Kahn *et al.*, 2005). It has also been shown that gonorrhoea increases transmission and acquisition of human immunodeficiency virus (HIV) through genital shedding of the HIV (WHO, 2016b).

Antimicrobial resistance

For diagnostic purposes, the World Health Organization (WHO) recommends performing culture methods in parallel to nucleic acid amplification testing (NAAT) for analysis and monitoring the antibiotic susceptibility of the pathogen (Low & Unemo, 2016). In fact, gonorrhoea is more than ever a major global public health concern due to the emerging number of antibiotic resistant strains (WHO, 2012). In 2012 the WHO released a new “Global action plan to control the spread and impact of antimicrobial resistance in *Neisseria gonorrhoeae*” and in 2016 “Guidelines for the treatment of *Neisseria gonorrhoeae*” to keep pace with the antimicrobial resistance progress of the “superbug”. Due to its natural competence and selective pressure *N. gonorrhoeae* has acquired all known resistance mechanisms to every antimicrobial by gaining genes and mutations throughout the genome. The history of the gonococcal antimicrobial resistance (AMR) began only five years after introducing sulphonamides as the first antibiotics for treatment of gonorrhoea with the discovery of the first resistant strain (Goire *et al.*, 2014). In the following years a vicious cycle manifested, which contained the introduction of a new antibiotic, discovery of a resistant strain and changing the treatment by introducing a new antimicrobial. Penicillin,

tetracycline, spectinomycin, ceftriaxone, ciprofloxacin, cefixime and azithromycin were the applied antibiotics in the last 80 years (Figure 1.1). The third generation cephalosporin ceftriaxone is considered the last line of defence, although recently there have been reports from Japan and Europe about two gonococcal strains *N. gonorrhoeae* H041 and *N. gonorrhoeae* F89, which were resistant against this and most other applied antibiotics (Ohnishi *et al.*, 2011a, Unemo *et al.*, 2012). The therapy type has to be chosen carefully and has to take the local data on antimicrobial susceptibility into consideration.

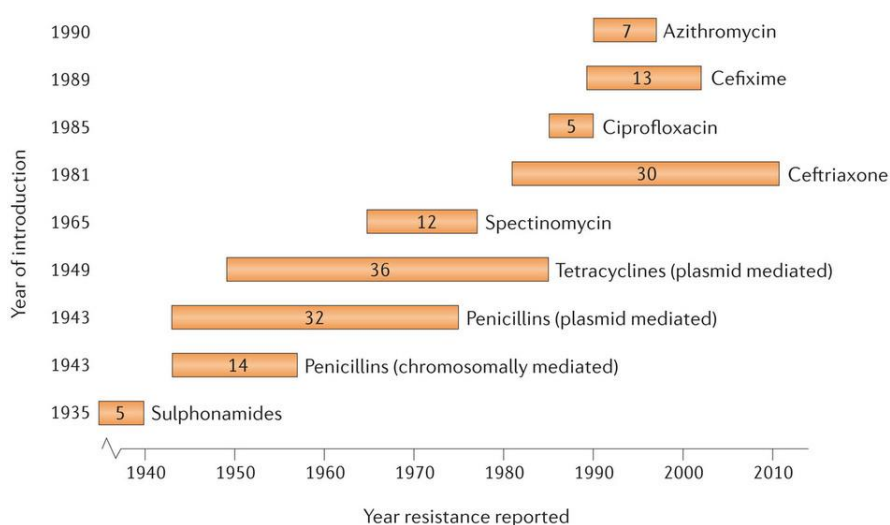


Figure 1.1: History of applied antimicrobials against gonorrhoea. The graph shows the introduced antibiotics against gonorrhoea from 1935 till 2014 starting with the year the antimicrobial came into clinical use until the first case of resistance was reported. The numbers in the bars indicate the years the antibiotics were applied before the resistance has been observed. Reproduced with permission from *Nat Rev Microbiol* (Goire *et al.*, 2014) p. 224.

Immune response and vaccination

Due to the emerging antimicrobial resistances of *N. gonorrhoeae* there is an increased need for a vaccine. However, only two clinical trials have been performed for *N. gonorrhoeae* vaccines. The first was a crude killed whole cell vaccine that was tested on an Inuit population in northern Canada and the second a single-antigen Pili vaccine, which was examined amongst the US military personnel stationed in Korea (Greenberg, 1975, Greenberg *et al.*, 1974, Boslego *et al.*, 1991). The result of both trials was the absence of the vaccine protection from *N. gonorrhoeae* infection. There are various reasons why vaccine development is challenging. One reason is the high reinfection rate, which indicates a poor naturally acquired immunity to *N. gonorrhoeae* infections. Furthermore, the surface antigens of *N. gonorrhoeae* are highly variable and the pathogen developed mechanisms to evade

and manipulate the host immunity. The understanding of the human immune response to the gonococcal infection is thus an important factor in the vaccine development.

1.1.3 Virulence factors

N. gonorrhoeae expresses a set of common as well as species-specific virulence factors, which ensure a successful infection of human cells, evasion of the immune system and transmission. The initial step in the invasion process is the adherence of the pathogen by its type IV pili to the host cells. The bacteria can use several surface proteins and therefore different pathways to invade the host cell. These include the opacity-associated (Opa) proteins or the outer membrane protein PorB. Further important virulence factors are the immunoglobulin A1 (IgA) protease, which is not only secreted to support the invasion of human mucosa by specifically cleaving the human immunoglobulin IgA1, but has also been shown to cleave the lysosomal protein LAMP1 to promote bacterial intracellular survival (Lin *et al.*, 1997).

Another fundamental virulence factor is lipooligosaccharide (LOS), the major glycolipid of the pathogen's outer membrane. LOS is an analogue to lipopolysaccharides (LPS) from other Gram-negative bacteria. The composition of LPS is a lipid moiety (lipid A), which is linked through 2-keto-3-deoxyoctulosonic acid (core oligosaccharides) to the O antigens, consisting of repeating units of oligosaccharides. LOS lacks the O antigen unit and is known to contribute to *N. gonorrhoeae* virulence in different ways, for example by enhancing resistance to normal human serum and acting as putative adhesins by interaction with asialoglycoprotein receptors (ASP-R) (Rice *et al.*, 1987, Harvey *et al.*, 2001, Porat *et al.*, 1995). The neisserial surface molecules LOS but also the type IV pili and Opa proteins are undergoing steady phase variation, which helps the pathogen to evade the host immune system.

Type IV pilus

The type IV pili of *N. gonorrhoeae* are surface-exposed filamentous structures with a diameter of 6 - 9 nm and an average length of $0.9 \pm 0.1 \mu\text{m}$ (Craig & Li, 2008, Holz *et al.*, 2010). Piliated and non-piliated colonies growing on appropriate laboratory agar plates can be distinguished by binocular microscopy. Colonies expressing pili appear as smaller and darker structures with sharp edges. The neisserial pilus is a multifunctional tool, which is

responsible for the initial adhesion of the bacteria to the host cell, immune evasion, surface motility, DNA transformation and complement inhibition. Though pili are important for the adherence of *N. gonorrhoeae* to the host cell, their inhibitory effect could be demonstrated on the internalization (Makino *et al.*, 1991). The adhesion process is initiated by the proteins PilC and PilV that are assumed to interact with the transmembrane receptor CD46 (Kallstrom *et al.*, 1997). Since the gonococcal pilus is localized extracellularly and is accessible for the immune response, the bacteria have developed an evasion system comprised of antigen variation and post-translational modification in form of glycosylation and phosphorylation (Marceau *et al.*, 1998, Forest *et al.*, 1999).

Additionally, *Neisseria* have the unique characteristic of taking up single- as well as double-stranded DNA by their pilus. Therefore, the transformed DNA requires a DNA uptake sequence (DUS; GCCGTCTGAA), which is distributed throughout the whole genome (Elkins *et al.*, 1991). The transformation process can be divided in donation, binding and uptake of DNA. The DNA is donated either by type IV secretion or by release of DNA through autolysis of the bacterial cell. Several pilus-associated components are required for a transformation process. However, the whole transformation machinery and process is still object of ongoing research.

Opacity-associated (Opa) proteins

The Opa proteins are localized in the outer membrane of *N. gonorrhoeae* and are predicted to form β -barrel structures with eight antiparallel β -strands and four extracellular loops (de Jonge *et al.*, 2002). The protein name is based on the fact that agar-grown colonies appear opaque when viewed under a binocular microscope. The proteins are encoded by 11 genes and are constitutively transcribed (Bhat *et al.*, 1991). The expression is regulated at a translational level and undergoes phase variation with a frequency of approximately 10^{-3} per cell division (Mayer, 1982). Opa proteins function as virulence factors for the adherence to and invasion in epithelial cells and neutrophils (King & Swanson, 1978). The proteins can be categorized in two classes depending on their cellular host receptor. Opa₅₀ (Opa_{HS}) binds to the heparan sulphate proteoglycans (HSPG) receptor and extracellular matrix protein such as vitronectin and fibronectin (Chen *et al.*, 1995, van Putten & Paul, 1995, Gomez-Duarte *et al.*, 1997). However, the majority of the Opa proteins (Opa₅₁₋₆₀) interact with receptors of the

human carcinoembryonic antigen-related cell adhesion molecules (CEACAM) family (Virji *et al.*, 1996).

Major outer membrane protein PorB

The gonococcal major outer membrane protein PorB is a homotrimeric β -barrel porin. Each monomere is about 35 kDa large and consist of 16 antiparallel transmembrane-spanning β -strands with 8 elongated and extracellular loops (L1 - L8) (Zeth *et al.*, 2013). The pore functions not only as an ion channel for small nutrients and waste products, but also plays a crucial role for pathogenicity. There are two alleles of PorB, PorB_{IA} and PorB_{IB}, whereas bacteria contain only one version of the gene. The alleles exhibit high homology among them and the majority of the variations are localized in their extracellular loop regions (Fudyk *et al.*, 1999). A study from 2003 that analysed 282 clinical isolates over a course of 10 years could demonstrate that 22.3 % of the strains expressed PorB_{IA} and 77.7 % PorB_{IB} (McKnew *et al.*, 2003). However, the PorB_{IA} serotype is strongly connected to DGI, since 79 % of bacterial strains isolated from DGI patients expressed PorB_{IA} (Morello & Bohnhoff, 1989, Bash *et al.*, 2005). The invasion in epithelial cells is mediated by PorB_{IA}, not PorB_{IB}, and takes place under low-phosphate conditions found in the blood stream (van Putten *et al.*, 1998, Kühlewein *et al.*, 2006). Crystallisation of PorB_{IA} in the presence of ATP and phosphate demonstrated an ATP binding site and the binding of two phosphate ions at the two arginine residues Arg⁹² and Arg¹²⁴ (Figure 1.2). Mutation of Arg⁹² resulted in a reduced invasion that pointed out the importance of this residue for neisserial pathogenicity (Zeth *et al.*, 2013).

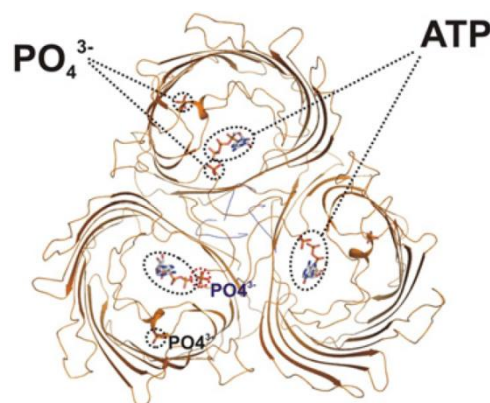


Figure 1.2: Crystal structure of *N. gonorrhoeae* PorB_{IA}. Trimeric structure of the porin viewed from the top with marked positions of ATP and two phosphate ions (PO₄³⁻). Graphic obtained from (Zeth *et al.*, 2013) p. 634.

The host cell receptor of PorB_{IA} has been shown to be the scavenger receptor expressed by endothelial cells 1 (SREC-I, also known as SCARF1) (Rechner *et al.*, 2007). It belongs to the class F of the scavenger receptor family and is expressed by endothelial cells, dendritic cells and macrophages (Adachi *et al.*, 1997, Tamura *et al.*, 2004). The 86 kDa protein consists of an extracellular domain with five epidermal growth factor (EGF)-like cysteine-rich repeats and a carboxy-terminal cytoplasmic tail composing serine- and proline-rich regions (Ramirez-Ortiz *et al.*, 2013). The receptor binds the ligand acetylated low-density lipoprotein (acLDL), heat-shock proteins HSP70, HSP90 and Gp96, as well as calreticulin and the pancreatic zymogen GP2 (Tamura *et al.*, 2004, Berwin *et al.*, 2004, Jeannin *et al.*, 2005, Holzl *et al.*, 2011, Murshid *et al.*, 2010). Furthermore, SREC-I is involved in the internalization of pathogenic fungi (Means *et al.*, 2009).

Recently, a model has been developed that explains the low phosphate-dependent invasion (LPDI) of *N. gonorrhoeae* in two steps: the human heat shock glycoprotein Gp96 binds in a phosphate-sensitive manner to the outer membrane protein PorB_{IA} upon invasion of *N. gonorrhoeae*. This results in strong adhesion to the host cell and the interaction of PorB_{IA} to SREC-I, which leads to an engulfment of the bacteria (Rechner *et al.*, 2007). The invasion requires clathrin-coated pit formation and involves actin and Rho GTPases, while it is independent of microtubules, acidic sphingomyelinase, phosphatidylinositol 3-kinase, myosin light chain kinase and Src kinases (Kühlewein *et al.*, 2006). The interaction of PorB_{IA} and SREC-I results in a re-localization of SREC-I to membrane rafts. Furthermore, caveolin-1 is activated and the signalling molecules phosphoinositide 3-kinase (PI3K) and PLC γ 1 are recruited to phosphorylated caveolin-1. The neutral sphingomyelinase is required to recruit PI3K to caveolin-1. The activation of PI3K and PLC γ 1 leads to phosphorylation of PKD1 and the activation of Rac-1 that initiates the required cytoskeletal rearrangements for the bacterial uptake (Faulstich *et al.*, 2013, Faulstich *et al.*, 2015). Though PorB_{IA} is sufficient for LPDI, additional gonococcal factors might be involved in this invasion pathway (Kühlewein *et al.*, 2006).

Besides being a key player in LPDI, PorB_{IA} is also important for serum resistance of *N. gonorrhoeae* (Morello & Bohnhoff, 1989). The protein binds the factor H, a regulator of the alternative pathway of the complement system, or the C4b-binding protein to evade complement-mediated killing (Ram *et al.*, 1999, Ram *et al.*, 2001).

Another characteristic of the neisserial PorB is the ability to translocate into artificial planar lipid bilayer membranes and host cell membranes (Lynch *et al.*, 1984, Rudel *et al.*, 1996). Additionally, PorB_{IA} resembles the mitochondrial voltage-dependent anion channel (VDAC), which led to the investigation of its role in the induction of apoptosis. PorB_{IA} has been shown to target the outer membrane of mitochondria, induce cytochrome *c* release through pore formation, break down the mitochondrial membrane potential and activate caspases, which subsequently leads to apoptosis (Muller *et al.*, 2000). However, in a subsequent study PorB_{IA} was not sufficient to induce the release of cytochrome *c*, which implies that other factors are required to trigger the apoptosis (Muller *et al.*, 2002). Furthermore, PorB_{IA} has been shown to increase the transcription of several anti-apoptotic genes (Binnicker *et al.*, 2004). In the case of meningococcal PorB an association of the porin with the mitochondria resulted in a stabilization of the mitochondrial membrane and enhanced cellular survival (Massari *et al.*, 2000).

Neisserial macrophage infectivity potentiator (Ng-MIP)

The macrophage infectivity potentiator (MIP) that exhibits a peptidyl prolyl *cis-trans* isomerase (PPIase) enzyme activity was identified as a virulence-associated protein in various pathogens. PPIases belong to a superfamily of ubiquitously distributed proteins that are found in eukaryotes, prokaryotes and some giant viruses. The family comprises three structurally unrelated members, which are distinguished due to the susceptibility to naturally occurring inhibitors. Cyclophilins were the first identified proteins with PPIase activity that are inhibited by cyclosporine A, which was isolated from the fungus *Trichoderma polysporum* and was applied for prevention of allograft rejection due to its immunosuppressive properties (Takahashi *et al.*, 1989). Besides, a secondary metabolite of *Streptomyces tsukabensis* FK506 (Tacrolimus) has also been shown to inhibit the T cell activation and was used to identify the FK506-binding protein (FKBP) exhibiting PPIase activity (Harding *et al.*, 1989, Siekierka *et al.*, 1989). The macrolide rapamycin (Sirolimus) isolated from *Streptomyces hygroscopicus* belongs also to the inhibitors of FKBP, but has furthermore been shown to inhibit the serine/threonine kinase mammalian target of rapamycin (mTOR) of the PI3K family (Sabers *et al.*, 1995, Brown *et al.*, 1994). The last family member are the parvulins inhibited by juglone (5-hydroxy-1,4-naphthoquinone) (Hennig *et al.*, 1998, Rahfeld *et al.*, 1994).

PPIases catalyse the *cis-trans* isomerization of peptidyl-prolyl bonds in polypeptide backbones during protein folding. Peptide bonds without prolyl residues strongly favour *trans* conformation due to the steric hindrance of the side chains in the *cis* formation. The free energy difference is estimated to be 2.6 kcal/mol. However, the pyrrolidine ring of proline (Pro) results in a low free energy difference between the *cis* and *trans* isomers of 0.5 kcal/mol for Xxx-Pro (Xxx any residue). Therefore, neither the *cis* nor the *trans* conformation is favourable and the protein dynamics are slowed down by a factor of 100. The prolyl *cis-trans* isomerisation is a molecular switch that influences protein folding and denaturation kinetics of proteins (Brandts *et al.*, 1975, Stewart *et al.*, 1990, Pal & Chakrabarti, 1999). PPIases assist during the *cis-to-trans* and *trans-to-cis* conversion of these prolyl bonds and have been shown to be important for numerous biological processes such as gene expression, signal transduction, protein secretion, development and tissue regeneration (Unal & Steinert, 2014).

PPIases are also associated with the virulence of several pathogenic bacteria and parasitic protozoa and occur as cytosolic, periplasmic or extracellularly secreted proteins. The first and best investigated PPIase under this aspect was the MIP of *Legionella pneumophila* (Lp-MIP), which belongs to the FKBP family. Inactivation of Lp-MIP resulted in a decreased survival of *L. pneumophila* Wadsworth in protozoan cells, macrophage-like cells U937 and human alveolar macrophages (Cianciotto & Fields, 1992). Furthermore, infection of guinea pigs with *Legionella* expressing the mutated Lp-MIP form showed reduced virulence (Cianciotto *et al.*, 1990). However, whether the PPIase activity is required for the contribution to the intracellular survival is still under discussion, since reduced PPIase activity did not affect the bacterial survival, and moreover numerous non-pathogenic bacteria are known to express proteins with PPIase activity (Wintermeyer *et al.*, 1995).

The discovery of Lp-MIP triggered the identification of other MIP-like proteins from pathogens such as *Chlamydia trachomatis*, *N. gonorrhoeae* and *N. meningitidis*. *N. gonorrhoeae* expresses the 30 kDa membrane-localized, homodimeric, surface-exposed lipoprotein MIP of the FKBP family, which has a homology of 43.8 % to Lp-MIP. The PPIase activity of the protein can be inhibited by rapamycin. Deletion of Ng-MIP results in a decreased intracellular survival in macrophages, while the attachment was not impaired (Leuzzi *et al.*, 2005). Furthermore, sera from 20 patients with urethritis or DGI recognized

the purified recombinant Ng-MIP, which indicates the expression of the protein during infection and its immunogenic character (Rotman & Seifert, 2014).

A homologue of Ng-MIP was also described in *N. meningitidis* (Williams *et al.*, 2007). Due to its conservation, surface exposition and the ability to induce the generation of cross-protective bactericidal antibodies, the Nm-MIP is suggested as potential antigen in the development of a vaccine against meningococcal infection (Hung *et al.*, 2011). Even an antibody against a recombinant truncated Nm-MIP showed bactericidal activity. The recombinant protein contained no human sequence similarity, which is important to avoid cross-reaction with the human FKBP (Bielecka *et al.*, 2015).

1.1.4 Interaction of *N. gonorrhoeae* with neutrophils

During infection, *N. gonorrhoeae* interacts by its adhesins and invasins with different cell surface receptors on epithelial cells and innate immune cells such as macrophages and dendritic cells. LOS and PorB are recognized by the toll-like receptors (TLRs) and peptidoglycan fragments in outer-membrane vesicles are recognized by NOD-like receptors (NLRs) (Massari *et al.*, 2002, Fiset *et al.*, 2003, Kaparakis *et al.*, 2010, Mavrogiorgos *et al.*, 2014). This binding leads to the release of inflammatory cytokines such as interleukin-8 (IL-8) and IL-6, which in turn results in the recruitment and activation of polymorphonuclear leukocytes (PMNs) (Waage *et al.*, 1989, Ramsey *et al.*, 1995). Furthermore, the outer membrane protein Opa binds CEACAM receptors on the surface of PMNs, which leads to increased killing of Opa-expressing bacteria in contrast to Opa-negative bacteria. Especially the receptor CEACAM3 has been shown to promote phagocytic uptake of bacteria (Billker *et al.*, 2002, Schmitter *et al.*, 2004, Pils *et al.*, 2008).

PMNs have many mechanisms to kill bacteria, such as neutrophil extracellular traps (NETs), clearance of intracellular bacteria by reactive oxygen species (ROS), phagocytosis, degrading enzymes and antimicrobial peptides. However, *Neisseria* have also developed numerous mechanisms to evade this killing and even to utilize PMNs for their purposes, since PMNs are the first line of defence during infection. For the killing of adherent and extracellular bacteria, PMNs generate extracellular ROS through the NADPH oxidase (oxidative burst) at the plasma membrane to damage bacterial lipids, proteins and DNA. Gonococci have several antioxidant mechanisms such as the expression of catalase for detoxification or the Mn(II) transport system (MntABC) for quenching (Johnson *et al.*, 1993,

Tseng *et al.*, 2001). In several studies, however, it could be demonstrated that ROS does not play a role in killing gonococci, since a mutation of neisserial antioxidant genes did not affect bacterial survival in the presence of neutrophils (Seib *et al.*, 2005). Another mechanism of PMNs is the release of NETs, which are composed of the PMNs chromatin and granule components to trap and kill microbes. Gonococci have been shown to suppress and induce NET formation depending on the multiplicity of infection (MOI). A higher MOI (>20) stimulates NET formation, but *Neisseria* are able to resist the NET-mediated killing (Gunderson & Seifert, 2015).

Besides factors that are involved in oxidative damage, PMNs produce also non-oxidative antibacterial components. However, the neutrophil mechanisms for killing extracellular bacteria are not sufficient, since more than 81 % stay alive after association with PMNs for 2 h (Criss *et al.*, 2009). *N. gonorrhoeae* has a system for avoiding phagocytosis by PMNs through antigenic variation and limiting opsonization with antibodies or complements. Nevertheless, internalized bacteria are still detected within PMNs isolated from gonorrhoea patient (Ovcinnikov & Delektorskij, 1971). *In vitro* infections revealed that 41 % of internalized bacteria stay alive (Criss *et al.*, 2009). However, not only survival but also intracellular replication of gonococci was observed in PMNs (Casey *et al.*, 1986, Simons *et al.*, 2005). Moreover, PMNs challenged with gonococci showed a prolonged lifespan, due to the inhibition of spontaneous and induced apoptosis by intrinsic (staurosporine) and extrinsic (tumor necrosis factor-related apoptosis-inducing ligand) factors (Chen & Seifert, 2011, Simons *et al.*, 2006).

Based on these facts, it can be assumed that *Neisseria* take advantage of the recruited PMNs. Neutrophils could be a protective bacterial niche that helps the gonococci to acquire new nutrients and transmit into deeper tissues (Criss & Seifert, 2012).

1.2 *Chlamydia trachomatis*

1.2.1 The order of Chlamydiales

The order of Chlamydiales comprises the four families Chlamydiaceae, Parachlamydiaceae, Waddliaceae and Simkaniaceae (Everett *et al.*, 1999). The Gram-negative obligate intracellular pathogens parasitize within diverse organisms ranging from humans to amoeba. Chlamydiaceae is the best investigated family containing the two genera *Chlamydophila* and *Chlamydia* that include altogether 11 species. *Chlamydia* was described for the first time in 1907 by Halberstaedter and von Prowatzek, who observed *Chlamydia*-containing vacuoles by Giemsa staining in cells from conjunctiva scrapings of individuals suffering from trachoma (Halberstaedter, 1907). At the beginning *Chlamydia* was thought to be a virus, however improving laboratory techniques contributed to research and identified *Chlamydia* as bacteria in the 1960's. Chlamydiaceae such as *C. psittaci* and *C. muridarum* are animal pathogens, while the pathogens *C. trachomatis* and *C. pneumoniae* are the major causes of several human diseases.

1.2.2 *C. trachomatis* infection diseases

C. trachomatis was responsible for 131 million ocular and sexually transmitted infections (STIs) in 2012 (WHO, 2016a). The bacteria are divided into three biovars that are subdivided in up to 18 serovars. Serotyping was originally performed by monoclonal antibodies on basis of differences in the variable, serotype- and species-specific epitopes of OmpA (Wang, 1971, Wang *et al.*, 1975, Wang *et al.*, 1985). The serovars A - C cause trachoma, an infection of the upper inner eyelid that is the major cause of preventable blindness in the world. The disease is spread by direct contact with infected individuals and affects 8 million people mainly from poor communities with low hygiene standards and poor water supply (Wright *et al.*, 2007, Resnikoff *et al.*, 2004). The lympho-granuloma venereum (LGV) biovar comprises the serovars L1 - 3 and is an invasive form of *C. trachomatis* that results in urogenital or anorectal infection. It affects submucosal connective tissue and spreads into regional lymph nodes. An untreated LGV infection can lead to rectal fistula or stricture. The last biovar is divided in the serotypes D-K that cause the most prevalent sexually transmitted diseases. The course of disease is asymptomatic in 70 - 80 % of women and 50 % of men (Malhotra *et al.*, 2013). Uncomplicated infection in women manifests in abnormal vaginal discharge,

dysuria and intermenstrual bleeding. Symptomatic men suffer from urethritis and women from cervicitis. Untreated infection in women can lead to pelvic inflammatory disease, ectopic pregnancy and salpingitis. However, a spontaneous clearance of the infection is also possible (Parks *et al.*, 1997). Pregnancy during chlamydial infection can result in infection of the child during delivery, which leads to neonatal conjunctivitis, nasopharyngeal infection and neonatal pneumonia (WHO, 2016a).

Clinically evident resistance to antibiotics has not developed in *Chlamydia* yet. However, 15 isolates, of which 11 were the result of treatment failure, exhibited a so-called heterotypic-resistance (Jones *et al.*, 1990, Mourad *et al.*, 1980, Lefevre & Lepargneur, 1998, Misyurina *et al.*, 2004, Somani *et al.*, 2000). This form of resistance comprises a heterogenic chlamydial population containing susceptible and resistant bacteria, although the whole population would be able to express resistance. The mechanisms behind chlamydial resistances are not known, because less than 1 - 10 % of the population expresses resistance, genetic differences between these populations are missing, isolated bacteria do not survive long-passages and often lose their resistances (Somani *et al.*, 2000).

Clinical treatment failure can not only lead to development of antibiotic resistances but can also result in persistence, though distinguishing the two forms is challenging. This chlamydial form has not only been observed in *in vitro* studies, but there is evidence for persistence *in vivo*. Atypical *C. trachomatis* was found in fibroblasts and macrophages from synovial membranes of patients with *Chlamydia*-associated reactive arthritis or Reiter's syndrome (Nanagara *et al.*, 1995). Furthermore, a long-term study showed several reinfections with the same genotype, although the patients were treated with antibiotics (Dean *et al.*, 2000). This study provides evidence that chronic chlamydial infection could occur due to the persisting *Chlamydia*, which are reactivated and establish a new infection.

Until now, no protective vaccination is available but research is still ongoing. Understanding the immune response during an infection is essential for vaccine development. Most of the current knowledge was gained by infection experiments with *C. muridarum* in mice and observations from human infection with *C. trachomatis*. However, not only pathogen evasion mechanisms impede vaccine development but also an incomplete knowledge about *C. trachomatis*-induced immune response in the genital tract, as well as limited genetic tractability of *Chlamydia*. For a long time it has been assumed that *C. trachomatis* cannot be genetically manipulated due to its intracellular niche. However,

transformation systems and other genetic approaches have been established, which promoted the chlamydial research. The first examined vaccination attempts were performed with whole inactivated *C. trachomatis*, which resulted in temporal protection but has also been shown to worsen the disease during reinfection (Grayston & Wang, 1978, Grayston *et al.*, 1985). Thus, research focused on subunit vaccines against certain chlamydial antigens. The most important proteins, recognized by human or mice T cells are: CrpA, Cap1, PmpD, Omp2, HSP60, YopD homologue, enolase and the most promising candidate OmpA (Brunham & Rey-Ladino, 2005).

1.2.3 Developmental cycle of *C. trachomatis*

Chlamydia performs a biphasic developmental cycle within the host cell (Figure 1.3). During the cycle, the bacteria occur in two morphologically and structurally distinct forms: the elementary bodies (EBs) and the reticulate bodies (RBs) (Constable, 1959, Gaylord, 1954). The developmental cycle begins with the attachment of the EBs to epithelial cells. EBs have an average size of 0.3 μm and appear as round and electron dense structures (Eb *et al.*, 1976). This chlamydial form is highly infectious but thought to be metabolically inert due to compactly condensate nuclear material. However, a recent study has proven EBs metabolic and biosynthetic activity using glucose-6-phosphate (G-6-P) as energy source to generate ATP (Omsland *et al.*, 2012). The attachment and entry mechanism of EBs is still under investigation. A two-step adhesion process is proposed, which is initialized by electrostatic interactions of the bacteria with the cell surface located HSPG from the glycosaminoglycan family (Zhang & Stephens, 1992). The chlamydial outer membrane protein OmpA (also called major outer membrane protein MOMP) is one of the major adhesins interacting with HSPG (Su *et al.*, 1996, Su *et al.*, 1990). Further potential adhesins are LPS, HSP70, OmcB and polymorphic membrane proteins (Pmps) (Raulston *et al.*, 2002, Fadel & Eley, 2007, Grimwood *et al.*, 2001, Grimwood & Stephens, 1999). This first step is mediated by reversible low-affinity interactions, while the second involves an irreversible and high-affinity binding to still unidentified host receptors (Carabeo & Hackstadt, 2001, Elwell *et al.*, 2016).

The bacterial entry into the host cell contains features of the trigger as well as the zipper mechanism. Signal transduction pathways can be induced by the zipper mechanism through binding of bacteria to certain host receptors. Indirect evidence suggests that EBs

express a Type III secretion system (T3SS) with spike-like structures triggering the bacterial entry by secretion of effector molecules into the host cell (Nichols *et al.*, 1985, Fields *et al.*, 2003). One of the effectors is the translocated actin-recruiting phosphoprotein (Tarp) that nucleates and bundles actin using its globular actin (G-actin) and filamentous actin (F-actin) domains (Jewett *et al.*, 2006). Furthermore, the effector protein CT166 has been shown to be interfering with Rac-dependent cytoskeletal changes (Thalmann *et al.*, 2010). *C. trachomatis* stimulates the Rho family GTPase Rac1, which recruits several actin regulators and induce cytoskeletal rearrangements (Carabeo *et al.*, 2004).

After endocytosis of *C. trachomatis*, the bacteria remain throughout the cycle in a vacuole called 'inclusion'. The fusion with late endosomes or lysosomes is inhibited, which enables the bacteria to develop intracellularly (Hackstadt, 2000). In the first 8 h post-infection the EBs differentiate to the larger (1 μm), non-infectious, replicative and metabolically active RBs. Belland *et al.* categorized the bacterial gene expression due to the temporal expression during the development in early, mid- and late-cycle genes (Belland *et al.*, 2003). The expression of early genes leads to modification of the inclusion membrane, inclusion transport to peri-Golgi region, redirection of exocytic vesicles for the fusion with the inclusion and establishment of required host-pathogen interactions (Scidmore *et al.*, 1996). The RBs express mid-cycle genes for biogenesis of the cell envelope, energy metabolism, protein folding, T3SS, DNA replication, modification, repair and recombination (Nicholson *et al.*, 2003). If more than one bacterium has been internalized, multiple inclusions are fused by homotypic fusion. RBs replicate until 24 h post-infection and are triggered by an unknown mechanism asynchronously to redifferentiate back to EBs. Late-cycle effectors such as proteins for DNA condensation are required for packaging of progeny EBs. The *in vitro* *C. trachomatis* developmental cycle is complete after 48 h and ends with cell lysis or extrusion, which results in the release of new infectious particles (Hybiske & Stephens, 2007). Before this time point, *C. trachomatis* has been shown to interfere with pro-apoptotic pathways to maintain the survival of the host cells (Fan *et al.*, 1998, Fischer *et al.*, 2001, Rajalingam *et al.*, 2001).

The bacterial developmental cycle can be reversibly arrested during the replication stage. *Chlamydia* appear as enlarged, pleomorphic aberrant RBs (ABs), whose cell division and differentiation to EBs is inhibited (Hogan *et al.*, 2004). This state is called 'persistence'

and can be induced *in vitro* by various factors such as exposition to β -lactam antibiotics, Interferon- γ (IFN- γ) and amino acid or iron deficiency.

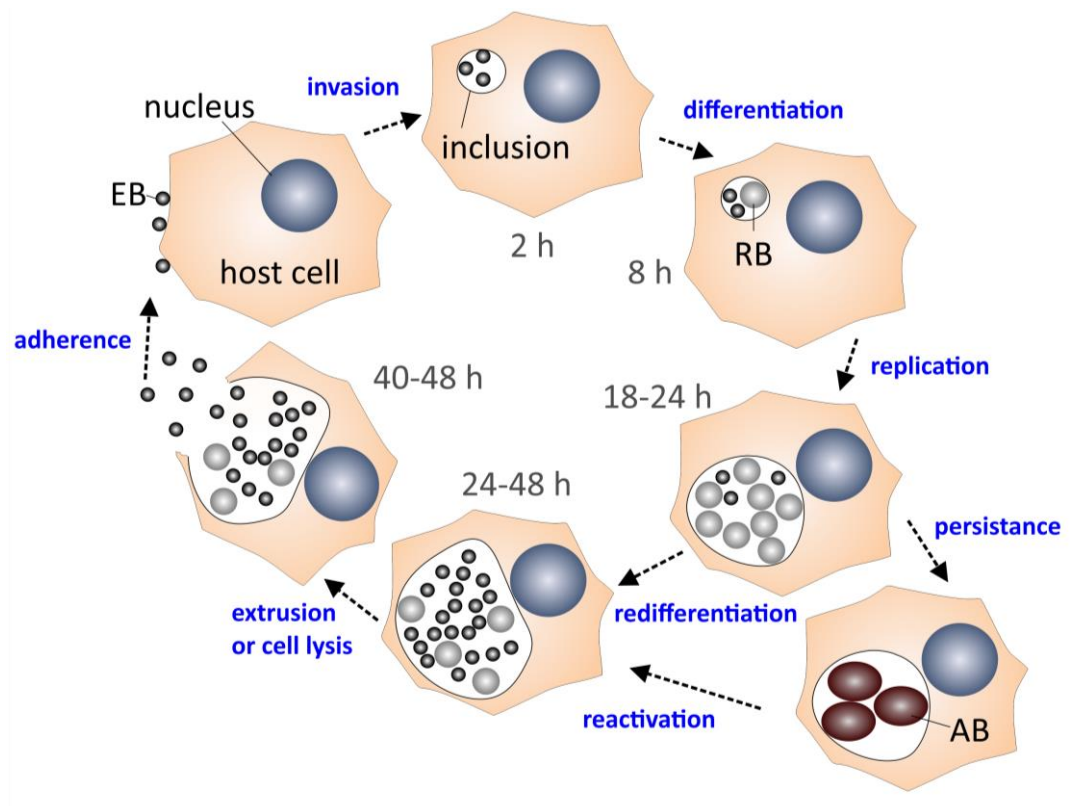


Figure 1.3: Biphasic developmental cycle of *C. trachomatis*. Infectious EBs adhere to and invade the host cell. Within the bacteria-containing vacuole, the so-called inclusion, EBs differentiate to RBs, which replicate and then redifferentiate back to EBs. The new infectious EBs are released by either cell lysis or extrusion and are able to infect neighbouring cells. If factors such as penicillin or Interferon- γ are present during infection, *C. trachomatis* acquires a persistent form. Removal of the stimulus reactivates the bacteria that enter the developmental cycle again. EB: elementary body, RB: reticulate body, AB: aberrant body

1.2.4 Host-pathogen interaction

C. trachomatis has a strongly reduced genome of 1 Mb encoding approximately 1 000 open reading frames (ORFs) and additionally possesses a 7.5 kb cryptic plasmid. Therefore, the bacteria lack several metabolic enzymes and the present ORFs are assumed to be essential. The inability to provide their own nutrients for development results in dependency on the host cell that is used by the bacteria for acquisition of nutrients such as amino acids, lipids and iron. The bacteria established a close interaction system to cell organelles such as the Golgi, mitochondria, multivesicular bodies, lipid droplets and lysosomes.

Mitochondria play an important role during the infection, though a direct contact between the inclusion and these organelles could not be observed for *C. trachomatis* as it

has been shown for *C. psittaci* (Matsumoto *et al.*, 1991). Deletion of the mitochondrial proteins Tom22 and Tom40, which are involved in recognition and import of proteins to mitochondria, reduced the infection with *C. caviae* but did not influence *C. trachomatis* infection (Derre *et al.*, 2007). Nevertheless, mitochondria are key players in the programmed cell death (apoptosis), generation of ROS and production of energy in the form of adenosine triphosphate (ATP) - all processes in which *C. trachomatis* intervenes and from which it derives benefits. ROS is generated in the mitochondrial respiratory chain and membrane-bound NADPH oxidase and is required during chlamydial infection along with K⁺ efflux for activation of NLRP3-dependent pro-inflammatory cysteine protease caspase-1 (Abdul-Sater *et al.*, 2009, Abdul-Sater *et al.*, 2010). It has been shown that *C. trachomatis* infection leads to increased ROS levels in the first hours of infection that decline afterwards and return back to a basal level after 9 h (Boncompain *et al.*, 2010). Another study has reported an increased ROS production after 20 h post-infection that increases until 24 h and returns to the basal levels at 36 h post-infection (Abdul-Sater *et al.*, 2009). The sources of the ROS generation are the NADPH oxidase NOX and the member of the intracellular NLR family NLRX1 that is localized in mitochondria. Depletion of NLRX1 leads to a reduced growth of *C. trachomatis* and an inhibition of NOX resulted in a strong reduction of the infection, implying that NOX is essential for chlamydial development, while NLRX1 is needed for an optimal growth (Abdul-Sater *et al.*, 2010).

Furthermore, mitochondria provide the cell with ATP and *C. trachomatis* is assumed to obtain cellular ATP; therefore, the bacteria were often termed as 'energy parasites'. ATP is generated during glycolysis in the cytosol and cellular respiration comprising the tricarboxylic acid (TCA) cycle and oxidative phosphorylation (OXPHOS) inside of mitochondria. These organelles possess membranes that separate mitochondria into four biochemically distinct compartments: the inner mitochondrial membrane (IMM), the outer mitochondrial membrane (OMM), the intermembrane space between IMM and OMM (IMS) and the matrix within the IMM. The IMM forms diverse invaginations termed cristae, which increase the inner membrane surface and harbour the four complexes of the electron transport chain: complex I (NADH:ubiquinone oxidoreductase), complex II (succinate dehydrogenase), complex III (ubiquinol:cytochrome *c* oxidoreductase, cytochrome *bc*₁ complex) and complex IV (cytochrome *c* oxidase) (Frey & Mannella, 2000). The proton translocation across the IMM by the complexes I, III and IV results in an electrochemical

gradient consisting of the mitochondrial membrane potential ($\Delta\psi$) ranging from 180 - 220 mV due to an excess of positively charged protons, and the pH gradient (ΔpH) with a pH 7 in the intermembrane space and pH 7.5 to 8 in the matrix (Santo-Domingo & Demaurex, 2012). The mitochondrial F_0F_1 -ATP synthase/ F_0F_1 -ATPase uses this gradient and the proton-motive force to catalyse ATP from ADP and inorganic phosphate. The F_0F_1 -ATPase is a huge 500 kDa complex with 16 to 18 subunits that is not only found in mammals but is also conserved in various bacteria and plants (Capaldi & Aggeler, 2002). The complex consists of a membrane-embedded hydrophobic F_0 motor, which rotates due to the proton translocations and causes a conformational change of the hydrophilic F_1 module facing the mitochondrial matrix that result in ATP synthesis (Abrahams *et al.*, 1994, Collinson *et al.*, 1994).

The energy supply in *C. trachomatis* is a controversially discussed topic. In the beginning, the hypothesis of the 'energy parasite' was supported by the missing evidence for glycolytic enzymes activity and components of the electron chain. Additionally, it has been demonstrated that the bacteria are auxotrophic for ATP, GTP and UTP, while CTP could be synthesized by *C. trachomatis* using UTP (Tipples & McClarty, 1993). Further indications were the two identified ATP/ADP translocases and nucleotide symporter Npt1_{Ct} and Npt2_{Ct}, which facilitate the exchange of bacterial ADP for ATP from the host cell (Stephens *et al.*, 1998, Tjaden *et al.*, 1999). However, there are also arguments against this hypothesis. Subsequent genome sequencing revealed the existence of genes encoding for proteins that are involved in energy metabolism, glycolysis and TCA cycle including the pyruvate kinase, phosphoglycerate kinase, glyceraldehyde-3-phosphate dehydrogenase and glucose-6-phosphate dehydrogenase (Stephens *et al.*, 1998, Iliffe-Lee & McClarty, 1999). The final evidence against *C. trachomatis* being an 'energy parasite' was the demonstration of ATP production in cell-free (axenic) culture system by EBs using G-6-P, while RBs utilize ATP (Omsland *et al.*, 2012).

1.2.5 Chlamydial macrophage infectivity potentiator (Ctr-MIP)

A 27 kDa MIP-like protein, exhibiting a 37 % homology to the Lp-MIP has been identified in *C. trachomatis* (Ctr-MIP) (Lundemose *et al.*, 1991, Lundemose *et al.*, 1992). The protein is also expressed by five other chlamydial species such as *C. pneumoniae*, *C. muridarum* and *C. caviae*. The Ctr-MIP, which is synthesized 14 h post-infection, has been shown to possess

PPIase activity that can be inhibited by FK506 and rapamycin (Lundemose *et al.*, 1991, Lundemose *et al.*, 1993a). Furthermore, it has been identified as surface-exposed lipoprotein that is present in EBs and RBs (Lundemose *et al.*, 1993b, Neff *et al.*, 2007). A dual localisation of the protein in the inner and outer membrane of EBs has been suggested (Neff *et al.*, 2007). The pre-treatment of *C. trachomatis* with the PPIase inhibitors FK506 and rapamycin or the addition during infection reduced infectivity in McCoy cells. The presence of the inhibitors during 24 h of infection resulted in the development of morphologically abnormal and persistent-like bacteria. These data indicate the involvement of the Ctr-MIP in intracellular infection (Lundemose *et al.*, 1993a). A study of Bas *et al.* analysed seven chlamydial antigens regarding their ability to induce the production of proinflammatory cytokines by human monocytes, macrophages and THP-1 cells (Bas *et al.*, 2008). The recombinant Ctr-MIP (rCtr-MIP) has been shown the highest proinflammatory activity through stimulation of the synthesis of IL-1 β , TNF- α , IL-6 and IL-8. Involved in this pathway were the receptors TLR2, TLR1 and TLR6 with the help of CD14. This kind of immune response could not be induced by a non-lipidated rCtr-MIP, which was generated by the mutation of the lipobox cysteine to an alanine (C20A). Additionally, the same was true for a Ctr-MIP treated with lipases. Therefore, Ctr-MIP is assumed to play an important role during chlamydial pathogenesis, which can be attributed to its lipid modifications (Bas *et al.*, 2008).

1.3 Antimicrobials

The alarming numbers of antibiotic resistances, bacterial persistence and the lack of vaccines triggered the search for new antimicrobials against the major causative agents of sexually transmitted diseases *N. gonorrhoeae* and *C. trachomatis*. In the following chapter three classes of small compounds with different sources are introduced, which were screened for their antimicrobial properties in this study.

1.3.1 Plant-derived compounds

The usage of plants in herbal medicine for therapeutic purposes is the oldest treatment procedure that was applied throughout the history of mankind in all cultures. Nowadays, research is focused on the identification, isolation and structural elucidation of plant-derived compounds with antimicrobial properties, which may be further processed to drugs used in modern medicine. Possible sources for novel natural compounds are tropical lianas of the families Dioncophyllaceae and Ancistrocladaceae occurring in Africa, South and Southeast Asia. They have been shown to produce naphthylisoquinoline alkaloids with extraordinary inhibitory properties against *Plasmodium*, *Leishmania* and *Trypanosoma* (Bringmann *et al.*, 2003a, Bringmann *et al.*, 2003b, Francois *et al.*, 1997). Recently, further novel compounds, the so-called naphthoquinones, which are structurally related to the naphthylisoquinoline alkaloids, were identified. The naphthoquinones from *Triphyophyllum peltatum* of the Dioncophyllaceae family were named dioncoquinones and exhibit antiprotozoal properties against *Leishmania major* and anti-tumoral activities (Bringmann *et al.*, 2008). Also other isolated quinones such as the anthraquinone chrysophanol isolated from the plant *Colubrina greggii* showed antimicrobial activity against *Bacillus subtilis* and *Staphylococcus aureus* (García-Sosa, 2006).

These bioactive compounds are the structural basis for the synthesis of simplified analogues, the side effects of which are aimed to be removed by focusing on the mode of action of the compound.

1.3.2 Pipecolic acid derivatives

MIP PPIases have been associated with virulence in pathogens such as *N. gonorrhoeae*, *C. trachomatis*, *L. pneumophila* and *B. pseudomallei*. Therefore, researchers started to investigate inhibitors against the bacterial MIPs. The known inhibitors FK506 and rapamycin

are not suitable because of their immunosuppressant properties and the inhibition of the human PPIase FKBP12. However, the immunosuppression is not due to the inhibition of the PPIase activity, but it has been shown that the binding of the inhibitors FK506 and rapamycin to FKBP12 promotes the association to calcineurin or mTOR (mechanistic target of rapamycin), respectively (Bierer *et al.*, 1990, Liu *et al.*, 1991, Chiu *et al.*, 1994, Sabers *et al.*, 1995). Therefore, different structure-based approaches were applied to identify and synthesize compounds that specifically inhibit only the PPIase activity of bacterial MIP proteins without having immunomodulatory side effects. Beneficial for the design of pathogenic MIP inhibitors are the available structural data from the crystal structures of Lp-MIP, Tc-MIP (*Trypanosoma cruzi*) and BpML1 (*Burkholderia pseudomallei*) (Riboldi-Tunnicliffe *et al.*, 2001, Pereira *et al.*, 2002, Norville *et al.*, 2011). Until now, inhibitors were designed against the Lp-MIP, Bp-MIP and the MIP of *P. falciparum* using structure- and substrate-based techniques (Juli *et al.*, 2011, Begley *et al.*, 2014, Harikishore *et al.*, 2013). The structure of the Lp-MIP-rapamycin complex revealed that a pipercoline moiety of rapamycin mediates the binding to the protein (Ceymann *et al.*, 2008). Therefore, two compounds possessing a pipercoline moiety were used in a study as basis for the synthesis of novel small-molecule pipercolic acid derivatives applying structural data and computational docking methods (Juli *et al.*, 2011). A protease-coupled PPIase assay was performed to measure the Lp-MIP PPIase activity in the presence of the novel inhibitors showing that several of the inhibitors affected the isomerase activity negatively. Furthermore, Begley *et al.* were able to co-crystallize BpML1 with four different pipercolic acid derivatives, which allowed the authors to identify the chemical scaffold of the binding (Begley *et al.*, 2014). Several inhibitors have not only been shown to inhibit the PPIase activity of BpML1 but also to reduce the infectivity of *B. pseudomallei* without having cytotoxic effects on macrophages.

1.3.3 Antimicrobials derived from marine sponges or sponge-associated bacteria

Sponges are sessile animals from the phylum Porifera, which filter organic material and microorganisms through their pores for nutrition. More than 8 000 species were identified in diverse marine and freshwater ecosystems (Laport *et al.*, 2009). Marine sponges have been discovered as a rich source of bioactive compounds that are produced as secondary metabolites for protection against predators and the settling of larva from other organisms

on their surface, since sponges lack any physical defence mechanisms (Anjum *et al.*, 2016). Around 5 300 different novel compounds are isolated from marine sponges every year (Faulkner, 2000, Faulkner, 2001, Faulkner, 2002). A characteristic of these chemicals is their diversity, which includes nucleosides, amino acid derivatives, cyclic peptides, terpenes, sterols, alkaloids, peroxides and fatty acids (Donia & Hamann, 2003, Blunt *et al.*, 2005, Blunt *et al.*, 2006, Sipkema *et al.*, 2005, Piel, 2006). The natural compounds have exhibited antiviral, antibacterial, antifungal, antiprotozoal, antitumor, immunosuppressive and anti-inflammatory activities (Laport *et al.*, 2009). Several of the compounds were tested in clinical trials or are even in clinical use for years such as the antiviral ara-A (vidarabine). The synthesis of ara-A was based on nucleosides isolated from *Tectitethya crypta* (formerly *Cryptotethya crypta*) (Bergmann & Feeney, 1950, Bergmann & Feeney, 1951).

However, the origin of the secondary metabolites is a controversially discussed topic. Sponges are hosts for various microorganism communities, which represent 50 - 60 % of the marine sponge biomass (Bergmann & Burke, 1955, Wang, 2006). This cohabitation has many advantages such as nutrient acquisition, waste disposal and stabilization of the sponge skeleton. To this date fungi, microalgae, virus and at least ten different bacterial phyla such as Actinobacteria have been identified as sponge-associated microorganisms using denaturing gradient gel electrophoresis (DGGE), 16S rRNA gene sequencing and fluorescence *in situ* hybridization (FISH) (Thomas *et al.*, 2010). It has been hypothesised that the microorganisms are the actual producers of the bioactive metabolites since the same compounds have been found in unrelated sponges or some of them are known to be produced by certain microorganisms (Piel, 2004). Approximately 65 % of the compounds derive from fungi and 35 % from bacteria associated with sponges (Thomas, 2010). About 50 % of the bacterial metabolites were produced by marine filamentous actinomycetales species such as *Streptomyces*, of which over 10 000 bioactive compounds have been discovered (Berdy, 2005).

The synthesis or isolation of these sponge-derived metabolites on a large scale is difficult due to their complex structures and the demanding cultivation of sponges (Belarbi *et al.*, 2003). Furthermore, although several laboratory culture-based techniques are available for the culturing of microorganisms, there are only few bacteria species that can be cultured without their host (Hentschel *et al.*, 2003).

1.4 Aim of the work

In rare cases *N. gonorrhoeae* infection can lead to the development of DGI, which is associated with the expression of the neisserial porin PorB_{IA} (Morello & Bohnhoff, 1989, Bash *et al.*, 2005). Although SREC-I has been identified as the cellular receptor of PorB_{IA}, a direct interaction has never been demonstrated (Rechner *et al.*, 2007). Thus, using different approaches, this work aimed to analyse the porin-receptor interaction.

The rising number of antibiotic resistances makes *N. gonorrhoeae* a major threat for public health. Therefore, in search for novel antimicrobials against the PorB_{IA}-mediated invasion of *N. gonorrhoeae*, 68 small molecule compounds were screened in this study. The *in vitro* screening was also performed to identify inhibitors of *C. trachomatis* infection. The analysed compounds were grouped in the following three classes according to their respective origin: i) plant-derived compounds, ii) extracts or pure compounds from marine sponges or sponge-associated bacteria, iii) pipecolic acid derivatives synthesized specifically for the inhibition of bacterial MIP proteins.

I analysed the inhibitory effect of two highly bioactive pipecolic acid derivatives, PipN3 and PipN4, on the PPlase activity of the recombinant and purified Ctr-MIP and Ng-MIP. Additionally, I studied their impact during *C. trachomatis* infection of HeLa cells and *N. gonorrhoeae* infection of PMNs isolated from human blood.

I also investigated the natural compound SF2446A2, which was isolated from *Streptomyces sp.* strain RV15. The substance showed extraordinary bactericidal activity against *C. trachomatis* in the screening. Thus, I analysed the mode of action of the compound during infection. The substance negatively impacted mitochondrial functionality. Therefore, I investigated further the dependency of *C. trachomatis* on the host cell mitochondria and ATP.

2 MATERIAL AND METHODS

2.1 Material

2.1.1 Bacterial strains

All used *N. gonorrhoeae* strains in this study derived from the *N. gonorrhoeae* strain MS11. *Escherichia coli* (*E. coli*) strain DH5 α was used for amplification of plasmids and the *E. coli* strain BL-21 for the expression of recombinant proteins.

Table 2.1: *N. gonorrhoeae* strains

Strain	characteristics	Genotype/ Plasmids	Source
N917	PorB _{IB} , Pili ⁺ , Opa ⁻	$\Delta pilE2$, $cat< >porB_{IB}>ermC$	(Bauer, 1997)
N920	PorB _{IA}	$\Delta pilE2$, $cat<porB_{IA}<>ermC$	(Bauer, 1997)
N924	PorB _{IB} , Pili ⁻ , Opa ⁻	$\Delta pilE1/2$, $cat<porB_{IA}<>ermC$	(Bauer, 1997)
N927	PorB _{IA} , Pili ⁻ , Opa ⁻	$\Delta pilE1/2$, $cat<porB_{IA}<>ermC$	(Bauer, 1997)
N931	PorB _{IB} , Pili ⁻ , Opa50	$\Delta pilE1/2$, $cat<porB_{IB}< >ermC$ pTH6a (opa50)	(Bauer, 1997)
N2009	PorB _{IA} , Pili ⁺ , Opa ⁻	$cat<porB_{IA}<>ermC$	(Sprenger, 2010)
N2011	PorB _{IA} , Pili ⁻ , Opa ⁻	$cat<porB_{IA}<>ermC$	(Faulstich, 2012)
ΔNg -MIP	N2009, ΔNg -MIP	N2009, $\Delta ng-mip::kan$	this study
ΔNg -MIP ^C	ΔNg -MIP, Ng-MIP ^C	ΔNg -MIP, pLAS::pPIIE_ <i>ng-MIP</i>	this study
PorB _{IA} -FLAG	PorB _{IA} -FLAG, Pili ⁻ , Opa ⁻	$cat<porB_{IA}loop1FLAG(G41-A42)<>ermC$	this study
PorB _{IB} -FLAG	PorB _{IB} -FLAG, Pili ⁻ , Opa ⁻	$cat<porB_{IB}loop1FLAG(D41-G42)<>ermC$	this study

Arrowheads indicate 5' end (> or <) and 5' to 3' orientation (>) of genes.

Table 2.2: Further used bacterial strains

Strain	Comment	Source
<i>Chlamydia trachomatis</i> (L2/434/BU)	wild type strain	ATCC VR-902B
<i>Chlamydia trachomatis</i> GFP (L2/434/BU)	green fluorescent protein (GFP)-expressing strain	pGFP::SW2 plasmid (Wang <i>et al.</i> , 2011)
<i>Escherichia coli</i> K-12	wild type strain	ATCC 25404
<i>Staphylococcus aureus</i> RN4220	wild type strain	(Kreiswirth <i>et al.</i> , 1983)
<i>Neisseria lactamica</i> 2358	wild type strain	N78, Max-Planck-Institut für Infektionsbiologie

2.1.2 Cell lines

Table 2.3: Cell lines

Cell line	Properties	Source
Chang	human conjunctiva epithelial cells	ATCC CCL20.2
HeLa229	human epithelial cervical carcinoma cells	ATCC CCL-227
HEK 293T	human kidney epithelial cells	ATCC CRL-11268
HeLa KRAB	HeLa cells with the gene encoding the KRAB-tTR repressor integrated into the chromosomal DNA	(Kozjak-Pavlovic <i>et al.</i> , 2007); Alexander Karlas
<i>f18kd-2</i>	HeLa KRAB cells with inducible shRNA-mediated knockdown of F1 β	this study
<i>mtx2kd-2</i>	HeLa KRAB cells with inducible shRNA-mediated knockdown of Mtx2	(Kozjak-Pavlovic <i>et al.</i> , 2007)
<i>glskd-1</i>	HeLa KRAB cells with inducible shRNA-mediated knockdown of GlS	Kozjak-Pavlovic, Elke Maier, 2013

All cell lines except CHO and HEK 293T cells were grown in RPMI 1640 medium. CHO cells were cultured in Ham's F12 medium and HEK 293T cells in DMEM medium. All media were supplemented with 10 % fetal calf serum (FCS) and the cells were grown at 37 °C and 5 % CO₂.

2.1.3 Plasmids

Table 2.4: Plasmids

Plasmid	Comment	Source
pET15b_Ng-MIP	neisserial <i>mip</i> without putative leader sequence amplified with Ng-MIP F/R from N927 (NdeI/BamHI)	this study
pET15b_Ctr-MIP	chlamydial <i>mip</i> without putative leader sequence amplified with Ctr-Mip F/R from <i>Ctr</i> wt (NdeI/BamHI)	this study
pET15b_PorB _{IA}	<i>PorB_{IA}</i> without putative leader sequence amplified with PorB _{IA} _pET15b F/R from gDNA N927 (NdeI/BamHI)	this study
pet15b_PorB _{IB}	<i>PorB_{IB}</i> without putative leader sequence amplified with PorB _{IB} _pET15b F/R from gDNA N924 (NdeI/BamHI)	this study
pET15b_Ng-MIP Δ DD	amplified with oligo number 13, 14, 15, 16 and 17 from pET15b_Ng-MIP (NdeI/BamHI)	Jutta Ebert, 2016
pET15b_Ng-MIP_D-L	amplified with oligo number 16, 17, 18 and 19 from pET15b_Ng-MIP (NdeI/BamHI)	Jutta Ebert, 2016

pET15b_Ng-MIP_Y-A	amplified with oligo number 16, 17, 20, 21 and 22 from pET15b_Ng-MIP (NdeI/BamHI)	Jutta Ebert, 2016
pcDNA3-GFP-SREC-I	extracellular domain of SREC-I was amplified from cDNA (IRATp970A0758D6, rzpd: Deutsches Ressourcenzentrum für Genforschung GmbH) with SRECI Ex. Dom. F/R (HindIII/ BamHI)	this study
pLVTHM_F1β-1	oligoannealing with ATP5B-1 FOR/ REV (Mlu/Cla)	Elke Maier
pLVTHM_F1β-2	oligoannealing with ATP5B-2 FOR/ REV (Mlu/Cla)	Elke Maier
pLAS::pPIIE_ngo-MIP	Ng-MIP amplified with Ng-MIP F/ R from gDNA N2009 (PacI/FseI)	this study
pET15b	protein expression vector with 6xHis and thrombin cleavage site	Merck Millipore
pcDNA3-GFP	cloning vector with GFP sequence (EcoRI/BamHI)	Vera Kozjak-Pavlovic
pLVTHM	shRNA expression vector; Addgene plasmid 12247	Wiznerowicz and Trono, 2003
pLAS::pPIIE mCherry	complementation vector for <i>N. gonorrhoeae</i> with NGFG_01468 and NGFG_01471 sequences	Prof. Dr. Berenike Maier
psPAX	viral packaging vector; Addgene plasmid 12260	Wiznerowicz and Trono, 2003
pCMV-VSV-G	viral envelope vector; Addgene plasmid 8454	Stewart et al., 2003

2.1.4 Oligonucleotides

Table 2.5: Oligonucleotides for performance of polymerase chain reaction (PCR)

Name	Sequence (5' → 3')	Comment
SRECI Ex. Dom. F	CTCGCAAGCTTATGGGGCTGGGG	extracellular domain of SRECI; HindIII site
SRECI Ex. Dom. R	CTGCTGGATCCAGTGTCCTCGACT	extracellular domain of SRECI; BamHI site
Ng-MIP F	CTCGCTTAATTAACCGCGTCCGGAAATCA	<i>N. gonorrhoeae mip</i> ; PacI site
Ng-MIP R	CTGCTGGCCGCAAGCCATGCCGTCTGA	<i>N. gonorrhoeae mip</i> ; FseI site
Ng-MIP-pET15b F	CTCGCCATATGAAGAATATATTA	<i>N. gonorrhoeae mip</i> without signal peptide; NdeI site
Ng-MIP-pET15b R	CTGCTGGATCCCTATTCTGTAAC	<i>N. gonorrhoeae mip</i> ; BamHI site
Ctr-Mip F	CTCGCCATATGAAGAATATATTA	<i>C. trachomatis mip</i> without signal peptide; NdeI site
Ctr-Mip R	CTGCTGGATCCCTATTCTGTAAC	<i>C. trachomatis mip</i> ; BamHI site

PorB _{IA} _pET15b NdeI F	CTCGCCATATGGACGTTACCCTGTACG	<i>N. gonorrhoeae porB_{IA}</i> without signal peptide; NdeI
PorB _{IA} _pET15b BamHI R	CTGCTGGATCCTTAGAATTTGTGGCGC	<i>N. gonorrhoeae porB_{IA}</i> ; NdeI
PorB _{IB} _pET15b NdeI F	CTCGCCATATGGATGTCACCCTG	<i>N. gonorrhoeae porB_{IB}</i> without signal peptide; NdeI
PorB _{IB} _pET15b BamHI R	CTGCTGGATCCGAATTTGTGGCGC	<i>N. gonorrhoeae porB_{IB}</i> ; NdeI

Table 2.6: Oligonucleotides for construction of gene mutants

Name	Sequence (5' → 3')	Comment
Ng-MIP UP F	GCCGTCTGAAAGCCGGCAACGCGGCAACCT	500 bp upstream of <i>N. gonorrhoeae mip</i>
Ng-MIP UP R	TGAGACACAATTCATCGATGATGTCCGAATC CATGCCCGAAA	500 bp upstream of <i>N. gonorrhoeae mip</i>
Ng-MIP Down F	TGCAGGCATGCAAGCTTCAGGATGGATCTTC GCTGTCGAT	500 bp downstream of <i>N. gonorrhoeae mip</i>
Ng-MIP Down R	CATGCCGTCTGACACATCCG	500 bp downstream of <i>N. gonorrhoeae mip</i>
Kan F	ATCATCGATGAATTGTGTCTCAAATCTCTG AT	kanamycin resistance cassette
Kan R	CTGAAGCTTGCATGCCTGCA	kanamycin resistance cassette
13_pET15b Fwd	TATGCGACTCCTGCATTAGGAA	sequence in pET15b
14_DiDom Rev	GCTTTAGCCTGCTG GCCCTGCGCGGCAGAA	<i>mip</i> without dimerization domain
15_DiDom Fwd	GCCGCGCAGGGCCAGCAGGCTAAAGCCGTA GA	<i>mip</i> without dimerization domain
16_MIP NdeI Fwd	CTCGCCATATG GGCAAAAAGAAGCCGCC	<i>mip</i> without dimerization domain; NdeI
17_MIP BamHI_Rev	CTGCTGGATCCATTTACTTTTTTGATGTCGAC TTGATC	<i>mip</i> ; BamHI
18_MIP D-L 165 Rev	TTTGCTGCTTAGGAATACGGTAC	D165→L165 (<i>gac</i> → <i>gcc</i>)
19_MIP D-L 165 Fwd	ACCGTATTCCTAAGCAGCAAA	D165→L165 (<i>gac</i> → <i>gcc</i>)
20_MIP Y-A 208 Rev	TGTTTCGCGGGCGGCAAGGTT	Y208→A208 (<i>tac</i> → <i>aga</i>)
21_MIP Y-A 208 Fwd	AACCTTGCCGCCCGCGAACA	Y208→A208 (<i>tac</i> → <i>aga</i>)
22_pET15b Rev	TTTCATGTTTGACAGCTTATCATCGATAAGC	sequence in pET15b
PorB _{IA} -FLAG loop1 F	AAGGATGACGACGATAAGGCTCAGGCGGAT CG	G41-DYKDDDDK-A42 in <i>porB_{IA}</i>
PorB _{IA} -FLAG loop1 R	TATCGTCGTCATCCTTGTAATCTCCATGGTGA GCTA	G41-DYKDDDDK-A42 in <i>porB_{IA}</i>
PorB _{IB} -FLAG loop1 R	TATCGTCGTCATCCTTGTAATCGTCTGTATGT TCTA	D41- DYKDDDDK -G42 in <i>porB_{IB}</i>

PorB _{IB} -FLAG loop1 F	ACAAGGATGACGACGATAAGGGCAAGGTA AGTAA	D41- DYKDDDDK -G42 in <i>porB_{IB}</i>
FJB4	GCTTGCCGTCTGAATTACGCCCCGCCCTGCC ACTCATGC	<i>catGC</i>
ISO3	GCTTGCCGTCTGAATTACGCCCCGCCCTGCC ACTCATGC	<i>ErmC</i>

Table 2.7: Oligonucleotides for qRT-PCR

Name	Sequence (5' → 3')	Comment
MIP Comp RT-PCR F	GATTTTGTACTGCAGACCG	sequence in <i>mip</i>
MIP Comp RT-PCR R	GGCTAAAGCCGTAGAAAAA	sequence in <i>mip</i>
5S F	CGGCCATAGCGAGTTGGT	sequence in 5S
5S R	TTGGCAGTGACCTACTTTCG	sequence in 5S

Table 2.8: Oligonucleotides for shRNAs

Name	Sequence (5' → 3')	Comment
ATP5B-1 FOR	CGCGTCCCCGCAGAATCATGAATGTCATTGTTCAAG AGACAATGACATTCATGATTCTGCTTTTTGGAAAT	shRNA F1β 1
ATP5B-1 REV	CGATTTCCAAAAAGCAGAATCATGAATGTCATTGTC TCTTGAACAATGACATTCATGATTCTGCGGGGA	shRNA F1β 1
ATP5B-2 FOR	CGCGTCCCCGGTTTCAGAGGTGTCTGCATTATTCAAG AGATAATGCAGACACCTCTGAACCTTTTTGGAAAT	shRNA F1β 2
ATP5B-2 REV	CGATTTCCAAAAAGTTTCAGAGGTGTCTGCATTATC TCTTGAATAATGCAGACACCTCTGAACCGGGGA	shRNA F1β 2

2.1.5 Antibodies

Table 2.9: Primary antibodies for western blot (WB) and immunofluorescence staining (IF)

Antibody	Origin	Dilution	Source
<i>N. gonorrhoeae</i>	rabbit polyclonal	IF 1:500	US Biological N0600-02
cHSP60	mouse monoclonal	IF 1:300, WB 1:1 000	Santa Cruz
SREC-I	rabbit polyclonal	WB 1:1 000	Santa Cruz
Omp85	rabbit polyclonal	IF 1:250, WB 1:1 000	Davids Biotechnology (self-made)
PorB _{IA}	rabbit polyclonal	IF 1:100, WB 1:1 000	Davids Biotechnology (self-made)
PorB _{IB}	rabbit polyclonal	IF 1:100, WB 1:1 000	Davids Biotechnology (self-made)
PorB _{IB} peptide	rabbit polyclonal	IF 1:100, WB 1:1 000	Davids Biotechnology (self-made)

OmpA	rabbit polyclonal	WB 1:1 000	Annette Fischer (self-made)
β -actin	mouse monoclonal	WB 1:5 000	Sigma-Aldrich
β -tubulin	rabbit polyclonal	WB 1:1 000	Santa Cruz
α -tubulin	mouse monoclonal	WB 1:1 000	Santa Cruz
ICDH	rabbit polyclonal	WB 1:500	Biogenesis 0200-0498
SDHA	mouse monoclonal	WB 1:200	Invitrogen
F1 α	mouse monoclonal	WB 1:10 000	BD Biosciences
6xHIS	mouse monoclonal	WB 1:1 000	GeneTex GTX18184
FLAG	rabbit polyclonal	WB 1:1 000	Sigma-Aldrich
Glutaminase	Rabbit monoclonal	WB 1:10 000	Abcam
GFP	mouse monoclonal	WB 1:500	Santa Cruz
Biotin	goat HRP-linked	WB 1:1 000	Cell signaling technology

Table 2.10: Secondary antibodies

Antibody	Origin	Dilution	Source
ECL TM anti-mouse IgG HRP linked	goat	WB 1:3 000	Santa Cruz sc2005
ECL TM anti-rabbit IgG HRP linked	goat	WB 1:3 000	Santa Cruz sc2005
Anti-rabbit IgG Cy2 TM -linked	goat	IF 1:100	Dianova
Anti-rabbit IgG Cy5 TM -linked	goat	IF 1:100	Dianova
Anti-mouse IgG Cy5 TM -linked	goat	IF 1:100	Dianova

2.1.6 Kits

Table 2.11: Kits used in this study

Kit	Manufacturer
GeneJET TM Gel Extraction Kit	Thermo Scientific
Wizard [®] SV Gel and PCR Clean-Up System	Promega
PureYield TM Plasmid Midiprep System	Promega
AxyPrep TM Plasmid Miniprep Kit	Axygen
RNeasy [®] Mini Kit	Qiagen
RevertAid First Strand cDNA Synthesis Kit	Thermo Scientific
Luminescent ATP Detection Assay Kit	Abcam

2.1.7 Buffers, solutions and media

Table 2.12: Media and solutions for cell culture

Medium/ Chemicals	Manufacturer/ ingredients
RPMI 1640	GIBCO
RPMI 1640, no glucose	GIBCO
SILAC RPMI 1640 Flex Medium, no glucose, no phenol red	GIBCO
CHO Medium	GIBCO
DMEM	Sigma-Aldrich
DPBS	GIBCO
TrypLETM Express	GIBCO
Fetal calf serum (FCS)	PAA
Fetal calf serum (FCS) dialysed 10 kDa	Sigma-Aldrich
Cell stocking medium	FCS, 10 % dimethyl sulfoxide (DMSO) (v/v)
XF Base medium	Seahorse Bioscience
2 x HBS	50 mM Hepes pH 7.05, 140 mM NaCl, 1.5 mM Na ₂ HPO ₄
Chloroquine	25 mM in PBS

Table 2.13: Bacterial culture media and buffers

Medium/Buffer	Ingredients
Lysogeny broth (LB) medium	10 g/l tryptone, 5 g/l yeast extract, 10 g/l NaCl
LB agar	11 g/l tryptone, 5 g/l yeast extract, 10 g/l NaCl, 15 g agar
TSB medium	27.5 g/l Tryptone Soya Broth, 5 ml 50 % glucose (w/v)
TSB agar	30 g/l Tryptone Soya Broth, 15 g/l agar
GC agar	36.23 g/l GC Agar base (Oxoid), after autoclaving 1 % vitamin mix is added
SPG buffer	0.22 M sucrose, 10 mM Na ₂ HPO ₄ , 3.8 mM K ₂ HPO ₄ , 5 mM glutamate, pH 7.4
Proteose peptone (PPM) medium	15 g/l proteose peptone, 5 g/l NaCl, 0.5 g/l soluble starch, 1 g/l KH ₂ PO ₄ , 4 g/l KH ₂ PO ₄ . Adjust to pH 7.2 and sterilize by sterile filtration. Add 1 % vitamin mix and 0.5 % NaHCO ₃ directly before experiments.
Vitamin mix	combine vitamin mix Solution I and II (add dH ₂ O up to 2 l)
Vitamin mix solution I	200 g D(+)-glucose, 20 g L-glutamine, 0.026 g 4-aminobenzoic acid, 0.2 g cocarboxylase, 0.04 g iron(III) nitrate nonahydrate,

	0.006 g thiamine hydrochloride (vitamin B1), 0.5 g NAD, 0.02 g vitamin B12, 52 g L-cysteine hydrochloride monohydrate; add 1 l dH ₂ O
Vitamin mix solution II	2.2 g L-cystine, 0.3 g L-arginine monohydrochloride, 1 g uracil, 0.06 g guanine-hydrochloride, 2 g adenine hemisulfate, add 600 ml dH ₂ O, 30 ml 32 % HCl
HEPES medium (phosphate free medium)	50 ml solution I, 10 ml solution II, 200 µl solution III, 3 ml solution IV/V, 5 ml solution VI, 50 ml solution VII, 50 ml solution VIII, in dH ₂ O up to 500 ml, pH 7.3, sterilize by filtration
HEPES-solution I	0.1 % (w/v) L-alanine, 0.15 % (w/v) L-arginine, 0.025 % (w/v), L-asparagine, 0.025 % (w/v) glycine, 0.018 % (w/v) L-histidine, 0.05 % (w/v) L-lysine, 0.015 % (w/v) L-methionine, 0.05 % (w/v) proline, 0.05 % (w/v) L-serine, 0.05 % (w/v) L-threonine, 0.061 % (w/v) L-cysteine, 0.036 % (w/v) L-cystine, 0.05 % (w/v) L-glutamine, 0.046 % (w/v) GSH, 0.0032 % (w/v) hypoxanthine, 0.008 % (w/v) uracil, 0.004 % (w/v) D-biotin, in 18 % 1 N NaOH and 82 % ddH ₂ O, pH 7.2
HEPES-solution II	37.5 % (w/v) glucose
HEPES-solution III	1 % (w/v) Fe(NO ₃) ₃ ·9H ₂ O
HEPES-solution IV/V	0.33 % (w/v) NAD, 0.33 % (w/v) cocarboxylase, 0.33 % (w/v) thiamine, 0.33 % (w/v) calcium pantothenate, 0.188 % (w/v) CaCl ₂ ·2H ₂ O, 4.17 % (w/v) sodium lactate, 15.33 % (w/v) glycerol, 3.33 % (w/v) oxaloacetate
HEPES solution VI	5 % (w/v) MgCl ₂ ·7H ₂ O
HEPES solution VII	5 % (w/v) NaCl, 3.4 % (w/v) sodium acetate
HEPES solution VIII	2.38 % (w/v) Hepes
Stocking solution <i>E. coli</i>	50 % glycerol, 2.9 % NaCl
Stocking solution <i>N. gonorrhoeae</i>	25 % glycerol, 75 % PPM medium
<i>N. gonorrhoeae</i> transformation medium	PPM medium, 1 % vitamin mix, 10 mM MgCl ₂ , 0.5 % (v/v) NaHCO ₃
Buffer I for neisserial genomic DNA isolation	50 mM glucose, 25 mM Tris/HCl pH 8.0, 10 mM ethylenediaminetetraacetic acid (EDTA)

Table 2.14: Buffers for agarose gel electrophoresis, SDS-PAGE and WB

Buffer	Ingredients
1 x TAE buffer	2 M Tris, 0.05 M EDTA, 1 M acetic acid (pH 8.5)
2 x Laemmli buffer	4 % SDS, 20 % glycerol, 120 mM Tris pH 6.8, 0.4 - 2 % β-mercaptoethanol, 0.02 g bromphenolblue
12.5 % SDS gel solution	6.9 ml Acrylamid/bis (30/0.8), 3.5 ml 1.875 M Tris pH 8.8, 0.1 % (w/v) SDS, 6.3 ml dH ₂ O, 100 µl 10 % (w/v) ammonium persulfate (APS), 10 µl tetramethylethylenediamine (TEMED)

SDS stacking gel solution	0.83 ml Acrylamid/bis (30/0.8), 0.5 ml 0.8 M Tris pH 6.8, 50 µl 10 % (w/v) SDS, 3.55 ml dH ₂ O, 50 µl 10 % (w/v) APS, 10 µl TEMED
SDS running buffer	25 mM Tris, 0.191 M glycine, 1 % (w/v) SDS
Coomassie staining solution	40 % ethanol, 7 % acetic acid, 0.2 % (w/v) coomassie R-250
Coomassie destaining solution	30 % ethanol, 10 % acetic acid
Colloidal fixation solution	7 % acetic acid, 40 % methanol
Colloidal staining solution A	2.375 % phosphoric acid, 10 % (w/v) ammonium sulfate
Colloidal staining solution B	5 % (w/v) coomassie G-250
Colloidal neutralization solution	1.2 % (w/v) Tris, pH 6.5 adjust with phosphoric acid
Colloidal washing solution	25 % methanol
10 x (tris buffered saline) TBS buffer	1.5 M NaCl, 200 mM Tris/HCl, pH 7.5
10 x transfer buffer	20 mM Tris, 150 mM glycine, 0.02 % SDS; for 1 x transfer buffer add 20 % methanol
Blocking buffer for WB	1 x TBS, 5 % non-fatty milk powder
TBS-T	1 x TBS, 0.2 % Tween-20
ECL solution 1	2.5 mM Luminol, 0.4 mM p-coumaric acid
ECL solution 2	100 mM Tris/HCl pH 8.5, 0.02 % H ₂ O ₂

Table 2.15: Buffers for IF and transmission electron microscopy (TEM)

Buffer	Ingredients
Blocking solution for IF	1 x PBS, 1 % (w/v) bovine serum albumin (BSA) (for <i>N. gonorrhoeae</i> staining) 1 x PBS, 2 % (v/v) FCS (for <i>C. trachomatis</i> staining)
Permeabilization solution	1 x PBS, 0.1 % or 0.2 % (v/v) Triton X-100
Mowiol	35 g glycerol, 12 g Mowiol, 30 ml dH ₂ O, 60 ml 0.2 M Tris/HCl pH 8.5
TEM solution	2.5 % glutaraldehyde, 50 mM KCl, 50 mM cacodylate (pH 7.2)

Table 2.16: Buffers for analysis of protein-protein interactions

Buffer	Ingredients
IP (immunoprecipitation) buffer I	10 mM NaCl, 10 mM NaH ₂ PO ₄ , 1 mM EDTA, 0.5 % glycerol, 1 % NP-40, 1.5 % BSA, pH 7.6
IP buffer II	10 mM Tris/HCl, 200 mM NaCl, 0.5 mM EDTA, 0.5 % glycerol, 1 % NP-40, pH 7.6
PD (pull-down) lysis buffer	20 mM Hepes pH 7.4, 150 mM NaCl, 1 % Triton, 0.5 mM EDTA, 1 x protease inhibitor

PD wash buffer	20 mM Hepes pH 7.4, 150 mM NaCl, 0.5 mM EDTA, 1 x protease inhibitor
PD elution buffer	0.1 M glycine pH 3.5
SPR buffer	10 mM Hepes (pH 7.4), 150 mM NaCl, 3.4 mM EDTA, 0.005 % Tween-20 and 0.01 % Zwittergent

Table 2.17: Buffers for protein purification

Buffer	Ingredients
Buffer A _Q (Source Q)	20 mM Tris/HCl, pH 7.5, 10 mM EDTA, 0.05 % Zwittergent, 0.01 % Na-Azide, pH 8.6
Buffer B _Q	Buffer A _Q supplemented with 1 M NaCl
Buffer A _S (Source S)	50 mM MES, pH 6.1, 0.05 % Zwittergent, 0.01 % Na-Azide, pH 6
Buffer B _S	Buffer A _S supplemented with 1 M NaCl
Buffer A _G (Source G)	20 mM Tris, pH 7.5, 200 mM NaCl, 0.05 % Zwittergent, 0.01 % Na-Azide
NC (native condition) lysis buffer	50 mM NaH ₂ PO ₄ , 300 mM NaCl, 10 mM imidazole, pH 8
NC wash buffer	50 mM NaH ₂ PO ₄ , 300 mM NaCl, 20 mM imidazole, pH 8
NC elution buffer	50 mM NaH ₂ PO ₄ , 300 mM NaCl, 250 mM imidazole, pH 6
TC (thrombin cleavage) wash buffer 1	150 mM NaH ₂ PO ₄ , 300 mM NaCl, 10 % glycerol, pH 7.6
TC wash buffer 2	20 mM Imidazole, 400 mM NaCl, 10 % glycerol, pH 7.6
TC wash buffer 3	40 mM imidazole, 500 mM NaCl, 10 % glycerol, pH 7,6
Thrombin wash buffer	20 mM Tris/HCl, 200 mM NaCl, pH 7.5
Thrombin buffer	1.5 M Tris/HCl, 1.5 M NaCl, 25 mM CaCl ₂ , pH 8.4
Buffer MIP_A _Q	50 mM Tris/HCl, 10 mM EDTA, 0.01 % Na-Azid, pH 8.5
Buffer MIP_B _Q	50 mM Tris/HCl, 10 mM EDTA, 1M NaCl, 0.01 % Na-Azid, pH 7.5
Buffer MIP_A _G	20 mM Hepes, 200 mM NaCl, 0.01 % Na-Azid, pH 7.5
DC (denaturing condition) binding buffer	20 mM Tris/HCl, 8 M Urea, 500 mM NaCl, 5 mM imidazole, pH 7.4
DC elution buffer	20 mM Tris/HCl, 8 M Urea, 500 mM NaCl, 500 mM imidazole, pH 7.4
Carbonate Buffer	20 mM Na ₂ CO ₃ , 180 mM NaHCO ₃ , in H ₂ O pH 9

Table 2.18: Buffers for experiments with isolated mitochondria and bacterial membrane vesicles

Buffer	Ingredients
1 x phosphate buffered saline (PBS)	137 mM NaCl, 2.7 mM KCl, 8 mM Na ₂ HPO ₄ , 1.5 mM KH ₂ PO ₄
Solution A	buffer B containing 2 mg/ml BSA
Solution B	20 mM Hepes pH 7.6, 220 mM mannitol, 70 mM sucrose, 1 mM EDTA, 0.5 mM phenylmethylsulfonyl fluoride (PMSF)
Solution C	buffer B containing 5 mM MgCl ₂ , 2 mM glutathione, 1 mM Na-succinate, 10 mM K ₂ HPO ₄
Lysis buffer for isolation of bacterial membrane vesicles	50 mM MOPS, 15 mM MgCl ₂ , 1 x protease inhibitors and 5 µg/ml DNaseI

Table 2.19: Annealing buffer for shRNA oligonucleotides

Buffer	Ingredients
Annealing buffer	100 mM K-acetate, 30 mM Hepes KOH pH 7.4, 2 mM Mg-acetate

2.1.8 Chemicals

Table 2.20: Antibiotics

Antibiotic	Comment
Penicillin/Streptomycin	supplemented in cell culture media
Ampicilin	100 µg/ml for <i>E. coli</i> selection
Erythromycin	7 µg/ml for <i>N. gonorrhoeae</i> selection
Kanamycin	40 µg/ml for <i>N. gonorrhoeae</i> selection
Spectinomycin	100 µg/ml for <i>N. gonorrhoeae</i> selection
Anhydrotetracycline (AHT)	induction of shRNA knockdown cell lines

Table 2.21: Enzymes

Enzymes	Manufacturer
Restriction enzymes	Thermo Scientific and New England BioLabs (NEB)
iProof™ High-Fidelity DNA Polymerase	BIO-RAD
Phusion High-Fidelity DNA polymerase	Thermo Scientific
Taq DNA polymerase	Genaxxon Bioscience
MolTaq DNA polymerase	Molzym
T4 DNA ligase	Fermentas

FastAP Thermosensitive Alkaline Phosphatase	Thermo Scientific
Dnase I	Thermo Scientific
Rnase A	Thermo Scientific

Table 2.22: DNA and protein markers

Size standard	Application	Manufacturer
GeneRuler™ 1 kb DNA ladder	DNA agarose gels	Thermo Scientific
PageRuler™ Prestained Protein Ladder	Protein PAGE	Thermo Scientific

Table 2.23: Fine chemicals

Chemicals	Manufacturer
(±)-6-hydroxy-2,5,7,8-tetramethylchromane-2-carboxylic acid (Trolox)	Sigma-Aldrich
6-hydroxy-2,5,7,8-tetramethylchroman-2-carboxylic acid (FCCP)	Sigma-Aldrich
Acrylamid Rotiphorese Gel 30 (37.5:1)	Roth
Adenosine diphosphate (ADP)	Sigma-Aldrich
Albumin Fraktion V (BSA)	Roth
Alexa Fluor 555 phalloidin	Invitrogen
Alexa Fluor 647 phalloidin	Invitrogen
Ammonium persulfate (APS)	Merck
ANTI-FLAG® M2 Affinity Gel	Sigma-Aldrich
Antimycin	Sigma-Aldrich
Bacto™ Proteose Peptone No. 3	BD
BioSensor Chip CM5	GE Healthcare
carbonyl cyanide m-chloro phenyl hydrazone (CCCP)	Sigma-Aldrich
CnBr-Sepharose beads	GE Healthcare
Coomassie G250	Roth
Coomassie R250	Roth
Digitonin	Sigma-Aldrich
dimethyl sulfoxide (DMSO)	Roth
Dynabeads® Protein G	Invitrogen
EZ-Link™ NHS-LC-Biotin	Thermo Scientific
Intas HD Green	Intas
Isopropyl-β-D-thiogalactopyranosid (IPTG)	Roth

Loading dye 6 x	Thermo Scientific
Lysostaphin	AMBI Products LLC
Mouse IgG2B Isotype Control	R&D Systems
Na-succinate	Fluka Analytica
Ni-NTA agarose	Qiagen
Oligomycin	Merck Milipore
PerfeCTa® SYBR® Green FastMix™, ROX	Quantabio
phenylmethanesulfonyl fluoride (PMSF)	Roth
Paraformaldehyde (PFA)	Morphisto
Protease inhibitor	Merck Milipore
Rapamycin	Alfa Aesar
Recombinant Human SREC-I/SCARF1 Fc Chimera	R&D Systems
Restore Plus Western Blot Stripping buffer	Thermo Scientific
Roti®Phenol/Chloroform/Isoamylalcohol (pH 7.5-8)	Roth
Rotinone	Sigma-Aldrich
Saponin	Sigma-Aldrich
SNARF®	Invitrogen
Soluble starch	Riedel-deHaen
tetramethylethylenediamine (TEMED)	Fluka Analytica
Tetramethylrhodamine, methyl ester (TMRM)	Sigma-Aldrich
Thrombin	Sigma-Aldrich
Trichloroacetic acid (TCA)	Roth
Zwittergent® 3-14 Detergent	Calbiochem

All other chemicals were obtained from Roth, Sigma-Aldrich, Serva or Merck Chemicals if not stated otherwise.

2.1.9 Technical equipment

Table 2.24: Technical equipment

Equipment	Manufacturer
2720 Thermal Cycler	Applied Biosciences
Advanced TC™ 96-well cell culture microplates	Greiner bio-one
Äkta pure	GE healthcare life science
Amicon® Ultra Centrifugal Filters	Merck Millipore

Anion exchanger column (Source Q)	GE Healthcare
Autoclave	WEBECO, Sytec VX 150
Avanti™ J-25T centrifuge	Beckham Coulter
Binocular SMZ-168	Motic
C6 Flow Cytometer	Accuri
Cation exchanger column (Source S)	GE Healthcare
Chemiluminescence camera system	Intas
Cold centrifuge 5417R	Eppendorf
Desalting column	Amersham Pharmacia Biotech AB
DMIL light microscope	Leica
FACSaria III	BD
Gel filtration column	GE Healthcare
Hera Cell 240i incubator	Thermo
Hera Safe sterile hood	Thermo
HisTrap HP column	GE Healthcare
Hoefer SE 600 Chroma™ gel system	Hoefer
ImageScanner III Labscan™ 6.0	GE Healthcare
Labtherm ET1311	Liebisch
Megafuge 1.0R	Heraeus
Mikro 200	Hettich Zentrifugen
Mini Rocker-Shaker MR-1	Biosan
NanoDrop 1000 spectrophotometer	Peqlab Biotechnology
Operetta LCS™	Perkin Elmer
Optima™ L-80-XP Ultracentrifuge	Beckman Coulter
Optima™ Max-XP ultracentrifuge	Beckham Coulter
PerfectBLue™ Semi-Dry Elektrobloetter	Peqlab Biotechnology
pH electrode SenTix	WTW series inolab
Plate reader infinite 200	Tecan
Power Pac 300	Biorad
ProteOn™ XPR36 Protein Interaction Array System	Bio Rad
RW16 basic drill-fitted Dounce homogenizer	IKA Labortechnik
Seahorse Bioscience XF ^e 96 Extracellular Flux Analyzer	Seahorse Bioscience
S-MONOVETTE®	Sarstedt
Sonifier	Branson VWR
Spectrophotometer Ultrospec 3100 pro	Amersham Bioscience
Step One Plus real-time PCR system	Applied Biosystems
T18 digital ULTRA TURRAX®	IKA Labortechnik
TCS SPE confocal microscope	Leica

Thermo mixer comfort	Eppendorf
Transmissionelectronmicroscope (EM900)	Carl Zeiss
Vortex Genie 2	Bender & Hobein AG

2.1.10 Software

Table 2.25: Applied software

Software	Manufacturer
Argus x1 version 7.6.17	Biostep® GmbH
ClustalW2	http://www.ebi.ac.uk/Tools/psa/
Coral Draw X7	Corel Corporation
EndNoteX7	Thomson Reuters
ExpASy – Translate Tool	http://www.expasy.org/
Harmony® High Content Imaging and Analysis Software	Perkin Elmer
Image J	W. Rasnband, National Institutes of Health
ImageScanner III Labscan™ 6.0	GE Healthcare
LabImage Chemostar	Intas, Science imaging
Leica LAS AF confocal microscopy software	Leica Microsystems
NCBI blast	http://blast.ncbi.nlm.nih.gov
ND-100 V3.7.1	NanoDrop Technologies, Inc. Wilmington
Office 2010	Microsoft
ProteOn™ Manager Software	Bio Rad
Serial Cloner 2.5	Franck Perez Serial Basics
StepOne Software v.2.3	Life Technologies
Tecan i-Control	Tecan
Unicorn 6.0	GE Healthcare
Wave 2.2.0276	Seahorse Bioscience, Inc.

2.2 Methods

2.2.1 DNA methods

Polymerase chain reaction (PCR)

PCR was applied to amplify DNA sequences from genomic or chromosomal DNA. A standard PCR required 100 to 500 ng of template DNA, 0.5 µl of forward and reverse primers (100 mM), 0.5 µl dNTPs (100 mM), 2 µl MgCl₂, 10 µl 5 x iProof™ buffer, 0.5 µl iProof™ polymerase and dH₂O to fill up to a total volume of 50 µl. The reaction was performed in a thermocycler with the following program: initial denaturation 10 sec at 98 °C, 30 cycles of 10 sec denaturation at 98 °C, annealing for 10 sec at 50 °C to 60 °C (depended on the melting temperatures of the oligonucleotides), elongation at 72 °C for 30 sec per 1 kb and a final elongation at 72 °C lasting 5 min. The PCR was cooled down to 4 °C, 5 µl of the reaction were mixed with 2 µl of 6 x loading dye and 5 µl dH₂O. The DNA was separated by a 1.5 % agarose gel (in TAE buffer) containing Intas HD Green applying 160 V for 35 min.

An overlap extension PCR was used to fuse two PCR fragments, which contained complementary overhangs. 25 - 100 ng of the smaller fragment were used in one reaction. The volume of the larger fragment was calculated according to the following formula:

$$\frac{\text{concentration (ng/}\mu\text{l)} \times \text{volume (}\mu\text{l)}}{\text{length (bp)}}_{\text{(of smaller fragment)}} = \frac{\text{concentration (ng/}\mu\text{l)} \times \text{volume (}\mu\text{l)}}{\text{length (bp)}}_{\text{(of larger fragment)}}$$

The fragments were added to a mixture of 4 µl 5 x HF buffer, 0.4 µl dNTPs (100 mM), 0.1 µl Taq DNA polymerase, 0.2 µl of Phusion High-Fidelity DNA polymerase and filled up to 20 µl dH₂O. The PCR program contained 98 °C for 30 sec, ten cycles of 98 °C 10 sec, 50 - 60 °C for 20 sec, 72 °C for 20 sec per kb and finally before cooling down to 4 °C a 72 °C step for 10 sec.

Furthermore, 6 µl 5 x HF buffer, 0.6 µl of dNTPs, 1 µl of forward and reverse primers (100 mM), 0.1 µl Taq DNA polymerase, 0.3 µl of Phusion High-Fidelity DNA polymerase and 21 µl dH₂O were added to the 20 µl sample. The following thermocycler program was applied: 98 °C for 30 sec, 25 cycles of 98 °C 10 sec, 50 - 60 °C for 20 sec, 50 sec per kb at 72 °C and a final elongation for 10 sec at 72 °C.

Cloning of PCR fragment into vector

The PCR sample was purified by GeneJet™ Gel Extraction Kit to remove salts, primers, enzymes and buffers. This step was applied after performing PCR or a DNA restriction. The PCR was separated on a 1.5 % agarose gel to cut out the PCR fragment of interest under UV light. Wizard® SV Gel and PCR Clean-Up System were used to extract the DNA from the agarose gel.

Furthermore, the PCR fragment and the cloning vector were cut using appropriate restriction enzymes and buffers. In the case of two different enzymes with incompatible buffers the restriction was performed in series with a PCR purification step in between. The vector was dephosphorylated after restriction using FastAP Thermosensitive Alkaline Phosphatase.

Ligation of insert in vector

The ligation of the cut insert and the vector was performed using T4 DNA ligase and T4 ligase buffer. The insert to vector ratio was 4:1 in a total volume of 15 µl. The ligation mixture was incubated overnight at 16 °C and transformed into chemo-competent *E. coli* DH5α.

Colony PCR

The screening for bacterial colonies, which express the transformed plasmid, was done by colony PCR. Therefore, bacterial material from five colonies was transferred in 50 µl dH₂O and streaked at the same time on a replica plate. The PCR master mix contained 0.5 µl of forward and reverse primers (100 mM), 0.5 µl dNTPs (100 mM), 1 µl Enhancer, 5 µl 10x PCR Buffer, 0.5 µl MolTaq polymerase and dH₂O to fill up to a total volume of 50 µl. The bacterial suspension was heated for 10 min at 95 °C and centrifuged for 2 min at 10 000 rpm. 5 µl of the supernatant were added to the master mix. The PCR program started with an initial denaturation at 94 °C for 5 min. The following 30 cycles contained 30 sec at 94 °C, 30 sec at 50 °C and 45 sec per 1 kb at 72 °C. After the final elongation step at 72 °C for 5 min the PCR was cooled down to 4 °C.

Quantitative real-time PCR (qRT-PCR)

In order to analyse the expression rate of a neisserial gene, qRT PCR was applied. Therefore, 3 ml PPM medium were inoculated at OD₅₅₀ 0.1 and was shaken at 37 °C until the culture

reached an OD₅₅₀ of 0.6. The bacteria were centrifuged at 5 000 x g for 5 min and the pellet was resuspended in 700 µl QIAzol Lysis Reagent (RNeasy® Mini Kit). After incubation for 5 min at room temperature (RT) 140 µl chloroform were added and shaken vigorously for 15 sec. The samples were incubated for 3 min at RT and centrifuged at 12 000 x g for 15 min at 4 °C. The upper phase was transferred in a new tube and 1.5 volume of 100 % ethanol were added. The probe was loaded on an RNeasy MinElute spin column and centrifuged at 8 000 x g for 15 sec. Further on, the DNase digest was performed on the column. The column membrane was washed with 350 µl RWT buffer (15 sec at 8 000 x g). 10 µl DNase I and buffer RDD were mixed and incubated on the membrane for 15 min at RT. Afterward, the column was washed with 350 µl RW1, 700 µl RWT, 500 µl RPE and 500 µl 80 % ethanol. In the last step, the column was centrifuged for 2 min at 8 000 x g and further for 5 min at 15 000 x g. The RNA was eluted with 14 µl of RNase-free water for 1 min at 15 000 x g.

The preparation of first strand cDNA was done according to the manufacturer's instruction from RevertAid First Strand cDNA synthesis Kit. Briefly, 1 µg of the isolated RNA was mixed with 1 µl Random Hexamer Primer in a total volume of 12 µl. In a separated tube 4 µl 5 x RT Buffer, 1 µl RiboLock RNase Inhibitor, 2 µl dNTPs (10 mM) and 1 µl RevertAid Reverse Transcriptase were mixed. Then, both solutions were mixed and incubated in a thermocycler at following temperatures: 25 °C for 5 min, 42 °C for 40 min, 10 min at 50 °C, 10 min at 60 °C and finally, 70 °C for 5 min. The synthesized cDNA was stored at - 80 °C.

The performance of the qRT-PCR was done using SYBR Green Fast Mix. Therefore, 10 µl of SYBR Green were mixed with 1.8 µl of 1:10 diluted primer and 1.4 µl dH₂O. The mix was pipetted in a 96 well PCR plate and 5 µl of the 1:10 diluted cDNA were added. Each sample was done in triplicates. The normalization of the input cDNA was done by analysing the neisserial constitutively expressed 5sRNA for each sample. The plate was centrifuged for 2 min at 1 000 rpm and placed in the StepOne Plus real-time PCR machine. The program was performed as followed: holding stage with one step at 95 °C for 10 min, 40 cycle stage with step one at 95 °C for 15 sec and step two at 60 °C for 1 min and a melt curve stage with step one for 15 sec at 95 °C, step 2 at 60 °C for 10 min and step three at 95 °C for 15 sec. The results were analysed by the StepOne Software.

2.2.2 Gel electrophoresis and western blot

Agarose gel

Agarose gel electrophoresis was applied for separation of DNA fragments. The DNA probes were mixed with 6 x loading dye and separated on a 1.5 % agarose gel supplemented with Intas HD Green (in TAE buffer) at 160 V for 35 min. UV light was used for visualisation of the DNA fragments.

TCA precipitation of proteins

For the precipitation of proteins sodiumdeoxycholate was added to a final concentration of 0.0125 % and TCA to 14.4 %. The proteins were incubated on ice for 30 min and centrifuged for 30 min at 14 000 rpm at 4 °C. The pellet was dried for 5 min at 37 °C and resuspended while shaking for 15 min at 65 °C in an appropriate amount of 2 x Laemmli buffer.

SDS-PAGE

SDS-PAGE was performed in order to separate proteins according to their masses by electrophoresis in a polyacrylamide gel. The samples were denatured with sodium dodecyl sulphate (SDS) containing 2 x Laemmli buffer and by heating at 95 °C for 5 min. The separation was performed on a gel consisting of a stacking gel and 12.5 % SDS gel at 25 mA and 200 V.

Coomassie and colloidal coomassie staining

Coomassie R-250 or colloidal coomassie G-250 were applied for the visualisation of proteins separated by SDS-PAGE. Gels stained with R-250 were incubated for 1 h in coomassie staining solution and were destained with coomassie destaining solution until the bands could be detected. The staining with G-250 required an incubation of the gel for 1 h at RT in coomassie fixation solution. The staining solution was prepared freshly before the staining by mixing 20 ml of the colloidal staining solution B with 800 ml of A under stirring and a subsequent addition of 200 ml methanol. After fixation, the gels were washed with dH₂O and incubated in the staining solution overnight (or for several days). The gels were incubated for 5 min in neutralization solution and washed twice for 15 min with washing

solution. Finally, the gels were incubated in dH₂O for 30 min at 4 °C and scanned with the ImageScanner III Labscan™ 6.0.

Western blot

The transfer of proteins separated by SDS on a polyvinylidene fluoride (PVDF) membrane was done by semi-dry blotting for 2 h at 1 mA/cm². Afterwards the membrane was stained with coomassie to control the transfer success and subsequently destained with destainer solution. The membrane was scanned and destained in methanol until no bands were visible. Non-specific antibody binding regions were blocked with 5 % milk in TBS for 1 h at RT. The membrane was incubated overnight at 4 °C in the first antibody diluted in 3 % BSA/TBS. Furthermore, the membrane was washed three times with TBS-T for 30 min and incubated in the HRP-linked secondary antibody (diluted 1:3 000 in 5 % milk/TBS) for 1 h at RT. The membrane was washed three times with TBS-T and overlaid with a 1:1 mixture of ECL solution 1 and 2. The signal was detected by the Intas LabImage Chemostar system.

Membranes could be reused for the detection of further proteins by removing the first bound antibody with stripping buffer. For this, the membrane was incubated for 10 min in stripping buffer and washed with TBS-T three times for 10 min. The membrane had to be blocked for 1 h in 5 % milk in TBS before applying the next antibody.

2.2.3 Cell culture methods

Cultivation of cell lines

All cell lines were cultured in 75 cm² culture flasks at 37 °C and 5 % CO₂ in medium supplemented with 10 % FCS. The cells were passaged every second day to maintain a confluency of 80 % and were cultivated for six weeks in total. Therefore, the cells were washed with pre-warmed phosphate buffered saline (PBS) and detached from the flask surface by adding 1 ml Trypsin. The flask was incubated for 5 min in 37 °C and 5 % CO₂ and the Trypsin was inactivated with medium containing 10 % FCS. The cells were split in a new cell culture flask or were seeded in well plates to perform experiments on the following day.

Preparation of cell cryostocks

Cells from a 75 cm² culture flask were washed with PBS and detached by using Trypsin. Afterwards, the cells were taken up in 10 ml medium and centrifuged at 800 x g for 5 min. The pellet was resuspended in FCS supplemented with 10 % DMSO and split into three cryo tubes, which were frozen in an isopropanol chamber at - 80 °C. For longer storage duration, the cryostocks were kept in a liquid nitrogen storage container.

In order to revitalize cryostocks, the frozen cells were thawed and taken up in 10 ml warm medium. The cells were centrifuged to remove the containing DMSO for 5 min at 800 rpm. The pellet was resuspended in medium and transferred into a cell culture flask.

Isolation of primary human PMNs

PMNs were isolated from human venous blood by using the Ficoll-Hypaque method. 10 ml heparinized blood were layered on top of 15 ml Ficoll reagent and were centrifuged at 1 000 rpm for 30 min at 20 °C (without brakes). The lower granulocyte layer was mixed 1:3 with 1 % polyvinyl alcohol in 0.85 % saline and kept at RT for 45 min. The upper layer was transferred in a new tube and centrifuged at 1 000 rpm for 5 min. The pellet was resolved in 16 ml H₂O and incubated for 30 sec on RT. Subsequently, 4 ml 5 x PBS were added to the mixture and the neutrophils were collected by centrifugation at 1 000 rpm for 5 min. The neutrophils were resuspended in 1 x Hank's Balanced Salt Solution (HBSS) and stored at RT.

CaPO₄ plasmid transfection of cells

5x10⁵ cells were seeded in a 6 well plate and were supplemented with 2 µl of 25 mM chloroquine before the transfection. 4 µg of a plasmid were mixed with 50 µl of 2.5 M CaCl₂ and 200 µl dH₂O. 250 µl of 2 x HBS were added slowly to the mixture while making bubbles with a pasteur pipette. The solution was incubated for 15 min RT and then added to the cells while shaking the plate. The medium was changed 24 h after transfection.

Generation of stable and inducible knockdown cell lines

The shRNA-mediated knockdown of F1β-subunit of the mitochondrial ATPase was performed by applying the lentiviral based expression system (Wiznerowicz & Trono, 2003). Oligonucleotides containing the shRNA were assembled by oligo annealing. 1 µl sense and oligonucleotide (1 mM) were mixed with 48 µl of annealing buffer and incubated for 4 min at

94 °C. Afterwards, the sample was incubated for 10 min at 70 °C and was further cooled down for 1 h at RT. The construct was cloned with the restriction enzymes ClaI and MluI in the pLVTHM vector. The plasmid contained GFP as a marker.

293T cells were seeded in three 6 well plates and transfected using the method of CaPO₄ plasmid transfection with the plasmid carrying the shRNA (2 µg) and the two viral packaging plasmids pCI-VSVG-G (1 µg) and psPAX (1 µg). The medium was changed after 24 h. The virus particles-containing supernatant was filtered with a 0.45 µm filter 48 h post-transfection. 3 ml of the supernatant were used to infect HeLa KRAB cells grown in a 25 cm² culture flask in the presence of 0.5 µg/ml polybrene. This HeLa cell line encodes the KRAB-tTR repressor, which suppresses the shRNA expression. After 24 h the cells were transferred into a 75 cm² flask. The knockdown was induced with 1 µg/ml AHT for seven days and analysed by western blot.

If the knockdown was successful, flow cytometry was applied to sort for single cell clones. Therefore, the knockdown was induced for maximal two days. Single cells were sorted according to the GFP signal in a 96 well plate in DMEM medium. As soon as the cells achieved a confluency of 80 %, they were transferred in 12 well plates and subsequently in 25 cm² flasks. The knockdown was tested by western blot and one positive clone was used for further experiments.

Cytotoxicity assay

The cytotoxicity assay was applied to determine the concentration of a compound, which is toxic for the cells. Therefore, cells were seeded in 12 well plates and pre-treated for 24 - 48 h with the substance to be tested. The cells were detached by Trypsin and washed once with PBS by centrifugation at 800 x g for 5 min. The cells were resuspended in 500 µl PBS and 1 µl of propidium iodide (PI) was added to stain the apoptotic cells. The analysis was performed at the flow cytometer using the red laser at 561 nm.

Crystal violet staining of cells

Crystal violet staining was applied for the measurement of the cell number, which was subsequently used for normalization purpose. Cells seeded in a 96 well plate were washed with PBS twice and fixed with 75 % EtOH for 10 min at RT. The EtOH was removed and the cells were dried for 15 min. Afterwards, 0.1 % crystal violet (in PBS) was added and

incubated for 30 min. The cells were washed three times with PBS and were dried overnight at RT. 100 µl of 10 % acetic acid were added and incubated for 5 min. 50 µl of the dyed cell were mixed with 150 µl dH₂O in a ELISA microplate and measured at a plate reader (Plate reader Tecan infinite 200) at 550/560 nm.

2.2.4 Bacterial culture techniques

2.2.4.1 *E. coli*

Cultivation and stock preparation

E. coli were grown on LB agar plates or shaken at 190 rpm in LB medium at 37 °C overnight. If selection was required, bacteria were grown on agar plates or in medium supplemented with the appropriate antibiotic.

For preparation of a bacteria stock 0.5 ml of an overnight culture were mixed with 0.5 ml of stocking solution and was frozen at - 80 °C.

Generation of chemo-competent *E. coli* DH5α

100 ml LB medium were inoculated 1:50 with a DH5α overnight culture and were shaken until OD₆₀₀ 0.6. The culture was incubated for 15 min on ice and centrifuged at 4 000 rpm for 10 min at 4 °C. The pellet was resuspended in 20 ml cold 0.1 M CaCl₂ and incubated on ice for 30 min. After another centrifugation step, the pellet was resuspended in 10 ml 0.1 M CaCl₂ and 20 % glycerol.

Transformation of chemo-competent *E. coli* DH5α

100 µl of chemo-competent *E. coli* DH5α were thawed on ice and incubated with 15 µl of the ligation on ice for 30 min. The heat-shock was achieved by incubating the bacteria for 90 sec at 42 °C followed by 2 min on ice. 1 ml of LB medium was added and the bacteria shaken for 45 min at 37 °C. Finally, the bacteria were plated on selective LB agar plates and incubated overnight at 37 °C.

2.2.4.2 *S. aureus*

S. aureus RN4220 were cultivated on TSB agar plates or grown in TSB medium at 37 °C while shaking at 190 rpm.

2.2.4.3 *N. gonorrhoeae*

Culturing and preparation of bacterial stocks

N. gonorrhoeae was grown on GC agar plates supplemented with 1 % vitamin mix for 14 - 17 h at 37 °C/ 5 % CO₂. Bacteria were streaked at least once more after thawing for performance of experiments. The selection for non-piliated or Opa-negative colonies was done using a binocular microscope.

Growth curves

PPM medium was inoculated at OD₅₅₀ 0.15 with not piliated *N. gonorrhoeae*. The preculture was shaken with 100 rpm at 37 °C until an OD₅₅₀ 0.6. The main culture was inoculated at OD₅₅₀ 0.1 either in Erlenmeyer flasks or in a 48 well plate in a total volume of 400 µl. The growth in the flasks was measured with cuvettes and a spectrophotometer every hour for 6 h. Growth of *Neisseria* in a 48 well plate was measured by Tecan plate reader every 10 min for 6 h while shaking with 100 rpm at 37 °C.

Isolation of genomic DNA

N. gonorrhoeae, grown for 14 - 17 h on GC agar plates, were taken up in 1 ml PPM medium and centrifuged for 5 min at 5 000 x g. The pellet was resuspended in buffer I, supplemented with 200 µg/ml RNase A and 0.1 % SDS and was shaken for about 10 min at 42 °C until the suspension got clear. One volume of phenol-chloroform was added and shaken vigorously prior to centrifugation for 5 min at 15 000 rpm. The upper phase was transferred in a new tube and the phenol-chloroform treatment was repeated three more times. The DNA was precipitated by addition of 0.1 volumes of 3 M sodium acetate and 2.5 volumes of cold ethanol and subsequently incubation for 1 h at - 20 °C. The mixture was centrifuged at 15 000 rpm for 15 min at 4 °C. The pellet was washed with cold 70 % ethanol and taken up in 100 µl dH₂O after drying at air for about 15 min.

Transformation

N. gonorrhoeae are natural competent bacteria and the transformation of PCR fragments requires a DNA uptake sequence (GCCGTCTGAA) (Goodman & Scocca, 1988, Elkins *et al.*, 1991). Bacterial material was taken from GC agar plate and was resuspended in PPM medium. 50 µl of an OD₅₅₀ 0.32 bacterial suspension were mixed with 10 ng of a PCR product and were dripped in small portions on a non-selection GC agar plate. The plate was incubated at 37 °C for 6 h. The grown bacteria were taken up in PPM medium, centrifuged for 5 min at 5 000 x g and plated on an appropriate selective GC agar plate. The screening for successfully transformed colonies was done by colony PCR.

Neisserial mutagenesis and complementation

The integration of a FLAG sequence into the loop 1 sequence of the *porB_{IA}* and *porB_{IB}* genes was performed according to the procedure of site-directed mutagenesis of PorB from Bauer *et al.* (Bauer *et al.*, 1999). Two overlapping PCR fragments were amplified from genomic DNA of N920 with the primers PorB_{IA}-FLAG loop1 F/ ISO3 and PorB_{IA}-FLAG loop1 R/ FJB4 (Table 2.6) for FLAG-tagging of *porB_{IA}*. The oligonucleotides PorB_{IB}-FLAG loop1 F/ ISO3 and PorB_{IB}-FLAG loop1 R/ FJB4 were applied to amplify from genomic DNA of N931 to introduce a FLAG-tag to *porB_{IB}*. The fragments were fused by overlap PCR with the primers ISO3 and FJB4 and transformed in the recipient strain N917. 7 µg/ml erythromycin were used for selection of positive colonies.

The knockout of neisserial *mip* gene was performed by replacing the gene with a kanamycin resistance cassette. Therefore, a PCR fragment was constructed, which contained a DUS sequence and the kanamycin sequence flanked by 500 bp upstream and downstream of the target gene (Figure 2.1). The PCR fragment was transformed in N2009 and was integrated in the genomic DNA by homologous recombination.

The plasmid pLAS::pPILemCherry (given by Berenike Maier), which was used for the complementation of a knockout, features an asparate aminotransferase (NGFG_01468) gene, a spectinomycin resistance cassette, mCherry under a PilE promotor and an L-lactate permease (NGFG_01471) gene. The target gene with its native promotor was cloned in the plasmid by exchanging it with mCherry and the PilE promotor. The plasmid was transformed in a knockout strain, which resulted in integration in the non-coding region between NGFG_01468 and NGFG_01471.

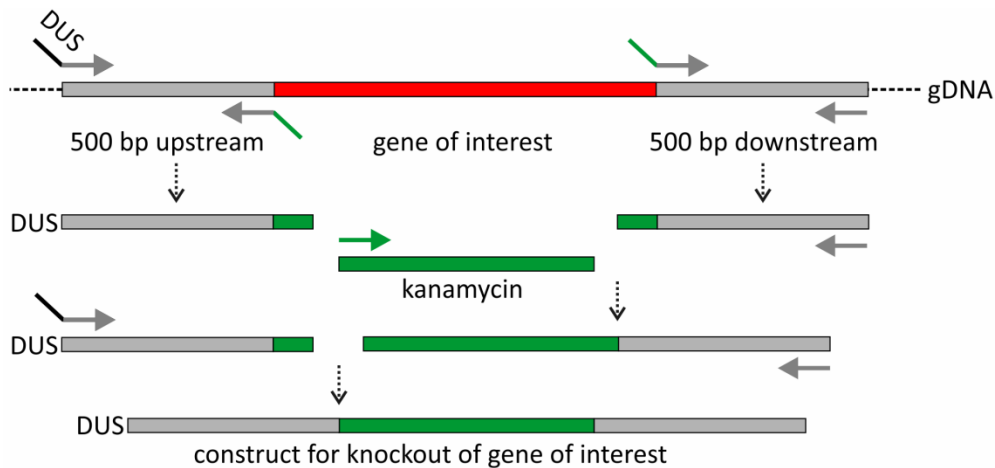


Figure 2.1: Overlap PCR strategy for targeted knockout of *N. gonorrhoeae* genes. 500 bp up- and downstream of the gene of interest were amplified from neisserial genomic DNA (gDNA) using oligonucleotides with overhangs complementary to kanamycin. The two fragments are combined with the kanamycin resistance cassette in the centre by applying overlap PCR.

Differential Immunostaining

Cells were grown on coverslips in 12 well plates to a confluency of 60 - 70 %. For infection at LPDI, HEPES medium was applied during the assay. The cells were washed once with HEPES to remove residual phosphate and incubated for 30 min at 37 °C / 5 % CO₂ prior infection. *N. gonorrhoeae* was taken up in 1 ml HEPES medium and was washed by centrifugation at 5 000 x g for 5 min. The cells were infected at MOI 10 and were centrifuged at 600 x g for 3 min to synchronize the infection that was performed for 1 h at 37 °C / 5 % CO₂. The cells were washed three times with HEPES, fixed with 4 % PFA for 15 min at RT and was washed three times with PBS. Unspecific antibody-binding sites were blocked with 1 % BSA in PBS for 1 h. The primary anti-*N. gonorrhoeae* antibody (in 1 % BSA/PBS) was incubated for 1 h on the cells to stain extracellular bacteria. The cells were washed three times with PBS and incubated for 1 h with the secondary Cy2-linked anti-rabbit IgG antibody. After washing with PBS the cells were permeabilised by treatment with 0.1 % Triton X-100 in PBS for 15 min. The intra- and extracellular bacteria were stained according to the protocol described above with the exception that a Cy5-linked anti-rabbit IgG antibody was used as secondary antibody. Additionally, the cellular nuclei were stained with DAPI (5 mg/ml stock solution diluted 1:3 000 in PBS) and the actin cytoskeleton with Phalloidin555 (1:100 in PBS) for 20 min. Afterwards, the cells were embedded in Mowiol on glass slides. The analysis was performed at the confocal microscope Leica TCS SPE using a 63x oil immersion objective.

Neutrophil survival assay

2×10^5 isolated PMNs were seeded in 24 well plates using RPMI medium without FCS by centrifugation at 1 000 rpm for 5 min. The cells were infected at MOI 50 with *N. gonorrhoeae* for 1 h at 37 °C under 5 % CO₂. Cells were washed three times with medium to remove extracellular bacteria and incubated for further 1-2 h. Afterwards, the cells were washed three times and lysed with 100 µl 1 % saponin for 7 min. 400 µl fresh medium were added to each well and the bacteria were plated at dilution 10^{-1} , 10^{-2} and 10^{-3} on GC agar plates. After overnight incubation at 37 °C the grown colonies were counted by using binocular microscope.

Isolation of neisserial blebs

Neisseria were inoculated at OD₅₅₀ 0.1 in 25 ml PPM medium and were grown at 37 °C (120 rpm) until an OD₅₅₀ 0.5 - 0.6. The bacteria were centrifuged for 20 min at 16 000 x g and the supernatant sterile filtrated with 0.2 µm filters. The isolation of the neisserial membrane vesicles (blebs) required an ultracentrifugation at 100 000 x g at 4 °C overnight. The blebs containing pellet was resuspended in HEPES medium.

2.2.4.4 *C. trachomatis*

Preparation

HeLa cells grown in T75 cell culture flask were infected with *C. trachomatis* at MOI 1 at 35 °C and 5 % CO₂ in RPMI supplemented with 5 % FCS. 48 h post-infection the cells were scraped off and vortexed for 3 min with glass beads to lyse the cells. The supernatant was collected and the cells were pelleted by centrifugation at 800 x g for 5 min. 100 µl of the supernatant were used to infect HeLa monolayers in T150 flasks. The cells were harvested 24 h post-infection and lysed with glass beads. After centrifugation at 2 000 rpm for 10 min at 4 °C the supernatant was centrifuged at 25 000 x g for 30 min at 4 °C to pellet the bacteria. The pellet was washed with 10 ml cold SPG buffer and centrifuged again. The bacterial pellet was resuspended in 1 ml cold SPG buffer and the bacteria were separated by passing the suspension through a 20G and 18G needle. Aliquots were prepared, stored at - 80 °C and were thawed freshly before infection experiments. After each preparation the titer of the stock was determined by infecting HeLa cells seeded in 12 well plates with 0.2 µl to 5 µl (in

0.2 μl steps) of the prepared bacteria. The bacterial amount that is needed to reach an MOI 1 was estimated by monitoring the infection at a bright field microscope.

Elementary body progeny assay

1×10^5 HeLa cells were seeded in two 12 well plates (plate A and B), which were infected at MOI 1 for 24 h at 35 °C and 5 % CO_2 in RPMI supplemented with 5 % FCS. Plate A (primary infection) was harvested after 24 h using 100 μl 2 x Laemmli buffer. Plate B was lysed with glass beads 48 h post-infection to allow *C. trachomatis* to finalize the developmental cycle in the host cells. The progeny infectious particles were released and 1 μl of the suspension was used to infect fresh HeLa cells in a 12 well plate (plate C, progeny infection). After 24 h of infection, plate C was harvested in the same manner as plate A. Cell lysates were analysed by western blot using antibodies against β -tubulin, α -tubulin or β -actin as a loading control and the chlamydial protein OmpA or cHSP60. The signals were measured by ImageJ and the bacterial bands were normalized against the loading control intensities.

Immunofluorescence staining

HeLa cells were grown on coverslips in 12 well plates and infected with *C. trachomatis* at MOI 1. 24 or 48 h post-infection the cells were washed three times with PBS and fixed for 30 min with 4 % PFA. The cell membrane and the inclusions were permeabilized with 0.2 % Triton X-100 in PBS for 30 min. The non-specific antibody binding sites were blocked with 2 % FCS in PBS for 1 h. The cells were incubated with the primary antibody cHSP60 for 1 h, were washed with PBS and stained for 1 h with the secondary Cy5-linked anti-mouse IgG antibody. The cell nuclei were detected with DAPI (1.5 $\mu\text{g}/\text{ml}$) and the actin cytoskeleton with Phalloidin555 (1:100). Finally, the coverslips were embedded in Mowiol and analysed at the confocal microscope Leica TCS SPE using a 63x oil immersion objective.

Transmission electron microscopy

HeLa cells were grown on coverslips in 12 well plates, infected with *C. trachomatis* for 48 h at MOI 1 and fixed with TEM fixation solution (2.5 % glutaraldehyde, 50 mM KCl, 50 mM cacodylate [pH 7.2]) for 1 h at 4 °C. The cells were transferred in 50 mM cacodylate buffer, contrasted with 2 % OsO_4 buffered with cacodylate buffer for 1 h, washed with H_2O and incubated in 0.5 % uranyl acetate (in H_2O) overnight. The samples were dehydrated by

increasing ethanol concentration steps beginning from 50 - 100 % and embedded in Epon812. Sections were analysed by the transmission electron microscope TEM900 (Zeiss) and negatives were digitalized by scanning.

2.2.4.5 ATP measurements

Isolation of bacterial membrane vesicles of *N. gonorrhoeae*, *E. coli* and *S. aureus* and ATP measurement

Bacteria were grown in 100 ml liquid culture until an OD₆₀₀ 0.5 - 0.6 and centrifuged for 12 min at 4 000 rpm. 10 ml lysis buffer were added to 5 g bacteria, which was supplemented either with 50 µg/ml lysostaphin for *S. aureus* or 1 mg/ml lysozyme for *E. coli* or *N. gonorrhoeae*. The lysis was performed for 45 min at RT while shaking at 800 rpm. The membrane vesicles were generated by sonification with three 20 sec strokes and 30 sec brakes or by applying the Turrax dispenser at the highest speed for 6 times for 10 sec. Then, the suspension was centrifuged at 12 000 x g for 10 min and afterwards at 100 000 x g for 45 min. The pellet was resuspended in lysis buffer without the enzymes and treated with 1 mM ADP to induce ATP production.

The ATP measurements were performed in white bottom 96 well plates using a Luminescence ATP detection assay kit (Abcam) as described in the manufacturer's protocol. Briefly, 50 µl of detergent were added to a sample and incubated for 5 min while orbital shaking at 700 rpm. 50 µl of the substrate were added and incubated for further 5 min in an orbital shaker. After 10 min incubation in the dark the Luminescence signal was measured in a Tecan plate reader.

Measurement of ATP production in *C. trachomatis*

HeLa cells grown in T175 cell culture flasks were infected at MOI 1 for 24 h with *C. trachomatis*. The preparation of the bacteria was performed according to the procedure described in 2.2.4.4. The bacterial pellet was resuspended in 500 µl of SPG buffer. 70 µl of the bacterial suspension was added to 130 µl of SILAC RPMI 1640 Flex Medium supplemented with 5 % FCS, 1.15 mM L-arginine and 0.22 mM L-lysine. The production of ATP was induced by addition of 0.5 mM glucose-6-phosphate and incubation at 35 °C for 2 h.

The ATP levels were measured with the Luminescent ATP Detection Assay Kit according to manufacturer's instructions.

2.2.5 Bioactivity testing of compounds

In *N. gonorrhoeae*

In order to screen for inhibitors against *N. gonorrhoeae* the neisserial strain N927 was prepared by streaking the bacteria on a GC agar plate (day 1) and restreaking on a new GC agar plate on the following day (day 2) (Figure 2.2A). 1.2×10^4 Chang cells were seeded in 96 black clear bottom plates (day 2). The cells were pre-treated for 1 h with three different concentrations of the inhibitors (1.6 μ M, 8 μ M and 40 μ M) in HEPES medium (day 3). 10 mM phosphate were applied as a control for a reduced invasion. The bacteria were resuspended in 500 μ l HEPES medium and were stained by adding 0.5 μ l of SNARF. This was followed by an incubation step at RT for 20 min in the dark and three times washing with HEPES medium (5 min for 5000 x g). Chang cells were infected at MOI 100 in the presence of the compounds for 1 h at 37 °C. Then, the cells were washed three times with HEPES and fixed with 4 % PFA for 15 min at RT. The cells were washed with PBS and the nuclei stained with 1.5 μ g/ml DAPI and the actin cytoskeleton with Phalloidin647 (1:100). The analysis of the number of bacteria per cells was done by the Operetta high content imaging system (day 4). The microscope took six pictures in one well at 20 \times magnification and counted the amount of nuclei and bacteria according to their fluorescent signal. Every condition was performed in three technical replicates and averagely 11×10^3 cells have been analysed.

In *C. trachomatis*

The procedure of screening for inhibitors against *C. trachomatis* was similar to that for *N. gonorrhoeae* (Figure 2.2B). 1.2×10^4 HeLa cells were grown in a 96 well black clear bottom plates (day 1). The cells were pre-treated for 1 h with the compounds (day 2) and were infected at MOI 1 for 24 h at 35 °C and 5 % CO₂ in RPMI supplemented with 5 % FCS with GFP-expressing *C. trachomatis* in the presence of the compounds. The cells were fixed and stained with DAPI and Phalloidin647 (day 3). The microscope measured the average cell surface area and the average inclusion surface area per well (day 4). The ratio between HeLa cell surface area and the *C. trachomatis* inclusion surface area was calculated by the system.

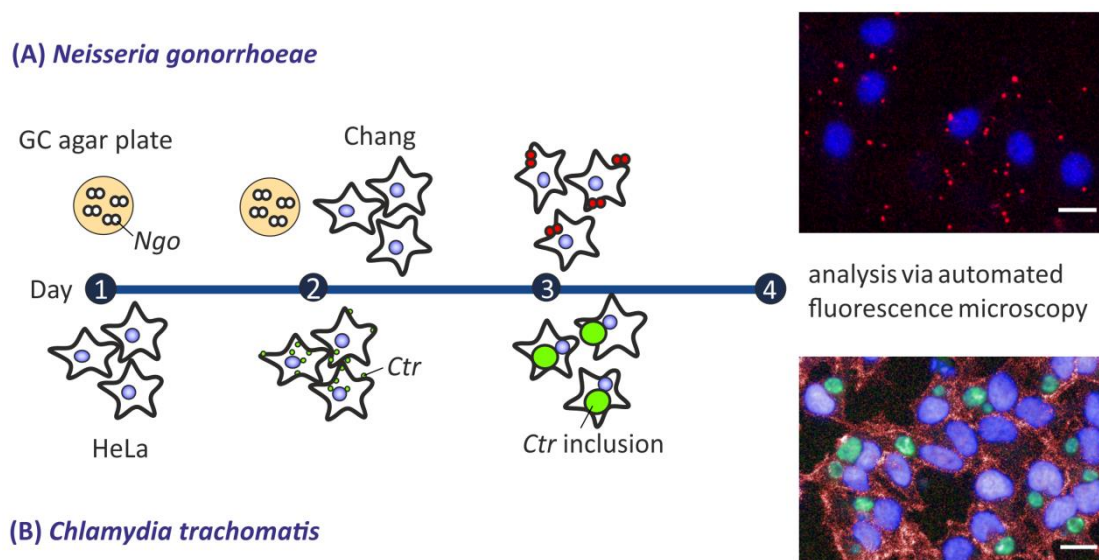


Figure 2.2: Procedure for the screening for inhibitors of *N. gonorrhoeae* and *C. trachomatis*. (A) For the compound screen in *N. gonorrhoeae* infection, bacteria (N927) were prepared by streaking (day 1) and restreaking (day 2) on GC agar plates. Chang cells were seeded in a 96 well plate (day 2), pre-incubated with the compounds and infected at MOI 100 for 1 h with SNARF stained bacteria (red) in the presence of the substances (day 3). The cells were washed, fixed with 4 % PFA and stained with DAPI (nuclei, blue). (B) In order to screen for inhibitors against *C. trachomatis* HeLa cells were seeded in a 96 well plate (day 1), pre-incubated with the substances and infected in the presence of the compounds at MOI 1 for 24 h with GFP-expressing *C. trachomatis* (day 2). The cells were fixed, the nuclei stained with DAPI (blue) and the actin cytoskeleton with Phalloidin647 (red) (day 3). The analysis of both assays was performed by automated fluorescence microscopy (day 4). Scale bar: 20 μ m

2.2.6 Mitochondria techniques

Isolation of mitochondria

Cells grown in 145 cm² dishes were washed with PBS and collected by using a cell scraper. The cells were centrifuged at 4 °C for 7 min at 800 x g. The pellet was resuspended in 4 ml buffer A and incubated on ice for 15 min. Afterwards, the cells were homogenised with 20 strokes drill-fitted Dounce homogenizer and centrifuged as before for 5 min. The supernatant was separated in Eppendorf Cups and centrifuged for 10 min at 10 000 x g and 4 °C. The pellet was washed with 1 ml buffer B and resuspended in 30 μ l of buffer B. The concentration of the isolated mitochondria was determined by resolving 2 μ l mitochondria in 100 μ l 0.1 % SDS and measure the absorption at 280 nm and 310 nm at the Nano Drop. The following formula was applied to calculate the concentration (Clarke, 1976):

$$\text{concentration [protein]} = \frac{A_{280 \text{ nm}} - A_{310 \text{ nm}}}{1.05} \times \frac{100}{2}$$

Preparation of inverted mitochondrial membrane vesicles and ATP measurements

Mitochondria were isolated and solubilized in 2 ml of solution B. The inverted vesicles were generated by sonification (three times for 20 sec with 30 sec pauses) and subsequently centrifuged at 12 000 x g for 10 min at 4 °C and afterwards at 100 000 x g for 45 min. The vesicles pellet was resuspended in 1.5 ml solution C and centrifuged for 5 min at 12 000 x g. In order to measure the ATP production of inverted mitochondrial vesicles or whole mitochondria (0.125 mg/ml per sample), 1 mM ADP was added as substrate to initiate the ATP production. The samples were incubated for 30 min at 37 °C in a rotary shaker prior ATP measurement using the Abcam Luminescence Kit as described in section 2.2.4.5.

Measurement of mitochondrial membrane potential

HeLa cells grown in 6 well plates were detached with 300 µl Trypsin and mixed with 700 µl RPMI supplemented with 10 % FCS. The cells were centrifuged at 800 x g for 5 min and dissolved in 500 µl RPMI medium. 20 nM Tetramethylrhodamine, methyl ester (TMRM) was added and the samples were incubated for 20 min at 37 °C on a rotary shaker. Afterwards, the cells were washed twice with PBS and resuspended in 500 µl PBS. The fluorescence was measured by flow cytometry using blue laser at 488 nm (BD Accuri C6 Flow Cytometer).

Cell Mito Stress Test

The oxygen consumption rate (OCR) and the extracellular acidification rate (ECAR) were measured by the Seahorse Bioscience XFe96 Extracellular Flux Analyzer (Seahorse Bioscience) using manufacturers protocol (Wu *et al.*, 2007). Briefly, 2×10^4 HeLa cells were seeded in a total volume of 80 µl in Seahorse 96 well XF Cell Culture Microplate. XF Base medium supplemented with 1 mM pyruvate, 2 mM L-glutamine and 10 mM glucose (pH 7.4 ± 0.05) was used for the measurements. The basal respiration, the ATP production, the maximal respiration and the non-mitochondrial respiration were determined by sequentially injecting 2 µM oligomycin, 0.5 µM or 1 µM FCCP, 0.5 µM rotenone and antimycin A, respectively. Data were normalized to the cell number of a replication plate, which was quantified by a crystal violet staining.

2.2.7 Purification of native and recombinant proteins and antibodies

Protein purification of native neisserial PorB_{IA} and PorB_{IB}

N. gonorrhoeae colonies from three GC agar plates were resuspended in 10 ml PPM medium. 200 ml preculture were inoculated at OD₅₅₀ 0.3 and were shaken at 37 °C for 6 h at 135 rpm. The main culture was inoculated with the preculture at OD₅₅₀ 0.1 in 1 l PPM medium and was shaken at 100 rpm for 8 h. The bacteria were pelleted by centrifugation for 30 min at 3 000 rpm at 4 °C. The pellet was resuspended in 10 ml 1 M sodium acetate (pH 4) supplemented with 1 mM PMSF. Zwittergent solubilized in 0.5 M CaCl₂ were added to a final concentration of 5 %. The cells were disrupted by applying the Turrax disperser several times at high speed on ice and were mixed with 90 ml of 5 % Zwittergent in 0.5 M CaCl₂ and 1 mM 3-Mercapto-1,2-Propanediol (alpha-Monothioglycerol). Further Turrax dispersion was performed and the probe was stirred for 1 h at RT. 100 % ethanol was added to a final concentration of 20 % dropwise while stirring until white precipitation started. The precipitants were pelleted by centrifugation at 15 000 rpm for 30 min at 15 °C. The porin containing supernatant was dialysed against a buffer consisting of 20 mM Tris/HCl (pH 7.5), 10 mM EDTA buffer and 0.05 % Zwittergent. The dialysis was performed for 1 h at 4 °C in 250 ml, then the buffer was exchanged with fresh 250 ml and dialysed for another 1 h. The buffer was changed for the third time and the probe was dialysed overnight. The protein was purified by anion-exchange chromatography (Source Q column) using the Äkta protein purification system. The column was equilibrated with 15 ml buffer A_Q. The protein was injected and should bind to the column, which was washed with 20 ml A_Q buffer. The elution was performed by a salt gradient with 20 ml buffer B_Q. Further purification was done by using cation-exchange chromatography (Source S column). Therefore, the sample was dialysed for buffer A_S, applied to Source S and eluted with 30 ml buffer B_S. Finally, the protein was purified with gel filtration chromatography using Superdex 200 10/30 and buffer A_G. The protein containing samples were pulled together and concentrated with Amicon® Ultra centrifugal filters. Each purification step was monitored by SDS-PAGE and coomassie staining.

Induction of recombinant protein expression and determination of the protein solubility

The purification of a recombinant protein required the expression of the protein in a small liquid culture to analyse the appropriate induction period as an initial step. 10 ml LB medium supplemented with 100 µg/ml ampicillin were inoculated with 500 µl of an appropriate *E. coli* BL-21 overnight culture. The culture was shaken for 30 min at 37 °C until an OD₆₀₀ 0.5-0.7. The protein expression was induced with 1 mM IPTG for 4 h. Every hour 1 ml of the culture was centrifuged at 15 000 x g for 1 min and the pellet resuspended in 2 x Laemmli. The protein expression was analysed by SDS-PAGE and coomassie staining.

Furthermore, the protein solubility had to be determined in order to analyse if the protein is expressed in a soluble form or if it accumulates in inclusion bodies. Therefore, 50 ml of a 4 h induced liquid culture was centrifuged at 4 000 rpm for 20 min. The pellet was frozen at -20 °C overnight and thawed the next day on ice. 5 ml NC lysis buffer supplemented with 1 mg/ml lysozyme were added to the pellet for 30 min on ice. Subsequently, the lysate was sonicated with six strokes and 10 sec pause and centrifuged at 10 000 x g for 30 min at 4 °C. The supernatant contained the soluble fraction and the pellet the insoluble fraction, which were analysed by SDS-PAGE and coomassie staining.

Protein purification of Ng-MIP and Ctr-MIP under native conditions

The neisserial *mip* gene was amplified by PCR from gDNA of N927 (Bauer, 1997) using the oligonucleotides 5' CTCGCCATATGGGCAAAAAGAAGC 3' (NdeI) and 5' CTGCTGGATCCATTTA CTTTTTGGATG 3' (BamHI). For the amplification of the chlamydial *mip*, the primers 5' CTCGCCATATGAAGAATATATTA 3' (NdeI) and 5' CTGCTGGATCCCTATTCT GTAAC 3' (BamHI) were applied. The genes were cloned without the signal peptide sequence into the vector pET15b using the restriction sites NdeI and BamHI, thus receiving an N-terminal 6xHis-tag. The plasmids were transformed in BL-21 *E. coli* cells using ampicillin (100 µg/ml) for selection. An overnight culture of the transformed plasmid containing *E. coli* was used to inoculate 1 l LB culture which was shaken vigorously at 37 °C until OD₆₀₀ 0.6. The protein expression was induced by adding 1 mM IPTG to the culture and incubating for additional 4 h. The bacteria were pelleted by centrifugation at 4 000 x g for 20 min and frozen overnight at -20 °C. Afterwards, the pellet was thawed for 15 min on ice and resuspended in 4 ml per gram wet weight NC lysis buffer. After addition of 1 mg/ml lysozyme and incubation for 30 min on ice the pellet was sonicated using 10 sec bursts with a 10 sec cooling period.

10 µg/ml ribonuclease A and 5 µg/ml desoxyribonuclease I were added and incubated on ice for 15 min. The lysate was centrifuged at 10 000 x g for 20 min. 7 ml of the supernatant were mixed in a column with 1.75 ml 50 % Ni-NTA slurry and incubated for 1 h at 4 °C on a rotary shaker. In the case of Ctr-MIP, the column was washed twice with NC wash buffer and eluted with 2 ml NC elution buffer. For the neisserial MIP, it was possible to cleave the 6xHis tag at the thrombin cleavage site. Therefore, after binding of the protein to the Ni-NTA beads, the column was washed twice with TC wash buffer 1, TC wash buffer 2, TC wash buffer 3 and thrombin wash buffer. The beads were mixed with 1 volume thrombin wash buffer, 0.1 volume thrombin buffer, 20 units thrombin and incubated overnight at 4 °C on a rotary shaker. The flow-through contained the His-tag free protein.

The Ctr-MIP and Ng-MIP were further purified using the Äkta protein purification system. Therefore, a desalting column was applied to exchange buffer to buffer MIP_{AQ}. The proteins were purified by anion exchanger column (Source Q) using elution buffer MIP_{BQ}. A desalting column was used to exchange the buffer to buffer MIP_{AG} for further purification by gel filtration. Finally, the proteins were dialysed against 35 mM Hepes pH 7.8.

Purification of recombinant proteins under denaturing conditions for antibody production

In order to generate antibodies against PorB_{IA}, PorB_{IB} and Omp85 of *N. gonorrhoeae* the appropriate genes were inserted without signal peptide sequence into the pET15b vector. The induction and centrifugations steps were performed according to procedure described for native conditions. The frozen bacterial pellet was thawed on ice for 15 min and was resuspended in 2 - 5 ml DC binding buffer per gram wet weight. 1 mg/ml lysozyme, 10 µg/ml RNase A, 5 µg/ml DNase I und 1 x protease inhibitor was added and incubated for 20 min at RT. The probe was centrifuged at 15 000 rpm at RT for 15 min and the protein containing supernatants was filtrated through a 0.45 µm filter. The purification was performed using a HisTrap HP column at the Äkta protein purification system. The proteins were eluted with 20 column volume DC elution buffer using a linear gradient. The protein containing fractions were identified by SDS-PAGE and coomassie staining and were concentrated with protein concentration columns. To determine the protein amount, BSA ranging from 0.25 µg to 2 µg was loaded next to 10 µl of the probe. Image J was used to analyse the intensities of the coomassie stained bands and calculate the concentration of the protein. Approximately 0.5 mg of the protein was sent to Davids Biotechnology GmbH (Regensburg, Germany) for

production of polyclonal antibodies in rabbits. Furthermore, a *N. gonorrhoeae* PorB_{IB} specific peptide antibody was obtained from Davids Biotechnology GmbH using a company synthesised peptide: SGKFTGNVLEISGMAKREHRYL.

Purification of antibodies using CNBr-activated Sepharose

In order to purify an antibody the appropriate purified recombinant protein (antigen) had to be bound to CNBr-activated Sepharose beads, which were then used to pull-down the antibody from the serum. Therefore, 100 µg of the protein were concentrated by centrifugation at 2 000 rpm and RT in Amicon® Ultra Centrifugal Filters to a volume of 200 µl. 4 ml of carbonate buffer were added and the protein was concentrated again. This step was repeated three times to exchange the buffer. The final volume of the protein was adjusted to 1 ml. 0.14 g of the CNBr-activated Sepharose beads were swelled for 30 min in 1 mM HCl, centrifuged at 600 x g for 2 min and were washed twice with carbonate buffer. The beads pellet was resuspended in the protein containing buffer. After an overnight incubation at 4 °C at a rotary shaker the beads were washed twice with carbonate buffer and were blocked at RT in 0.1 M Tris/HCl (pH 8) buffer. The beads were washed three times with carbonate buffer and resuspended in 1 ml 500 mM NaCl in PBS. 7 ml of the serum, 7 ml PBS and 1 ml protein were incubated overnight at 4 °C at a rotary shaker. The beads were washed three times with NaCl in PBS and eluted with 10 ml 0.1 M glycine (pH 2.5) in 500 µl steps. 100 µl 1 M Tris/HCl (pH 7.5) was added to each 500 µl eluate. The antibody containing fractions were pooled and determined by SDS-PAGE and western blot. The buffer was exchanged to PBS. The purified antibody was stored in 50 % glycerol at - 20 °C.

2.2.8 Co-immunoprecipitation (co-IP) and pull-down assays

Co-IP of PorB_{IA} using Dynabeads®Protein G coupled to SREC-I

20 µl of Dynabeads®Protein G were incubated on a rotary shaker overnight at 4 °C in IP buffer I to block non-specific binding regions. The beads were washed once with IP buffer II, which did not contain phosphate to interrupt a potential phosphate-dependent interaction of PorB_{IA} and SREC-I. 100 µl of the saturated beads were incubated with 100 µg/ml SREC-I Fc Chimera for 1 h at 4 °C on a rotary shaker. The beads were washed and incubated with 5 µg neisserial PorB for 1 h. After subsequent washing steps with IP buffer II the beads were

resuspended with 30 μ l 2 x Laemmli buffer, heated for 10 min at 95 °C and analysed by SDS-PAGE and western blot.

Pull-down of SREC-I using FLAG-tagged PorB_{IA} coated neisserial blebs

Chang cells were seeded in 145 cm² dishes. The cells were washed once with HEPES medium and 200 to 300 μ l of the isolated blebs were added to 10 ml HEPES, which were given to the cells. 2 h after incubation at 37 °C the cells were washed three times with HEPES and collected with a cell scraper. The cells were lysed in 770 μ l PD lysis buffer for 30 min on ice. The lysate was centrifuged for 10 000 x g for 10 min at 4 °C. The supernatant was mixed with 76 μ l M2 α -FLAG agarose beads, which were previously equilibrated with PD wash buffer. After an incubation of 1 h at 4 °C on a rotary shaker the flow-through was collected and the beads were washed three times with eight volumes of PD wash buffer. The elution was performed in six 100 μ l steps of 0.1 M glycine (pH 3.5) with a subsequent neutralization with 1 M Tris/HCl (pH 8). The proteins were precipitated with TCA and resuspended in 2 x Laemmli buffer while shaking at 65 °C for 15 min.

Pull-down of PorB_{IA}-expressing *N. gonorrhoeae* by soluble GFP-tagged SREC-I

293T cells were transfected with the plasmid pcDNA3-GFP-SREC-I by CaPO₄ transfection. After 24 h the medium was changed to HEPES medium for further 48 h. The GFP-tagged SREC-I containing medium was centrifuged at 4 000 x g for 10 min at 4 °C. 500 μ l of the supernatant were used to incubate 2x10⁶ *N. gonorrhoeae* colony forming units (cfus) for 30 min at RT at a rotary shaker. The bacteria were washed three times with HEPES medium and lysed in 10 μ l 2 x Laemmli buffer. The analysis was done either by western blot or flow cytometry using the blue laser at 488 nm.

2.2.9 Surface plasmon resonance (SPR) measurements

The analysis of the interaction of SREC-I Fc Chimera to the isolated neisserial PorB was done by surface plasmon resonance experiments at the Biorad ProteOn XPR36. The experiment was performed by Prof. Dr. Thomas Müller (Institute for Molecular Plant Physiology and Biophysics, University of Würzburg). The ProteOn™ GLC Sensor Chip was coated with NeutrAvidin and was used to immobilize the biotinylated neisserial PorB on the surface by loading 1200 resonance units (RU) first and then 1200 RUs more.

The biotinylation (Thermo Fisher) of PorB was done according to manufacturer's instructions. Briefly, EZ-Link NHS-LC Biotin was added in a 20-fold molar excess (calculations described in manufacturer's protocol) to 1 - 10 mg of the protein solubilized HEPES medium. After an incubation of 2 h on ice, the biotinylation was monitored by western blot using an antibody against biotin. The removal of excessive biotin was performed by gel filtration using the SPR buffer 10 mM Hepes (pH 7.4), 150 mM NaCl, 3.4 mM EDTA, 0.005 % Tween-20 and 0.01 % Zwittergent. SREC-I Fc Chimera was solubilized in the SPR buffer and injected at a flow rate of 100 μ l/ml over the chip surface at 25 °C. The association phase was 120 sec and dissociation phase 60 sec. The biosensor chip was regenerated with 2 M $MgCl_2$ for 2 min.

2.2.10 PPlase Assay

Peptidyl prolyl *cis-trans* isomerase (PPlase) activity of MIP proteins was determined in a coupled assay with the protease α -chymotrypsin, which was performed by Matthias Weiwad (Department of Enzymology, Institute of Biochemistry and Biotechnology, Martin-Luther-University Halle-Wittenberg) (Fischer *et al.*, 1989). The assay utilizes the specificity of α -chymotrypsin for the *trans* isomer of the Xaa-Pro bond in proline-containing oligopeptides. Thus, α -chymotrypsin only cleaves off the 4-nitroanilide from the used tetrapeptide substrate succinyl-Ala-Leu-Pro-Phe-4-nitroanilide when the Leu-Pro bond is in the *trans* conformation. At the applied high concentration of α -chymotrypsin (0.2 mg/ml), cleavage of the of the *trans* peptide occurs immediately during the mixing time. α -Chymotrypsin catalysed cleavage of 4-nitroaniline from the remaining peptide depends on the rate of *cis*-to-*trans* isomerization of the prolyl bond and can be followed by increase in absorbance at 390 nm. Catalysis of *cis-trans* isomerization by MIP proteins was measured at 10 °C for 6 min in a reaction mixture containing 35 mM Hepes buffer (pH 7.8), 40 μ M succinyl-Ala-Leu-Pro-Phe-4-nitroanilide, and 15 nM of the respective MIP protein. The reaction was started by addition of α -chymotrypsin and the release of 4-nitroanilide was monitored at 390 nm.

2.2.11 Statistical analysis

The analysis of statistical significance of the acquired data was calculated with the two-tailed Student's t-tests using Microsoft Excel.

3 RESULTS

3.1 Analysis of the interaction between SREC-I and PorB_{IA}

The outer membrane protein PorB_{IA} is sufficient for LPDI in host cells and is independent of other virulence factors, such as Pili or Opa (Kühlewein *et al.*, 2006). PorB_{IB}-expressing strains showed a significantly lower invasion rate of only 1 - 2 % in comparison to PorB_{IA}-expressing strains (Figure 3.4). SREC-I has been identified as the cellular receptor of the PorB_{IA}. The knockdown of SREC-I reduces the invasion significantly (Rechner *et al.*, 2007). Since a direct interaction of PorB_{IA} and SREC-I has never been shown, this study aimed at analysing this interaction by co-IP, pull-down assay, receptor-binding assay and surface plasmon resonance (SPR).

3.1.1 Co-IP of neisserial PorB_{IA}

The co-IP was performed using a SREC-I Fc Chimera, which is a commercially obtained N-terminal region of the human SREC-I protein (S20 - T421) fused to a C-terminal region of the human IgG₁ (P100 -K330). The Fc region of the SREC-I Fc Chimera was bound to protein G-coated magnetic beads (Dynabeads® Protein G) and this was used to capture the purified PorB_{IA} protein. The bound proteins were analysed by western blot using an anti-PorB_{IA} antibody (Figure 3.1). The control samples were untreated beads, beads incubated only with PorB_{IA} and beads bound to an IgG protein instead of SREC-I. All samples that included the treatment with PorB_{IA} showed a signal in the western blot independently of the antigen bound to the magnetic beads. Due to the unspecific binding of PorB_{IA} to the beads themselves, this experimental set up was not suitable to analyse the protein interaction.

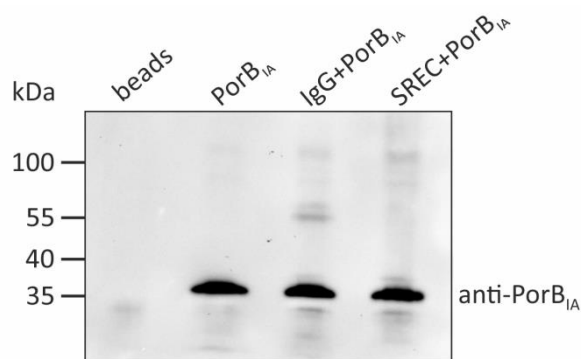


Figure 3.1: PorB_{IA} binds unspecifically to Dynabeads® Protein G during co-IP. PorB_{IA} was immunoprecipitated using uncoated beads (PorB_{IA}), beads covered with IgG (IgG+PorB_{IA}) or SREC-I (SREC+PorB_{IA}). The precipitation was analysed by SDS-PAGE and western blot using an antibody

against PorB_{IA}. Untreated beads were also lysed and used as a control (beads). Exemplary results of one out of three performed experiments are shown.

3.1.2 Pull-down of PorB_{IA} interaction partners with PorB_{IA}-FLAG coated neisserial blebs

N. gonorrhoeae has been shown to release neisserial outer membrane vesicles (blebs) with the size of 70 - 120 nm in diameter during their logarithmic growth phase (Dorward & Judd, 1988). The blebs contain not only DNA or RNA, but also different surface proteins such as PorB or LOS (Dorward & Judd, 1988, Dorward *et al.*, 1989). The idea was to use these PorB_{IA} coated vesicles for a pull down of the cellular receptor SREC-I of Chang cells. The proteins that bound to PorB could be analysed by mass spectrometry. Therefore, two neisserial strains were generated by site-directed mutagenesis that contained a FLAG-tag sequence (DYKDDDDK) in the extracellular loop 1 of either PorB_{IA} (G41-A42) or PorB_{IB} (D41-G42) (Bauer *et al.*, 1999). The PorB_{IB}-FLAG strain served as a negative control. The FLAG-tag enabled the isolation of the blebs with their interaction partners using M2 α -FLAG agarose beads.

In order to verify the expression of FLAG-tagged PorB_{IA} and PorB_{IB}, bacterial material (Figure 3.2A, B) and isolated neisserial blebs (Figure 3.2C) were lysed with 2 x Laemmli buffer and analysed by western blot using an anti-FLAG antibody. A signal could be detected for the PorB_{IA}-FLAG as well as for the PorB_{IB}-FLAG neisserial strain, proving a successful mutagenesis.

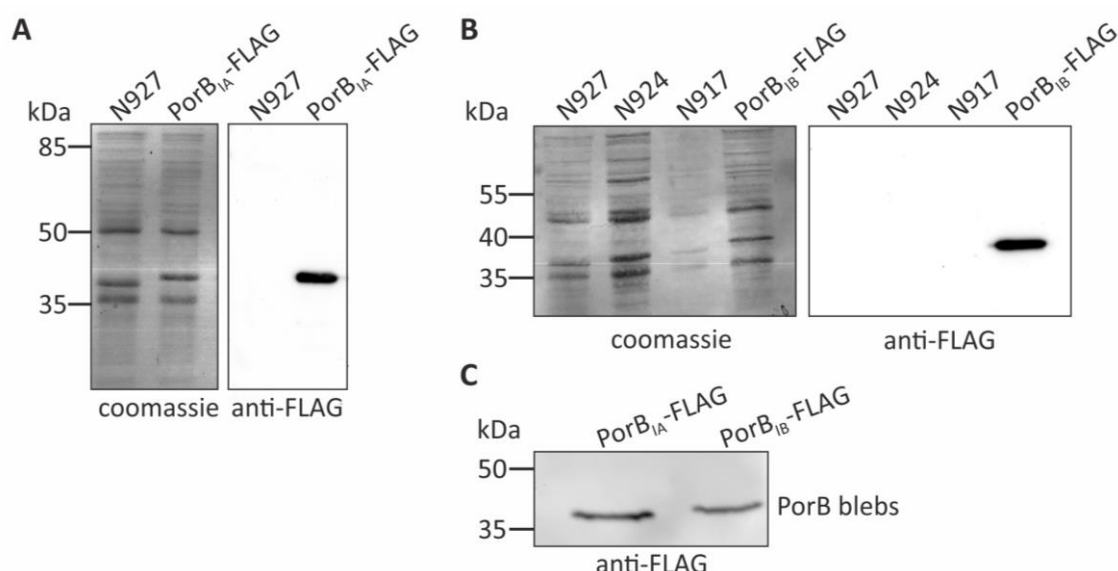


Figure 3.2: *N. gonorrhoeae* mutants PorB_{IA}-FLAG and PorB_{IB}-FLAG express a FLAG-tagged PorB. A FLAG-tag was introduced in loop 1 of the neisserial PorB_{IA} (A) and PorB_{IB} (B). The generated clones were analysed by SDS-PAGE and western blot by using an anti-FLAG antibody. As a control, N927 (PorB_{IA}) (A, B), N924 (PorB_{IB}) (B) and N917 (PorB_{IB}) (B) bacterial lysates were loaded next to the PorB_{IA}-FLAG (A) and PorB_{IB}-FLAG (B) clones. The coomassie stained membrane is shown next to the

immunoblot staining. (C) Isolated neisserial blebs from PorB_{IA}-FLAG and PorB_{IB}-FLAG were analysed by SDS-PAGE and western blot using the anti-FLAG antibody.

The growth behaviour of the strains PorB_{IA}-FLAG and PorB_{IB}-FLAG was measured in comparison to the wild type strains N927 (PorB_{IA}) or N924 (PorB_{IB}) (Figure 3.3). The strain expressing a FLAG-tagged PorB_{IA} grew similar to N927, while PorB_{IB}-FLAG showed a growth defect, growing as almost 50 % slower than the PorB_{IB}-expressing wild type N924, which indicated a negative growth effect of the FLAG-tag in the loop 1 of PorB_{IB}.

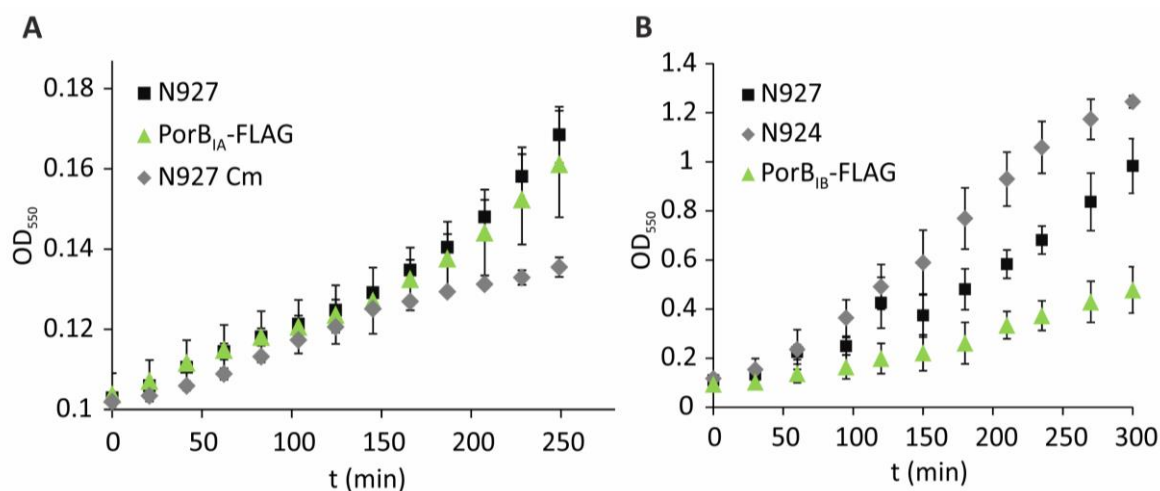


Figure 3.3: The introduction of a FLAG-tag in PorB_{IA} does not affect the bacterial growth, while FLAG-tagging of PorB_{IB} does. (A) The growth of N927 (PorB_{IA}), N927 in the presence of 15 μ g/ml chloramphenicol (Cm) and PorB_{IA}-FLAG was measured in liquid culture at OD₅₅₀ in a plate reader every 20 min for 250 min. (B) Growth curves of N927, N924 (PorB_{IB}) and PorB_{IB}-FLAG were generated by measuring OD₅₅₀ of the liquid culture every 30 min for 300 min. The graphs represent mean values \pm SD of three independent experiments.

The invasion and adherence behaviour of PorB_{IA}-FLAG and PorB_{IB}-FLAG was also analysed. Chang cells were infected with the mutant strains and the wild type strains N927 and N924 for 1 h at MOI 10 under low-phosphate condition. Phosphate was added as a control to decrease the infection rate. A differential immunostaining was performed and the amount of intra- and extracellular bacteria was determined. A non-significantly reduced invasion and adherence of PorB_{IA}-FLAG by approximately 40 % could be observed (Figure 3.4A). Nevertheless, the internalisation was phosphate-sensitive, since the addition of phosphate led to a decrease in invasion to only 9.5 %. The invasion and adherence of PorB_{IB}-FLAG was increased by about 20 % compared to the PorB_{IB}-expressing strain N924, but was still significantly less than the infection with N927 (Figure 3.4B). Although the strains PorB_{IA}-FLAG and PorB_{IB}-FLAG differed from the wild type strains in terms of infection, the

difference was not significant and the trend of the invasion and adherence was similar, which implied a still functional interaction of the FLAG-tagged PorB proteins with the cellular receptor.

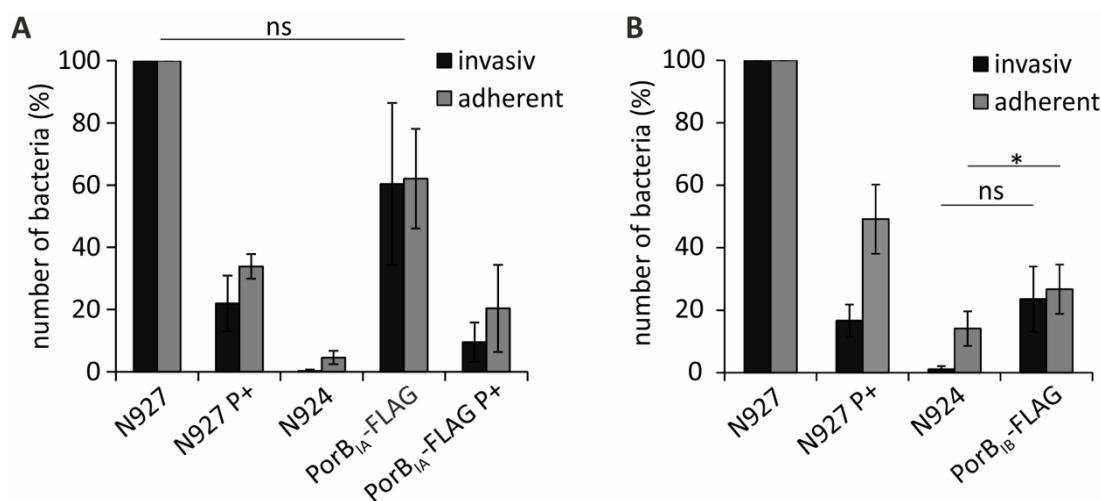


Figure 3.4: FLAG-tagging of PorB_{IA} and PorB_{IB} influences the bacterial infectivity and adherence. Chang cells were infected at MOI 10 with N927 (PorB_{IA}), N924 (PorB_{IB}), PorB_{IA}-FLAG (A) and PorB_{IB}-FLAG (B). The numbers of invasive and adherent bacteria were determined by differential immunostaining and fluorescence microscopy. 10 mM phosphate were added to the infection as a control (P+). The graph shows mean values \pm SD of three independent experiments. ns not significant, * $p < 0.05$

Neisserial blebs were isolated from PorB_{IA}-FLAG, PorB_{IB}-FLAG and N927 and were added to Chang cells for 2 h. The cells were lysed and the blebs with their interaction partners isolated by M2 α -FLAG agarose beads. The proteins were precipitated by TCA and analysed by colloidal coomassie staining. Differences between band patterns of the elution fraction of PorB_{IA}-FLAG (Figure 3.5A) and the controls PorB_{IA}-FLAG in the presence of phosphate (P+) (Figure 3.5B), PorB_{IB}-FLAG (Figure 3.5C) and N927 (Figure 3.5D) could not be detected, indicating that this approach was not appropriate to pull-down SREC-I or other interaction partners of PorB_{IA}.

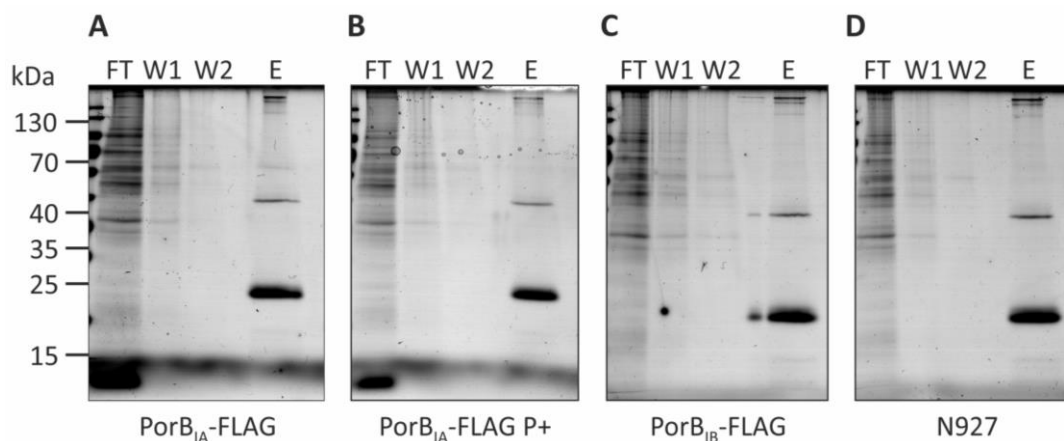


Figure 3.5: Pull-down of cellular interaction partners of PorB_{IA} by FLAG-tagged neisserial blebs. A pull-down was performed with blebs from PorB_{IA}-FLAG (A, B), PorB_{IB}-FLAG (C) and N927 (D) using anti-FLAG agarose beads. Phosphate (P+) was added to the incubation with PorB_{IA}-FLAG blebs as a control (B). The flow-through (FT), the two washing steps (W1, 2) and the eluate were precipitated with TCA and analysed by SDS-PAGE and colloidal coomassie staining. Exemplary results of one out of three performed experiments are shown.

3.1.3 Binding of soluble GFP-tagged SREC-I to PorB_{IA}-expressing *Neisseria*

Recently, it has been demonstrated that Opa_{CEA}-expressing *N. gonorrhoeae* binds species-specifically to the human CEACAM1 receptor and not to other mammalian orthologues (Voges *et al.*, 2010). This result was achieved by performing binding studies with the soluble GFP-tagged amino-terminal domains of CEACAM1, whose binding to whole bacteria was monitored by flow cytometry. The same approach was used in this study to analyse the interaction of PorB_{IA}-expressing *Neisseria* with the soluble GFP-tagged extracellular domain of SREC-I. To this purpose, HEK 293T cells were transfected with the pcDNA3 vector containing either GFP as a negative control or the GFP-tagged extracellular domain of SREC-I. The GFP signal in the cells was monitored by fluorescence microscopy (Figure 3.6A, B). Cells expressing only GFP exhibited a homogeneously distributed signal (Figure 3.6A), whereas the GFP-tagged SREC-I appeared in enclosed vesicles throughout the cell (Figure 3.6B). 24 h after transfection the growth medium of the cells was exchanged for HEPES medium and the cells were incubated for further 48 h. After this, the cells and the supernatant were analysed by western blot using antibodies against SREC-I (Figure 3.6C) and GFP (Figure 3.6D). The majority of the GFP-tagged SREC-I could be detected in the cellular fraction, which was also true for GFP protein. However, SREC-I-GFP and GFP were also present as soluble proteins in the supernatant.

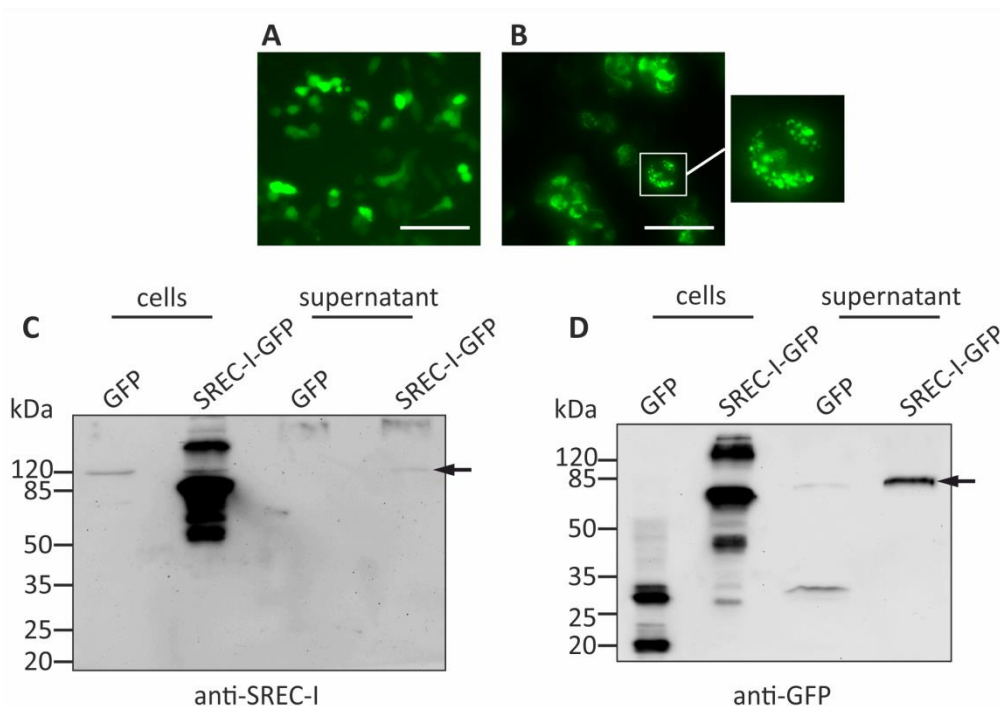


Figure 3.6: Soluble GFP-tagged SREC-I is detectable in the supernatant. (A, B) HEK 293T cells were transfected with pcDNA3 containing either GFP (A) or the GFP-tagged extracellular domain SREC-I (B). The distribution of GFP (green) in the cells was analysed by microscopy. Scale bar: 50 μ m. (C, D) HEK 293T cells expressing GFP or SREC-I-GFP (arrow) were cultivated for 48 h after transfection in HEPES. The cells and the supernatant were lysed with 2 x Laemmli buffer and analysed by SDS-PAGE and western blot using the antibodies against SREC-I (C) and GFP (D).

The supernatant containing either GFP as a control or the soluble GFP-tagged SREC-I was incubated with the *N. gonorrhoeae* strains N924, N927 and the non-pathogenic strain *N. lactamica*. The western blot (Figure 3.7A) and flow cytometry analysis (Figure 3.7B) of the washing fraction (supernatant) and the bacterial pellet revealed that the majority of the soluble SREC-I-GFP could be detected in the supernatant, while the GFP control was equally present in the wash fraction as well as in the bacterial pellet. The GFP in the pellet seemed to be cleaved, since two GFP bands could be observed at a height of 28 kDa and about 15 kDa. A slight SREC-I-GFP band was visible in the pellets of N924 and N927. The SREC-I content bound to N927 was slightly higher than to N924, but the same was also true for the GFP protein alone.

In contrast to the western blot, the flow cytometry measured the GFP fluorescence directly in the bacteria. The incubation with GFP control was hardly detectable. The highest SREC-I-GFP amount could be found in N927 bacteria. The signal was decreased in N924 bacteria, though the difference was not significant due to the high standard deviation.

However, a significant difference in the bound SREC-I-GFP could be observed between N927 and *N. lactamica*, which had bound less than 55 % of the protein.

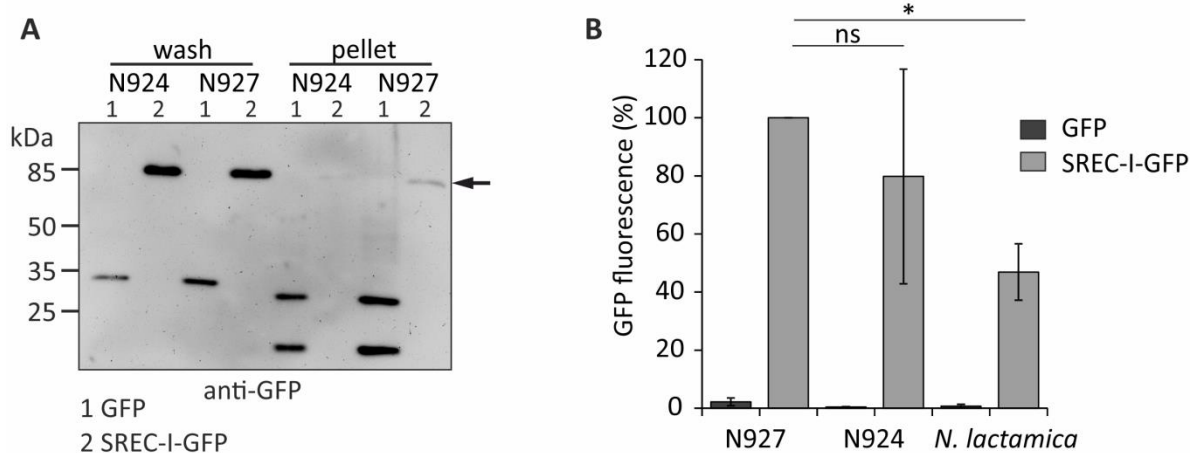


Figure 3.7: The binding of soluble SREC-GFP to PorB_{IA} is not significantly different to PorB_{IB}. (A, B) HEK 293T cells were transfected with pcDNA3-GFP (1) and pcDNA3-SREC-I-GFP (2) and were grown for 48 h. The supernatant was incubated for 30 min at 37 °C and 5 % CO₂ with *N. gonorrhoeae* N924 (PorB_{IB}), N927 (PorB_{IA}) and *N. lactamica*. The bacteria were washed three times with HEPES medium. The supernatant from the last wash and the pellet were analysed by western blot (A) or flow cytometry (B). The SREC-I band is marked with a black arrow. The experiment was performed three times and the mean values \pm SD were normalized to the GFP fluorescence signal of the N927 sample. ns not significant, * $p < 0.05$

3.1.4 Interaction analysis of SREC-I and PorB_{IA} by SPR

Another approach to analyse the interaction between PorB_{IA} and SREC-I *in vitro* was by SPR. For this, PorB_{IA} and PorB_{IB} (as a negative control) were isolated from *N. gonorrhoeae* strains N2011 and N924, respectively, under native conditions. After the final purification step, which consisted of applying a gel filtration column, the fractions not only contained PorB monomers at 35 kDa but also the trimeric conformation at 120 kDa (Figure 3.8A). The proteins were biotinylated (Figure 3.8B) and bound to the NeutrAvidin coated surface of the chip. The solubilized SREC-I Fc Chimera was injected over the PorB layer in six different concentrations ranging from 0.625 to 20 nM. It could be shown that the SPR signal increased in concentration-dependent manner and had a binding constant (K_D) of 5.79 nM (\pm 1.39 nM), which indicates a high-affinity interaction of SREC-I to PorB_{IA} due to the low K_D value (Figure 3.8C). However, the addition of phosphate to the measurement did not affect the K_D . Furthermore, performance of the experiment with PorB_{IB} revealed an even lower K_D of 3.84 nM (\pm 1.98 nM), indicating higher affinity.

In conclusion, several approaches were used to analyse the interaction between PorB_{IA} and SREC-I, however these methods proved to be not suitable for the analysis, which might be caused by unspecific protein binding.

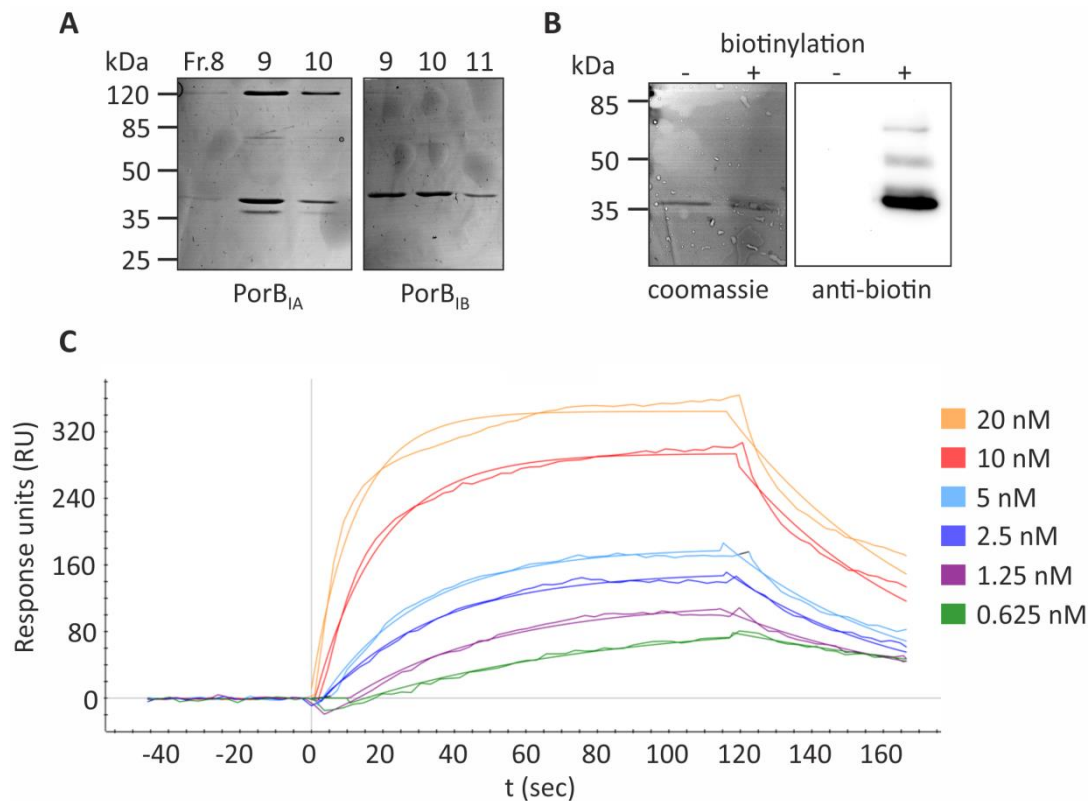


Figure 3.8: SREC-I binds to PorB_{IA} in a concentration-dependent manner. (A) PorB_{IA} and PorB_{IB} were isolated under native conditions from N2011 and N924, respectively. Gel filtration chromatography was applied as a final purification step and the proteins from three fractions (Fr.) were analysed without heat denaturation by SDS-PAGE and coomassie staining. (B) PorB_{IA} was examined before (-) and after (+) biotinylation with SDS-PAGE and western blot using an anti-biotin antibody. (C) The biotinylated PorB_{IA} was immobilized on the surface of the NeutrAvidin coated BioSensor Chip CM5. The solubilized SREC-I-Fc was injected over the PorB_{IA} surface in concentration ranging from 0.625 to 20 nM (indicated by different colours). The *in vitro* protein-protein interaction was analysed by SPR at the Biorad ProteOn XPR36.

3.1.5 Generation of antibodies against Omp85, PorB_{IA} and PorB_{IB}

A part of this work was dedicated to generation of antibodies specific for neisserial outer membrane proteins PorB_{IA}, PorB_{IB} and Omp85. To this end, proteins were expressed as a His-tagged fusions in *E. coli* and purified using affinity chromatography (Figure 3.9A). The purified proteins were sent to a company for the production of polyclonal antibodies in rabbits.

Additionally, a peptide antibody specific for PorB_{IB} was generated. The peptide corresponding to the sequence SGKFTGNVLEISGMAREHRYL was specific for PorB_{IB}. The

purified antibodies were tested in western blot (Figure 3.9B-E). They recognized both the purified proteins and the proteins in bacterial lysates with high affinity. The PorB antibodies, however, detected both proteins, while only the PorB_{IB} peptide antibody was specific for PorB_{IB}, as expected.

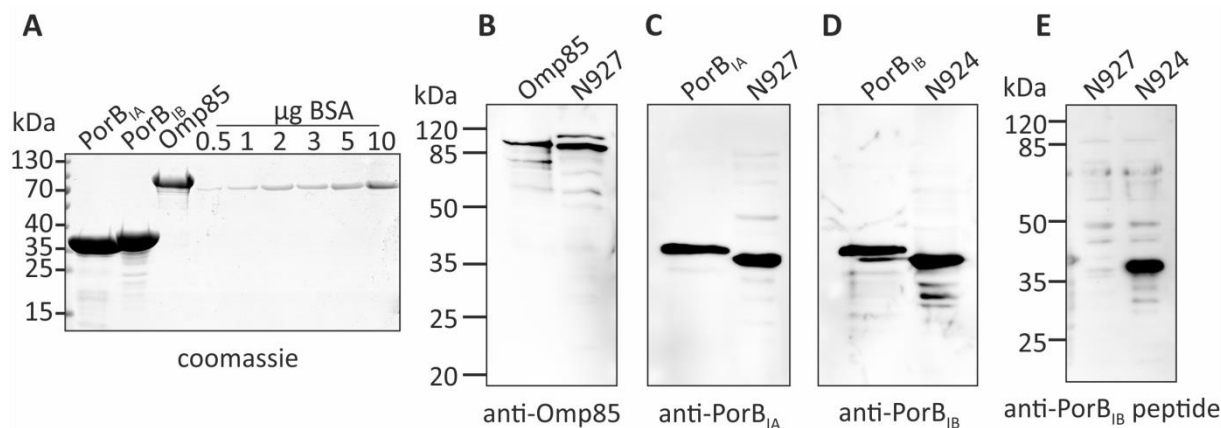


Figure 3.9: Generation of antibodies against PorB_{IA}, PorB_{IB} and Omp85. (A) The neisserial genes *porB_{IA}*, *porB_{IB}* and *omp85* were cloned in the vector pet15b resulting in a His-tagged fusion at the N-terminus. The protein expression was induced by 1 mM IPTG and the purification was done under denaturing conditions using the HisTrap column and the Äkta chromatography system. The protein concentration was determined with a BSA concentration gradient by performing SDS-PAGE and coomassie staining. The proteins were sent for production of polyclonal antibodies in rabbits. (B-E) The generated antibodies were purified and were tested in western blot. The purified proteins Omp85 (B), PorB_{IA} (C) and PorB_{IB} (D) were loaded next to bacterial lysates. Additionally, a PorB_{IB} peptide antibody was obtained and tested in western blot (E).

3.2 Screening for inhibitors of *N. gonorrhoeae* and *C. trachomatis*

N. gonorrhoeae and *C. trachomatis* are the most prevalent sexually transmitted pathogens worldwide. Due to the increased resistance of *N. gonorrhoeae* to nearly all available antibiotics and the high *C. trachomatis* infection and re-infection rates, this study aimed to identify novel antimicrobial agents against these two pathogens. Therefore, 68 different small molecule compounds including plant-derived compounds, pipercolic acid derivatives and substances from sponges or sponge-associated bacteria were screened for their bactericidal activities against *N. gonorrhoeae* and *C. trachomatis*. Especially, inhibitors of the PorB_{IA}-mediated invasion were in the focus of the work and the PorB_{IA}-expressing strain N927 was used for the screening. The N927 bacteria were stained with SNARF and were used to infect Chang cells, which were pre-treated with the compounds, under low-phosphate conditions in the presence of the compounds. For the screening in chlamydial infections, a GFP-expressing strain was used to infect pre-treated HeLa cells in the presence

of the small molecules. Subsequently, the cells were fixed, and nuclei and actin cytoskeleton stained. The analysis was performed by the automated fluorescence microscope Operetta. The output assessed the amount of intra- and extracellular bacteria per cell for *Neisseria* infection and the inclusion surface area per host cell surface area for *C. trachomatis* infection. Furthermore, the percentage of *Neisseria* per cell and chlamydial inclusion surface area per cell surface area relative to the DMSO control, respectively, were calculated. The compounds were tested in the three different concentrations of 1.6, 8 and 40 μM . Figure 3.10 shows examples for screening results of the substance CJ118 in *N. gonorrhoeae* infection and GP-RP-6 in chlamydial infection. Phosphate and tetracycline were used as positive controls during infection with *Neisseria* and *Chlamydia*, respectively.

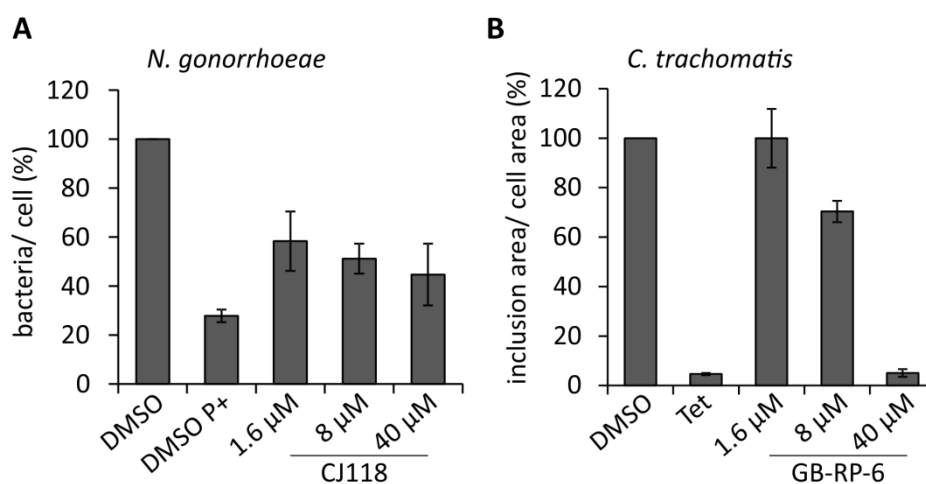


Figure 3.10: CJ118 and GB-RP-6 inhibit infection of *N. gonorrhoeae* and *C. trachomatis*, respectively. (A) Chang cells were infected with SNARF stained *N. gonorrhoeae* (N927) at MOI 100 for 1 h in the presence of DMSO, 1.6, 8 and 40 μM CJ118. The total number of bacteria was determined by automated fluorescence microscopy. The values referred to the DMSO control, which was set to 100 %. Phosphate (P+) was added as a negative control. (B) HeLa cells were infected with GFP-expressing *C. trachomatis* at MOI 1 for 24 h in the presence of DMSO, tetracycline (Tet), and 1.6, 8 and 40 μM GB-RP-6. DMSO was used as a negative control, and tetracycline as a positive control at 11.25 μM . The analysis was done by automated fluorescence microscopy. The graph represents mean values \pm SD of the inclusion surface area relative to the cell surface area from three technical replicates.

The results of the highest concentration (40 μM) were the criterion for the distribution of the compounds into the categories bioactive, moderately active and inactive (Table 3.1, 3.2). A compound was considered as active (green) against the bacteria when the number of *N. gonorrhoeae* or the chlamydial inclusion surface area was decreased by more than 70 %. A reduction of 40 - 70 % (yellow) was classified as moderate effect. A substance was categorized as inactive if 40 μM of a substance resulted in a decrease of less than 40 %

(red). When cell death was observed during the screening procedure the compound was rated as cytotoxic and was excluded from the categorization.

The screen led to the identification of seven active compounds against *C. trachomatis*, eight moderately effective substances against *Chlamydia* and seven against *N. gonorrhoeae*. However, none of the tested compounds decreased the neisserial infection by 70 % and thus, none was considered active. Five of the substances showing a moderate effect on *N. gonorrhoeae* were pipecolic acid derivatives such as CJ118 (Figure 3.10A) and two extracts from marine sponges. While the naphthoquinones did not affect *Neisseria* at all, four of them had a strong (Figure 3.10B) and three a moderate negative impact on the growth of *C. trachomatis*. Furthermore, four pipecolic acid derivatives and three sponge- and sponge-associated bacteria-derived substances affected the bacterial inclusion development.

Table 3.1: Overview of the screening results

pathogen	plant	pip. acid	sponge	
<i>N. gonorrhoeae</i>	0	0	0	% of infection reduction ≥ 70 % ≥ 40 % < 40 %
	0	5	2	
	8	22	10	
<i>C. trachomatis</i>	4	0	3	
	3	5	0	
	13	25	12	

Plant-derived small molecules (Plant), pipecolic acid derivatives (Pip. acid) and compounds extracted from marine sponges or sponge-associated bacteria (Sponge) were tested in infection of *N. gonorrhoeae* and *C. trachomatis*. An active compound (green) against the bacteria decreased the number of *N. gonorrhoeae* or the chlamydial inclusion surface area by more than 70 % at a concentration of 40 μ M. A reduction of 40 - 70 % was classified as moderate effect (yellow). A compound was categorized as inactive (red) when it decreased the infection by less than 40 %. The numbers in the cells represent the amount of compounds showing a specific percentage of infection reduction.

Table 3.2: Results of the screening for inhibitors against *N. gonorrhoeae* and *C. trachomatis*

compound	information	anti <i>Ngo</i>	anti <i>Ctr</i>
GB-RP-6	naphthoquinone ¹		
GB-RP-7	chrysophanol ¹		
GB-RP-8	naphthylisoquinoline alkaloids ¹		
GB-RP-9	michellamin A ¹	toxic	toxic
GB-RP-10	8-aminoquinoline ¹	toxic	toxic
GB-RP-11	naphthoquinone ¹		
GB-RP-12	naphthoquinone ¹	toxic	toxic
GB-RP-13	naphthoquinone ¹		
GB-RP-14	naphthoquinone ¹	-	
GB-RP-15	naphthoquinone ¹	-	toxic
GB-RP-16	naphthoquinone ¹	-	
GB-RP-17	naphthoquinone ¹	-	toxic
GB-RP-18	naphthoquinone ¹	-	
GB-RP-19	naphthoquinone ¹	-	toxic
GB-RP-20	naphthoquinone ¹	-	toxic
GB-RP-21	naphthoquinone ¹	-	
GB-RP-22	naphthoquinone ¹	-	toxic
GB-RP-23	naphthoquinone ¹	-	toxic
GB-RP-24	naphthoquinone ¹	-	toxic
GB-RP-25	naphthoquinone ¹	-	
CJ57	pipecolic acid derivative ²		
CJ73	pipecolic acid derivative ²		
CJ74	pipecolic acid derivative ²		
CJ84	pipecolic acid derivative ²		
CJ114	pipecolic acid derivative ²		
CJ118	pipecolic acid derivative ²		
CJ183	pipecolic acid derivative ²		
CJ208	pipecolic acid derivative ²		
FS55	pipecolic acid derivative ²	toxic	toxic
SF12	pipecolic acid derivative ²		
SF30	pipecolic acid derivative ²		
SF110	pipecolic acid derivative ²		
SF181	pipecolic acid derivative ²		
SF84	pipecolic acid derivative ²		
SF45	pipecolic acid derivative ²		

Compound	information	anti <i>Ngo</i>	anti <i>Ctr</i>
CJ89	pipecolic acid derivative ²		
CJ103	pipecolic acid derivative ²		
CJ120	pipecolic acid derivative ²		
CJ257	pipecolic acid derivative ²		
CJ248	pipecolic acid derivative ²		
CJ198	pipecolic acid derivative ²		
SF10	pipecolic acid derivative ²		
SF11	pipecolic acid derivative ²		
SF130	pipecolic acid derivative ²		
SF170	pipecolic acid derivative ²	toxic	toxic
SF233	pipecolic acid derivative ²		
SF275	pipecolic acid derivative ²		
SF171	pipecolic acid derivative ²	-	
SF263	pipecolic acid derivative ²	-	
SF260	pipecolic acid derivative ²	-	toxic
UR1	extract from marine sponges ³		
UR2	extract from marine sponges ³		
UR3	extract from marine sponges ³	toxic	-
UR4	extract from marine sponges ³	toxic	-
UR5	extract from marine sponges ³	toxic	-
UR6	extract from marine sponges ³		
UR7	extract from marine sponges ³		
UR8	pure compound from marine sponges ³	toxic	toxic
UR9	pure compound from marine sponges ³		
UR10	pure compound from marine sponges ³		
Gelliusterol E	acetylenic sterol ³		
SF2446A2	naphthacene glycoside ³		
L1	pure compound from marine sponges ³	-	
L2	pure compound from marine sponges ³	-	toxic
L3	pure compound from marine sponges ³	-	
Ageloline A	quinolinone ³	-	
UB	pure compound from marine sponges ³	-	toxic
UC	pure compound from marine sponges ³	-	

The screened compounds are listed with name and information about their structural class or background. Plant-derived small molecules (1), pipecolic acid derivatives (2) and extracts or pure compounds of marine sponges or sponge-associated bacteria (3) were tested in *N. gonorrhoeae* (Ngo) and *C. trachomatis* (Ctr) infection of epithelial cells. Compounds that revealed cytotoxicity were marked with 'toxic'. Active compounds (green) reduced the infection by more than 70 %, moderately active (yellow) by 40 - 70 % and inactive (red) decreased the infection by less than 40 % at a concentration of 40 μ M.

3.3 Inhibitors of neisserial and chlamydial MIP

3.3.1 PipN3 and PipN4 inhibit the PPIase activity of Ng-MIP and Ctr-MIP

It has been demonstrated that the peptidyl prolyl *cis-trans* isomerase MIP, identified in various pathogenic protozoans and bacteria such as *N. gonorrhoeae* and *C. trachomatis*, is associated with virulence. Thus, the protein was considered a possible therapeutic drug target. Small-molecule pipercolic acid derivatives were designed in the group of Prof. Ulrike Holzgrabe (Institute for Pharmacy and Food Chemistry, University of Würzburg), exhibiting inhibitory activity against the Lp-MIP and BpML1 without having immunosuppressive features (Juli *et al.*, 2011, Begley *et al.*, 2014). In this study 30 different pipercolic acid derivatives were screened for their inhibitory effect against infection of *N. gonorrhoeae* and *C. trachomatis*. Several of them were categorized as active or moderately active. However, it could not be concluded if they targeted the bacterial MIP protein or were effective due to other side effects. Therefore, the selected active or moderately active pipercolic acid derivatives were further analysed for their impact on the neisserial and chlamydial MIP protein in a protease α -chymotrypsin-based assay, which measured the PPIase activity of the proteins in the presence of the compounds.

In order to purify the MIP proteins for the PPIase activity assay, the *ng-mip* (from genomic DNA of N927) and *ctr-mip* (from genomic DNA of *C. trachomatis* L2) were cloned in the expression vector pet15b without signal peptide. The expression of the N-terminally His-tagged recombinant proteins was induced with IPTG. The analysis of the solubility of the expressed proteins revealed that both MIPs exist not only as insoluble proteins in inclusion bodies but also as soluble proteins in the supernatant (Figure 3.11A, C). The proteins were purified under native conditions using affinity chromatography, anion-exchange chromatography and gel filtration (Figure 3.11B, D). The His-tag of Ng-MIP could be removed by thrombin cleavage, which was not possible for Ctr-MIP.

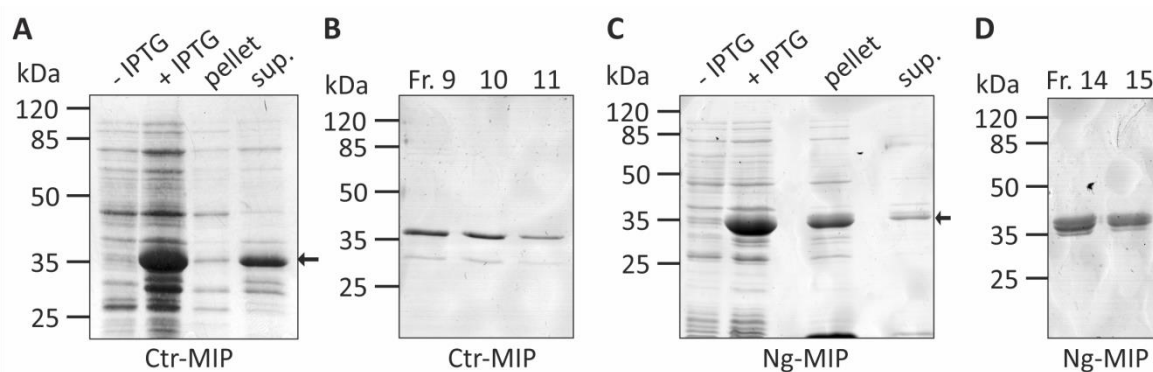


Figure 3.11: Purification of recombinant His-tagged Ctr-MIP and Ng-MIP under native conditions. (A, C) The protein expression of Ctr-MIP (A) and Ng-MIP (C) was induced in *E. coli* (BL-21) transformed with pet15b vectors containing *ctr-mip* or *ng-mip* without signal peptide. The IPTG (1 mM) induction was performed for 4 h in liquid culture. The solubility of the proteins was determined by sonification and subsequent centrifugation. The pellet (insoluble) and supernatant (sup., soluble) were analysed by SDS-PAGE and coomassie staining. (B, D) The final purification step of Ctr-MIP (B) and Ng-MIP (D) was performed using gel filtration. The protein-containing fractions (Fr.) were pulled together and concentrated applying an Amicon® Ultra Centrifugal Filter. The analysis was done by SDS-PAGE and coomassie staining.

The PPlase activity of Ng-MIP and Ctr-MIP was measured in the presence of increasing concentrations of the pipercolic acid derivatives. The known MIP inhibitor rapamycin was used as a positive control. The IC_{50} was determined, which is the compound concentration inhibiting the PPlase activity by 50 %. Eight of ten measured compounds were shown to inhibit the PPlase activity in the range between 0.2 μM (lowest) and 15.8 μM (highest) (Table 3.3). Rapamycin had an IC_{50} of 0.0158 μM (\pm 0.0042) for neisserial and 0.0079 μM (\pm 0.0006) for chlamydial MIP. Especially the compounds SF10 and SF11 exhibited an extraordinary low IC_{50} . SF10 showed an IC_{50} of 0.0956 μM (\pm 0.022) for Ng-MIP and 0.0646 μM (\pm 0.011) for Ctr-MIP, and SF11 an IC_{50} of 2.79 μM (\pm 0.78) for Ng-MIP and 0.241 μM (\pm 0.031) for Ctr-MIP (Table 3.3, Figure 3.12). For this reason, both compounds were in the focus of further analysis. The structural difference between the pipercolic acid derivatives was the NO_2 group, which was located either in *meta* (3) or *para* (4) position at the benzene ring (Figure 3.12). Thus, the compounds were renamed to PipN4 (SF10) and to PipN3 (SF11).

Table 3.3: IC₅₀ of pipecolic acid derivatives on Ng-MIP and Ctr-MIP

Compound	IC ₅₀ (μM) Ng-MIP	IC ₅₀ (μM) Ctr-MIP
CJ183	5.1 (± 0.2)	6.3 (± 0.6)
SF45	0.274 (± 0.020)	0.179 (± 0.014)
CJ103	> 50	> 50
CJ120	> 50	> 50
CJ257	10.1 (± 2.1)	15.8 (± 4.6)
CJ248	8 (± 1.4)	18.1 (± 2.1)
CJ198	7.4 (± 2.1)	4.5 (± 1.4)
PipN4 (SF10)	0.0956 (± 0.022)	0.0646 (± 0.011)
PipN3 (SF11)	2.79 (± 0.78)	0.241 (± 0.031)
SF275	3.8 (± 0.1)	3.1 (± 0.3)
Rapamycin	0.0158 (± 0.0042)	0.0079 (± 0.0006)

The concentration (IC₅₀ in μM) of pipecolic acid derivatives and rapamycin that reduced the PPIase activity of Ng-MIP and Ctr-MIP by 50 % was determined by a protease-coupled assay with the oligopeptide substrate succinyl-Ala-Leu-Pro-Phe-4-nitroanilide.

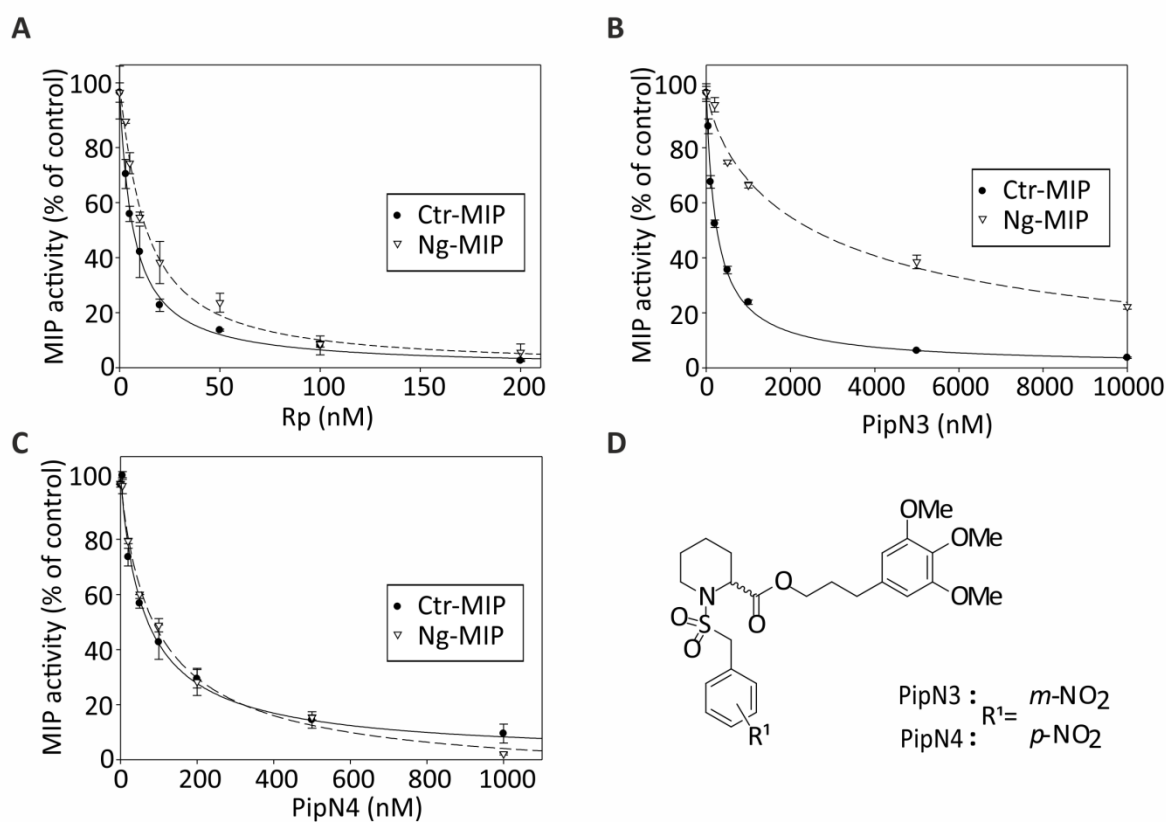


Figure 3.12: PipN3 and PipN4 inhibit the PPIase activity of the neisserial and chlamydial MIP. (A-C) The PPIase activity of the recombinant proteins Ctr-MIP and Ng-MIP was analysed in the presence of increasing concentrations of rapamycin (Rp, A), PipN3 (B) and PipN4 (C). A protease-coupled assay with the oligopeptide substrate succinyl-Ala-Leu-Pro-Phe-4-nitroanilide was used to determine the

enzyme activity. The data were normalized to a DMSO-containing control and represented as means \pm SD of three independent measurements. (D) Structure of the pipercolic acid derivatives PipN3 and PipN4.

3.3.2 PipN3 and PipN4 decrease chlamydial infection in a dose-dependent manner

The pipercolic acid derivatives of interest PipN3 and PipN4 showed moderate activity against *C. trachomatis* during the compound screen, while no effect could be observed on *N. gonorrhoeae*. To verify the screening results for *C. trachomatis*, HeLa cells were infected in the presence of the compounds and rapamycin. Both inhibitors decreased the chlamydial inclusion surface area significantly by approximately 40 - 45 % at 30 and 40 μ M compared to the DMSO control (Figure 3.13). Rapamycin was applied as a positive control and reduced the inclusion surface area in a dose-dependent manner significantly by 74.3 % at 20 μ M.

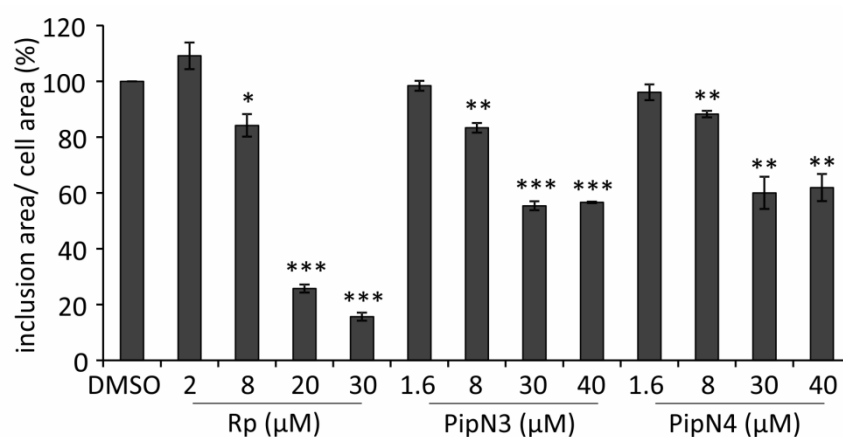


Figure 3.13: PipN3 and PipN4 decrease chlamydial inclusion surface area in a dose-dependent manner. HeLa cells were infected with GFP-expressing *C. trachomatis* at MOI 1 for 24 h in the presence of DMSO and an appropriate concentration (in μ M) of rapamycin (Rp), PipN3 and PipN4. The cells were fixed and stained with DAPI and Phalloidin647. The inclusion surface area per cell surface area was determined by automated fluorescence microscopy. The graph represents mean values \pm SD of three technical replicates in relation to DMSO control at 100 %. * p <0.05, ** p <0.01, *** p <0.0005

A PI cytotoxicity assay was performed to determine a working concentration of the inhibitors that exhibited no cytotoxic effect on the cells. Therefore, HeLa229 cells were incubated for 48 h with the inhibitors before performing the PI assay. The percentage of PI positive and therefore dead cells was under 20 %, indicating a low cytotoxic effect of the compounds. 5 μ M was the highest concentration that showed no cytotoxicity and was applied in further experiments (Figure 3.14).

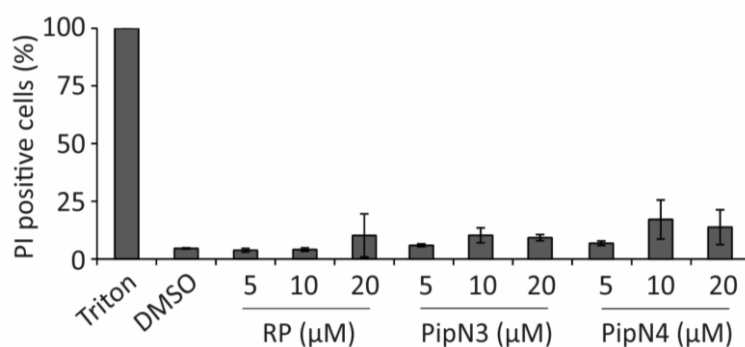


Figure 3.14: 5 μM is the highest non-cytotoxic concentration of rapamycin, PipN3 and PipN4. HeLa cells were treated for 48 h with 5, 10 and 20 μM rapamycin (Rp), PipN3 and PipN4. The amount of dead cells was determined using PI staining and flow cytometry. 0.1 % Triton was used as a positive control and was set to 100 %. The graph shows mean values ± SD of three independent experiments.

3.3.3 PipN3 and PipN4 affect chlamydial developmental cycle

The pipercolic acid derivatives PipN3 and PipN4 have been shown to reduce the primary *C. trachomatis* infection and inhibit the PPIase activity of the neisserial and chlamydial MIP. The effect of the compounds was further investigated on the chlamydial progeny. To this purpose, two HeLa 12 well plates per experimental approach were infected with *C. trachomatis* for 48 h. In the first approach, the compounds and rapamycin were added either in the beginning, 8 h or 24 h post-infection (Figure 3.15A). In the other approach, the MIP inhibitors were removed 8, 24 and 33 h after infection by washing out with fresh medium (Figure 3.15C). The first plate was lysed 48 h post-infection in 2 x Laemmli and served for analysis of the primary infection. The infected cells of the second plate were lysed with glass beads and the newly developed chlamydial progeny was used to infect fresh HeLa cells. These were lysed 24 h post-infection with 2 x Laemmli. The analysis of the primary and progeny infection was done by western blot (Figure 3.15A, C) and immunofluorescence (Figure 3.15B, D, E).

It was observed that the presence of rapamycin and the MIP inhibitors during infection affected the chlamydial progeny infectivity even when the compounds were added 24 h post-infection (Figure 3.15B). Rapamycin reduced the number of inclusions by 73.7 %, while the addition of PipN3 and PipN4 led to a decrease of averagely 63.4 % in inclusion number when added in the beginning of the infection (Figure 3.15B, E). The removal of the compounds during infection resulted in a recovery of the chlamydial progeny, thus leading to a restored progeny infectivity (Figure 3.15C). When the compounds were removed 8 h

post-infection, a reduction of only 20 - 30 % in inclusion number could be observed, while the removal 33 h after infection decreased the inclusion number by 30 - 40 % (Figure 3.15D).

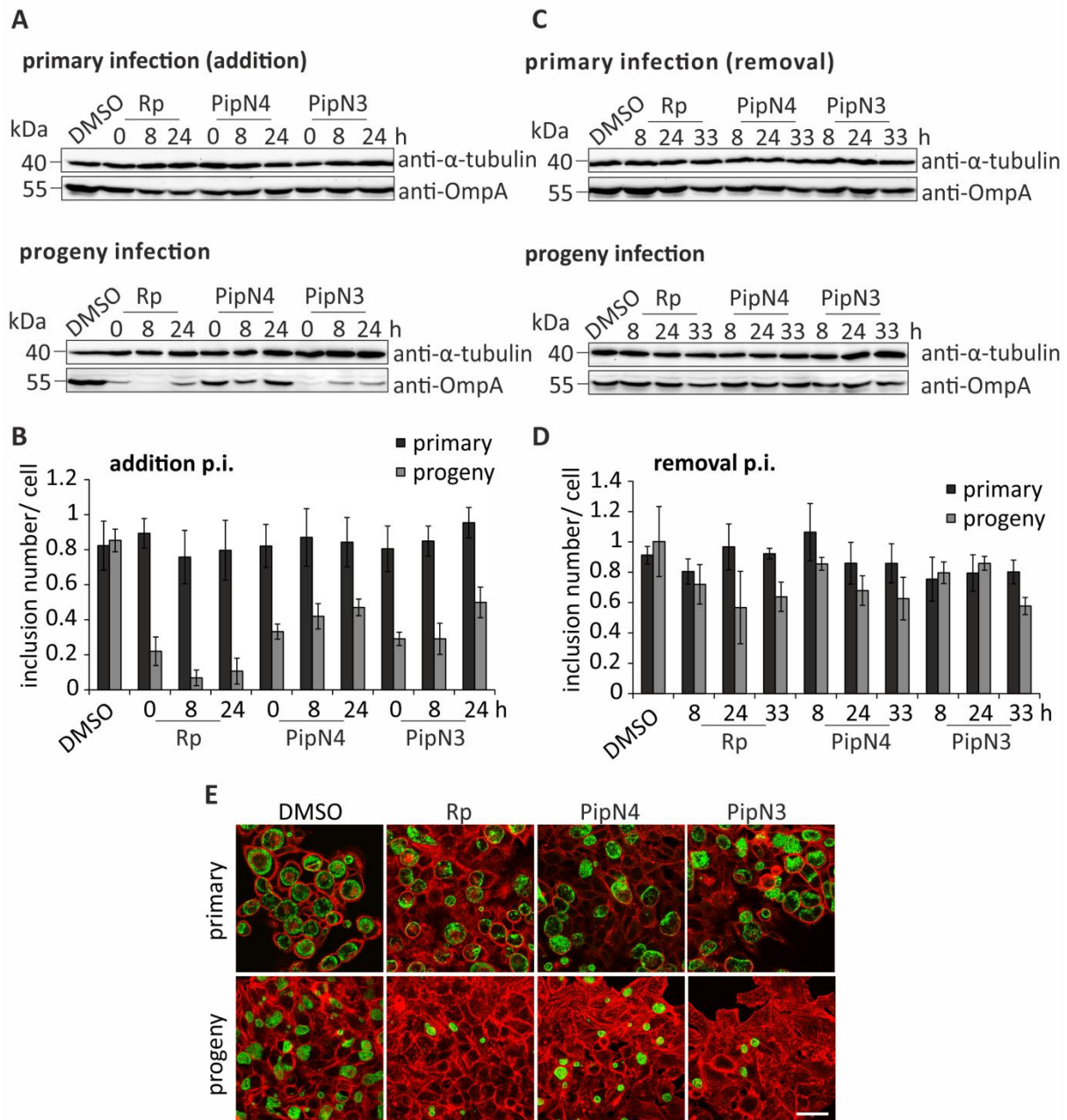


Figure 3.15: PipN3 and PipN4 affect infectivity of chlamydial progeny in a reversible manner. (A, B) Two replicates of HeLa cells were infected at MOI 1 for 48 h with *C. trachomatis* in the presence of DMSO or 5 μ M rapamycin, PipN3 and PipN4. The MIP inhibitors were added in the beginning of the infection (0 h) and 8 h or 24 h post-infection. One replicate was lysed in 2 x Laemmli buffer after 48 h for analysis of the primary infection. The other replicate was lysed after 48 h and the lysate was used to infect new HeLa cells. These were lysed with 2 x Laemmli buffer 24 h post-infection for examination of the progeny infection. The infection was analysed by SDS-PAGE and western blot using antibodies against α -tubulin as a loading control or OmpA to determine the chlamydial content (A). The experiments from A were performed in parallel on coverslips and the infection was analysed by immunofluorescence staining using antibodies against cHSP60 (green) and Phalloidin555 (red). Inclusions from 300 cells were counted at the microscope and normalized to the cell number (B). (D, E) Experiments were done as described for A and B with the difference that rapamycin, PipN3 and

PipN4 were added in the beginning of the infection and were removed by washing 8, 24 and 33 h post-infection. (E) Cells infected in the presence of DMSO or 5 μ M Rp, PipN3 and PipN4 were either fixed 48 h post-infection (primary infection) or lysed to infect new HeLa cells (progeny infection) and then fixed. The staining was performed as described for B. The experiments of B and D were performed in three technical replicates, representing mean values \pm SD, which were normalized to the DMSO control. Scale bar: 50 μ m

It has been demonstrated that rapamycin and the MIP inhibitors PipN3 and PipN4 affected the chlamydial developmental cycle, which resulted in less infectious and viable progeny (Figure 3.15). To analyse this effect, bacterial particles within the inclusions treated for 48 h with the compounds were analysed by electron microscopy (Figure 3.16). The percentage of EBs, RBs and Abs was determined by counting bacteria in 100 inclusions per sample (Figure 3.16E). In the DMSO control an inclusion contained 60.7 % EBs and 39.3 % RBs. This ratio is changed upon treatment with rapamycin to 37.2 % EBs and 50.7 % RBs. This trend could also be observed for the PipN3- and PipN4-treated cells. Furthermore, the number of ABs was increased to 12.2 % for rapamycin and to 5 - 6 % in the presence of PipN3 and PipN4. Besides enlarged Abs, other membranous structures could be detected, which appeared as empty, small, but also expanded bacterial particles.

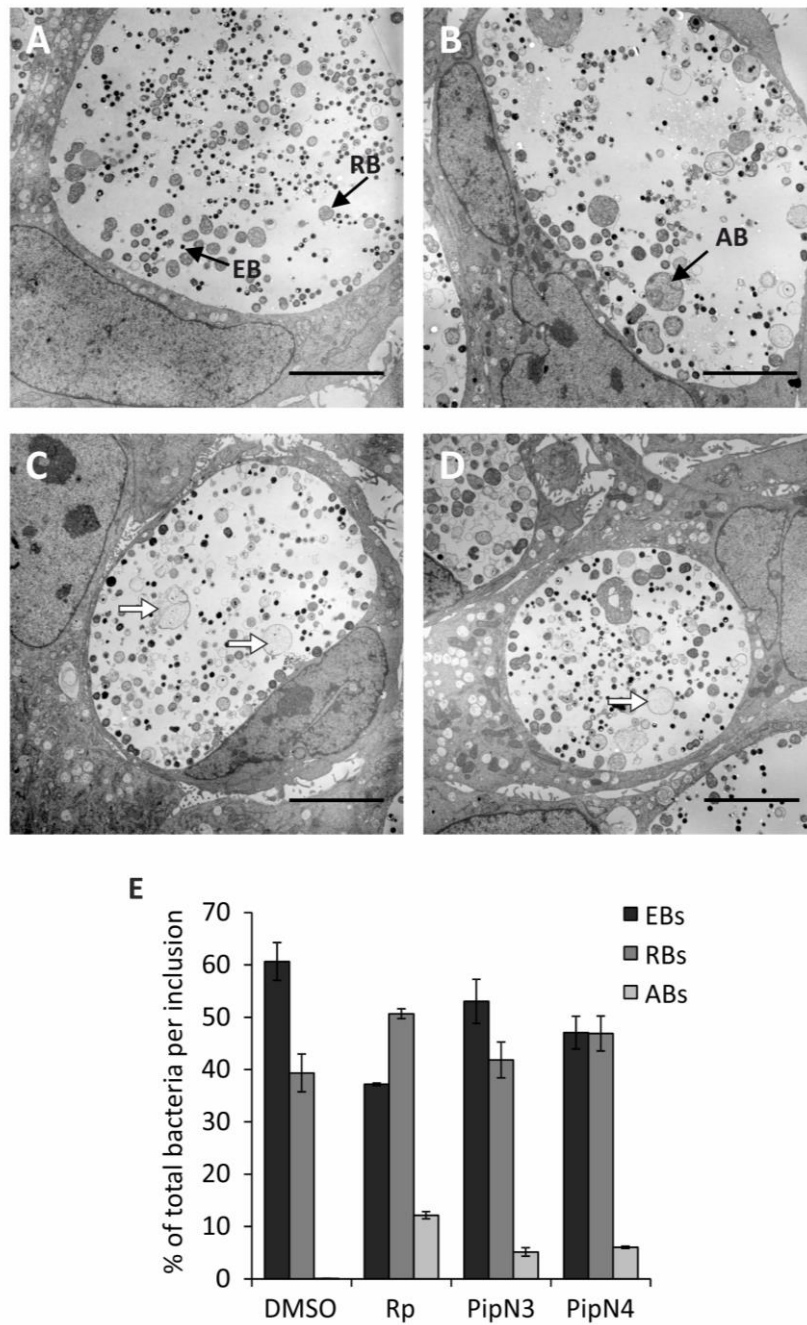


Figure 3.16: PipN3 and PipN4 change the content of chlamydial inclusions. (A-D) HeLa cells were infected at MOI 1 for 48 h in the presence of DMSO (A), rapamycin (B), PipN3 (C) and PipN4 (D). The cells were fixed and analysed by TEM. (E) The percentage of the mean number of EBs, RBs and ABs from the samples A - D was determined by counting the particles in 100 inclusions. Scale bar: 5 μ M. White arrows mark empty membrane vesicles. EB, elementary body. RB, reticulate body. AB, aberrant body.

3.3.4 PipN3 and PipN4 decrease the survival of *N. gonorrhoeae* in neutrophils

It could be demonstrated that mutagenesis of *L. pneumophila* MIP resulted in decreased survival of the pathogen in macrophages (Cianciotto & Fields, 1992). Likewise, the knockdown of the *N. gonorrhoeae* MIP led to a reduced intracellular survival in macrophages (Leuzzi *et al.*, 2005). However, since PMNs are the first line of defence during a *Neisseria* infection and the bacteria are not only able to survive in PMNs but can even replicate intracellularly, the role of Ng-MIP was investigated during infection of PMNs (Criss *et al.*, 2009, Casey *et al.*, 1986, Simons *et al.*, 2005).

In order to analyse if Ng-MIP is involved in PMN infection, a MIP deletion mutant (Δmip) was generated by site-directed mutagenesis in the strain N2009. Additionally, a complementation strain (Δmip^C) was produced using the plasmid pLAS::pPIIEmCherry, which enabled the integration of the *mip* gene in the non-coding region between NGFG_01468 and NGFG_01471 of Δmip . The knockdown and the complementation could be verified by q-RT-PCR (Figure 3.17A). Δmip^C has been shown to express slightly more *mip* compared to the wild type strain (N2009). In addition, the growth of the mutant strains was analysed by OD measurement (Figure 3.17B). The knockout mutant exhibited a growth defect only after 180 min of growing in liquid culture. However, the normal growth could be restored by complementation, since the strain Δmip^C grew similarly to the wild type. Next, these mutant strains and the wild type were used to infect PMNs isolated from venous human blood, which were attached to the surface of 24 well plates by centrifugation. The infection was performed for 1 h at MOI 50, and after washing, the cells were incubated for further 2 h. The survival of Δmip was significantly reduced by 28.7 % (Figure 3.17C). The complementation of the deletion, however, restored the wild type phenotype (Figure 3.17D). The survival of Δmip^C was even slightly increased in comparison to the wild type by 35.5 %, albeit not significantly, due to high standard deviation.

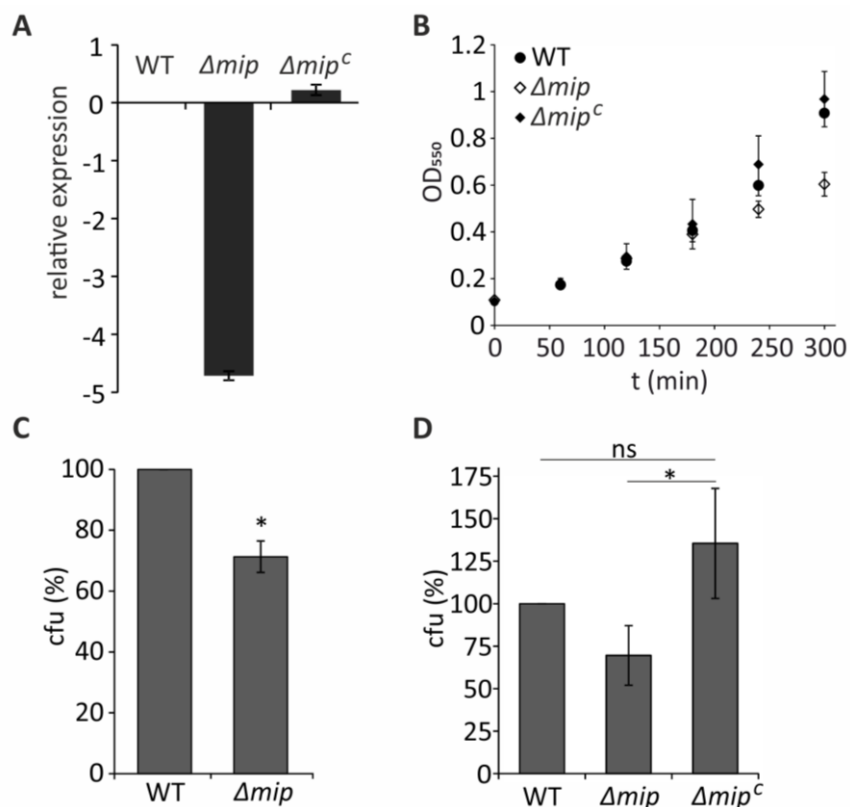


Figure 3.17: The knockout of neisserial *mip* affects survival of *N. gonorrhoeae* in PMNs. (A) Q-RT-PCR was performed to measure the RNA levels of *ng-mip* in WT (N2009), Δmip and Δmip^C . (B) Growth curves of neisserial wild type (WT), MIP knockout mutant (Δmip) and the complementation strain (Δmip^C) were generated by measuring the OD₅₅₀ in liquid culture for 300 min every 60 min. (C, D) PMNs were infected with WT, Δmip or Δmip^C at MOI 50 for 2 h. The cells were lysed, plated on GC agar and the cfus determined by counting. The graphs represent means \pm SD values from three independent experiments which were normalized to the WT. ns not significant, * $p < 0.05$

We could demonstrate that Ng-MIP played a role in the bacterial survival in the presence of PMNs (Figure 3.17). However, it could not be concluded if the MIP protein itself or its PPIase activity was required for the prolonged survival. To investigate the role of the PPIase activity, the pipecolic acid derivatives PipN3 and PipN4 and rapamycin, as a positive control, were applied. Initially, the growth behaviour of bacteria was analysed in the presence of the MIP inhibitors (Figure 3.18A), but no growth defect could be observed. The compounds were then added during infection to analyse if the inhibition of the neisserial PPIase would affect the survival of *Neisseria* in PMNs. All compounds reduced bacterial survival significantly. The bacterial amount was decreased by 34.7 % in the presence of rapamycin, by 25.6 % of PipN3 and by 16.7 % when PipN4 was added (Figure 3.18B).

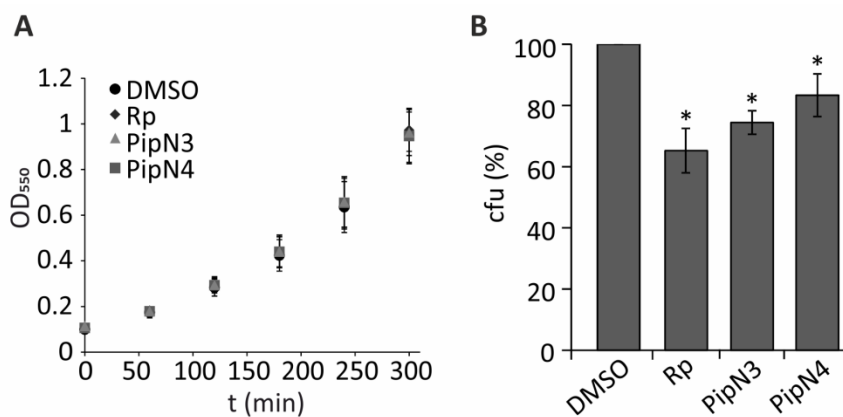


Figure 3.18: PipN3 and PipN4 inhibit survival of *N. gonorrhoeae* in PMNs. (A) Neisserial wild type strain (N2009) was grown in liquid culture in the presence of DMSO, rapamycin (Rp), PipN3 and PipN4. The OD was measured at 550 nm for 300 min every 60 min. (B) PMNs were infected in the presence of DMSO, Rp, PipN3 and PipN4 for 2 h. The neutrophils were lysed and the bacteria plated on GC agar. The cfus were determined by counting with a binocular. The graph represents mean values \pm SD of three independent experiments normalized to the DMSO control. * $p < 0.05$

3.3.5 Site-specific mutation of Ng-MIP inhibits PPIase activity

In previous studies site-directed mutagenesis of the Lp-MIP has been performed, in order to identify amino acids involved in the PPIase activity. The substitution of Tyr185 to Ala reduced the PPIase activity to 0.6 % and Asp142 to Leu to 5.3 % (Wintermeyer *et al.*, 1995). However, the deletion of the first 77 N-terminal amino acids, which harbour the dimerization domain, did not affect the activity (Kohler *et al.*, 2003). The same mutations were integrated in Ng-MIP to analyse if these amino acids and the dimerization domain play a similar role in the neisserial MIP. For this, the mutated Ng-MIP variants MIP ^{Δ 22-91} (dimerization domain), MIP^{D165L} (Lp-MIP: D142L) and MIP^{Y208A} (Lp-MIP: Y185A) were expressed in *E. coli* by induction with 1 mM IPTG for 4 h. The protein purification was performed similar to the wild type Ng-MIP protein under native conditions (Figure 3.19A, B). The PPIase activity was tested using the α -chymotrypsin-coupled assay. The deletion of the dimerization domain led to a decrease in the PPIase activity by 25 % in the monomeric MIP protein. The activity of MIP^{D165L} was strongly reduced to 11.6 % of the wild type Ng-MIP, while in the case of MIP^{Y208A} it was diminished to 1.1 % of the original activity (Figure 3.19C).

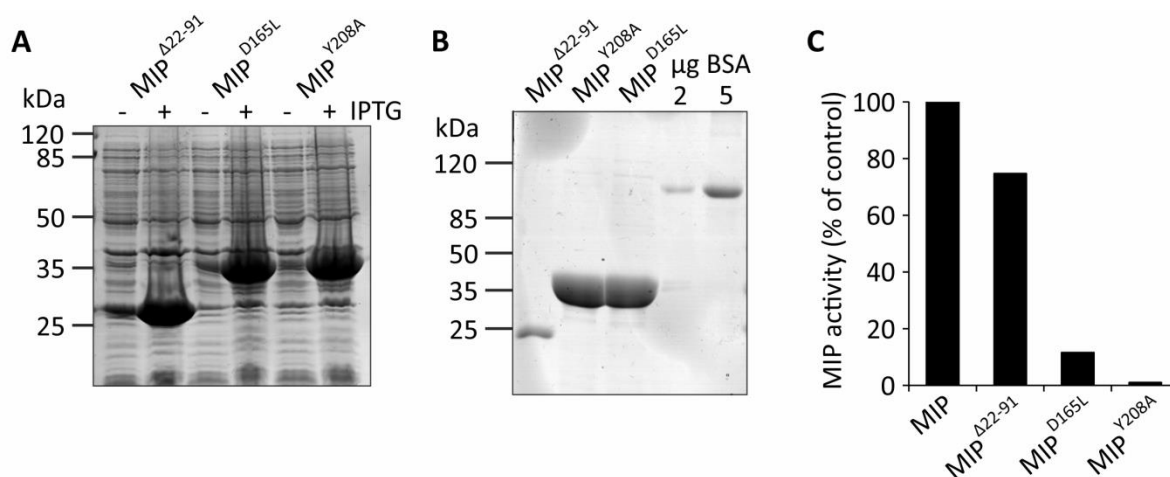


Figure 3.19: Expression, purification and activity assay of the His-tagged recombinant proteins MIP Δ 22-91, MIP^{D165L} and MIP^{Y208A}. (A) The protein expression of MIP Δ 22-91, MIP^{D165L} and MIP^{Y208A} was induced in *E. coli* (BL-21) by addition of 1 mM IPTG for 3 h in liquid culture. (B) The proteins were purified under native conditions and were analysed by SDS-PAGE and coomassie staining after gel filtration. 2 μ g and 5 μ g BSA were loaded to estimate the protein concentrations. (C) PPIase assay was performed with the purified recombinant Ng-MIP, MIP Δ 22-91, MIP^{D165L} and MIP^{Y208A}. The PPIase activity of the mutant MIP variants was normalized to the wild type MIP.

3.4 Analysis of the bioactive compound SF2446A2

3.4.1 Gelliusterol E and SF2446A2 inhibit chlamydial inclusion formation

Marine sponges are the source of a huge variety of secondary metabolites that exhibit antibacterial, antifungal and antiviral properties. Sponge-associated bacteria are also producers of numerous bioactive natural compounds. Within the scope of screening for inhibitors of *N. gonorrhoeae* and *C. trachomatis*, 18 different compounds, derived from sponges or sponge-associated bacteria were analysed. Since the two compounds gelliusterol E and SF2446A2 exhibited a strong antichlamydial activity, their IC₅₀ and impact on the chlamydial progeny was further investigated. Gelliusterol E (26,27-bisnorcholest-5,16-dien-23-yn-3 β ,7 α -diol) was isolated from the Red Sea sponge *Callyspongia aff. Implexa*, while the naphthacene glycoside SF2446A2 originated from *Streptomyces sp.* strain RV15 that was obtained from the Mediterranean sponge *Dysidea tupa*. The compound SF2446A2 (Figure 3.21A) has already been identified in 1988 and has been shown bioactivity against *S. aureus* and different *Mycoplasma* strains (Takeda *et al.*, 1988, Gomi *et al.*, 1988).

Both substances inhibited the chlamydial inclusion formation in a dose-dependent manner, whereas no inclusions could be detected at the highest applied concentration of 40 μ M (Figure 3.20A-C). The determined IC₅₀ of gelliusterol E was 2.34 μ M and of SF2446A2 2.61 μ M (Figure 3.20B, C). An EB progeny assay was performed to analyse the infectivity of

chlamydial progeny made by bacteria treated with DMSO, or 1.6 μM , 8 μM and 40 μM of the compounds. The results revealed a negative impact starting from 8 μM (Figure 3.20D, E). At 40 μM almost no infection could be established, which indicated a lack of viable and infectious progeny EBs.

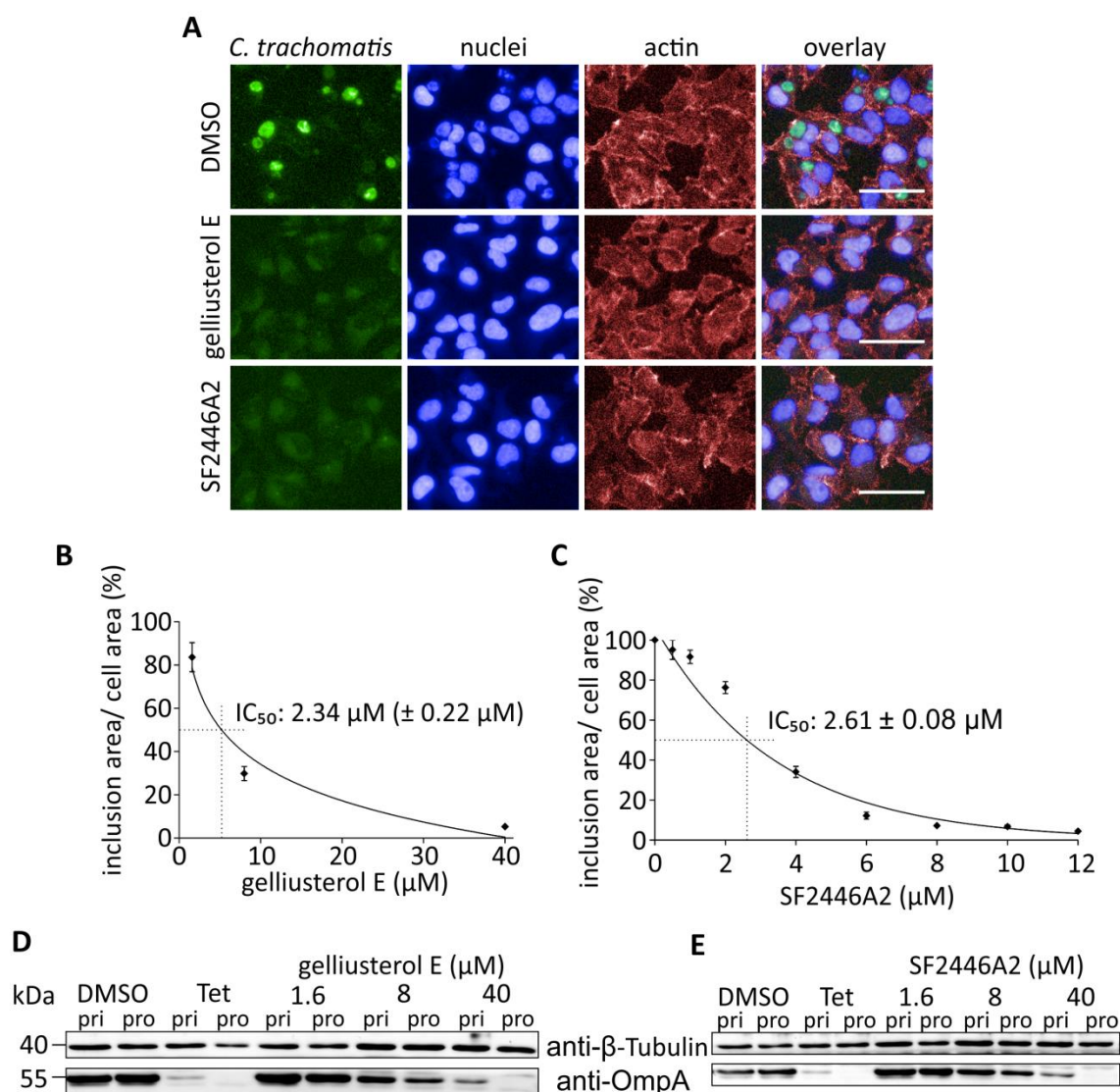


Figure 3.20: Gelliusterol E and SF2446A2 inhibit chlamydial inclusion formation and progeny. (A-C) HeLa cells were infected with GFP-expressing *C. trachomatis* (green) at MOI 1 for 24 h in the presence of DMSO or an appropriate concentration of gelliusterol E or SF2446A2 (40 μM for A). The cells were fixed and stained with DAPI (blue) and Phalloidin647 (red) and analysed by automated fluorescence microscopy (A). The graphs B and C represent mean values \pm SD of the inclusion surface area relative to the cell surface area from three independent experiments. The IC_{50} of gelliusterol E (B) and SF2446A2 (C) was calculated using a logarithmic trend line. The concentration of the compounds at 50 % of the relative inclusion surface area was determined as the IC_{50} . (D, E) HeLa cells were infected in duplicates with *C. trachomatis* for 24 h in the presence of DMSO, tetracycline (Tet), 1.6, 8 and 40 μM gelliusterol E (D) and SF2446A2 (E). One replicate was lysed in 2 x Laemmli buffer for analysis of the primary infection (pri). The other replicate was lysed after 48 h infection with glass beads. The lysate was used to infect fresh HeLa cells. These were lysed in 2 x Laemmli buffer 24 h post-infection and represented the progeny infection (pro). The lysates were analysed by SDS-PAGE

and western blot using antibodies against chlamydial OmpA and β -Tubulin as a loading control. Scale bar: 50 μ m

Both compounds were considered for further examinations, however due to the difficult isolation of a bigger amount of gelliusterol E, SF2446A2 was selected for further investigation of its mode of action. A cytotoxicity assay was performed to determine the non-cytotoxic working concentration using a PI staining and flow cytometry. Starting with 30 μ M, the amount of PI positive and therefore dead cells was increased. Thus, the applied concentrations in the following experiments were 20 μ M at maximum (Figure 3.21B).

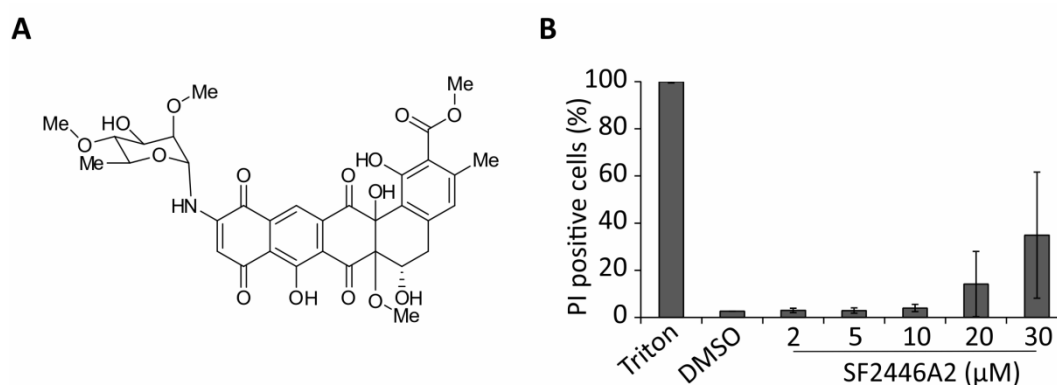


Figure 3.21: SF2446A2 shows cytotoxic activity in HeLa cell at concentrations greater than 20 μ M. (A) Structure of SF2446A2 with a molecular formula of $C_{34}H_{35}NO_{15}$ (Reimer *et al.*, 2015). (B) HeLa cells were treated for 24 h with DMSO, 2, 5, 10, 20 and 30 μ M SF2446A2. The cells were stained with PI and analysed by flow cytometry. 0.1 % Triton was used as a positive control for PI positive/ dead cells and was set to 100 %. The graph shows mean values \pm SD of three independent experiments.

3.4.2 Properties of SF2446A2

3.4.2.1 SF2446A2 affects fusion of chlamydial inclusions

The internalization of more than one *C. trachomatis* bacterium leads to homotypic fusion of single inclusions to one bacteria-containing vacuole. It was investigated whether SF2446A2 interferes with this process. HeLa cells were infected with *C. trachomatis* at MOI 1, 2, 4 and 10 in the presence of 20 μ M SF2446A2. Control cells were infected at MOI 1 and 10 and were treated with DMSO. Fusion of inclusions could be observed in DMSO treated cells, while it was inhibited in the presence of SF2446A2 (Figure 3.22). The infected cells mostly contained several small separated inclusions.

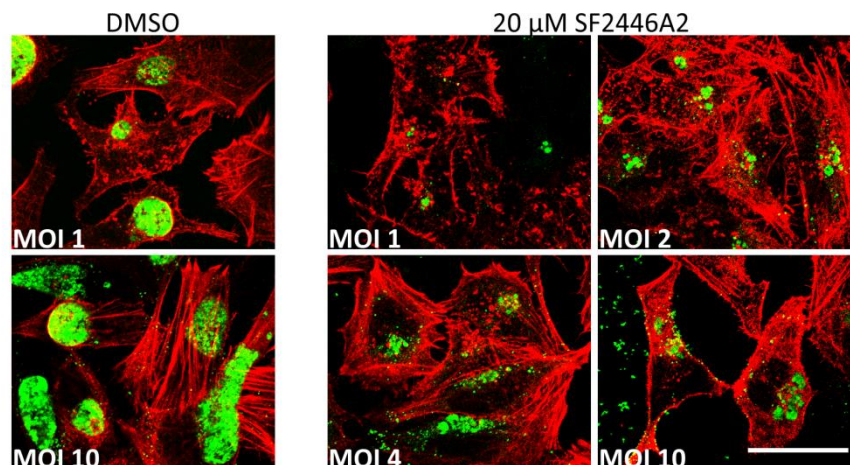


Figure 3.22: Fusion of chlamydial inclusions is inhibited in the presence of SF2446A2. HeLa cells were infected with *C. trachomatis* at MOI 1 and 10 for 24 h in the presence of DMSO and MOI 1, 2, 4 and 10 in the presence of 20 μ M SF2446A2. The cells were fixed and stained with Phalloidin555 (red) and an antibody against cHSP60 (green). Scale bar: 50 μ m

3.4.2.2 Antichlamydial effect of SF2446A2 is partially reversible

For further understanding of the compound dynamics during infection, two approaches were applied. In one approach 20 μ M SF2446A2 was added in the beginning of infection and 4 h, 8 h, 10 h and 16 h post-infection. The other approach comprised the removal of the compound 4 h, 8 h, 10 h and 16 h after infection. The cells were infected for 24 h and analysed by immunofluorescence (Figure 3.23A) and western blot (Figure 3.23B). The addition of SF2446A2 until 10 h post-infection reduced the infection strongly. However, 16 h after infection only a small negative effect was observed on the inclusion. The later the compound was added the more bacterial content could be detected. The effect of SF2446A2 could be reversed to some extent by removing the compound in the early time points of infection (4 h and 8 h). This was not the case after 10 h and 16 h post-infection.

The presence of the compound in the early time point of infection affected the bacteria more than the addition at latter time points. When SF2446A2 was added in the beginning of the infection and was removed after 8 h, the negative effect on the *Chlamydia* was stronger than the effect of the presence of the compound in the last 8 h of infection.

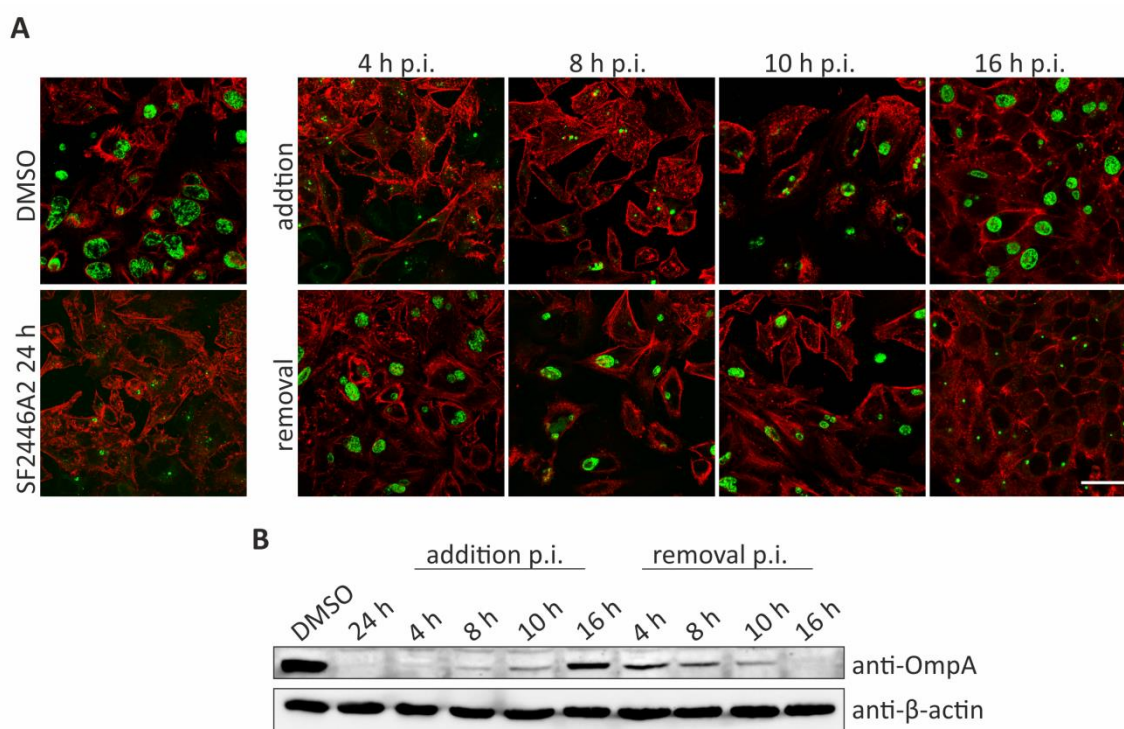


Figure 3.23: Addition of SF2446A2 after infection impedes chlamydial inclusion formation, which can be partly reversed by the removal of the compound. HeLa cells were infected with *C. trachomatis* at MOI 1 for 24 h in the presence of DMSO or SF2446A2 (24 h). The compound was either added or removed by washing 4 h, 8 h, 10 h or 16 h post-infection (p.i.). (A) The infection was analysed by immunofluorescence using Phalloidin555 (red) and antibodies against cHSP60 (green). (B) The analysis was also done by SDS-PAGE and western blot with antibodies against the chlamydial OmpA and β -actin as a loading control. Scale bar: 50 μ M

3.4.2.3 SF2446A2 exhibit antioxidant potential

In the context of investigating the mode of action of SF2446A2, the effect of the compound on cellular ROS generation and its antioxidant properties were analysed by Dr. Eman Maher Othman (Institute of Pharmacology and Toxicology, University of Würzburg) (Reimer *et al.*, 2016). A microscopic analysis was applied that contained staining with the cell-permeable dye DHE (dihydroethidium), which forms a red fluorescent product that intercalates within the DNA upon reaction with ROS (Figure 3.24A). Furthermore, the cell permeable H₂DCF-DA (2,7-dichlorodihydrofluorescein diacetate), which is a reduced form of fluorescein was used as an indicator for ROS to verify the results of the microscopy analysis (Figure 3.24B). The ROS inducer 4-nitroquinoline 1-oxide (NQO) was applied as a positive control. The cells were treated with SF2446A2 alone or in combination with NQO. SF2446A2 alone has shown no effect on the cellular ROS production. However, when the cells were treated with NQO and

different concentrations of the compound, the ROS generation was decreased in comparison to cells treated with NQO, indicating an antioxidant activity of SF2446A2.

In order to examine if the antioxidant properties are responsible for the antichlamydial effect of the compound, the known antioxidant Trolox was used as a control during chlamydial infection. Microscopic analysis and the dye DHE were applied to determine the Trolox concentration with an appropriate antioxidant activity (Figure 3.24C). Chlamydial infection was subsequently performed for 24 h in the presence of 12 and 24 μM of Trolox (Figure 3.24D). Since no effect of the antioxidant could be observed, we concluded that the antioxidant properties were not responsible for SF2446A2's antichlamydial activity.

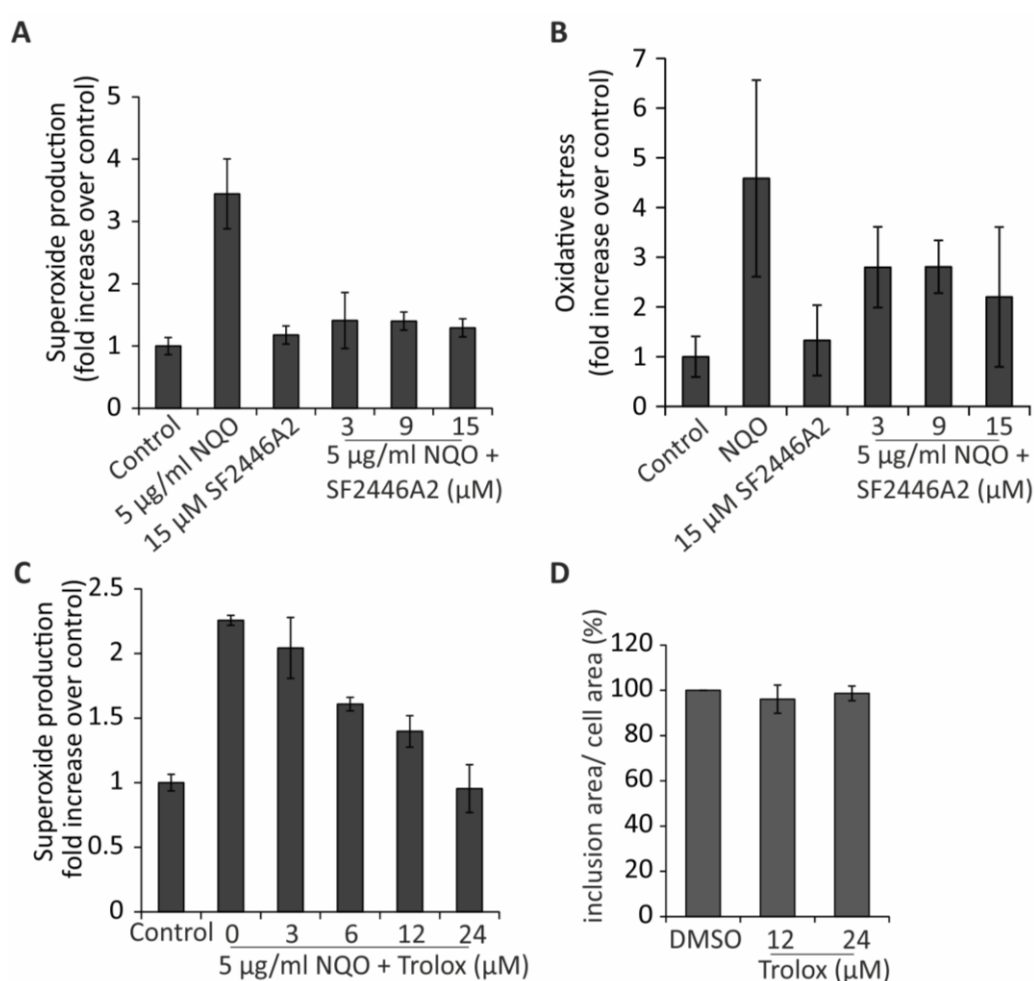


Figure 3.24: SF2446A2 exhibit antioxidant potential. (A, B) HeLa cells were treated with 5 $\mu\text{g/ml}$ NQO, 15 μM SF2446A2 or with a combination of NQO and 3, 9 and 15 μM SF2446A2. Superoxide formation was detected by microscopy using 10 μM DHE dye (A). 10 μM $\text{H}_2\text{DCF-DA}$ was added during the last 20 min at 37 $^\circ\text{C}$ and the fluorescence was measured by flow cytometry (B). (C) Microscopic detection of superoxide formation using the dye (10 μM) DHE in HeLa cells treated with 5 $\mu\text{g/ml}$ NQO or with a combination of NQO and 3, 6, 12 and 24 μM Trolox. (D) HeLa cells were infected in the presence of DMSO, 12 μM and 24 μM Trolox. The inclusion surface area relative to the cell surface area was determined by automated fluorescence microscopy. The graph shows mean values \pm SD of three independent experiments.

3.4.3 SF2446A2 inhibits mitochondrial respiration and enhances glycolysis

It has been reported that SF2446A2 affects the human parasite *Schistosoma mansoni* by impairing its vitality, morphology, oogenesis and spermatogenesis (Reimer *et al.*, 2015). Since the compound has shown effects on the trematode, we took into consideration that SF2446A2 could also target the eukaryotic cell. Thus, the mitochondrial respiration and glycolytic activity were analysed in the presence of the natural compound applying a Mito Stress Test at the Seahorse Bioscience XF^e96 Extracellular Flux Analyzer. This enabled the measurement of the oxygen consumption rate (OCR) in cells treated for 1 h with DMSO, 10 μ M, 15 μ M and 20 μ M of SF2446A2 and 5 μ M oligomycin (Figure 3.25A). For analysis of the functionality of mitochondria, the inhibitors oligomycin, FCCP (p-trifluoromethoxy carbonyl cyanide phenyl hydrazone) and a mixture of antimycin A and rotenone were added sequentially during the measurements. The program XF Mito Stress Test Report Generator was applied to calculate the basal respiration, proton leak, maximal respiration capacity, spare respiratory capacity and ATP production (Figure 3.25B). These phases are illustrated in Figure 3.25C for the DMSO control.

The basal respiration was determined prior to the addition of the first inhibitor. Cells treated with 20 μ M SF2446A2 showed already a decrease in the OCR by 28 % (Figure 3.25A, B). The pre-treatment of cells with 5 μ M oligomycin resulted in a reduction of the OCR levels by 86 %. Afterwards, oligomycin was injected in all samples to inhibit the mitochondrial F₀F₁-ATPase and thus decreased the OCR levels drastically. This reduction can be assigned to the mitochondria-linked ATP production that is inhibited in a dose-dependent manner by SF2446A2. The remaining basal respiration the so-called proton leak is uncoupled from mitochondrial respiration and is doubled in the presence of 20 μ M SF2446A2. The uncoupling agent FCCP was added thereafter, leading to a breakdown of the proton gradient and the mitochondrial membrane potential ($\Delta\psi$). The measured increase in the OCR levels represented the maximal respiration rate based on the uninhibited electron flow and the maximal consumed oxygen. The maximal respiration was decreased in a dose-dependent manner by SF2446A2. At 20 μ M of the compound the OCR levels were reduced by 60 % compared to the DMSO control. The spare respiratory capacity that represents the ability of cells to respond to cellular energy demand is reduced to 0 % in SF2446A2 treated cells. However, the pre-treatment with oligomycin did not affect the maximal respiration since the OCR levels increased to 110 % upon treatment with FCCP. Finally, antimycin A and rotenone,

the inhibitors of the mitochondrial complex I and III, were added in combination, resulting in a shutdown of the mitochondrial respiration. The measured non-mitochondrial respiration did not differ between DMSO and SF2446A2 treated cells.

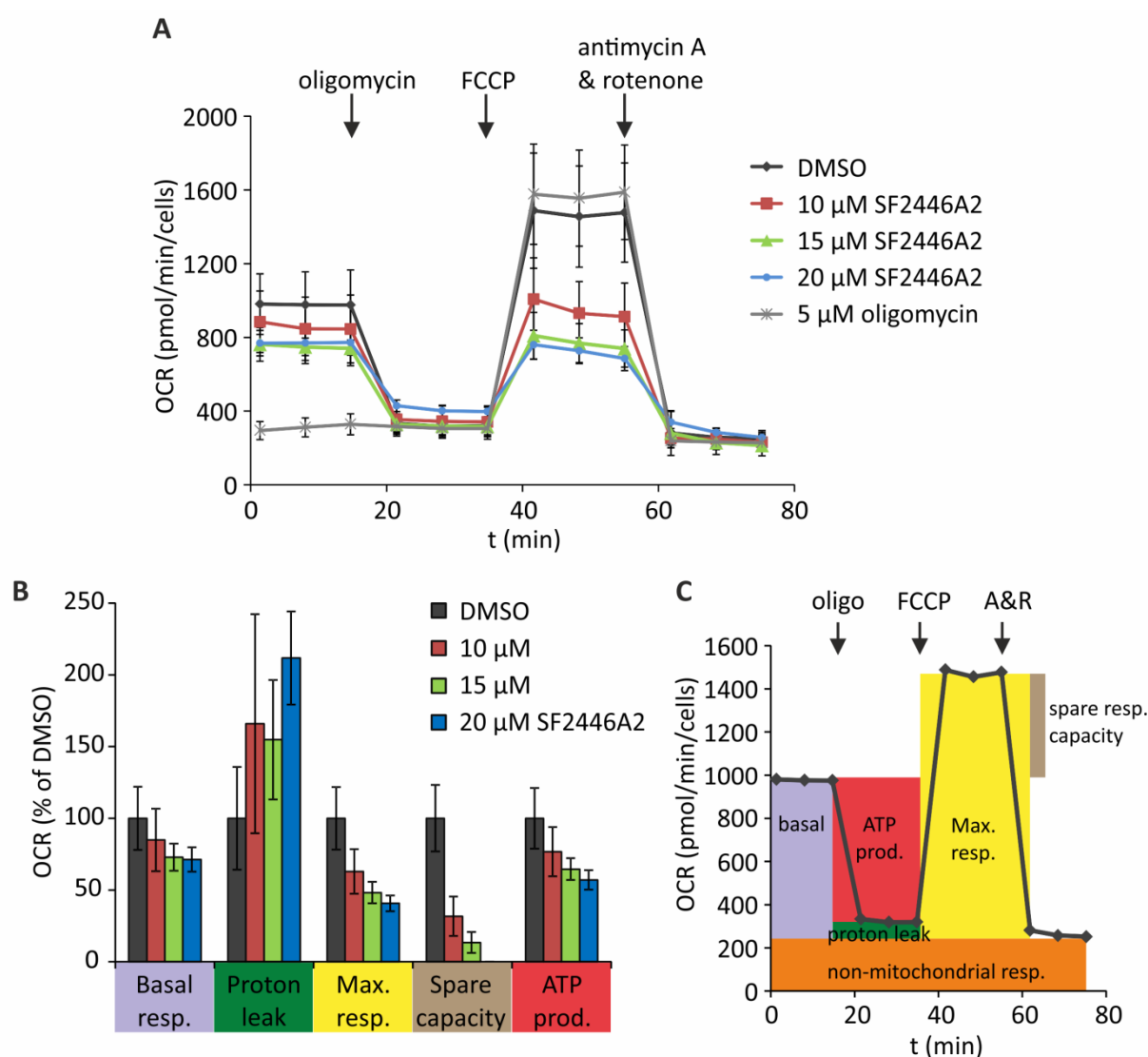


Figure 3.25: SF2446A2 affects mitochondrial respiration in a dose-dependent manner. HeLa cells were treated for 1 h with DMSO and 10, 15, 20 μM SF2446A2. The oxygen consumption rate (OCR) was measured at the Seahorse Bioscience Analyser. Oligomycin (oligo, 2 μM), FCCP (1 μM) and antimycin A/rotenone (A&R, 0.5 μM) were added during the measurements (arrows). (B) The XF Mito Stress Test Report Generator calculated the basal respiration (basal resp.), proton leak, maximal respiration capacity (max. resp.), spare respiratory capacity (spare resp. capacity) and the ATP production (ATP prod.) as % of the DMSO controls, respectively. (C) The DMSO control was used to illustrate the respiration phases determined by the Mito Stress Test. The experiments were performed three times with six technical replicates and the results of one experiment are shown exemplary.

Besides the OCR, the extracellular acidification rate (ECAR) was measured, which represents the rate of lactic acid production and therefore the glycolytic activity of the cell. Pre-treatment of cells with oligomycin increased the ECAR levels strongly, which was also

observed for 20 μM SF2446A2, indicating higher cellular glycolysis rates (Figure 3.26A). The cells seemed to compensate their ATP loss from the inhibited mitochondrial respiration by increasing their glycolytic activity.

To prove this hypothesis, cells were grown in medium containing galactose as carbohydrate substituent for glucose. It has been reported that the use of galactose instead of glucose as carbohydrate source leads to increased mitochondrial respiration, enhanced synthesis of respiratory chain proteins and remodelling of mitochondrial structure (Rossignol *et al.*, 2004). Galactose is metabolised by the cell slowly to G-6-P, forcing the cells to obtain their ATP from oxidative phosphorylation (OXPHOS) (Dott *et al.*, 2014). HeLa cells grown in glucose-containing medium revealed no difference in the survival when treated with DMSO or SF2446A2 (Figure 3.26B). However, the number of cells grown after 24 h in galactose-supplemented medium in the presence of SF2446A2 was decreased significantly by approximately 45 % compared to DMSO-treated cells. The results showed that the cell viability is impaired in the presence of SF2446A2 when the cells are forced to use the OXPHOS as their energy source, indicating an inhibitory effect of the compound on the mitochondrial respiration.

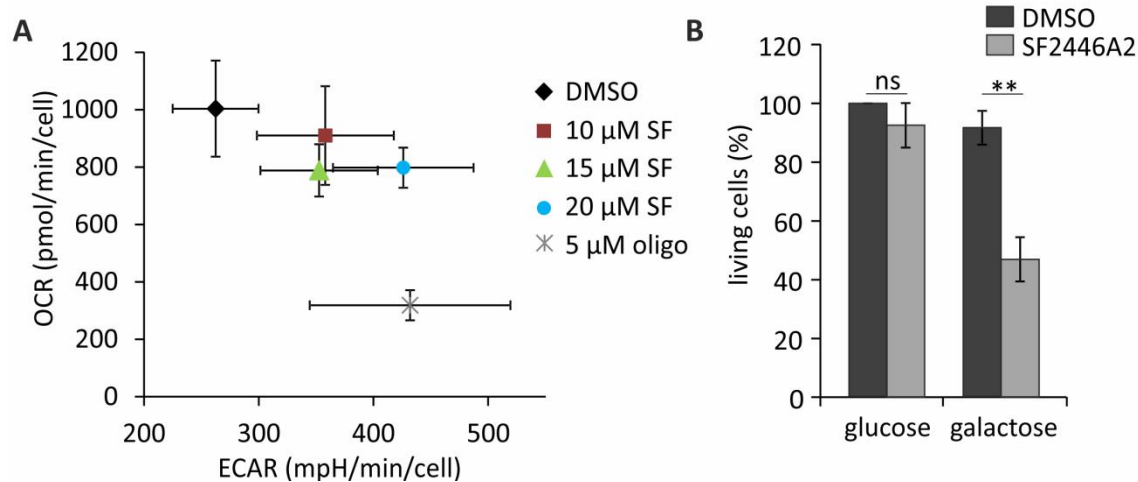


Figure 3.26: SF2446A2 increases the cellular glycolysis rate and decreases the cell viability in the presence of galactose-containing medium. (A) HeLa cells were treated for 1 h with DMSO and 10, 15, 20 μM SF2446A2 (SF) and 5 μM oligomycin (oligo). The extracellular acidification rate (ECAR) was measured at the Seahorse Bioscience Analyser. The experiment was performed three times with six technical replicates and the results of one experiment are shown exemplary. (B) HeLa cells were grown in the presence of DMSO and 10 μM SF2446A2 for 24 h in 11 mM glucose or galactose-containing medium. The cell viability was analysed by tryptophan blue staining and counting. The graph was normalized to the result obtained with DMSO-treated cells, which were incubated in glucose-containing medium. The experiment was performed in three independent replicates. ns not significant, ** $p < 0.01$

3.4.4. SF2446A2 impairs the mitochondrial ATP production

In the Mito Stress Test SF2446A2 has been shown to inhibit the mitochondrial respiration in a dose-dependent manner. For further investigation of this effect the $\Delta\Psi$ was measured using the fluorescent lipophilic cationic dye TMRM (Tetramethylrhodamine, methyl ester). HeLa cells were treated for 4 h with DMSO and SF2446A2. Furthermore, oligomycin and the uncoupling agent CCCP (carbonyl cyanide m-chloro phenyl hydrazone) were applied as a control. Oligomycin increased the $\Delta\Psi$ significantly by 42.5 % due to the inhibition of the F_0F_1 -ATPase (Figure 3.27A). The mitochondrial membrane is hyperpolarized because of the reduced amount of protons pumped by the ATPase in the mitochondrial matrix from the intermembrane space, thus resulting in a more negatively charged matrix. The cationic dye TMRM accumulates in the matrix, which leads to an increased fluorescence signal. In contrast, the addition of the proton ionophore CCCP decreased the $\Delta\Psi$ by 59.1 %. The mitochondrial membrane is depolarized due to the destroyed proton gradient. The matrix becomes less negatively charged, thus preventing an accumulation of TMRM. Cells treated with SF2446A2 showed a significant increase of 24.9 % in the $\Delta\Psi$, verifying an interfering effect on the mitochondrial respiratory chain.

In the next step, the ATP content of cells in glucose or galactose medium in the presence of DMSO, SF2446A2 and oligomycin was analysed using the Luminescence ATP detection assay kit (Figure 3.27B). In the presence of glucose no significant difference between the samples could be detected. However, when the cells were transferred to galactose-supplemented medium, a significant decrease in the ATP levels by approximately 20 % could be observed in cells treated with SF2446A2 and oligomycin. To verify these results, inverted mitochondrial membrane vesicles were isolated from HEK 293T cells and treated with DMSO, SF2446A2, oligomycin and CCCP (Figure 3.27C). The ATP production was induced by the addition of ADP and the measurement was performed using the ATP detection assay kit. SF2446A2 reduced the ATP production significantly by 28.2 %, similar to the controls oligomycin and CCCP.

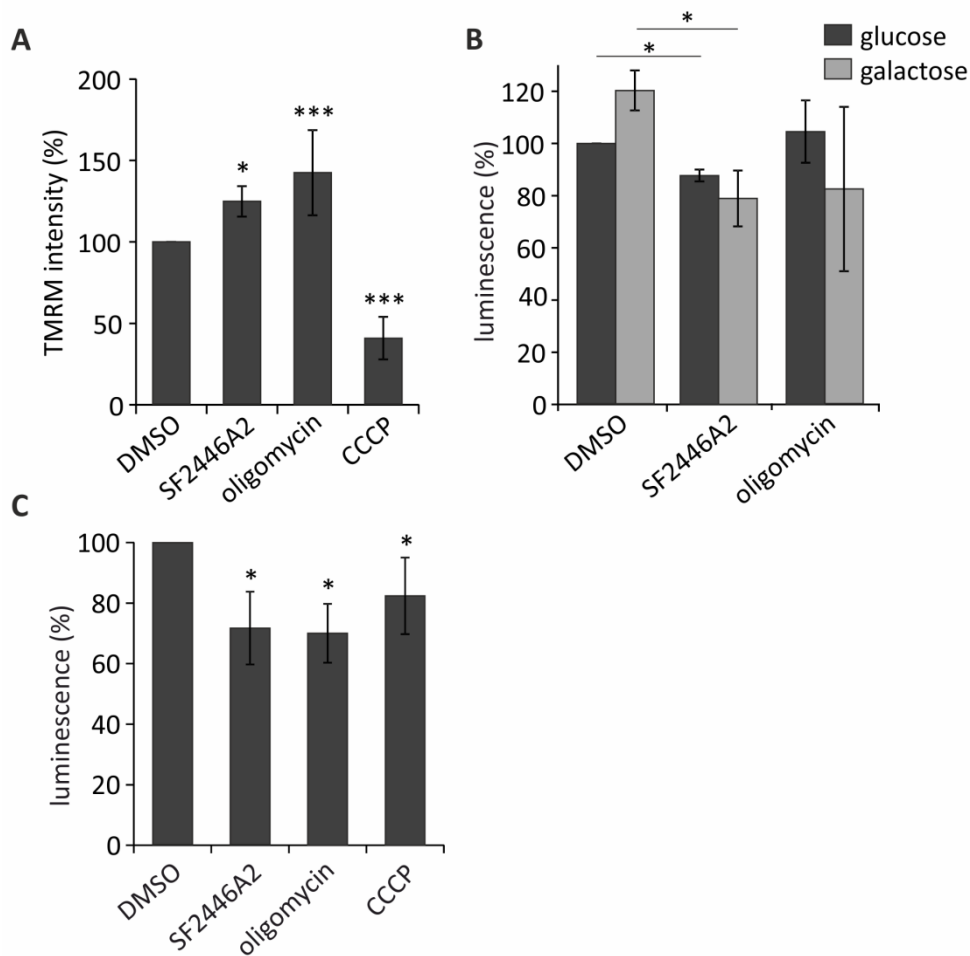


Figure 3.27: SF2446A2 increases mitochondrial membrane potential and inhibits ATP production. (A) HeLa cells were treated with DMSO, 20 μ M SF2446A2 and 20 μ M oligomycin for 4 h and 10 μ M CCCP for 10 min. The cells were stained with 20 nM TMRM and analysed by flow cytometry. (B) HeLa cell were grown either in medium supplemented with 11 mM glucose or galactose and were treated with DMSO, 20 μ M SF2446A2 and 20 μ M oligomycin for 4 h. The ATP content was measured with the ATP Luminescence Kit. (C) Inverted mitochondrial membrane vesicles were isolated from HEK 293T cells and were treated with DMSO, 20 μ M SF2446A2, 20 μ M oligomycin and 10 μ M CCCP for 30 min. The ATP production was induced by the addition of 1 mM ADP and measured using the ATP Luminescence Kit. All experiments were performed in three independent replicates. Mean values \pm SD were normalized to DMSO. * p <0.05, *** p <0.0005

Since the antichlamydial compound SF2446A2 showed to inhibit the mitochondrial respiration it was investigated, if the inhibition of the respiratory chain by oligomycin, antimycin A and rotenone would also affect the chlamydial infection. Therefore, HeLa cells were infected for 24 h in the presence of 0.5 - 5 μ M oligomycin, antimycin A, rotenone and the controls DMSO (solvent of oligomycin and antimycin A) and EtOH (solvent of rotenone) (Figure 3.28). Oligomycin and antimycin A decreased the inclusion surface area in a dose-dependent manner. At 2 μ M the inclusion area was diminished to approximately 30 %.

Rotenone reduced the inclusion surface area by about 30 % at all applied concentrations, indicating a saturation effect.

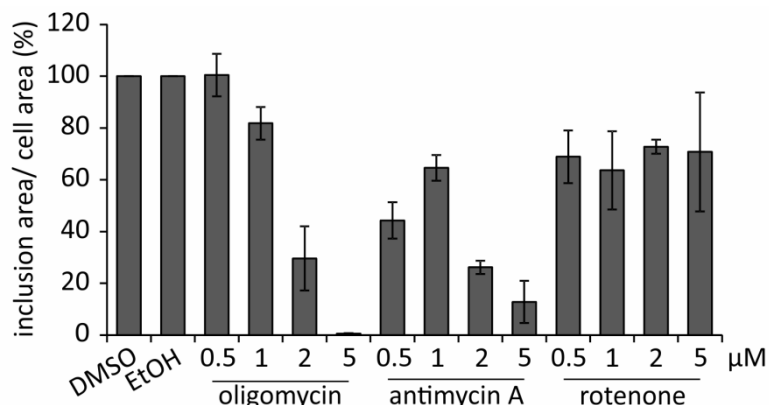


Figure 3.28: Oligomycin, antimycin A and rotenone decrease the chlamydial inclusion surface area. HeLa cells were infected for 24 h with GFP-expressing *C. trachomatis* in the presence of DMSO, oligomycin, antimycin A and rotenone using concentration ranging from 0.5 to 5 μM. The cells were fixed and stained with Phalloidin555 and DAPI. The analysis was performed by automated fluorescence microscopy. The mean inclusion surface area relative to the cell surface area was normalized to DMSO. The graph shows mean values ±SD of three technical experiments.

3.4.5. *C. trachomatis* is affected by the knockdown of F₀F₁-ATPase and detraction of glucose

We could demonstrate an inhibitory effect of the compound SF2446A2 on the mitochondrial respiration and ATP production. Furthermore, we could show that the known inhibitors of the mitochondrial respiratory chain oligomycin, antimycin A and rotenone decreased the chlamydial inclusion surface area, as well. Thus, we analysed whether a depletion of mitochondrial ATP would affect the chlamydial infection. To this purpose, the F₀F₁-ATPase knockdown cell line (*f1βkd-2*) was created using a lentiviral based expression system. In the following experiments the metaxin 2 knockdown cell line (*mtx2kd-2*) was used as a control. It has been shown that a knockdown of the mitochondrial protein metaxin 2 did not affect the mitochondrial respiration (Kozjak-Pavlovic *et al.*, 2007). The knockdown of F1β was induced for seven days with AHT and was confirmed by western blot using an antibody against the F1α-subunit, which depends on the presence of the F1β-subunit (Figure 3.29A).

Furthermore, the ATP production of the mitochondria of the cell lines *f1βkd-2* and *mtx2kd-2* was analysed. For this, mitochondria were isolated from induced and non-induced cells and the ATP production was initiated by addition of ADP. Oligomycin, which was applied as a positive control, inhibited the ATP generation significantly by 58.7 %. No significant difference could be detected for *mtx2kd-2* upon AHT induction. However, the

knockdown of F1 β by addition of AHT led to a decrease in ATP generation by 36.9 %, verifying the deficiency of the ATPase (Figure 3.29B).

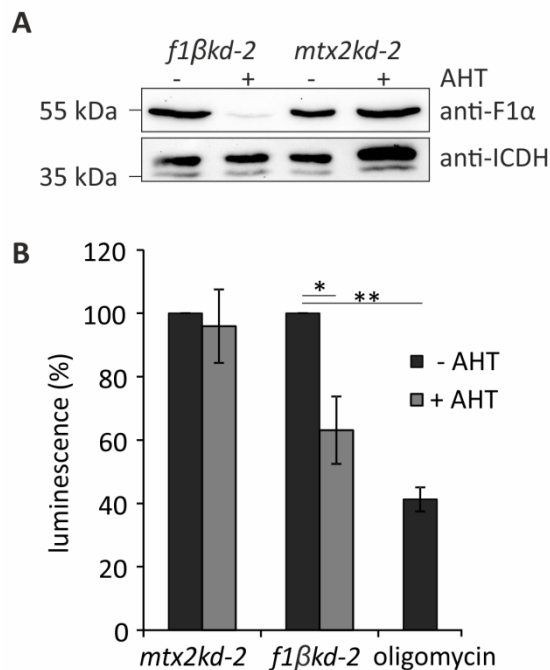


Figure 3.29: Knockdown of the ATPase F1 β -subunit leads to a reduced mitochondrial ATP production. The cell lines *mtx2kd-2* and *f1βkd-2* were induced for seven days with 1 μ g/ml AHT. The effect of the knockdown of metaxin 2 and F1 β on the levels of F₀F₁-ATPase was analysed by western blot (A) using antibodies against F1 α and ICDH as a loading control. The mitochondria of the induced cells were isolated and the ATP production was induced by the addition of 1 mM ADP and determined by ATP Luminescence Kit. 20 μ M oligomycin was added as a control. The graph represents the mean values \pm SD of three independent experiments, which were normalized to the ATP production of the non-induced *mtx2kd-2* cell line. *p<0.05, **p<0.01

The *f1βkd-2* and *mtx2kd-2* cell lines, induced and non-induced, were infected with *C. trachomatis* for either 24 h in glucose-containing medium or for 16 h in glucose and 8 h in galactose-supplemented medium. The infection was monitored by microscopic analysis of the inclusion surface area in relation to the cell surface area (Figure 3.30A), western blot (Figure 3.30B) and immunofluorescence staining (Figure 3.30C). The inclusion area and the bacterial content were not significantly different in the samples when the infection was performed in glucose-containing medium. A switch from glucose- to galactose-supplemented medium after 16 h resulted in a significantly decreased inclusion surface area of 72.9 % in the induced *f1βkd-2*, indicating a dependency of *C. trachomatis* on the cellular ATP.

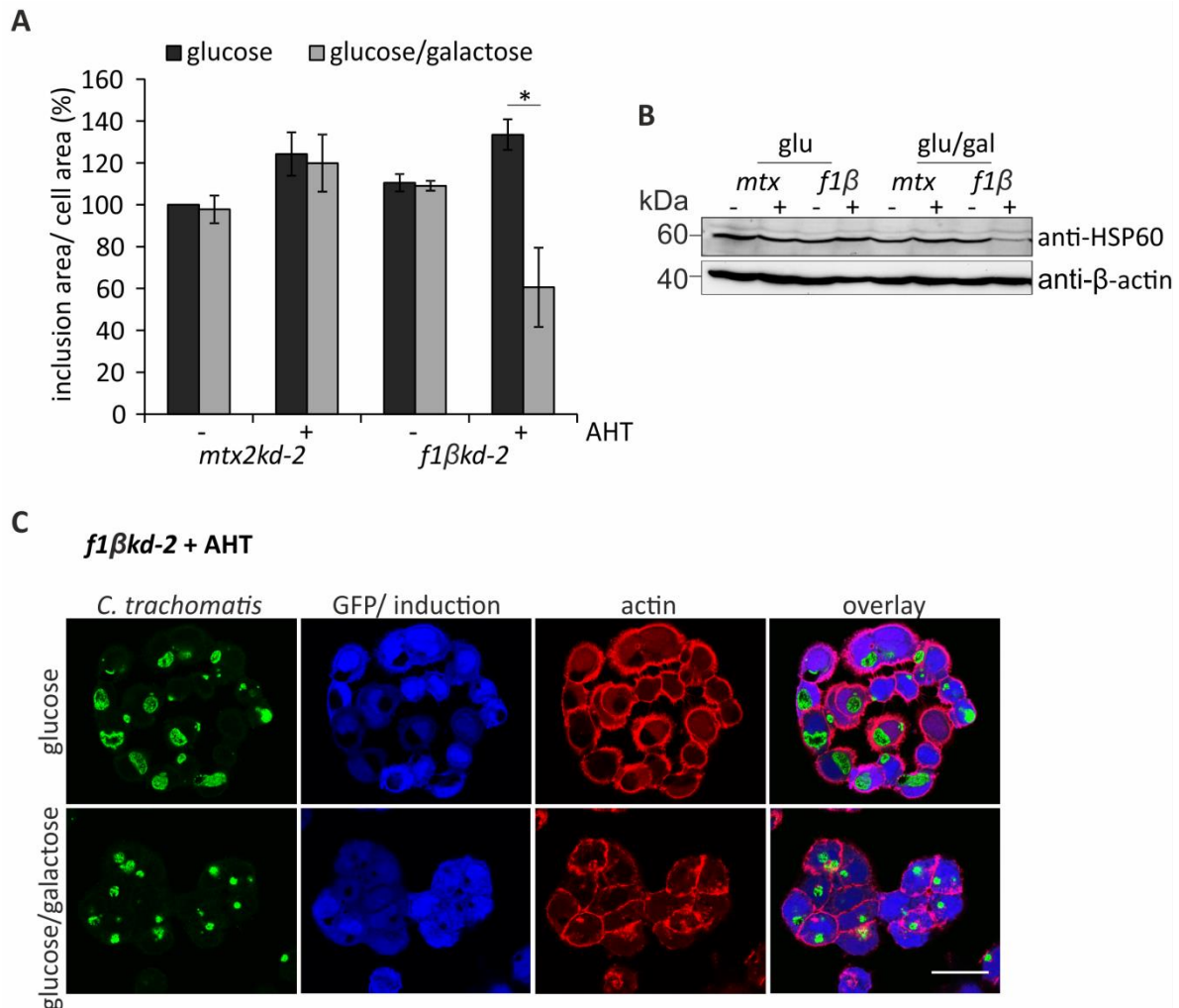


Figure 3.30: Knockdown of the mitochondrial ATPase F1 β -subunit decreases chlamydial inclusion surface area. (A-C) The cell lines *mtx2kd-2* and *f1 β kd-2* were induced for seven days with 1 μ g/ml AHT and were infected with *C. trachomatis* at MOI 1 in the presence of glucose (glu, 11 mM) for 24 h or for 16 h in glucose and subsequently in galactose-containing (gal, 11 mM) medium. The infection was analysed by automated fluorescence microscopy (A), western blot (B) and immunofluorescence (C). Infected cells were fixed and stained with Phalloidin555, DAPI and an antibody against cHSP60 (A). The inclusion surface area relative to the cell surface area was normalized to the results obtained for the non-induced *mtx2kd-2* infected in glucose-containing medium. The graph represents mean values \pm SD of three independent replicates. The western blot was done using antibodies against cHSP60 and β -actin as a loading control (B). Immunofluorescence staining was performed with induced (blue) *f1 β kd-2*, infected in glucose- or glucose/galactose-supplemented medium (C). The cells were stained with Phalloidin555 (red) and an antibody against cHSP60 (green). * $p < 0.05$, Scale bar: 50 μ m

3.4.6 Depletion of glucose and glutamine reduces chlamydial infection

In HeLa cells 4 - 5 % of glucose enters the tricarboxylic acid (TCA) cycle, while the majority of 80 % is metabolised by glycolysis. The substitution of glucose as energy source for cancer cells by galactose forces the cells to use glutamine for 98 % of their ATP production (Reitzer *et al.*, 1979). Glutamine is the most abundant amino acid in the blood plasma (Reitzer *et al.*,

1979, Bergstrom *et al.*, 1974). The conditionally essential amino acid glutamine is hydrolysed by the mitochondrial glutaminase to glutamate, an anaplerotic substrate, which is subsequently used as a precursor of glutathione, alanine, aspartate, serine and glycine (Lacey & Wilmore, 1990). Additionally, glutamate is converted by glutamate dehydrogenase to α -ketoglutarate that is used to drive the TCA cycle, produce oxaloacetate and subsequently acetyl-CoA.

Since we have observed that the depletion of cellular ATP generation by inhibiting glycolysis and OXPHOS led to reduced *C. trachomatis* infection, we investigated the effect of glutamine depletion by knockdown of the mitochondrial glutaminase. The knockdown was induced for seven days by AHT and was verified by western blot applying an anti-glutaminase antibody and an antibody against mitochondrial SDHA as a loading control (Figure 3.31A). The *mtx2kd-2* cell line was used as a control.

For analysis of ATP production mitochondria were isolated from induced and non-induced cells, which were cultivated for 24 h in galactose-supplemented medium. ADP was added for induction of ATP generation that was subsequently measured. Upon induction of *mtx2* knockdown no changes in the ATP levels could be observed (Figure 3.31B). A knockdown of glutaminase, however, led to a reduction in ATP generation by 20.1 %.

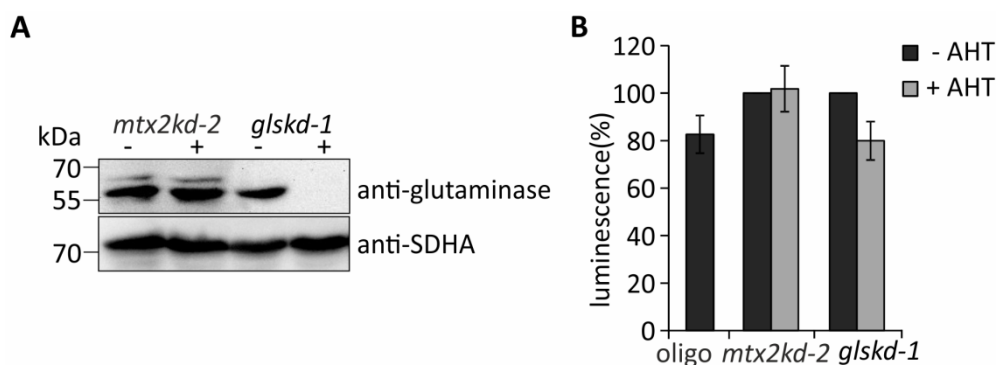


Figure 3.31: Knockdown of glutaminase in cells grown in galactose-containing medium reduces the mitochondrial ATP production. (A) The knockdown of the *mtxkd-2* and *glskd-1* cell lines was induced by 1 μ g/ml AHT for seven days. The cells were lysed in 2 x Laemmli buffer and analysed by SDS-PAGE and western blot using antibodies against glutaminase and SDHA as a loading control. (B) The ATP production of the isolated mitochondria from non-induced (-AHT) and induced (+AHT) *mtxkd-2* and *glskd-1* cells, cultivated in galactose-containing medium for 24 h, was induced with 1 mM ADP and measured with an ATP Luminescence Kit. 20 μ M oligomycin (oligo) was added as a control to the non-induced mitochondria from *mtxkd-2*. The mean values \pm SD of three replicates were normalized to non-induced samples, respectively.

The non-induced and induced *mtx2kd-2* and *glskd-1* cells were infected under different conditions. The medium was supplemented with either 5 % dialysed or non-

dialysed FCS. Dialysis at the cut-off of 10 kDa enabled the exclusion of small molecules such as glutamine or glucose from FCS. Furthermore, the infection was performed in glucose- or galactose-containing medium with or without glutamine. Western blot analysis (Figure 3.32A, B) and automated fluorescence microscopy (Figure 3.32C, D) were performed to monitor the infection.

A condition consisting of glucose-containing medium with glutamine and non-dialysed FCS was set as the control for each cell line (-AHT). In general, the application of dialysed FCS reduced the chlamydial inclusion surface area independently of the cell line or the condition by 30 % on average (Figure 3.32C, D). Furthermore, the substitution of glucose by galactose in medium supplemented with dialysed FCS diminished the inclusion surface area by 45 % on average in the *mtx2kd-2* (-/+ AHT) control cell line. A similar effect was achieved when glutamine was depleted in the presence of glucose, which affected the surface area of the inclusions negatively by roughly 40 %. The average chlamydial inclusion area in *mtx2kd-2* (-/+ AHT) and *glskd-1* (- AHT) in medium with galactose, without glutamine and dialysed FCS was 15 % of the control. However, the same conditions with or without glutamine resulted in a strong reduction of the infection in the induced *glskd-1* cell line to approximately 5 % of the control. When 2 mM glutamine were added to this condition, a strong OmpA band could be detected for *mtx2kd-2* (-/+ AHT) and *glskd-1* (- AHT), indicating a rescue of the infection. This effect could not be observed for the knockdown of the glutaminase, since the present glutamine cannot be converted by the glutaminase to glutamate and NH₃. These results demonstrate the dependency of *C. trachomatis* on the cellular energy supply through glycolysis or glutaminolysis during infection.

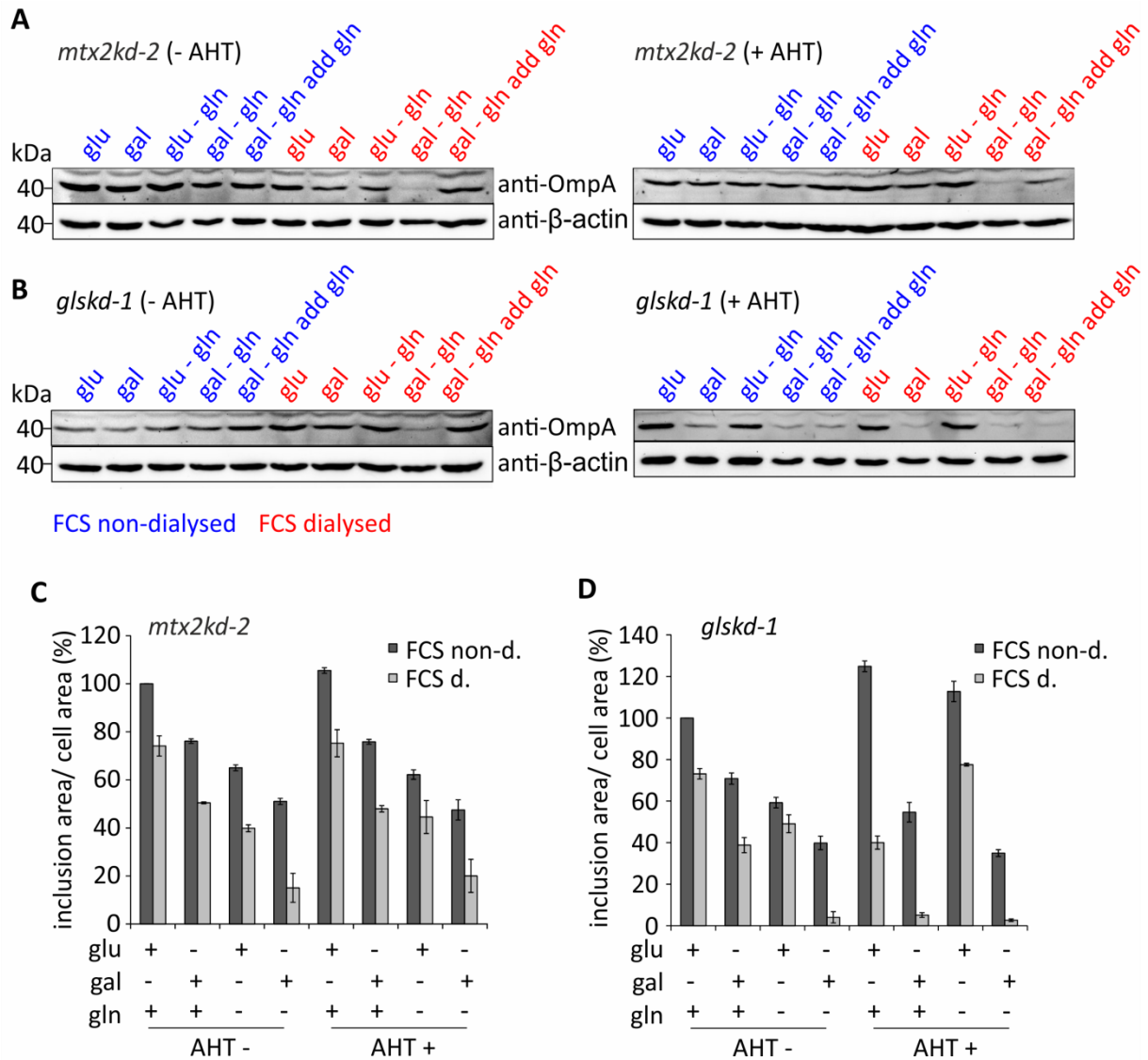


Figure 3.32: Knockdown of the mitochondrial glutaminase results in a diminished chlamydial infection in galactose-containing medium. The knockdown of the *mtxkd-2* and *glskd-1* cell lines was induced by 1 $\mu\text{g}/\text{ml}$ AHT for seven days. Non-induced and induced *mtxkd-2* (A, C) and *glskd-1* (B, D) cells were infected at MOI 1 for 24 h with *C. trachomatis*. The RPMI 1640 Medium (no glucose, L-glutamine) was used for experiments with glutamine and without glutamine the SILAC RPMI 1640 Flex Medium (supplemented with 1.15 mM L-arginine and 0.22 mM L-lysine) was applied. The content of infection medium was shown below the graph: glucose (glu, 11 mM), galactose (gal, 11 mM), glutamine (-gln) and glutamine added to the medium (add gln, 2 mM). The medium was supplemented with 5 % non-dialysed (non-d., blue) or dialysed FCS (d., red). The cells were either analysed by western blot using antibodies against the chlamydial protein OmpA and β -actin as a loading control (A, B) or automated fluorescence microscopy (C, D). The experiments were done in triplicates and the mean value \pm SD of the inclusion surface area relative to the cell surface area was normalized to non-induced *mtxkd-2* cells infected in the medium containing non-dialysed FCS.

3.4.7 SF2446A2 affects the growth of *N. gonorrhoeae* and *S. aureus*

The natural compound SF2446A2 has been shown to inhibit the mitochondrial respiration and the ATP production. However, depletion of ATP generated by OXPHOS did not affect the chlamydial inclusion surface area when the cells could use glycolysis for ATP supply. The effects of SF2446A2 could, however, be observed in glucose-containing medium, as well. Therefore, the compound might also possess a bacterial target. It has already been demonstrated that SF2446A2 shows antibacterial activity against different *Staphylococcus* strains, *Bacillus anthracis* and four *Mycoplasma* strains (Takeda *et al.*, 1988). We could confirm the bactericidal effect on *S. aureus* by measuring growth curves in the presence of DMSO, 5 μ M, 10 μ M and 20 μ M SF2446A2 (Figure 3.33A). Furthermore, the compound affected the growth of *N. gonorrhoeae* (Figure 3.33B), but did not impair the growth of *E. coli* (Figure 3.33C).

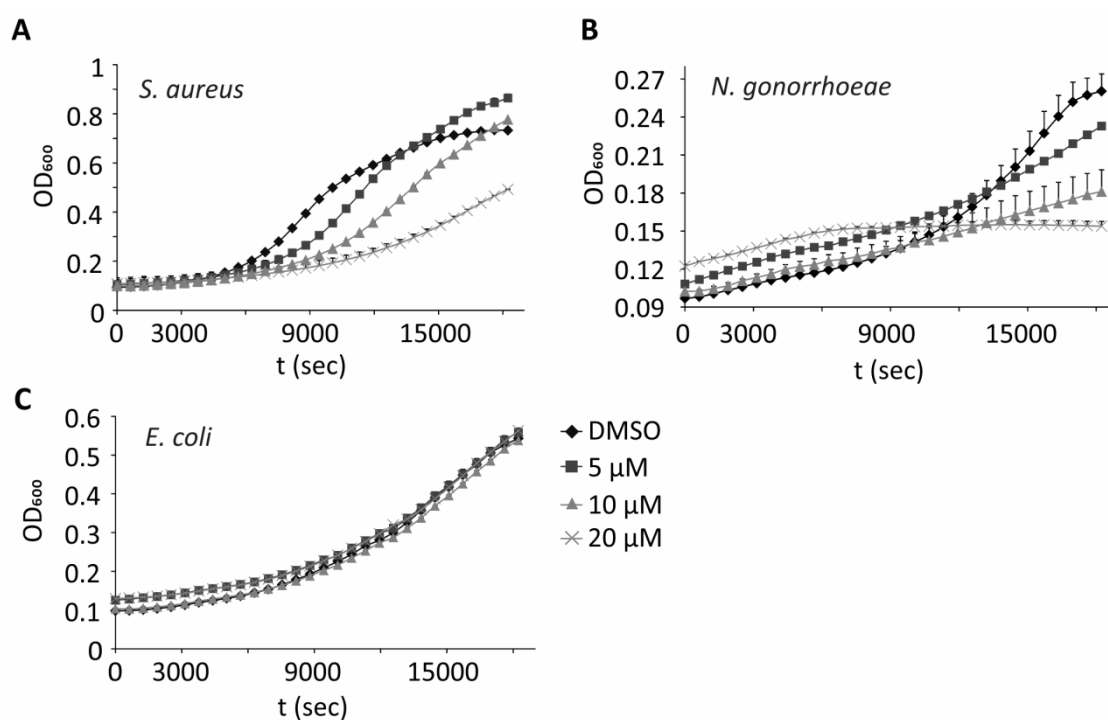


Figure 3.33: SF2446A2 affects growth of *N. gonorrhoeae* and *S. aureus*. The growth of *N. gonorrhoeae* (A), *S. aureus* (B) and *E. coli* (C) was analysed in the presence of DMSO, 5, 10 and 20 μ M SF2446A2. OD₆₀₀ was measured every 600 sec for 18 000 sec in liquid culture by Tecan plate reader. The graphs represent means \pm SD values from three technical replicates.

Since SF2446A2 inhibited the mitochondrial respiration we considered an inhibitory effect of the compound on the membrane-associated respiratory chain of bacteria. Therefore, the ATP generation of bacterial inverted membrane vesicles from *E. coli* (Figure

3.34A), *S. aureus* (Figure 3.34B) and *N. gonorrhoeae* (Figure 3.34C) was analysed in the presence of DMSO, 10 μM and 20 μM of SF2446A2. The ATP generation was induced by addition of ADP and measured with the Luminescent ATP Detection Assay Kit. The treatment with SF2446A2 resulted in no significant decrease of the ATP production. Additionally, no difference could be observed between the two compound concentrations. However, the ATP content was reduced not significantly in the presence of SF2446A2 by approximately 25 % in *E. coli* and *S. aureus* vesicles and by about 15 % in *N. gonorrhoeae* vesicles. Oligomycin was applied as a control, but impaired the ATP production of the bacterial vesicles by maximally 11 %. It has been shown that oligomycin has a similar IC_{50} for the inhibition of the ATP synthesis of the mitochondrial ATPase and the bacterial ATPases of *E. coli* and *S. aureus* (Balemans *et al.*, 2012). Since oligomycin did not show the expected inhibitory effect, we concluded that the assay was not suitable for the measurement of the bacterial ATPase functionality.

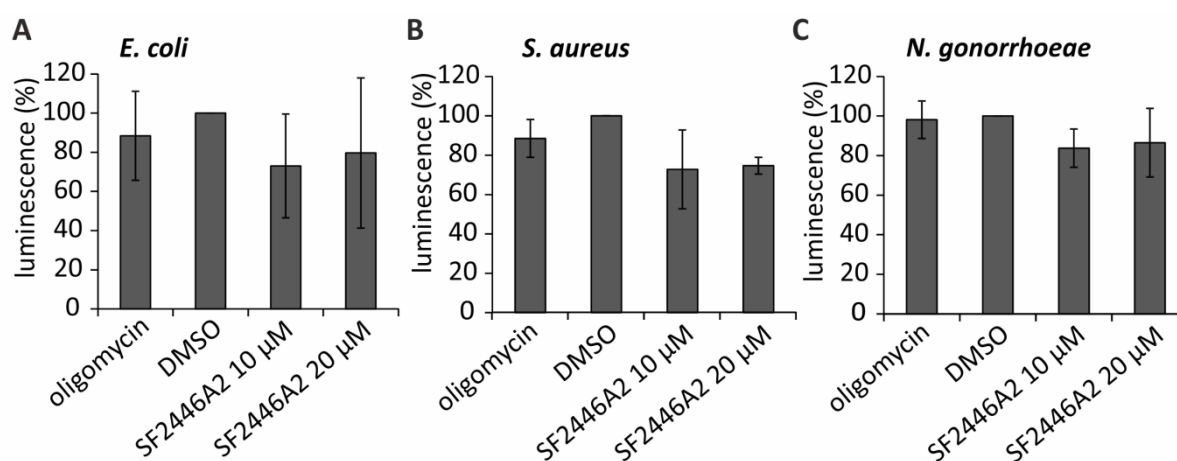


Figure 3.34: Analysis of the effect of SF2446A2 on the ATP synthesis of *E. coli*, *S. aureus* and *N. gonorrhoeae*. Inverted bacterial membrane vesicles were isolated from *E. coli* (A), *S. aureus* (B) and *N. gonorrhoeae* (C). The vesicles were treated with 20 μM oligomycin, DMSO, 10 μM and 20 μM SF2446A2. The ATP content was determined with the ATP Luminescence Kit. The experiments were performed in three replicates. The mean values \pm SD were normalized to the DMSO control.

Previously, it has been demonstrated that chlamydial EBs are able to generate ATP using G-6-P (Omsland *et al.*, 2012). Since, we have shown that not only SF2446A2 but also the mitochondrial respiratory inhibitors oligomycin, antimycin A and rotenone affected chlamydial infection, it was analysed if these compounds interfere with the chlamydial ATP production. *C. trachomatis* was isolated after 24 h infection of HeLa cells and was incubated for 2 h in a medium containing glucose, galactose or G-6-P (Figure 3.35). Furthermore,

Chlamydia was treated with DMSO, SF2446A2, oligomycin and a mixture of antimycin A and rotenone in the presence of G-6-P. In glucose-supplemented medium the ATP levels were reduced by 51.8 % and in galactose by 37.6 % in comparison to G-6-P. The treatment of *C. trachomatis* with SF2446A2 resulted in an insignificant increase in the ATP production by 7.8 %. Oligomycin decreased the ATP production by 16.5 % in bacteria, while a combination of antimycin A and rotenone reduced the ATP generation by 36.6 %, indicating that the ATP production of *C. trachomatis* by utilizing G-6-P is sensitive for these respiratory chain inhibitors but not for SF2446A2.

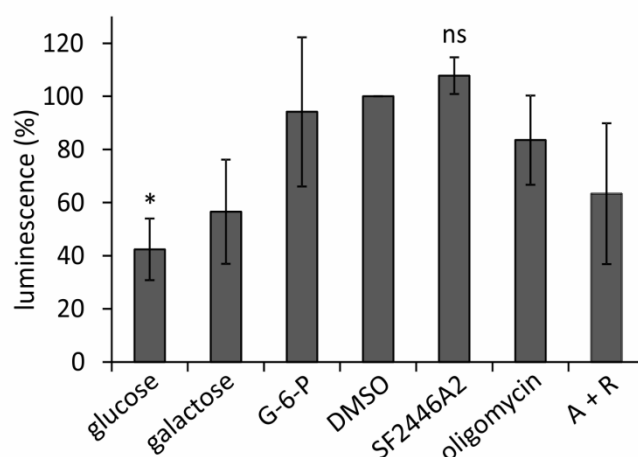


Figure 3.35: SF2446A2 has no significant effect on the chlamydial ATP level. *C. trachomatis* isolated 24 h post-infection from HeLa cells were incubated for 2 h at 35 °C in medium containing glucose, galactose and G-6-P. The bacteria were treated with DMSO, 20 µM SF2446A2, 20 µM oligomycin and a mixture of 0.5 µM antimycin A and rotenone (A + R) in G-6-P-supplemented medium. The ATP production was measured using the ATP Luminescence Kit. The graph shows mean values \pm SD of three independent experiments normalized to the DMSO control. ns not significant, * $p < 0.05$

4 DISCUSSION

Gonorrhoea is the second most prevalent sexually transmitted disease worldwide. The causative agent *N. gonorrhoeae* has recently been described as a 'superbug', the treatment of which will become an enormous challenge due to its resistance to nearly all available antibiotics (Ohnishi *et al.*, 2011b). Especially the discovery of two resistant strains against ceftriaxone, which was considered the last line of defence, led to an outcry in research and even in media (Ohnishi *et al.*, 2011a, Unemo *et al.*, 2012).

Another problem is the emerging number of coinfections with *C. trachomatis*, which is responsible for the most widespread sexually transmitted diseases. A study of coinfections in male patients with urethritis in Greece revealed that 30 % of *N. gonorrhoeae* positive diagnosed patients were also infected with *C. trachomatis* (Papadogeorgakis *et al.*, 2010). However, until this date *C. trachomatis* infections are treatable with antibiotics and resistances have not yet emerged. The difficulties of chlamydial infection lie elsewhere. An estimated number of 70 - 80 % of women and 50 % of men are asymptotically infected with *C. trachomatis* (Malhotra *et al.*, 2013). Furthermore, treatment failure can result in persistence and repeated reinfections. Thus, diagnosed gonorrhoea but not identified chlamydial infection can lead to wrong application of antibiotics and therefore persistent *Chlamydia*. Additionally, lateral gene transfer has been identified *in vitro* in *C. trachomatis*, hence offering the possibility for the uptake of resistance genes (Demars *et al.*, 2007). Besides these difficulties, there are no vaccines available against both of the human pathogens, which make them crucial model organisms in the search for novel antimicrobial agents.

4.1 The interaction of cellular SREC-I with neisserial PorB_{IA}

N. gonorrhoeae has developed various ways for adherence to and invasion into the host cell, involving virulence factors such as LOS, type IV pili and Opa proteins. It has been proposed that the bacteria use their porin PorB_{IA} during DGI infections to bind Gp69 in a phosphate-sensitive manner to invade the host cell by interacting with the cellular receptor SREC-I (Rechner *et al.*, 2007). The extracellular domain of the receptor contains six EGF domains, which are considered to be responsible for the binding of the bacteria. Also, other receptors possessing EGF domains have been shown to be involved in bacterial recognition (Adachi & Tsujimoto, 2002, Zhou *et al.*, 2001). It has been demonstrated that the presence of one EGF-

like domain of SREC-I is enough for bacterial internalization. An increasing number of EGF-like domains resulted in rising invasion numbers (Faulstich, 2009).

This work aimed to prove a direct interaction between the protein PorB_{IA} and its cellular receptor by co-IP, pull-down assays and SPR. Additionally, the establishment of the SPR assay would offer the possibility to screen for inhibitors specifically against the PorB_{IA}-mediated invasion pathway. The Gp96 protein was not included in the experiments due to its unknown role during infection. Since the depletion of Gp96 did not affect bacterial invasion, a function in innate immune system was considered (Rechner *et al.*, 2007).

The first analysis included co-IP of PorB_{IA} by SREC-I bound beads. However, this approach was not suitable since the porin bound unspecific to the beads. The reason could be an improper composition of blocking and washing buffer or an unspecific binding to protein G due to modifications or certain features of PorB_{IA} (Feller & Lewitzky, 2012).

In the following experiment PorB_{IA} and PorB_{IB} were FLAG-tagged at their extracellular loop 1. Isolated neisserial blebs were used to pull-down the interaction partners of PorB_{IA}. However, the coomassie staining revealed no extra bands in the sample with PorB_{IA} coated blebs in comparison to the control PorB_{IB} blebs and untagged N927 blebs. This can be explained by the FLAG-tagging of the porin, which might interfere with a proper binding, since the tagging itself decreased the bacterial adherence and invasion. Furthermore, the elution fractions did not contain a PorB band at 35 kDa. A PorB_{IA} signal could only be detected by western blot analysis, indicating a low binding efficiency of the pulled down neisserial blebs to the anti-FLAG beads (data not shown). Therefore, the potential receptor might be present in a low concentration in the elution fraction and not detectable by coomassie staining. The identification of proteins which are present in the sample but not in the control can be achieved by analysing the whole elution fraction lane using mass spectrometry.

The interaction was also analysed by monitoring the binding of the soluble GFP-tagged extracellular domain of SREC-I to PorB_{IA}-expressing *N. gonorrhoeae*. The difference in the binding to PorB_{IA}- and PorB_{IB}-expressing bacteria was not significant. However, the binding of SREC-I to the commensal *N. lactamica* was significantly reduced. These bacteria express only one porin that shows a homology of roughly 84 % to gonococcal PorB_{IB}. The

differences between pathogenic and non-pathogenic porins are variable sequences in the extracellular loops, which might hinder the binding to the soluble SREC-I (Derrick *et al.*, 1999). However, to exclude an unspecific binding of SREC-I and to verify a proper folding of the protein further controls should be applied. The controls would include the pre-incubation of SREC-I with its natural ligand AcLDL, which should lead to decreased binding of the receptor to the bacteria. Moreover, given that the type of the interaction is unknown, the applied pull-down and binding assays might in general not be suitable for the interaction analysis, since the binding might be not be strong or long-lasting enough.

The expected difference in the binding of PorB_{IA} and PorB_{IB} to SREC-I was also missing in the SPR experiment. The low K_D value revealed a high-affinity interaction of SREC-I to PorB_{IA} and PorB_{IB}. The addition of phosphate did not affect the binding, which supported the findings of Rechner *et al.* that the interaction of PorB_{IA} to SREC-I is phosphate independent (Rechner *et al.*, 2007). However, in order to exclude an unspecific binding of SREC-I to the porin coated chip, another protein such as IgG should be used as a negative control for the measurement. Additionally, the SREC-I ligand AcLDL or a SREC-I antibody could be used during the interaction assay for interruption of the protein-protein interaction. Furthermore, it has been taken into consideration that the SPR analysed the binding of the extracellular domain of SREC-I to biotinylated monomers and trimers of PorB. The fact that the majority of the PorB proteins were available as monomers and not trimers could have an influence on the binding. PorB_{IB} in its trimeric form might not interact with SREC-I to such extent.

Providing that the results of the interaction assays were not caused by unspecific binding, the question arises concerning the reasons for the equal binding efficiency of both porins to SREC-I, although gonococci cannot use PorB_{IB} for invasion into the host cell. It has been observed that SREC-I is able to form an oligomer in the membrane, which was described as homophilic *cis*-interaction (Shibata *et al.*, 2004). Receptor oligomerization upon contact to bacteria has also been described for other receptors, such as the Toll-like receptor 4 (TLR4) (Zhang *et al.*, 2002). LPS is recognized by TLR4 associated with the LPS binding protein (LBP), CD14 and myeloid differentiation protein MD-2, which leads to homotypic oligomerization of the receptor and induction of a signalling cascade. This might also apply for SREC-I. PorB_{IA}, but not PorB_{IB}, might be able to induce SREC-I oligomerization *in vivo*.

Another possibility is that SREC-I operates not as a single receptor but requires co-receptors for binding to the pathogen. Examples are the bone morphogenetic proteins (BMPs), cytokines from the TGF- β superfamily and their type I and II receptors. The BMPs possess a high affinity to the extracellular domain of the type I and a low affinity to the type II receptor. After formation of the ligand-type I receptor complex the affinity is increased for the type II receptor (Kirsch *et al.*, 2000). Other TGF- β ligands or Activin have shown a high affinity only to type II receptors and do not interact with the single type I receptor. Only after binding to the type II receptor, the type I receptor is incorporated (Massague, 1998). The interaction between PorB_{IA} and SREC-I might also recruit another receptor in a phosphate-sensitive manner, which is not possible when PorB_{IB} interacts with SREC-I. Such a co-receptor could be SREC-II, another member of the type F scavenger receptor family expressing seven EGF-like repeats in the extracellular domain. It has been demonstrated that the heterophilic *trans*-interaction of SREC-I and II is stronger than the homophilic *trans*-interaction of SREC-I (Ishii *et al.*, 2002). A scenario could be hypothesized in which PorB_{IA} binds to SREC-I, leading to an increased affinity to a co-receptor. The receptor is recruited and binds in a phosphate-sensitive manner to the SREC-I/PorB_{IA} complex, resulting in an induction of a signalling cascade and bacterial internalisation.

4.2 Search for novel antimicrobials

In order to find novel small compounds inhibiting the infection of *N. gonorrhoeae* and *C. trachomatis*, 68 substances were analysed using an *in vitro* infection assay that was evaluated at an automated fluorescence microscope. Three different concentrations of the compounds were tested and the results of the highest concentration were used as criterion for distinguishing between active, moderately active and inactive compounds. Additionally, the cytotoxicity and the dose-dependency of the effect of the compounds were taken into consideration.

No bioactive compounds against neisserial infection could be identified, while seven inhibitors could be found against infection with *C. trachomatis*. The reason for finding more inhibitors against *C. trachomatis* than against *N. gonorrhoeae* could be a variation in the target sites and screen output. The search for anti-neisserial substances was limited to the PorB_{IA}-mediated invasion pathway, whereas chlamydial inhibitors were not restricted to one adhesin or invasine, such as PorB_{IA}. During the 1 h infection period of *N. gonorrhoeae* the

substances could interfere with the interaction of PorB_{IA} with its cellular receptor, which would lead to decreased number of adherent and invasive bacteria. A cellular target involved in the intracellular signalling might be possible as well, which could result in impeding the signalling cascade that is responsible for bacterial internalisation. However, the 1 h infection period was not enough to obtain information about the bacterial viability, since the bacteria have an average doubling time of 60 min (Tobiason & Seifert, 2006). It was also not possible to monitor intracellular replication of gonococci due to the fact that the neisserial replication is usually measured starting from 4 h post-infection (Hagen & Cornelissen, 2006). Chlamydial inhibitors however, had at least 16 h to target their binding site, since an inhibitory effect on the chlamydial inclusions could be detected even after 16 h post-infection. The viability and replication could be directly monitored by measuring the inclusion surface area. To obtain the same information of *Neisseria* several types of screens would be necessary, which would focus on the growth of the bacteria in the presence of compounds and survival of intracellular bacteria over a longer time period.

The number of potential target sites of small molecules is higher during chlamydial infection due to the dependency of the bacteria on their cellular host. *C. trachomatis* require different factors from the cell for establishing its replicative niche and for performance of the developmental cycle. After entry of *C. trachomatis* into the host cell, the inclusion is transported along the microtubules in a dyneine-dependent manner to the peri-Golgi region (Clausen *et al.*, 1997, Grieshaber *et al.*, 2003). Several host cell factors such as Rab GTPases and SNARE proteins involved in membrane trafficking processes, organelle identity and the membrane fusion machinery are recruited to the inclusion. Besides Golgi, the bacteria were also found to interact with other host cell organelles for the acquisition of lipids or essential amino acids. It could be shown that only five amino acids (aspartate, glycine, γ -L-glutamyl-L-cystenylglycine, glutamic acid and proline) are non-essential for chlamydial growth while the others are essential or advantageous (Karayiannis & Hobson, 1981). All these dependencies of *C. trachomatis* can be targeted by compounds and inhibit proper inclusion formation.

4.3 Inhibitors of the macrophage infectivity potentiator

MIP-like PPlases has been shown to be connected to bacterial virulence, which led to investigation of these proteins as potential drug targets. The known MIP inhibitors rapamycin and FK506 are not appropriate for infection treatments because of their immunosuppressive properties. To avoid side effects, pipercolic acid derivatives were synthesised on the basis of the binding of rapamycin/FK506 to Lp-MIP and BpML1 and were tested successfully as MIP inhibitors (Juli *et al.*, 2011, Begley *et al.*, 2014, Norville *et al.*, 2011). During the screening for antimicrobials of *N. gonorrhoeae* and *C. trachomatis* 30 different pipercolic acid derivatives were tested, one of which was active, four were moderately active against *C. trachomatis* and five had a moderate effect on *N. gonorrhoeae*. Only one compound (CJ183) affected both pathogens. An *in vitro* enzymatic PPlase assay was performed to verify the inhibitory effect of the pipercolic acid derivatives on the PPlase activity of recombinant Ng-MIP and Ctr-MIP. The IC₅₀ was determined for ten selected pipercolic acid derivatives and rapamycin. Two compounds showed no effect on either of both enzymes. The IC₅₀s of six compounds differed between the neisserial and chlamydial MIP by approximately the factor of 1.5, which underlines the conserved binding pocket of the inhibitors. Minor variations in the structure, such as the position of NO₂ group in *para*- or *meta*-substitution of PipN3 and PipN4, resulted in severe changes of the IC₅₀. Since neither a crystal structure of Ng-MIP and Ctr-MIP nor a co-crystallisation of the MIP proteins with rapamycin/FK506 is available, a screening of compounds using the PPlase assay is suitable to search for the optimal pipercolic acid derivative structure.

However, the determined IC₅₀ values of the compounds from the PPlase assay do not entirely correspond to the inhibitory effect on *N. gonorrhoeae* and *C. trachomatis* during the infection assay. The compound CJ257 for example had an IC₅₀ of 15.8 μM and inhibited the inclusion surface area by 65 % at a concentration of 40 μM. In contrast to that, SF275 with an IC₅₀ of 3.1 μM decreased the inclusion area only by 30 %. The reason for these mismatches might be that the screening procedure was not specifically designed for the analysis of MIP inhibitors, but was a fast tool for identification of inhibitors of the PorB_{IA}-mediated invasion pathway of *N. gonorrhoeae* and of the primary infection of *C. trachomatis*. However, further investigation revealed the importance of neisserial MIP during infection of PMNs and not epithelial cells. Moreover, the major effect of chlamydial

MIP inhibition could be detected during progeny infection. Therefore, the observed inhibitory effects of the pipecolic acid derivatives during the compound screening could be caused by unknown side effects. The screening procedure has to be repeated under adjusted conditions for each pathogen.

Besides, there are more unknown factors that might influence the screening results. These include the ability of the compounds to enter the host cell. A compound with a low IC_{50} might not access the target site as efficiently as another compound with a higher IC_{50} due to hindrances in the entry through the membranes or pores in the cell membrane. Furthermore, unspecific binding to other target sites might reduce the amount of the compound at the MIP binding region. Additionally, it should be considered that the *in vitro* PPIase assay is performed with succinyl-Ala-Leu-Pro-Phe-4-nitroanilide as a substrate, which might not reflect the actual enzyme efficiency for its natural substrates.

4.3.1 The role of chlamydial MIP during bacterial developmental cycle

Previously, an inhibitory effect of 25 μ M rapamycin was demonstrated on chlamydial infectivity in McCoy cells (Lundemose *et al.*, 1993a). Furthermore, a rising number of chlamydial particles with abnormal morphology could be observed. We could confirm these results by applying rapamycin during infection of HeLa cells with *C. trachomatis*. Lundemose *et al.* detected a decrease of 80 % in the inclusion numbers after 36 h. We measured a reduction of 74.3 % in the total inclusion surface area after 24 h (20 μ M), which is in agreement with the former results. Rapamycin served in our study as a positive control for the analysis of the specifically designed MIP inhibitors PipN3 and PipN4, which emerged during the compound screening as the promising compounds and exhibited a low inhibitory concentration on the isomerase activity of Ctr-MIP. However, these compounds decreased the inclusion surface area by only about 30 % and therefore affected the primary infection less than rapamycin did. The reason might be the much lower IC_{50} of rapamycin of 0.015 μ M, which is 0.241 μ M for PipN3 and 0.0646 μ M for PipN4. However, the applied compound concentration of 5 μ M during the experiments should be sufficient enough to inhibit the chlamydial MIP isomerase activity, providing that rapamycin and the pipecolic acid derivatives reach the target site with similar efficiency. Since rapamycin is a known immunosuppressant due to the inhibition of mTOR, off-target effects cannot be excluded.

The serine/threonine kinase mTOR is responsible for regulation of several cellular pathways and plays a role in cellular proliferation, growth, autophagy, glucose and lipid metabolism (Gingras *et al.*, 2001, Richardson *et al.*, 2004, Schmelzle & Hall, 2000). The protein is known to modulate the translational regulators S6K1 and S6K2 (ribosomal S6 kinases) and eIF4E (eukaryotic initiation factor 4E) (Holz *et al.*, 2005). A proteomic profiling of *C. trachomatis*-infected HeLa cells revealed an increased mTOR protein expression and activation upon chlamydial infection (Tan *et al.*, 2016). The authors hypothesised a modulation of the mTOR pathway by *C. trachomatis* in order to stimulate the host cell glycolysis and gain ATP for RBs proliferation. Blockage of the mTOR signalling pathway by rapamycin could therefore affect the chlamydial development. Furthermore, treatment of cells for 24 h with more than 20 μM rapamycin resulted in cellular vacuole formation and cell detachment (data not shown). Therefore, the strong antichlamydial effect of rapamycin at 20 and 30 μM might be due to the cytotoxic effect of the compound, which arises through the inhibition of the mTOR pathway that is important for cell viability.

Although, it cannot be excluded that the pipercolic acid derivatives PipN3 and PipN4 have off-target effects as well, the effect on chlamydial growth differed from rapamycin during primary infection. While 30 μM rapamycin reduced the inclusion surface area by 84.4 %, a reduction by only approximately 40 % could be detected upon treatment with 30 μM PipN3 and PipN4. Furthermore, the application of 40 μM of the pipercolic acid derivatives did not lead to an enhanced effect, which indicated saturation in the inhibition of the Ctr-MIP PPIase activity. However, the effect on the primary infection was minor compared to the detected main influence of the compounds on the progeny infection. The developmental cycle of the bacteria is affected by rapamycin and the pipercolic acid derivatives PipN3 and PipN4, which resulted in less infectious progeny EBs. The compounds might negatively influence the replication of RBs. However, since the addition of the inhibitors 24 h post-infection also decreased the progeny infectivity, an inhibitory effect on the redifferentiation of RBs to EBs might also be considered. The observed effect can be reversed by washing out of the compounds post-infection. Electron microscopic pictures revealed a declined number of EBs, an increase in ABs and membranous structures. These results indicate the induction of chlamydial persistence by the compounds.

In this study, I could demonstrate the importance of the protein for the intracellular development for *C. trachomatis*. However, no bacterial or host cell substrate of Ctr-Mip is known so far. Previously, human collagen IV was identified as the target of Lp-MIP, which is important for interaction of the bacteria with lung epithelial cells and transmigration across epithelial cell barriers (Wagner *et al.*, 2007, Unal *et al.*, 2011). *C. trachomatis* is also known to bind the collagen types I and IV (Kihlstrom *et al.*, 1992). The pre-incubation of the bacteria with rapamycin reduced chlamydial infection, which could be due to the blocked interaction of Ctr-MIP to collagen IV (Lundemose *et al.*, 1993a). However, another study has shown that the lipoprotein is expressed only 12 h to 14 h post-infection that would exclude its role in the bacterial internalisation (Lundemose *et al.*, 1991). I also pre-treated the isolated chlamydial particles with rapamycin at different concentrations and infected cells for 24 h (data not shown). Unfortunately, I did not observe an effect on the chlamydial infection and therefore could not reproduce the already published results (Lundemose *et al.*, 1993a). The reason for this discrepancy could be the performance of the experiments with different cell types; while we used HeLa cells Lundemose *et al.* performed the studies with McCoy cells.

It was further proposed that Ctr-MIP might play a role in the modulation of nutrient transport into the inclusion, the inhibition of which could result in persistent bacteria (Lundemose *et al.*, 1993a). This idea arose due to a study of Brandl & Deber, who showed that the majority of integral membrane transport proteins possess membrane-buried proline residues (Brandl & Deber, 1986). *Cis-trans* isomerisation of these proteins could lead to a modulation of the transport state. However, this hypothesis would require the secretion and integration of Ctr-MIP in the inclusion membrane for interaction with the inclusion membrane proteins, which could not be demonstrated by now. Therefore, further assumptions regarding the Ctr-MIPs role in autophagy by interfering with the FKBP12-dependent signalling pathway or other cellular processes can only be considered when the MIP have been localised outside the inclusion (Unal & Steinert, 2014).

Ctr-MIP might also be important for production of chlamydial progeny in the process of redifferentiation of RBs to EBs. Ctr-MIP is expressed in the inner and outer membrane of EBs and on the surface of RBs (Lundemose *et al.*, 1993b, Neff *et al.*, 2007). Therefore, the PPIase activity of Ctr-MIP in the inner membrane might be important for catalysing the

folding of bacterial outer membrane or periplasmic proteins after the translocation across the membrane (Neff *et al.*, 2007).

Furthermore, a role of Ctr-MIP has also been suggested in the pathogenesis by induction of inflammatory responses during chlamydial infection. Recombinant Ctr-MIP exhibits a strong proinflammatory activity and has been shown to induce the release of IL-1 β , TNF- α , IL-6 and IL-8 in human monocytes/macrophages (Bas *et al.*, 2008). The lipid modifications of the lipoprotein have been identified as the inducers of this process. Also lipoproteins and lipopeptides of other pathogens such as *L. monocytogenes* and *N. gonorrhoeae* have been shown to trigger a strong inflammatory response (Flo *et al.*, 2000, Reglier-Poupet *et al.*, 2003, Fiset *et al.*, 2003). The benefits of *C. trachomatis* from induction of inflammation during infection are yet unknown. It is proposed that pathogens utilize this process for disruption of host cell barriers and entrance into deeper tissue layers. It is conceivable that *C. trachomatis* uses inflammation to reach a persistent state, thus evading the host cell immune system and establishing a chronic infection. *In vitro* studies have demonstrated the induction of persistence upon addition of TNF- α to the infection (Shemer-Avni *et al.*, 1988). Since TNF- α is secreted during chlamydial infection it might induce a persistent state.

4.3.2 Neisserial MIP and relation to bacterial survival in PMNs

The Ng-MIP is important for gonococcal intracellular survival in mouse and human macrophages (Leuzzi *et al.*, 2005). However, an acute infection is characterised by purulent exudates consisting of PMNs, exfoliated epithelial cells, and intracellular as well as extracellular bacteria (Jerse *et al.*, 2014). Since PMNs are the first-line of defence during neisserial infection, I analysed the role of Ng-MIP during neutrophil infection. I could demonstrate the importance of the enzyme during neutrophil infection by using an Ng-MIP deletion mutant and the MIP inhibitors PipN3 and PipN4. Deletion of Ng-MIP led to a significant reduction of intracellular bacteria by 28.7 %. To ensure that this knockdown is responsible for the effect, a complementation was performed, which restored the wild type phenotype. Furthermore, the MIP specific inhibitors PipN3 and PipN4 and the positive control rapamycin were applied during gonococcal PMN infection. This reduced the bacterial

survival significantly by 34.7 % in the presence of rapamycin, by 25.6 % in the presence of PipN3 and by 16.7 % when PipN4 was added.

Since *N. meningitidis* has also been shown to express a MIP protein that is highly homologous to Ng-MIP the inhibitors (Hung *et al.*, 2011) PipN3 and PipN4 were tested in meningococcal infection (Reimer *et al.*, 2016). Adherent and invasive bacteria were analysed 6 h post-infection after treatment with DMSO, rapamycin and the MIP inhibitors. PipN3 and PipN4 reduced the adherence as well as the invasion of *N. meningitidis* significantly. These results indicate that the Nm-MIP plays a crucial role during infection of pharyngeal epithelial cells, while Ng-MIP is responsible for the prolonged survival of *N. gonorrhoeae* within PMNs.

The effect of the compounds on the intracellular survival of *N. gonorrhoeae* was less pronounced compared to the effect of the knockout mutant. The explanation could be that the PPIase activity was not reduced to 0 % and the residual activity was sufficient enough to increase the bacterial survival. It might also be possible that not the PPIase activity but another property of the Ng-MIP is important during the bacterial survival in PMNs. The observed inhibition of the compounds might therefore be due to certain off target effects. The role of the enzyme activity was questioned previously in several studies regarding the *L. pneumophila* MIP. The deletion of this protein reduced the intracellular survival of the bacteria in protozoan cells, macrophage-like cells U937 and human alveolar macrophages (Cianciotto & Fields, 1992). The introduction of point mutations in the Lp-MIP, which decreased the PPIase activity to 5.3 % (D142L) and to 0.6 % (Y185A), did not affect the pathogen' survival in macrophage-like cell line U937, human blood monocytes and the amoeba *Acanthamoeba castellanii* (Wintermeyer *et al.*, 1995). The deletion of the part of the N-terminal domain (Δ 77-123) that prevents dimerization of Lp-MIP did not affect the proteins PPIase activity (Kohler *et al.*, 2003). However, the expression of this truncated protein decreased bacterial survival in *Acanthamoeba*. Nevertheless, the full PPIase activity of Lp-MIP has been shown to be important in the infection of guinea pig animal models. Similar mutations of the Ng-MIP are required to prove that the PPIase activity correlates with the prolonged survival in PMNs. First steps to address these issues have already been made by purifying three Ng-MIP variants including the mutations D165L (Lp-MIP: D142L), Y208A (Lp-MIP: Y185A) and deletion of the dimerization domain (Δ 22-91). The *in vitro* PPIase assay results were comparable to the mutated Lp-MIP, representing the high sequence

conservation of the MIP proteins. The enzyme activity of the monomeric MIP variant was reduced by only 25 %, while Y208A decreased the activity to 1.1 % and D142L to 11.6 %. The effect of these mutations needs to be investigated using a PMN survival assay.

Therefore, the MIP inhibitors PipN3 and PipN4 can only be used for supportive argumentation, since off-target effects cannot be excluded. Eight different PPIase proteins were identified in *N. gonorrhoeae* using NCBI databases and their functionality might be impaired by the MIP inhibitors as well (Humbert *et al.*, 2015). Furthermore, the PMN survival assay faced several complications such as the isolation of PMNs from different blood donors. Additionally, we observed the formation of NETs upon treatment of PMNs with DMSO (data not shown). The effect could be minimized using a concentration of 0.1 %, but still, these are the factors that could influence the results of the assay.

The role of neisserial MIP during survival in macrophages or neutrophils is unknown. The deletion of Ng-MIP seems to affect the bacteria themselves since the knockout mutant showed a slight growth defect. The membrane integrity might be damaged by the missing outer membrane protein. The MIP protein might as well be needed for assembly of certain bacterial outer membrane proteins. This effect was not observed upon treatment of the bacteria with the MIP inhibitors, which might be due to the residual activity of the MIP protein. However, it is also possible that another property of MIP instead of the PPIase activity is important for the bacteria.

The question arises how the Ng-MIP could contribute to the survival of *N. gonorrhoeae* in PMNs. There are several possibilities for pathogens to stay viable inside neutrophils, such as the inhibition of the phagosome/lysosome fusion, survival inside the phagolysosome by resisting oxidative burst and escape to the cytoplasm. Previously, it has been demonstrated that *N. gonorrhoeae* is able to avoid maturation of phagolysosomes by delaying fusion of the phagosome with primary granules (Johnson & Criss, 2013). The authors could show that this process is presumably mediated by unknown gonococcal surface characteristics and not by active secretion of certain effectors. It can be speculated whether Ng-MIP is the surface-exposed protein that contributes to the delayed fusion, therefore helping the pathogen to survive inside the neutrophils.

The exploitation of PMNs by the gonococci has many benefits for the pathogen such as the evasion from the host cell immune system, but also the acquirement of new nutrients

and transmission into deeper tissues. The Ng-MIP might play a direct role in the transmigration process, since the LP-MIP has been shown to contribute to bacterial dissemination in lung tissue by binding to collagen IV and promoting transmigration (Wagner *et al.*, 2007, Unal *et al.*, 2011).

The Lp-MIP, like the neisserial MIP, is a surface-exposed protein that resides within the bacterial cell wall/ cytomembrane. Electron microscopic studies using immunogold staining revealed the localisation of Lp-MIP during infection of *A. castellanii* within host membranes, which formed multilamellar structures (Helbig *et al.*, 2001). It is considered that Lp-MIP is delivered to the host cell membrane by shedding of outer membrane vesicles that have been shown to contain the MIP protein (Galka *et al.*, 2008). Lp-MIP might interfere with the host cell FKBP12 signalling pathway due to the high similarity of both proteins. This could result in changes of the host cell autophagy machinery that is regulated by FKBP12 signalling pathways (Unal & Steinert, 2014). A recent study provided evidence that autophagy can be induced in neutrophils (Mitroulis *et al.*, 2010). Since rapamycin has been shown to be one of the inducers, the observed effect of the compound on the survival of gonococci during the PMN survival assay could be due to autophagy processes and not due to the inhibition of the PPIase activity of Ng-MIP. Whether the neisserial MIP is also incorporated into host cell membranes is not known, but *N. gonorrhoeae* are also able to release outer membrane vesicles (blebs) that contain different surface proteins (Dorward & Judd, 1988, Dorward *et al.*, 1989). Therefore, it can be imagined that the Ng-MIP is interfering with neutrophil processes, which were optimized for the killing of pathogens.

Furthermore, one report presented an unknown type II secretion system-dependent exoenzyme with p-nitrophenol phosphorylcholine (p-NPPC) hydrolase activity as a potential target of the Lp-MIP (Debroy *et al.*, 2006). It was observed that the C-terminal domain of Lp-MIP is required for p-NPPC hydrolysis in cultured supernatants, but is not a p-NPPC hydrolase itself. The authors proposed two hypotheses, in which the Lp-MIP acts as a chaperone for the release of the p-NPPC hydrolase or is required for the activation of the secreted hydrolase by the PPIase activity. The authors demonstrated that a membrane bound protein is involved in the activation or secretion of proteins beyond the outer membrane. This finding shows that the functions of bacterial MIPs are not limited by their

membrane localisation. The neisserial MIP might also have an accessory role in the secretion and correct assembly of certain virulence-associated proteins that modulate the host cell and prolong bacterial survival.

4.4 Mode of action of antichlamydial compound SF2446A2

4.4.1 Antioxidant property and antibacterial activity of SF2446A2

18 compounds derived from marine sponges or sponge-associated bacteria were screened for their antichlamydial and antineisserial properties. The three compounds gellusterol E, ageloline A and SF2446A2 were highly active against *C. trachomatis*, of which the latter two exhibited antioxidant activity (Abdelmohsen *et al.*, 2015, Cheng *et al.*, 2016, Reimer *et al.*, 2015). Major producers of superoxide radicals, the precursors of the most reactive oxygen species, are the mitochondrial complexes I-III and the NADPH oxidase (Martinez-Reyes & Cuezva, 2014). Superoxide radicals are converted by superoxide dismutases to hydrogen peroxide, which can react with iron to form hydroxyl radicals. Cellular enzymes such as peroxiredoxins, glutathione peroxidases and catalase are required for removal of cellular hydrogen peroxide. Oxidative stress leads to DNA, protein and lipid damage and finally to apoptosis. However, lower concentrations of ROS function as second messenger in various signalling pathways (Sena & Chandel, 2012). Therefore, the question arose if the antioxidant properties of the antichlamydial compounds are connected to their bioactivity. In general, a correlation between antioxidant and antimicrobial activity has not been demonstrated, despite the finding that various natural compounds such as polyphenolic phytochemicals exhibit both properties (Stevenson & Hurst, 2007). However, the scavenging of radicals by antioxidants might play a role during chlamydial infection, since the cellular ROS levels are increased upon infection within a few hours and are decreased to the basal levels after 9 h post-infection (Boncompain *et al.*, 2010). The production of ROS is triggered by K⁺ efflux in infected cells and results in NLRP3-mediated caspase-1 activation (Abdul-Sater *et al.*, 2009). This cellular response on chlamydial infection is impaired by antioxidants due to the blockage of caspase-1 activation. Furthermore, the induction of ROS by *C. trachomatis* has also been shown to promote cellular necrosis (Chen *et al.*, 2016). Although ROS plays a role during chlamydial infection, the addition of the known antioxidants Trolox and n-acetylcysteine (data not shown) revealed that these substances have no impact on the

chlamydial infection. Previously, the effect of the antioxidants EDTA and vitamin C have been analysed on *C. trachomatis* (Lampe *et al.*, 2004, Wang *et al.*, 1992). While EDTA showed a moderate effect, vitamin C enhanced the chlamydial infection. A direct connection between antioxidants and an inhibitory effect on *C. trachomatis* have not been demonstrated yet. Therefore, we concluded that ageloline A and SF2446A2 are not impairing the bacterial infection through their antioxidant properties but through another mechanism. However, the antioxidant properties might play a role *in vivo*, since the host defence mechanisms against *C. trachomatis* comprise oxygen-mediated killing (Yong *et al.*, 1987, Yong *et al.*, 1982).

4.4.2 Inhibition of mitochondrial respiration by SF2446A2

The compound produced by the *Streptomyces sp.* strain RV15, SF2446A2 inhibited the chlamydial inclusion formation in a dose-dependent manner. We could demonstrate that this compound is not only affecting the primary, but also the progeny infection. However, the main effect was observed on the formation and establishment of the primary infection, the consequence of which was the development of a less viable progeny. This highly antichlamydial naphthoquinone antibiotic SF2446A2 might be of polyketide origin as the majority of naphthoquinones in bacteria (Izumikawa *et al.*, 2011, Medentsev *et al.*, 2005, Funa *et al.*, 1999, Metsa-Ketela *et al.*, 2013). Polyketides are the most important class of natural products among bacterial symbionts of marine sponges regarding drug discovery, since they exhibit various pharmacological activities (Della Sala *et al.*, 2014, Larsen *et al.*, 2015, Hochmuth & Piel, 2009). SF2446A2 had an IC₅₀ of 2.6 µM during infection of *C. trachomatis* without inducing persistence in the bacteria and was therefore an attractive compound for analysis of its mode of action. Since not only SF2446A2 but also four plant-derived naphthoquinones were classified as active and two as moderately active substances against *C. trachomatis* infection during the screening procedure, it could be speculated whether the class of quinones harbour an antichlamydial mechanism.

Naphthoquinones are known inhibitors of different parasites such as *Plasmodium*, *Leishmania* and several *Trypanosoma* species (Bringmann *et al.*, 2008, Menna-Barreto *et al.*, 2009). Furthermore, antitumoral properties could be demonstrated against cells derived from B cell lymphoma and multiple myeloma (Bringmann *et al.*, 2008). Pieretti *et al.*

investigated the possible target sites of the 2-phenoxy-1,4-naphthoquinone in *Trypanosoma brucei rhodesiense* (Pieretti *et al.*, 2013). They could demonstrate an inhibition of the glycosomal glycerol kinase and glycosomal glyceraldehyde-3-phosphate dehydrogenase (TbGAPDH). TbGAPDH is one of the catalysing enzymes in the glycolysis and a validated anti-parasitic target (Verlinde *et al.*, 2001). Furthermore, naphthoquinones have been shown to damage mitochondria (Menna-Barreto *et al.*, 2009, Boveris *et al.*, 1978, Morello *et al.*, 1995). The analysis of the mode of action of anti-typanosomal naphthofuranquinones revealed that the compound causes a collapse of the $\Delta\psi$ and decreases the complex I-III activity (Menna-Barreto *et al.*, 2009). The hypothesis was proposed that naphthoquinones accumulate in the IMM and are reduced by complex I. The reduced form interacts with oxygen and leads to the development of reactive oxygen species, which causes the mitochondrial dysfunctionality. The ROS generation might be the reason for the cytotoxic effect of naphthoquinones, which was also observed during the compound screen, since eight of the 16 tested naphthoquinones exhibited cytotoxicity.

Due to these known effects of quinones and the fact that the compound SF2446A2 was also active against the eukaryotic human parasite *S. mansoni*, the idea arose that the SF2446A2 is not inhibiting *C. trachomatis* directly but indirectly by interfering with certain cellular factors. Severe effects could be demonstrated on the mitochondrial respiration, including a decrease in the basal respiration and ATP production, an increase of the proton leak, a reduction of the maximal respiratory capacity and spare respiratory capacity in a dose-dependent manner. Furthermore, a simultaneous increase of the $\Delta\psi$ was observed. A hyperpolarized mitochondrial membrane is usually the result of an increased accumulation of protons in the IMS, which can be achieved by inhibition of the F_0F_1 -ATPase with the inhibitor oligomycin (Rego *et al.*, 2001). Blockage of complex I to IV or uncoupling have been shown to reduce the $\Delta\psi$ (Li *et al.*, 2003, Drose, 2013, Kalbacova *et al.*, 2003, Lee *et al.*, 2002). Therefore, the strongly reduced ATP production and the hyperpolarized membrane indicated an effect of SF2446A2 on the mitochondrial F_0F_1 -ATPase. However, the Mito Stress Test profile of oligomycin treated cells differed from those treated with SF2446A2. The basal mitochondrial respiration was reduced by 90 % in the presence of 5 μ M oligomycin, while 20 μ M SF2446A2 diminished the respiration by only 30 %. Furthermore, the maximal respiration was induced by FCCP to OCR levels of DMSO treated cells, despite of the pre-

treatment with oligomycin. This was not the case for cells treated with SF2446A2, which showed decreased maximal respiration levels. Based on the differences in the Mito Stress Test profiles it can be concluded that SF2446A2 is not only inhibiting complex V. Besides, the inhibition of complex I can also result in mitochondrial membrane hyperpolarization depending on the cell-type, inhibitor concentration and treatment duration. This effect has already been described in immortalized mouse embryonic fibroblasts (MEFs) and in 143B osteosarcoma cells (Valsecchi *et al.*, 2012, Barrientos & Moraes, 1999). A study of Forkink *et al.* has shown a hyperpolarisation of the mitochondrial membrane upon inhibition of complex I in HEK293T cells by the addition of 0.1 μ M rotenone for 24 h (Forkink *et al.*, 2014). It was accompanied by a decrease in mitochondrial oxygen consumption, low activity of complex II, III and IV, insensitivity of the oxygen consumption to FCCP treatment and upregulated glycolysis. A similar profile was observed when SF2446A2 was used to treat cells: reduced OCR levels, decreased maximal respiratory capacity and increased glycolysis. Therefore, it can be considered that SF2446A2 might impair the activity of complex I, which leads to changes in the mitochondrial respiration and results in increased $\Delta\psi$.

The reduced activity of complex IV and II could be associated with the diminished maximal respiration capacity, which is analysed by addition of the uncoupling agent FCCP and results in the maximal consumption of oxygen by complex IV. SF2446A2 reduced this capacity in a dose-dependent manner until no spare respiratory capacity was available, which is the difference between maximal and basal respiration. The spare respiratory capacity is crucial when the cellular energy demand is increased and has been shown to correlate with enhanced survival (Nickens *et al.*, 2013). Recently, it has been demonstrated that complex II, which is the link between the TCA cycle and the electron transport chain, is the main source of the spare respiratory capacity (Pfleger *et al.*, 2015). Inhibition of complex II by 3-nitropropionate (3NP) led to a complete loss of the spare respiratory capacity, while the OCR levels were only decreased by 10 - 18 %. It can be suggested that SF2446A2 reduced the FCCP-induced maximal oxygen consumption by diminishing the activity of complex II and complex IV.

Additionally, an uncoupling effect was observed upon treatment with SF2446A2, which implies an increased proton leak through the mitochondrial membrane. However, it

can be excluded that the compound acts as an uncoupling agent since the OCR was decreased and the $\Delta\psi$ increased upon treatment. 64 % of the proton leak is catalysed by the adenine nucleotide translocase (ANT), 11 % by the uncoupling proteins (UCP) and 25 % by other pathways that lead to the return of protons in the mitochondrial matrix independently of the F_0F_1 -ATPase pump (Brand *et al.*, 2005, Parker *et al.*, 2009, Parker *et al.*, 2008). 20 - 30 % of the oxygen consumption is generated by the proton leak in hepatocytes and 50 % are generated in rat skeletal muscles (Brand *et al.*, 1999). It has been shown that mild uncoupling from the ATP production reduces oxidative stress in the cell (Miwa & Brand, 2003). Therefore, it is hypothesized that ROS itself induces the proton leak by lipid peroxidation products such as aldehydes, alkenals, hydroxyalkenals and HNE (4-hydroxynonenal) and therefore generates a negative feedback loop, which attenuates its own production (Brand, 2000, Esterbauer *et al.*, 1991). Since SF2446A2 increased the proton leak, it can be assumed that the compound acts as a pro-oxidant and induces mitochondrial ROS production. It has been shown that polyphenolic natural compounds can scavenge ROS-species as well as produce radicals under certain conditions (Touriño *et al.*, 2008). Therefore, it is conceivable that SF2446A2 has a dual function as pro- and antioxidant.

However, uncoupling would inevitably lead to a depolarisation of the membrane, but instead a hyperpolarisation was measured. The $\Delta\psi$ plays a role in controlling the directionality of the F_0F_1 -ATPase and the ADP to ATP exchange by ANT through the IMM (Chinopoulos, 2011). Computer simulations and experiments with isolated mitochondria revealed that hyperpolarisation can be linked to the reverse mode of the ATPase and could be a response to a depolarisation of mitochondrial membrane (Chinopoulos *et al.*, 2010, Chinopoulos, 2011). Therefore, it would be interesting to analyse if SF2446A2 steadily increases the $\Delta\psi$ or if an initial depolarisation is occurring.

All in all, the performed Mito Stress Test and ATP measurements demonstrated a mitochondrial dysfunctionality upon treatment with SF2446A2, which led to reduced ATP levels. However, the target site of the compound could not be determined on the basis of these experiments. The compound might be metabolised in the cell and thus possess multiple functions, interfering with the mitochondrial respiration through several collective disruptions.

4.4.3 Blockage of mitochondrial respiration and the antichlamydial effect

The inhibition of the mitochondrial respiration by SF2446A2 resulted in increased glycolysis in order to compensate for the energy loss. Exchange of glucose as the carbon source in the medium by galactose led to a rapid dying of the cells in the presence of SF2446A2, which is likely due to the blockage of mitochondrial energy production and, thus, to the lack of ATP. To investigate the question if the ATP loss is responsible for the antichlamydial effect of the compound, the mitochondrial F_0F_1 -ATPase was knocked down using a shRNA-mediated approach. However, the knockdown of the F_0F_1 -ATPase itself did not affect the growth of *C. trachomatis*. These findings verified a report, which showed that the growth of *C. trachomatis* was not impaired during infection of a mutant Chinese-hamster-lung-fibroblast cell line (CCL 16-B2) with a 90 % reduced mitochondrial respiration (Tipple & McClarty, 1993). However, a combination of the absent ATPase and exchange of glucose to galactose medium prevented formation of chlamydial inclusions. Since SF2446A2 affected the bacteria in glucose-containing medium, it can be excluded that the antichlamydial effect came from the loss of ATP synthesized by mitochondria.

The knockdown of the mitochondrial ATPase and the simultaneous cultivation of the cells in galactose medium resulted in severe cell death as was observed for SF2446A2 treated cells. Previously, it has already been demonstrated that the ATP production of cells grown in galactose medium is sensitive to inhibition of OXPHOS by rotenone (Lanning *et al.*, 2014). Therefore, the F_0F_1 -ATPase knockdown cells were switched to galactose-supplemented medium only 16 h post-infection to prevent the establishment of the infection in already impaired cells. The depletion of glucose led to inhibition of further inclusion growth. *C. trachomatis* expresses the ATP/ADP translocases Npt1_{Ct} and Npt2_{Ct}, which transport the host cell ATP in the bacteria (Stephens *et al.*, 1998, Tjaden *et al.*, 1999). Depletion of cellular ATP levels could therefore impair the bacterial growth. However, the bacteria encode also a variety of proteins involved in the energy metabolism, such as enzymes of the chlamydial TCA cycle, oxidoreductases and enzymes of the glycolysis and gluconeogenesis pathway (Ilfie-Lee & McClarty, 1999, Nicholson *et al.*, 2003). Furthermore, chlamydial EBs use the sugar-phosphate/inorganic-phosphate antiporter UhpC to import G-6-P from the host cell and metabolise it to pyruvate applying glycolysis (Schwoppe *et al.*, 2002, Omsland *et al.*, 2012). The bacteria have the ability to generate ATP subsequently by

the enzymes phosphoglycerate kinase and pyruvate kinase (Iliffe-Lee & McClarty, 1999). The subtraction of glucose from cells with inhibited OXPHOS leads to a situation where the bacteria are not able to utilize cellular ATP by using translocases and are also not capable of generating their own ATP from G-6-P, thus resulting in inhibited bacterial growth.

Moreover, the dependency of *C. trachomatis* on the cellular ATP was investigated using a mitochondrial glutaminase knockdown cell line. During glutaminolysis glutamine is converted by the glutaminase to glutamate, which is metabolised to α -ketoglutarate for the TCA cycle in the mitochondrial matrix. The absence of glucose in the medium drives the cell to use glutaminolysis for production of 98 % of their cellular ATP (Reitzer *et al.*, 1979). In order to analyse the role of glutamine during chlamydial infection different conditions were applied including glucose- and galactose-containing medium in the absence or presence of glutamine or the glutaminase. Furthermore, the medium was supplemented either with non-dialysed or dialysed FCS for exclusion of small molecules. We observed a reduction of the infection in all cell lines, when dialysed FCS was supplemented, indicating that other small molecules such as vitamins or amino acids, independently of glucose or glutamine, were needed for chlamydial infection. Moreover, we demonstrated that the addition of glutamine positively affected the infection in the control cell lines, independently of the sugar added. It has already been shown that removal of glutamine from the cell culture medium reduced the production of inclusion and the infectivity yield and glutamine was therefore, classified as an advantageous amino acid for *C. trachomatis* (Karayiannis & Hobson, 1981, Reitzer *et al.*, 1979). The bacteria express glutamine transporters, which indicates a direct consumption of glutamine by the bacteria (Nicholson *et al.*, 2003). However, glutamine did not act as an advantageous amino acid when the glutaminase was knocked down. In this case, the addition of glutamine reduced the infection in the presence of glucose and dialysed FCS. The interference in the cellular metabolism might have resulted in certain cellular changes that were favourable for the chlamydial development.

The infection of the induced *glskd-1* cell line in the presence of glucose was reduced by only 40 %. The glycolysis provides the bacteria with enough cellular ATP and G-6-P for their own ATP production to balance the loss of glutamine as energy source. However, when glucose was absent the infection was decreased by 95 %. Glutamine as energy source is indispensable during infection when glucose is lacking.

Furthermore, *C. trachomatis* is believed to exploit the host cell vesicular transport for nutrient acquisition. The close association of the chlamydial inclusion to the Golgi apparatus enables the bacteria to obtain sphingomyelin and cholesterol-containing exocytic vesicles, which is mediated by Rab6 and 11 (Heuer *et al.*, 2009, Rejman Lipinski *et al.*, 2009). The intracellular transport of cargo vesicles is mediated by motor proteins such as kinesins and dyneins, which move along actin filaments or microtubules and require energy in form of ATP hydrolysis (Alberts *et al.*, 2010). Depletion of ATP sources will lead to changes in the cellular transport system and might impair the transport of essential nutrients to the chlamydial inclusion. The induction of F₀F₁-ATPase or mitochondrial glutaminase knockdown and simultaneous cultivation of the cells in galactose-containing medium resulted in an altered actin cytoskeleton structure, as observed after Phalloidin staining. Decrease in ATP levels might be the reason for the observed crumbled and patch-like filaments, since actin microfilaments require ATP hydrolysis for polymerisation (Korn *et al.*, 1987). Furthermore, the presence of the mitochondrial respiration inhibitor SF2446A2 blocked the fusion of several inclusions during a simultaneous infection of different bacteria. Homotypic fusion of inclusions is mediated by the transport of the bacteria-containing vacuoles by dynein proteins along microtubules (Richards *et al.*, 2013). It can be speculated if the missing ATP from OXPHOS could affect the transport of the single inclusions.

In general, ATP is the energy-currency of the cell and is required for nearly all cellular processes, of which numerous are exploited by the intracellular pathogens. It can be assumed that changes in these processes by inhibition of ATP production would affect the proper bacterial growth and development.

4.4.4 SF2446A2 and a direct effect on *C. trachomatis*

I demonstrated an inhibitory effect of the natural compound SF2446A2 on the mitochondrial respiration. However, further investigations revealed that the detected effect is not responsible for the antichlamydial properties of the compound. Since the substance also affected the growth of *S. aureus* and *N. gonorrhoeae* I assumed that SF2446A2 might also directly affect *C. trachomatis*. Also, other inhibitors of the mitochondrial respiration including oligomycin, rotenone and antimycin A impaired the chlamydial inclusion formation when the host cells were grown in the glucose-containing medium. Oligomycin is not only

affecting the host cell mitochondrial respiration, but has also been shown to inhibit the V-type ATP synthase of chlamydial EBs (Huijing & Slater, 1961, Peeling *et al.*, 1989). Besides, *C. trachomatis* also possesses genes that encode for NADH dehydrogenase (complex I), succinate dehydrogenase (complex II) and cytochrome bd oxidase (complex IV), which might be targeted by inhibitors of the mitochondrial respiration (Stephens *et al.*, 1998, Kalman *et al.*, 1999, Carlson *et al.*, 2005, Thomson *et al.*, 2008). *C. trachomatis* has the potential to generate its own ATP with the help of host cell substrates, which support the glycolysis, the incomplete TCA cycle and the respiratory chain. However, it is not known if the respiratory chain is used to generate ATP by the V-type ATP synthase, since the enzyme has been shown to hydrolyse ATP to ADP and inorganic phosphate (Peeling *et al.*, 1989). Instead, it has been proposed that the electron transport chain is used by *C. trachomatis* to build up an electrochemical membrane potential across the plasma membrane, which drives transport processes including the transport of lysine as it has been demonstrated for *C. psittaci* (Hatch *et al.*, 1982). Additionally, the respiratory chain is also useful for oxidation of NADH and FADH₂, which can be further reduced by glycolysis or TCA cycle. The treatment of isolated *C. trachomatis* in axenic medium with oligomycin and a combination of antimycin A and rotenone decreased the ATP levels, which might be due to the blockage of the respiratory chain, subsequent depolarization of the membrane and bacterial death. Disruption of the membrane potential in other bacteria such as *B. subtilis* or *E. coli* resulted in inhibited cell division (Strahl & Hamoen, 2010, Chimere *et al.*, 2012). Nevertheless, the measurement of ATP of isolated bacteria in the presence of SF2446A2 revealed a minor but not significant effect on the ATP levels. Either the compound does not affect the bacterial respiration at all or it needs to be metabolised by the cell to achieve its active form. Furthermore, it has been taken into consideration that *C. trachomatis* possesses a differential gene expression pattern throughout its complex developmental cycle (Nicholson *et al.*, 2003). Therefore, the metabolic status of the bacteria after cell lysis and cultivation in cell-free medium is unknown and is presumably altered. Thus, from the performed experiments it cannot be concluded but only speculated how SF2446A2 is affecting the human pathogen *C. trachomatis*.

The natural compound also inhibited the growth of the bacteria *N. gonorrhoeae* and *S. aureus*, while *E. coli* was not affected. All three bacteria possess a functional aerobic electron chain, whose inhibition could lead to impaired bacterial growth (Poole & Haddock,

1975, Suzuki *et al.*, 1992, Miller *et al.*, 1977). Therefore, it can be considered that SF2446A2 interferes with the aerobic respiration of *N. gonorrhoeae* and *S. aureus*. Several reasons are conceivable why *E. coli* is not affected by SF2446A2, including less uptake of the compound, efflux of the compounds by transporter proteins, metabolisation and inactivation of the compound or in contrast lack of metabolisation and thus, non-activation of SF2446A2. Additionally, the target sites of the compound in *S. aureus* and *N. gonorrhoeae* might be different in *E. coli*, therefore hindering the binding of the compound. Furthermore, compensatory mechanisms might be available that protect *E. coli* from the harmful effect of SF2446A2.

4.5 Conclusion and outlook

This study aimed to demonstrate a direct interaction of the neisserial virulence factor PorB_{IA} and its proposed cellular receptor SREC-I, which is important for phosphate-sensitive internalisation of *N. gonorrhoeae* in epithelial cells. In applying SPR I could show a high affinity binding of PorB_{IA} to SREC-I in a phosphate-independent manner. However, since PorB_{IB} possessed similar binding properties, the experiment has to be repeated with more controls to exclude unspecific binding. The experiment should be performed with saturated SREC-I binding sites using its natural ligand AcLDL or the SREC-I antibody. Additionally, instead of SREC-I the IgG protein control could be used to inject over the PorB coated chip. Furthermore, the analysis of this protein-receptor interaction can be performed using other approaches, such as the yeast-two hybrid method or a chemical cross-linking study (Fields & Song, 1989, Vasilescu *et al.*, 2004).

Moreover, 68 small molecule compounds were tested in an automated microscopy approach for their ability to inhibit the PorB_{IA}-mediated invasion of *N. gonorrhoeae* into epithelial cells, and their activity against the human pathogen *C. trachomatis*. While no active substances against *N. gonorrhoeae* could be identified, seven highly antichlamydial compounds were detected, including four naphthoquinones and the three compounds gelliusterol E, SF2446A2 and ageloline A, which were purified from marine sponges or sponge-associated bacteria (Abdelmohsen *et al.*, 2015, Reimer *et al.*, 2015, Cheng *et al.*, 2016). Additionally, I screened pipecolic acid derivatives for their inhibitory properties against *N. gonorrhoeae* and *C. trachomatis* and investigated the role of neisserial and

chlamydial MIP during infection. These compounds were synthesized as potential inhibitors of the *L. pneumophila* and *B. pseudomallei* MIP. I could demonstrate that several pipercolic acid derivatives were able to inhibit the PPIase activity of recombinant Ng-MIP and Ctr-MIP. The compounds with the lowest IC₅₀, PipN3 and PipN4 had severe effects on the chlamydial developmental cycle, resulting in less infectious progeny. Since the compound screening was used to analyse inhibitory effects on the primary chlamydial infection, repeating the screening procedure and measuring the EB progeny infectivity instead should be considered. For further investigation, an anti-Ctr-MIP antibody should be obtained to monitor the protein's localisation during different time points in the developmental cycle. Additionally, since Ctr-MIP has strong pro-inflammatory properties, it would be interesting to test PipN3 and PipN4 *in vivo* in a mouse infection model.

Moreover, I could demonstrate that the neisserial MIP is required for the intracellular survival in PMNs. Infection with a MIP knockout mutant or the application of PipN3 and PipN4 resulted in significant reduction of surviving bacteria. However, the initial compound screening was performed in epithelial cells, therefore it should be redone using isolated PMNs instead of Chang cells. To limit the variability due to different blood donors, the establishment of an infection model in immortalized neutrophil-like cells such as HL-60 should be considered. For further investigation of the role of Ng-MIP a proteome analysis of the knockout mutant and a wildtype strain as a control could be performed. Such an analysis would give some indication if the neisserial MIP have an accessory role in the secretion and correct assembly of certain virulence-associated proteins that prolong bacterial survival in the presence of PMNs. Additionally, to analyse if the PPIase activity of neisserial MIP is the factor prolonging the survival, creating neisserial strains that express the Ng-MIP containing point mutations D165L and Y208A would be a way to test for this. Strains containing the MIP with deletion of the dimerization domain (Δ 22-91) would allow analysing the effect of a structurally changed protein that has still a residual enzymatic activity of 75 % on bacterial survival and infectivity.

Furthermore, I investigated the mode of action of the highly antichlamydial naphthacene glycoside SF2446A2. I could demonstrate an inhibitory effect of the compound on the mitochondrial respiration, which led to an increased glycolytic activity in HeLa cells. The cellular ATP levels were decreased and the $\Delta\psi$ increased in the presence of SF2446A2. However, I could show that the inhibited OXPHOS was not responsible for the antichlamydial

properties of the compound. Knockdown of the cellular ATPase revealed that the chlamydial infection is only impaired when glucose was absent as an energy-source, indicating that *C. trachomatis* does not depend on the mitochondrial ATP. I could confirm this result by knocking down the mitochondrial glutaminase, which likewise resulted in an impaired infection under glucose-depleted conditions. Since SF2446A2 also affected the growth of *S. aureus* and *N. gonorrhoeae*, it might impair *C. trachomatis* directly. Further investigation is required to discover the mode of action of SF2446A2, but the current results imply that the compound might have multiple functions. For simplification of further research it is advisable to focus initially on the antibacterial effect on *S. aureus* and *N. gonorrhoeae*, since *C. trachomatis* complicates the situation through its obligate intracellular lifestyle. The compound contains an aminoglycoside group, and aminoglycoside antibiotics such as kanamycin and gentamicin have been shown to interfere with bacterial protein biosynthesis. Therefore, protein analysis in form of proteomics of untreated and SF2446A2 treated *N. gonorrhoeae* and *S. aureus* would be advisable. Furthermore, RNA sequencing would enable the monitoring of possible changes of the transcriptome. Additionally, it might be interesting to perform a metabolomics analysis to determine if SF2446A2 is metabolized by the bacteria. When medical application of SF2446A2 eventually is considered, all these investigations are important for discovery of the functional group of SF2446A2, which is responsible of the antibacterial properties. The compound was already tested in mice for toxicology and revealed no toxicity at 300 mg/kg for oral administration and a median lethal dose (LD₅₀) of 100 mg/kg for the intraperitoneal route (Takeda *et al.*, 1988). According to the Hodge and Sterner toxicity scale the compound can be classified as moderately toxic (Hodge & Sterner, 2005). Knowing the functional group of SF2446A2 would allow the use of computer-aided drug discovery methods and simulations to minimize the cytotoxic side effects.

5 REFERENCES

- Abdelmohsen, U.R., C. Cheng, A. Reimer, V. Kozjak-Pavlovic, A.K. Ibrahim, T. Rudel, U. Hentschel, R. Edrada-Ebel & S.A. Ahmed, (2015) Antichlamydial sterol from the Red Sea sponge *Callyspongia aff. implexa*. *Planta Med* **81**: 382-387.
- Abdul-Sater, A.A., E. Koo, G. Hacker & D.M. Ojcius, (2009) Inflammasome-dependent caspase-1 activation in cervical epithelial cells stimulates growth of the intracellular pathogen *Chlamydia trachomatis*. *J Biol Chem* **284**: 26789-26796.
- Abdul-Sater, A.A., N. Said-Sadier, V.M. Lam, B. Singh, M.A. Pettengill, F. Soares, I. Tattoli, S. Lipinski, S.E. Girardin, P. Rosenstiel & D.M. Ojcius, (2010) Enhancement of reactive oxygen species production and chlamydial infection by the mitochondrial Nod-like family member NLRX1. *J Biol Chem* **285**: 41637-41645.
- Abrahams, J.P., A.G.W. Leslie, R. Lutter & J.E. Walker, (1994) Structure at 2.8-Angstrom Resolution of F₁-Atpase from Bovine Heart-Mitochondria. *Nature* **370**: 621-628.
- Adachi, H. & M. Tsujimoto, (2002) FEEL-1, a novel scavenger receptor with in vitro bacteria-binding and angiogenesis-modulating activities. *J Biol Chem* **277**: 34264-34270.
- Adachi, H., M. Tsujimoto, H. Arai & K. Inoue, (1997) Expression cloning of a novel scavenger receptor from human endothelial cells. *J Biol Chem* **272**: 31217-31220.
- Alberts, B., D. Bray, K. Hopkin, A. Johnson, J. Lewis, M. Raff, K. Roberts & P. Walter, (2010) Essential cell biology. Garland Science, New York, USA, Abingdon, UK.
- Anjum, K., S.Q. Abbas, S.A.A. Shah, N. Akhter, S. Batool & S.S. ul Hassan, (2016) Marine Sponges as a Drug Treasure. *Biomol Ther* **24**: 347-362.
- Balemans, W., L. Vranckx, N. Lounis, O. Pop, J. Guillemont, K. Vergauwen, S. Mol, R. Gilissen, M. Motte, D. Lancois, M. De Bolle, K. Bonroy, H. Lill, K. Andries, D. Bald & A. Koul, (2012) Novel antibiotics targeting respiratory ATP synthesis in Gram-positive pathogenic bacteria. *Antimicrob Agents Chemother* **56**: 4131-4139.
- Barrientos, A. & C.T. Moraes, (1999) Titrating the effects of mitochondrial complex I impairment in the cell physiology. *J Biol Chem* **274**: 16188-16197.
- Bas, S., L. Neff, M. Vuillet, U. Spenato, T. Seya, M. Matsumoto & C. Gabay, (2008) The proinflammatory cytokine response to *Chlamydia trachomatis* elementary bodies in human macrophages is partly mediated by a lipoprotein, the macrophage infectivity potentiator, through TLR2/TLR1/TLR6 and CD14. *J Immunol* **180**: 1158-1168.
- Bash, M.C., P. Zhu, S. Gulati, D. McKnew, P.A. Rice & F. Lynn, (2005) por Variable-region typing by DNA probe hybridization is broadly applicable to epidemiologic studies of *Neisseria gonorrhoeae*. *J Clin Microbiol* **43**: 1522-1530.
- Bauer, F.J., (1997) Herstellung von PorB-Mutanten und Untersuchungen zur möglichen Rolle von PorB als Virulenzfaktor von *Neisseria gonorrhoeae*. Dissertation, Eberhard Karls Universität Tübingen.
- Bauer, F.J., T. Rudel, M. Stein & T.F. Meyer, (1999) Mutagenesis of the *Neisseria gonorrhoeae* porin reduces invasion in epithelial cells and enhances phagocyte responsiveness. *Mol Microbiol* **31**: 903-913.
- Begley, D.W., D. Fox, 3rd, D. Jenner, C. Juli, P.G. Pierce, J. Abendroth, M. Muruthi, K. Safford, V. Anderson, K. Atkins, S.R. Barnes, S.O. Moen, A.C. Raymond, R. Stacy, P.J. Myler, B.L. Staker, N.J. Harmer, I.H. Norville, U. Holzgrabe, M. Sarkar-Tyson, T.E. Edwards & D.D. Lorimer, (2014) A structural biology approach enables the development of antimicrobials targeting bacterial immunophilins. *Antimicrob Agents Chemother* **58**: 1458-1467.
- Belarbi, E., A.C. Gomez, Y. Chisti, F.G. Camacho & E.M. Grima, (2003) Producing drugs from marine sponges. *Biotechnol Adv* **21**: 585-598.
- Belland, R.J., G. Zhong, D.D. Crane, D. Hogan, D. Sturdevant, J. Sharma, W.L. Beatty & H.D. Caldwell, (2003) Genomic transcriptional profiling of the developmental cycle of *Chlamydia trachomatis*. *P Natl Acad Sci USA* **100**: 8478-8483.

- Bennett, J.S., D.T. Griffiths, N.D. McCarthy, K.L. Sleeman, K.A. Jolley, D.W. Crook & M.C. Maiden, (2005) Genetic diversity and carriage dynamics of *Neisseria lactamica* in infants. *Infect Immun* **73**: 2424-2432.
- Berdy, J., (2005) Bioactive microbial metabolites. *J Antibiot* **58**: 1-26.
- Bergmann, W. & D.C. Burke, (1955) Contributions to the Study of Marine Products .39. The Nucleosides of Sponges .3. Spongothymidine and Spongouridine. *J Org Chem* **20**: 1501-1507.
- Bergmann, W. & R.J. Feeney, (1950) The Isolation of a New Thymine Pentoside from Sponges. *J Am Chem Soc* **72**: 2809-2810.
- Bergmann, W. & R.J. Feeney, (1951) Contributions to the Study of Marine Products .32. The Nucleosides of Sponges .1. *J Org Chem* **16**: 981-987.
- Bergstrom, J., P. Furst, L.O. Noree & E. Vinnars, (1974) Intracellular free amino acid concentration in human muscle tissue. *J Appl Physiol* **36**: 693-697.
- Berwin, B., Y. Delneste, R.V. Lovingood, S.R. Post & S.V. Pizzo, (2004) SREC-I, a type F scavenger receptor, is an endocytic receptor for calreticulin. *J Biol Chem* **279**: 51250-51257.
- Bhat, K.S., C.P. Gibbs, O. Barrera, S.G. Morrison, F. Jahng, A. Stern, E.M. Kupsch, T.F. Meyer & J. Swanson, (1991) The opacity proteins of *Neisseria gonorrhoeae* strain MS11 are encoded by a family of 11 complete genes. *Mol Microbiol* **5**: 1889-1901.
- Bielecka, M.K., N. Devos, M. Gilbert, M.C. Hung, V. Weynants, J.E. Heckels & M. Christodoulides, (2015) Recombinant protein truncation strategy for inducing bactericidal antibodies to the macrophage infectivity potentiator protein of *Neisseria meningitidis* and circumventing potential cross-reactivity with human FK506-binding proteins. *Infect Immun* **83**: 730-742.
- Bierer, B.E., P.S. Mattila, R.F. Standaert, L.A. Herzenberg, S.J. Burakoff, G. Crabtree & S.L. Schreiber, (1990) Two distinct signal transmission pathways in T lymphocytes are inhibited by complexes formed between an immunophilin and either FK506 or rapamycin. *P Natl Acad Sci USA* **87**: 9231-9235.
- Billker, O., A. Popp, V. Brinkmann, G. Wenig, J. Schneider, E. Caron & T.F. Meyer, (2002) Distinct mechanisms of internalization of *Neisseria gonorrhoeae* by members of the CEACAM receptor family involving Rac1- and Cdc42-dependent and -independent pathways. *EMBO J* **21**: 560-571.
- Binnicker, M.J., R.D. Williams & M.A. Apicella, (2004) Gonococcal porin IB activates NF-kappaB in human urethral epithelium and increases the expression of host antiapoptotic factors. *Infect Immun* **72**: 6408-6417.
- Blunt, J.W., B.R. Copp, M.H. Munro, P.T. Northcote & M.R. Prinsep, (2005) Marine natural products. *Nat Prod Rep* **22**: 15-61.
- Blunt, J.W., B.R. Copp, M.H. Munro, P.T. Northcote & M.R. Prinsep, (2006) Marine natural products. *Nat Prod Rep* **23**: 26-78.
- Boncompain, G., B. Schneider, C. Delevoeye, O. Kellermann, A. Dautry-Varsat & A. Subtil, (2010) Production of reactive oxygen species is turned on and rapidly shut down in epithelial cells infected with *Chlamydia trachomatis*. *Infect Immun* **78**: 80-87.
- Boslego, J.W., E.C. Tramont, R.C. Chung, D.G. McChesney, J. Ciak, J.C. Sadoff, M.V. Piziak, J.D. Brown, C.C. Brinton, Jr., S.W. Wood & et al., (1991) Efficacy trial of a parenteral gonococcal pilus vaccine in men. *Vaccine* **9**: 154-162.
- Boveris, A., A.O. Stoppani, R. Docampo & F.S. Cruz, (1978) Superoxide anion production and trypanocidal action of naphthoquinones on *Trypanosoma cruzi*. *Comp Biochem Physiol C* **61**: 327-329.
- Brand, M.D., (2000) Uncoupling to survive? The role of mitochondrial inefficiency in ageing. *Exp Gerontol* **35**: 811-820.
- Brand, M.D., K.M. Brindle, J.A. Buckingham, J.A. Harper, D.F. Rolfe & J.A. Stuart, (1999) The significance and mechanism of mitochondrial proton conductance. *Int J Obes Relat Metab Disord* **23** Suppl 6: S4-11.
- Brand, M.D., J.L. Pakay, A. Ocloo, J. Kokoszka, D.C. Wallace, P.S. Brookes & E.J. Cornwall, (2005) The basal proton conductance of mitochondria depends on adenine nucleotide translocase content. *Biochem J* **392**: 353-362.

- Brandl, C.J. & C.M. Deber, (1986) Hypothesis about the function of membrane-buried proline residues in transport proteins. *P Natl Acad Sci USA* **83**: 917-921.
- Brandts, J.F., H.R. Halvorson & M. Brennan, (1975) Consideration of the Possibility that the slow step in protein denaturation reactions is due to cis-trans isomerism of proline residues. *Biochem* **14**: 4953-4963.
- Bringmann, G., V. Hoerr, U. Holzgrabe & A. Stich, (2003a) Antitrypanosomal naphthylisoquinoline alkaloids and related compounds. *Pharmazie* **58**: 343-346.
- Bringmann, G., K. Messer, B. Schwobel, R. Brun & L.A. Assi, (2003b) Acetogenic isoquinoline alkaloids. Part 151. Habropetaline A, an antimalarial naphthylisoquinoline alkaloid from *Triphyophyllum peltatum*. *Phytochem* **62**: 345-349.
- Bringmann, G., S. Rudenauer, A. Irmer, T. Bruhn, R. Brun, T. Heimberger, T. Stuhmer, R. Bargou & M. Chatterjee, (2008) Antitumoral and antileishmanial dioncoquinones and ancistroquinones from cell cultures of *Triphyophyllum peltatum* (Dioncophyllaceae) and *Ancistrocladus abbreviatus* (Ancistrocladaceae). *Phytochem* **69**: 2501-2509.
- Brown, E.J., M.W. Albers, T.B. Shin, K. Ichikawa, C.T. Keith, W.S. Lane & S.L. Schreiber, (1994) A mammalian protein targeted by G1-arresting rapamycin-receptor complex. *Nature* **369**: 756-758.
- Brunham, R.C. & J. Rey-Ladino, (2005) Immunology of Chlamydia infection: implications for a *Chlamydia trachomatis* vaccine. *Nat Rev Immunol* **5**: 149-161.
- Capaldi, R.A. & R. Aggeler, (2002) Mechanism of the F₁F₀-type ATP synthase, a biological rotary motor. *Trends Biochem Sci* **27**: 154-160.
- Carabeo, R.A., S.S. Grieshaber, A. Hasenkrug, C. Dooley & T. Hackstadt, (2004) Requirement for the Rac GTPase in *Chlamydia trachomatis* invasion of non-phagocytic cells. *Traffic* **5**: 418-425.
- Carabeo, R.A. & T. Hackstadt, (2001) Isolation and characterization of a mutant Chinese hamster ovary cell line that is resistant to *Chlamydia trachomatis* infection at a novel step in the attachment process. *Infect Immun* **69**: 5899-5904.
- Carlson, J.H., S.F. Porcella, G. McClarty & H.D. Caldwell, (2005) Comparative genomic analysis of *Chlamydia trachomatis* oculotropic and genitotropic strains. *Infect Immun* **73**: 6407-6418.
- Casey, S.G., W.M. Shafer & J.K. Spitznagel, (1986) *Neisseria gonorrhoeae* survive intraleukocytic oxygen-independent antimicrobial capacities of anaerobic and aerobic granulocytes in the presence of pyocin lethal for extracellular gonococci. *Infect Immun* **52**: 384-389.
- Caugant, D.A. & M.C. Maiden, (2009) Meningococcal carriage and disease-population biology and evolution. *Vaccine* **27** Suppl 2:B64-70.
- Ceymann, A., M. Horstmann, P. Ehses, K. Schweimer, A.K. Paschke, M. Steinert & C. Faber, (2008) Solution structure of the *Legionella pneumophila* Mip-rapamycin complex. *BMC Struct Biol* **8**: 17.
- Chen, A. & H.S. Seifert, (2011) *Neisseria gonorrhoeae*-mediated inhibition of apoptotic signalling in polymorphonuclear leukocytes. *Infect Immun* **79**: 4447-4458.
- Chen, L., C. Wang, S. Li, X. Yu, X. Liu, R. Ren, W. Liu, X. Zhou, X. Zhang & X. Zhou, (2016) Involvement of Lysosome Membrane Permeabilization and Reactive Oxygen Species Production in the Necrosis Induced by *Chlamydia muridarum* Infection in L929 Cells. *J Microbiol Biotechnol* **26**: 790-798.
- Chen, T., R.J. Belland, J. Wilson & J. Swanson, (1995) Adherence of pilus- Opa⁺ gonococci to epithelial cells in vitro involves heparan sulfate. *J Exp Med* **182**: 511-517.
- Cheng, C., E.M. Othman, A. Reimer, M. Grune, V. Kozjak-Pavlovic, H. Stopper, U. Hentschel & U.R. Abdelmohsen, (2016) Ageloline A, new antioxidant and antichlamydial quinolone from the marine sponge-derived bacterium *Streptomyces* sp SBT345. *Tetrahedron Letters* **57**: 2786-2789.
- Chimerel, C., C.M. Field, S. Pinero-Fernandez, U.F. Keyser & D.K. Summers, (2012) Indole prevents *Escherichia coli* cell division by modulating membrane potential. *Biochim Biophys Acta* **1818**: 1590-1594.
- Chinopoulos, C., (2011) Mitochondrial consumption of cytosolic ATP: not so fast. *FEBS Lett* **585**: 1255-1259.

- Chinopoulos, C., A.A. Gerencser, M. Mandi, K. Mathe, B. Torocsik, J. Doczi, L. Turiak, G. Kiss, C. Konrad, S. Vajda, V. Vereczki, R.J. Oh & V. Adam-Vizi, (2010) Forward operation of adenine nucleotide translocase during F_0F_1 -ATPase reversal: critical role of matrix substrate-level phosphorylation. *FASEB J* **24**: 2405-2416.
- Chiu, M.I., H. Katz & V. Berlin, (1994) RAPT1, a mammalian homolog of yeast Tor, interacts with the FKBP12/rapamycin complex. *P Natl Acad Sci USA* **91**: 12574-12578.
- Cianciotto, N.P., B.I. Eisenstein, C.H. Mody & N.C. Engleberg, (1990) A mutation in the mip gene results in an attenuation of *Legionella pneumophila* virulence. *J Infect Dis* **162**: 121-126.
- Cianciotto, N.P. & B.S. Fields, (1992) *Legionella pneumophila* mip gene potentiates intracellular infection of protozoa and human macrophages. *P Natl Acad Sci USA* **89**: 5188-5191.
- Clarke, S., (1976) A major polypeptide component of rat liver mitochondria: carbamyl phosphate synthetase. *J Biol Chem* **251**: 950-961.
- Clausen, J.D., G. Christiansen, H.U. Holst & S. Birkelund, (1997) *Chlamydia trachomatis* utilizes the host cell microtubule network during early events of infection. *Mol Microbiol* **25**: 441-449.
- Collinson, I.R., M.J. Runswick, S.K. Buchanan, I.M. Fearnley, J.M. Skehel, M.J. van Raaij, D.E. Griffiths & J.E. Walker, (1994) F_0 membrane domain of ATP synthase from bovine heart mitochondria: purification, subunit composition, and reconstitution with F_1 -ATPase. *Biochem* **33**: 7971-7978.
- Constable, F.L., (1959) Psittacosis elementary bodies. *Nature* **184**: Suppl 7: 473-474.
- Craig, L. & J. Li, (2008) Type IV pili: paradoxes in form and function. *Curr Opin Struct Biol* **18**: 267-277.
- Criss, A.K., B.Z. Katz & H.S. Seifert, (2009) Resistance of *Neisseria gonorrhoeae* to non-oxidative killing by adherent human polymorphonuclear leucocytes. *Cell Microbiol* **11**: 1074-1087.
- Criss, A.K. & H.S. Seifert, (2012) A bacterial siren song: intimate interactions between *Neisseria* and neutrophils. *Nat Rev Microbiol* **10**: 178-190.
- de Jonge, M.I., M.P. Bos, H.J. Hamstra, W. Jiskoot, P. van Ulsen, J. Tommassen, L. van Alphen & P. van der Ley, (2002) Conformational analysis of opacity proteins from *Neisseria meningitidis*. *Eur J Biochem* **269**: 5215-5223.
- Dean, D., R.J. Suchland & W.E. Stamm, (2000) Evidence for long-term cervical persistence of *Chlamydia trachomatis* by omp1 genotyping. *J Infect Dis* **182**: 909-916.
- Debroy, S., V. Aragon, S. Kurtz & N.P. Cianciotto, (2006) *Legionella pneumophila* Mip, a surface-exposed peptidylproline cis-trans-isomerase, promotes the presence of phospholipase C-like activity in culture supernatants. *Infect Immun* **74**: 5152-5160.
- Della Sala, G., T. Hochmuth, R. Teta, V. Costantino & A. Mangoni, (2014) Polyketide synthases in the microbiome of the marine sponge *Plakortis halichondrioides*: a metagenomic update. *Mar Drugs* **12**: 5425-5440.
- Demars, R., J. Weinfurter, E. Guex, J. Lin & Y. Potucek, (2007) Lateral gene transfer in vitro in the intracellular pathogen *Chlamydia trachomatis*. *J Bacteriol* **189**: 991-1003.
- Derre, I., M. Pypaert, A. Dautry-Varsat & H. Agaisse, (2007) RNAi screen in *Drosophila* cells reveals the involvement of the Tom complex in *Chlamydia* infection. *PLoS Pathog* **3**: 1446-1458.
- Derrick, J.P., R. Urwin, J. Suker, I.M. Feavers & M.C. Maiden, (1999) Structural and evolutionary inference from molecular variation in *Neisseria* porins. *Infect Immun* **67**: 2406-2413.
- Donia, M. & M.T. Hamann, (2003) Marine natural products and their potential applications as anti-infective agents. *Lancet Infect Dis* **3**: 338-348.
- Dorward, D.W., C.F. Garon & R.C. Judd, (1989) Export and intercellular transfer of DNA via membrane blebs of *Neisseria gonorrhoeae*. *J Bacteriol* **171**: 2499-2505.
- Dorward, D.W. & R.C. Judd, (1988) Characterization of naturally-evolved outer membrane blebs of *Neisseria gonorrhoeae*. In: Gonococci and meningococci. Kluwer Academic Publishers, Dordrecht, The Netherlands.
- Dott, W., P. Mistry, J. Wright, K. Cain & K.E. Herbert, (2014) Modulation of mitochondrial bioenergetics in a skeletal muscle cell line model of mitochondrial toxicity. *Redox Biol* **2**: 224-233.
- Drose, S., (2013) Differential effects of complex II on mitochondrial ROS production and their relation to cardioprotective pre- and postconditioning. *Biochim Biophys Acta* **1827**: 578-587.

- Eb, F., J. Orfila & J.F. Lefebvre, (1976) Ultrastructural study of the development of the agent of ewe's abortion. *J Ultrastruct Res* **56**: 177-185.
- Elkins, C., C.E. Thomas, H.S. Seifert & P.F. Sparling, (1991) Species-specific uptake of DNA by gonococci is mediated by a 10-base-pair sequence. *J Bacteriol* **173**: 3911-3913.
- Elwell, C., K. Mirrashidi & J. Engel, (2016) *Chlamydia* cell biology and pathogenesis. *Nat Rev Microbiol* **14**: 385-400.
- Esterbauer, H., R.J. Schaur & H. Zollner, (1991) Chemistry and biochemistry of 4-hydroxynonenal, malonaldehyde and related aldehydes. *Free Radic Biol Med* **11**: 81-128.
- Everett, K.D., R.M. Bush & A.A. Andersen, (1999) Emended description of the order *Chlamydiales*, proposal of *Parachlamydiaceae* fam. nov. and *Simkaniaceae* fam. nov., each containing one monotypic genus, revised taxonomy of the family *Chlamydiaceae*, including a new genus and five new species, and standards for the identification of organisms. *Int J Syst Bacteriol* **49 Pt 2**: 415-440.
- Fadel, S. & A. Eley, (2007) *Chlamydia trachomatis* OmcB protein is a surface-exposed glycosaminoglycan-dependent adhesin. *J Med Microbiol* **56**: 15-22.
- Fan, T., H. Lu, H. Hu, L. Shi, G.A. McClarty, D.M. Nance, A.H. Greenberg & G. Zhong, (1998) Inhibition of apoptosis in *Chlamydia*-infected cells: blockade of mitochondrial cytochrome c release and caspase activation. *J Exp Med* **187**: 487-496.
- Faulkner, D.J., (2000) Marine natural products. *Nat Prod Rep* **17**: 7-55.
- Faulkner, D.J., (2001) Marine natural products. *Nat Prod Rep* **18**: 1-49.
- Faulkner, D.J., (2002) Marine natural products. *Nat Prod Rep* **19**: 1-48.
- Faulstich, M., (2009) Interaktion von PorB von *Neisseria gonorrhoeae* mit dem SREC-I Rezeptor der Wirtszelle. Diploma thesis, Julius-Maximilians-Universität Würzburg.
- Faulstich, M., (2012) From local to disseminated infection: Mechanism of the porin-dependent gonococcal invasion. Dissertation, Julius-Maximilians-Universität Würzburg.
- Faulstich, M., J.P. Bottcher, T.F. Meyer, M. Fraunholz & T. Rudel, (2013) Pilus phase variation switches gonococcal adherence to invasion by caveolin-1-dependent host cell signaling. *PLoS Pathog* **9**: e1003373.
- Faulstich, M., F. Hagen, E. Avota, V. Kozjak-Pavlovic, A.C. Winkler, Y. Xian, S. Schneider-Schaulies & T. Rudel, (2015) Neutral sphingomyelinase 2 is a key factor for PorB-dependent invasion of *Neisseria gonorrhoeae*. *Cell Microbiol* **17**: 241-253.
- Feller, S.M. & M. Lewitzky, (2012) Very 'sticky' proteins - not too sticky after all? *Cell Commun Signal* **10**.
- Fields, K.A., D.J. Mead, C.A. Dooley & T. Hackstadt, (2003) *Chlamydia trachomatis* type III secretion: evidence for a functional apparatus during early-cycle development. *Mol Microbiol* **48**: 671-683.
- Fields, S. & O. Song, (1989) A novel genetic system to detect protein-protein interactions. *Nature* **340**: 245-246.
- Fischer, G., B. Wittmann-Liebold, K. Lang, T. Kiefhaber & F.X. Schmid, (1989) Cyclophilin and peptidyl-prolyl cis-trans isomerase are probably identical proteins. *Nature* **337**: 476-478.
- Fischer, S.F., C. Schwarz, J. Vier & G. Hacker, (2001) Characterization of antiapoptotic activities of *Chlamydia pneumoniae* in human cells. *Infect Immun* **69**: 7121-7129.
- Fisette, P.L., S. Ram, J.M. Andersen, W. Guo & R.R. Ingalls, (2003) The Lip lipoprotein from *Neisseria gonorrhoeae* stimulates cytokine release and NF-kappaB activation in epithelial cells in a Toll-like receptor 2-dependent manner. *J Biol Chem* **278**: 46252-46260.
- Flo, T.H., O. Halaas, E. Lien, L. Ryan, G. Teti, D.T. Golenbock, A. Sundan & T. Espevik, (2000) Human toll-like receptor 2 mediates monocyte activation by *Listeria monocytogenes*, but not by group B streptococci or lipopolysaccharide. *J Immunol* **164**: 2064-2069.
- Forest, K.T., S.A. Dunham, M. Koomey & J.A. Tainer, (1999) Crystallographic structure reveals phosphorylated pilin from *Neisseria*: phosphoserine sites modify type IV pilus surface chemistry and fibre morphology. *Mol Microbiol* **31**: 743-752.
- Forkink, M., G.R. Manjeri, D.C. Liemburg-Apers, E. Nibbeling, M. Blanchard, A. Wojtala, J.A. Smeitink, M.R. Wieckowski, P.H. Willems & W.J. Koopman, (2014) Mitochondrial hyperpolarization

- during chronic complex I inhibition is sustained by low activity of complex II, III, IV and V. *Biochim Biophys Acta* **1837**: 1247-1256.
- Francois, G., G. Timperman, W. Eling, L.A. Assi, J. Holenz & G. Bringmann, (1997) Naphthylisoquinoline alkaloids against malaria: evaluation of the curative potentials of dioncophylline C and dioncopeltine A against *Plasmodium berghei* in vivo. *Antimicrob Agents Chemother* **41**: 2533-2539.
- Frey, T.G. & C.A. Mannella, (2000) The internal structure of mitochondria. *Trends Biochem Sci* **25**: 319-324.
- Fudyk, T.C., I.W. Maclean, J.N. Simonsen, E.N. Njagi, J. Kimani, R.C. Brunham & F.A. Plummer, (1999) Genetic diversity and mosaicism at the por locus of *Neisseria gonorrhoeae*. *J Bacteriol* **181**: 5591-5599.
- Funa, N., Y. Ohnishi, I. Fujii, M. Shibuya, Y. Ebizuka & S. Horinouchi, (1999) A new pathway for polyketide synthesis in microorganisms. *Nature* **400**: 897-899.
- Galka, F., S.N. Wai, H. Kusch, S. Engelmann, M. Hecker, B. Schmeck, S. Hippenstiel, B.E. Uhlin & M. Steinert, (2008) Proteomic characterization of the whole secretome of *Legionella pneumophila* and functional analysis of outer membrane vesicles. *Infect Immun* **76**: 1825-1836.
- García-Sosa, K., Villarreal-Alvarez, N., Lübben, P., Peña-Rodríguez, L. M., (2006) Chrysophanol, an Antimicrobial Anthraquinone from the Root Extract of *Colubrina greggii*. *J Mex Chem Soc* **50**: 76-78.
- Gaylord, W.H., Jr., (1954) Intracellular forms of meningopneumonitis virus. *J Exp Med* **100**: 575-580.
- Gingras, A.C., B. Raught & N. Sonenberg, (2001) Regulation of translation initiation by FRAP/mTOR. *Genes Dev* **15**: 807-826.
- Goire, N., M.M. Lahra, M. Chen, B. Donovan, C.K. Fairley, R. Guy, J. Kaldor, D. Regan, J. Ward, M.D. Nissen, T.P. Sloots & D.M. Whitley, (2014) Molecular approaches to enhance surveillance of gonococcal antimicrobial resistance. *Nat Rev Microbiol* **12**: 223-229.
- Gomez-Duarte, O.G., M. Dehio, C.A. Guzman, G.S. Chhatwal, C. Dehio & T.F. Meyer, (1997) Binding of vitronectin to opa-expressing *Neisseria gonorrhoeae* mediates invasion of HeLa cells. *Infect Immun* **65**: 3857-3866.
- Gomi, S., T. Sasaki, J. Itoh & M. Sezaki, (1988) SF2446, new benzo[a]naphthacene quinone antibiotics. II. The structural elucidation. *J Antibiot (Tokyo)* **41**: 425-432.
- Goodman, S.D. & J.J. Scoocca, (1988) Identification and arrangement of the DNA sequence recognized in specific transformation of *Neisseria gonorrhoeae*. *P Natl Acad Sci USA* **85**: 6982-6986.
- Grayston, J.T. & S.P. Wang, (1978) The potential for vaccine against infection of the genital tract with *Chlamydia trachomatis*. *Sex Transm Dis* **5**: 73-77.
- Grayston, J.T., S.P. Wang, L.J. Yeh & C.C. Kuo, (1985) Importance of reinfection in the pathogenesis of trachoma. *Rev Infect Dis* **7**: 717-725.
- Greenberg, L., (1975) Field trials of a gonococcal vaccine. *J Reprod Med* **14**: 34-36.
- Greenberg, L., B.B. Diena, F.A. Ashton, R. Wallace, C.P. Kenny, R. Znamirowski, H. Ferrari & J. Atkinson, (1974) Gonococcal vaccine studies in Inuvik. *Can J Public Health* **65**: 29-33.
- Grieshaber, S.S., N.A. Grieshaber & T. Hackstadt, (2003) Chlamydia trachomatis uses host cell dynein to traffic to the microtubule-organizing center in a p50 dynamitin-independent process. *J Cell Sci* **116**: 3793-3802.
- Grimwood, J., L. Olinger & R.S. Stephens, (2001) Expression of *Chlamydia pneumoniae* polymorphic membrane protein family genes. *Infect Immun* **69**: 2383-2389.
- Grimwood, J. & R.S. Stephens, (1999) Computational analysis of the polymorphic membrane protein superfamily of *Chlamydia trachomatis* and *Chlamydia pneumoniae*. *Microb Comp Genomics* **4**: 187-201.
- Gunderson, C.W. & H.S. Seifert, (2015) *Neisseria gonorrhoeae* elicits extracellular traps in primary neutrophil culture while suppressing the oxidative burst. *MBio* **6**.
- Hackstadt, T., (2000) Redirection of host vesicle trafficking pathways by intracellular parasites. *Traffic* **1**: 93-99.

- Hagen, T.A. & C.N. Cornelissen, (2006) *Neisseria gonorrhoeae* requires expression of TonB and the putative transporter TdfF to replicate within cervical epithelial cells. *Mol Microbiol* **62**: 1144-1157.
- Halberstaedter, L., von Prowazek, S., (1907) Zur Aetiologie des Trachoms. *Dtsch. Med. Wschr.* **33** 1285-1287.
- Harding, M.W., A. Galat, D.E. Uehling & S.L. Schreiber, (1989) A receptor for the immunosuppressant FK506 is a cis-trans peptidyl-prolyl isomerase. *Nature* **341**: 758-760.
- Harikishore, A., M. Niang, S. Rajan, P.R. Preiser & H.S. Yoon, (2013) Small molecule *Plasmodium* FKBP35 inhibitor as a potential antimalaria agent. *Sci Rep* **3**: 2501.
- Harvey, H.A., M.P. Jennings, C.A. Campbell, R. Williams & M.A. Apicella, (2001) Receptor-mediated endocytosis of *Neisseria gonorrhoeae* into primary human urethral epithelial cells: the role of the asialoglycoprotein receptor. *Mol Microbiol* **42**: 659-672.
- Hatch, T.P., E. Alhossainy & J.A. Silverman, (1982) Adenine-Nucleotide and Lysine Transport in *Chlamydia Psittaci*. *J Bacteriol* **150**: 662-670.
- Helbig, J.H., P.C. Luck, M. Steinert, E. Jacobs & M. Witt, (2001) Immunolocalization of the Mip protein of intracellularly and extracellularly grown *Legionella pneumophila*. *Lett Appl Microbiol* **32**: 83-88.
- Hennig, L., C. Christner, M. Kipping, B. Schelbert, K.P. Rucknagel, S. Grabley, G. Kullertz & G. Fischer, (1998) Selective inactivation of parvulin-like peptidyl-prolyl cis/trans isomerases by juglone. *Biochem* **37**: 5953-5960.
- Hentschel, U., L. Fieseler, M. Wehrl, C. Gernert, M. Steinert, J. Hacker & M. Horn, (2003) Microbial diversity of marine sponges. *Prog Mol Subcell Biol* **37**: 59-88.
- Heuer, D., A. Rejman Lipinski, N. Machuy, A. Karlas, A. Wehrens, F. Siedler, V. Brinkmann & T.F. Meyer, (2009) *Chlamydia* causes fragmentation of the Golgi compartment to ensure reproduction. *Nature* **457**: 731-735.
- Hochmuth, T. & J. Piel, (2009) Polyketide synthases of bacterial symbionts in sponges-evolution-based applications in natural products research. *Phytochem* **70**: 1841-1849.
- Hodge, A. & B. Sterner, (2005) Toxicity classes. In: Canadian center for occupational Health and safety.
- Hogan, R.J., S.A. Mathews, S. Mukhopadhyay, J.T. Summersgill & P. Timms, (2004) Chlamydial persistence: beyond the biphasic paradigm. *Infect Immun* **72**: 1843-1855.
- Hollis, D.G., G.L. Wiggins & R.E. Weaver, (1969) *Neisseria lactamica* sp. n., a lactose-fermenting species resembling *Neisseria meningitidis*. *Appl Microbiol* **17**: 71-77.
- Holz, C., D. Opitz, L. Greune, R. Kurre, M. Koomey, M.A. Schmidt & B. Maier, (2010) Multiple pilus motors cooperate for persistent bacterial movement in two dimensions. *Phys Rev Lett* **104**: 178104.
- Holz, M.K., B.A. Ballif, S.P. Gygi & J. Blenis, (2005) mTOR and S6K1 mediate assembly of the translation preinitiation complex through dynamic protein interchange and ordered phosphorylation events. *Cell* **123**: 569-580.
- Holzl, M.A., J. Hofer, J.J. Kovarik, D. Roggenbuck, D. Reinhold, A. Goihl, M. Gartner, P. Steinberger & G.J. Zlabinger, (2011) The zymogen granule protein 2 (GP2) binds to scavenger receptor expressed on endothelial cells I (SREC-I). *Cell Immunol* **267**: 88-93.
- Huijing, F. & E.C. Slater, (1961) The use of oligomycin as an inhibitor of oxidative phosphorylation. *J Biochem* **49**: 493-501.
- Humbert, M.V., H.L. Almonacid Mendoza, A.C. Jackson, M.C. Hung, M.K. Bielecka, J.E. Heckels & M. Christodoulides, (2015) Vaccine potential of bacterial macrophage infectivity potentiator (MIP)-like peptidyl prolyl cis/trans isomerase (PPIase) proteins. *Expert Rev Vaccines* **14**: 1633-1649.
- Hung, M.C., O. Salim, J.N. Williams, J.E. Heckels & M. Christodoulides, (2011) The *Neisseria meningitidis* macrophage infectivity potentiator protein induces cross-strain serum bactericidal activity and is a potential serogroup B vaccine candidate. *Infect Immun* **79**: 3784-3791.

- Hybiske, K. & R.S. Stephens, (2007) Mechanisms of host cell exit by the intracellular bacterium *Chlamydia*. *P Natl Acad Sci USA* **104**: 11430-11435.
- Iliffe-Lee, E.R. & G. McClarty, (1999) Glucose metabolism in *Chlamydia trachomatis*: the 'energy parasite' hypothesis revisited. *Mol Microbiol* **33**: 177-187.
- Ishii, J., H. Adachi, J. Aoki, H. Koizumi, S. Tomita, T. Suzuki, M. Tsujimoto, K. Inoue & H. Arai, (2002) SREC-II, a new member of the scavenger receptor type F family, trans-interacts with SREC-I through its extracellular domain. *J Biol Chem* **277**: 39696-39702.
- Izumikawa, M., R. Satou, K. Motohashi, A. Nagai, Y. Ohnishi, M. Takagi & K. Shin-ya, (2011) Naphthoquinone-like Polyketide Isolated from *Streptomyces* sp RI-77 and Its Predicted Biosynthetic Pathway. *J Nat Prod* **74**: 2588-2591.
- Jeannin, P., B. Bottazzi, M. Sironi, A. Doni, M. Rusnati, M. Presta, V. Maina, G. Magistrelli, J.F. Haeuw, G. Hoeffel, N. Thieblemont, N. Corvaia, C. Garlanda, Y. Delneste & A. Mantovani, (2005) Complexity and complementarity of outer membrane protein A recognition by cellular and humoral innate immunity receptors. *Immun* **22**: 551-560.
- Jerse, A.E., M.C. Bash & M.W. Russell, (2014) Vaccines against gonorrhea: current status and future challenges. *Vaccine* **32**: 1579-1587.
- Jewett, T.J., E.R. Fischer, D.J. Mead & T. Hackstadt, (2006) Chlamydial TARP is a bacterial nucleator of actin. *P Natl Acad Sci USA* **103**: 15599-15604.
- Johnson, M.B. & A.K. Criss, (2013) *Neisseria gonorrhoeae* phagosomes delay fusion with primary granules to enhance bacterial survival inside human neutrophils. *Cell Microbiol* **15**: 1323-1340.
- Johnson, S.R., B.M. Steiner, D.D. Cruce, G.H. Perkins & R.J. Arko, (1993) Characterization of a catalase-deficient strain of *Neisseria gonorrhoeae*: evidence for the significance of catalase in the biology of *N. gonorrhoeae*. *Infect Immun* **61**: 1232-1238.
- Jones, R.B., B. Van der Pol, D.H. Martin & M.K. Shepard, (1990) Partial characterization of *Chlamydia trachomatis* isolates resistant to multiple antibiotics. *J Infect Dis* **162**: 1309-1315.
- Juli, C., M. Sippel, J. Jager, A. Thiele, M. Weiwad, K. Schweimer, P. Rosch, M. Steinert, C.A. Sottriffer & U. Holzgrabe, (2011) Pipecolic acid derivatives as small-molecule inhibitors of the *Legionella* MIP protein. *J Med Chem* **54**: 277-283.
- Kahn, R.H., D.J. Mosure, S. Blank, C.K. Kent, J.M. Chow, M.R. Boudov, J. Brock, S. Tulloch & S.T.D.P.M.P. Jail, (2005) *Chlamydia trachomatis* and *Neisseria gonorrhoeae* prevalence and coinfection in adolescents entering selected US juvenile detention centers, 1997-2002. *Sex Transm Dis* **32**: 255-259.
- Kalbacova, M., M. Vrbacky, Z. Drahota & Z. Melkova, (2003) Comparison of the effect of mitochondrial inhibitors on mitochondrial membrane potential in two different cell lines using flow cytometry and spectrofluorometry. *Cytometry A* **52**: 110-116.
- Kallstrom, H., M.K. Liszewski, J.P. Atkinson & A.B. Jonsson, (1997) Membrane cofactor protein (MCP or CD46) is a cellular pilus receptor for pathogenic *Neisseria*. *Mol Microbiol* **25**: 639-647.
- Kalman, S., W. Mitchell, R. Marathe, C. Lammel, J. Fan, R.W. Hyman, L. Olinger, J. Grimwood, R.W. Davis & R.S. Stephens, (1999) Comparative genomes of *Chlamydia pneumoniae* and *C. trachomatis*. *Nat Genet* **21**: 385-389.
- Kaparakis, M., L. Turnbull, L. Carneiro, S. Firth, H.A. Coleman, H.C. Parkinson, L. Le Bourhis, A. Karrar, J. Viala, J. Mak, M.L. Hutton, J.K. Davies, P.J. Crack, P.J. Hertzog, D.J. Philpott, S.E. Girardin, C.B. Whitchurch & R.L. Ferrero, (2010) Bacterial membrane vesicles deliver peptidoglycan to NOD1 in epithelial cells. *Cell Microbiol* **12**: 372-385.
- Karayiannis, P. & D. Hobson, (1981) Amino acid requirements of a *Chlamydia trachomatis* genital strain in McCoy cell cultures. *J Clin Microbiol* **13**: 427-432.
- Kerle, K.K., J.R. Mascola & T.A. Miller, (1992) Disseminated gonococcal infection. *Am Fam Physician* **45**: 209-214.
- Kihlstrom, E., M. Majeed, B. Rozalska & T. Wadstrom, (1992) Binding of *Chlamydia trachomatis* serovar L2 to collagen types I and IV, fibronectin, heparan sulphate, laminin and vitronectin. *Zbl Bakt-Int J Med M* **277**: 329-333.

- King, G.J. & J. Swanson, (1978) Studies on gonococcus infection. XV. Identification of surface proteins of *Neisseria gonorrhoeae* correlated with leukocyte association. *Infect Immun* **21**: 575-584.
- Kirsch, T., W. Sebald & M.K. Dreyer, (2000) Crystal structure of the BMP-2-BRIA ectodomain complex. *Nat Struct Biol* **7**: 492-496.
- Kohler, R., J. Fanghanel, B. Konig, E. Luneberg, M. Frosch, J.U. Rahfeld, R. Hilgenfeld, G. Fischer, J. Hacker & M. Steinert, (2003) Biochemical and functional analyses of the Mip protein: influence of the N-terminal half and of peptidylprolyl isomerase activity on the virulence of *Legionella pneumophila*. *Infect Immun* **71**: 4389-4397.
- Korn, E.D., M.F. Carlier & D. Pantaloni, (1987) Actin polymerization and ATP hydrolysis. *Science* **238**: 638-644.
- Kozjak-Pavlovic, V., K. Ross, N. Benlasfer, S. Kimmig, A. Karlas & T. Rudel, (2007) Conserved roles of Sam50 and metaxins in VDAC biogenesis. *EMBO Rep* **8**: 576-582.
- Kreiswirth, B.N., S. Lofdahl, M.J. Betley, M. O'Reilly, P.M. Schlievert, M.S. Bergdoll & R.P. Novick, (1983) The toxic shock syndrome exotoxin structural gene is not detectably transmitted by a prophage. *Nature* **305**: 709-712.
- Kühlewein, C., C. Rechner, T.F. Meyer & T. Rudel, (2006) Low-phosphate-dependent invasion resembles a general way for *Neisseria gonorrhoeae* to enter host cells. *Infect Immun* **74**: 4266-4273.
- Lacey, J.M. & D.W. Wilmore, (1990) Is Glutamine a Conditionally Essential Amino-Acid. *Nutr Rev* **48**: 297-309.
- Lampe, M.F., L.C. Rohan, M.C. Skinner & W.E. Stamm, (2004) Susceptibility of *Chlamydia trachomatis* to excipients commonly used in topical microbicide formulations. *Antimicrob Agents Chemother* **48**: 3200-3202.
- Lanning, N.J., B.D. Looyenga, A.L. Kauffman, N.M. Niemi, J. Sudderth, R.J. DeBerardinis & J.P. MacKeigan, (2014) A mitochondrial RNAi screen defines cellular bioenergetic determinants and identifies an adenylate kinase as a key regulator of ATP levels. *Cell Rep* **7**: 907-917.
- Laport, M.S., O.C. Santos & G. Muricy, (2009) Marine sponges: potential sources of new antimicrobial drugs. *Curr Pharm Biotechnol* **10**: 86-105.
- Larsen, E.M., M.R. Wilson & R.E. Taylor, (2015) Conformation-activity relationships of polyketide natural products. *Nat Prod Rep* **32**: 1183-1206.
- Lee, I., E. Bender & B. Kadenbach, (2002) Control of mitochondrial membrane potential and ROS formation by reversible phosphorylation of cytochrome c oxidase. *Mol Cell Biochem* **234-235**: 63-70.
- Lefevre, J.C. & J.P. Lepargneur, (1998) Comparative in vitro susceptibility of a tetracycline-resistant *Chlamydia trachomatis* strain isolated in Toulouse (France). *Sex Transm Dis* **25**: 350-352.
- Leuzzi, R., L. Serino, M. Scarselli, S. Savino, M.R. Fontana, E. Monaci, A. Taddei, G. Fischer, R. Rappuoli & M. Pizza, (2005) Ng-MIP, a surface-exposed lipoprotein of *Neisseria gonorrhoeae*, has a peptidyl-prolyl cis/trans isomerase (PPIase) activity and is involved in persistence in macrophages. *Mol Microbiol* **58**: 669-681.
- Li, N., K. Ragheb, G. Lawler, J. Sturgis, B. Rajwa, J.A. Melendez & J.P. Robinson, (2003) Mitochondrial complex I inhibitor rotenone induces apoptosis through enhancing mitochondrial reactive oxygen species production. *J Biol Chem* **278**: 8516-8525.
- Lin, L., P. Ayala, J. Larson, M. Mulks, M. Fukuda, S.R. Carlsson, C. Enns & M. So, (1997) The *Neisseria* type 2 IgA1 protease cleaves LAMP1 and promotes survival of bacteria within epithelial cells. *Mol Microbiol* **24**: 1083-1094.
- Liu, J., J.D. Farmer, Jr., W.S. Lane, J. Friedman, I. Weissman & S.L. Schreiber, (1991) Calcineurin is a common target of cyclophilin-cyclosporin A and FKBP-FK506 complexes. *Cell* **66**: 807-815.
- Low, N. & M. Unemo, (2016) Molecular tests for the detection of antimicrobial resistant *Neisseria gonorrhoeae*: when, where, and how to use? *Curr Opin Infect Dis* **29**: 45-51.
- Lundemose, A.G., S. Birkelund, S.J. Fey, P.M. Larsen & G. Christiansen, (1991) *Chlamydia trachomatis* contains a protein similar to the *Legionella pneumophila* mip gene product. *Mol Microbiol* **5**: 109-115.

- Lundemose, A.G., J.E. Kay & J.H. Pearce, (1993a) *Chlamydia trachomatis* Mip-like protein has peptidyl-prolyl cis/trans isomerase activity that is inhibited by FK506 and rapamycin and is implicated in initiation of chlamydial infection. *Mol Microbiol* **7**: 777-783.
- Lundemose, A.G., D.A. Rouch, S. Birkelund, G. Christiansen & J.H. Pearce, (1992) *Chlamydia trachomatis* Mip-like protein. *Mol Microbiol* **6**: 2539-2548.
- Lundemose, A.G., D.A. Rouch, C.W. Penn & J.H. Pearce, (1993b) The *Chlamydia trachomatis* Mip-like protein is a lipoprotein. *J Bacteriol* **175**: 3669-3671.
- Lynch, E.C., M.S. Blake, E.C. Gotschlich & A. Mauro, (1984) Studies of Porins: Spontaneously Transferred from Whole Cells and Reconstituted from Purified Proteins of *Neisseria gonorrhoeae* and *Neisseria meningitidis*. *Biophys J* **45**: 104-107.
- Makino, S., J.P. van Putten & T.F. Meyer, (1991) Phase variation of the opacity outer membrane protein controls invasion by *Neisseria gonorrhoeae* into human epithelial cells. *EMBO J* **10**: 1307-1315.
- Malhotra, M., S. Sood, A. Mukherjee, S. Muralidhar & M. Bala, (2013) Genital *Chlamydia trachomatis*: an update. *Indian J Med Res* **138**: 303-316.
- Marceau, M., K. Forest, J.L. Beretti, J. Tainer & X. Nassif, (1998) Consequences of the loss of O-linked glycosylation of meningococcal type IV pilin on piliation and pilus-mediated adhesion. *Mol Microbiol* **27**: 705-715.
- Martinez-Reyes, I. & J.M. Cuezva, (2014) The H⁺-ATP synthase: a gate to ROS-mediated cell death or cell survival. *Biochim Biophys Acta* **1837**: 1099-1112.
- Massague, J., (1998) TGF-beta signal transduction. *Annu Rev Biochem* **67**: 753-791.
- Massari, P., P. Henneke, Y. Ho, E. Latz, D.T. Golenbock & L.M. Wetzler, (2002) Cutting edge: Immune stimulation by neisserial porins is toll-like receptor 2 and MyD88 dependent. *J Immunol* **168**: 1533-1537.
- Massari, P., Y. Ho & L.M. Wetzler, (2000) *Neisseria meningitidis* porin PorB interacts with mitochondria and protects cells from apoptosis. *P Natl Acad Sci USA* **97**: 9070-9075.
- Matsumoto, A., H. Bessho, K. Uehira & T. Suda, (1991) Morphological studies of the association of mitochondria with chlamydial inclusions and the fusion of chlamydial inclusions. *J Electron Microsc (Tokyo)* **40**: 356-363.
- Mavrogiorgos, N., S. Mekasha, Y. Yang, M.A. Kelliher & R.R. Ingalls, (2014) Activation of NOD receptors by *Neisseria gonorrhoeae* modulates the innate immune response. *Innate Immun* **20**: 377-389.
- Mayer, L.W., (1982) Rates in vitro changes of gonococcal colony opacity phenotypes. *Infect Immun* **37**: 481-485.
- McKnew, D.L., F. Lynn, J.M. Zenilman & M.C. Bash, (2003) Porin variation among clinical isolates of *Neisseria gonorrhoeae* over a 10-year period, as determined by Por variable region typing. *J Infect Dis* **187**: 1213-1222.
- Means, T.K., E. Mylonakis, E. Tampakakis, R.A. Colvin, E. Seung, L. Puckett, M.F. Tai, C.R. Stewart, R. Pukkila-Worley, S.E. Hickman, K.J. Moore, S.B. Calderwood, N. Hachohen, A.D. Luster & J. El Khoury, (2009) Evolutionarily conserved recognition and innate immunity to fungal pathogens by the scavenger receptors SCARF1 and CD36. *J Exp Med* **206**: 637-653.
- Medentsev, A.G., A.Y. Arinbasarova & V.K. Akimenko, (2005) Biosynthesis of naphthoquinone pigments by fungi of the genus *Fusarium*. *Appl. Biochem. Microbiol.* **41**: 503-507.
- Menna-Barreto, R.F., R.L. Goncalves, E.M. Costa, R.S. Silva, A.V. Pinto, M.F. Oliveira & S.L. de Castro, (2009) The effects on *Trypanosoma cruzi* of novel synthetic naphthoquinones are mediated by mitochondrial dysfunction. *Free Radic Biol Med* **47**: 644-653.
- Metsa-Ketela, M., T. Oja, T. Taguchi, S. Okamoto & K. Ichinose, (2013) Biosynthesis of pyranonaphthoquinone polyketides reveals diverse strategies for enzymatic carbon-carbon bond formation. *Curr. Opin. Chem. Biol.* **17**: 562-570.
- Miller, R.D., K.E. Brown & S.A. Morse, (1977) Inhibitory action of fatty acids on the growth of *Neisseria gonorrhoeae*. *Infect Immun* **17**: 303-312.

- Misyurina, O.Y., E.V. Chipitsyna, Y.P. Finashutina, V.N. Lazarev, T.A. Akopian, A.M. Savicheva & V.M. Govorun, (2004) Mutations in a 23S rRNA gene of *Chlamydia trachomatis* associated with resistance to macrolides. *Antimicrob Agents Chemother* **48**: 1347-1349.
- Mitroulis, I., I. Kourtzelis, K. Kambas, S. Rafail, A. Chrysanthopoulou, M. Speletas & K. Ritis, (2010) Regulation of the autophagic machinery in human neutrophils. *Eur J Immunol* **40**: 1461-1472.
- Miwa, S. & M.D. Brand, (2003) Mitochondrial matrix reactive oxygen species production is very sensitive to mild uncoupling. *Biochem Soc Trans* **31**: 1300-1301.
- Morello, A., M. Pavani, J.A. Garbarino, M.C. Chamy, C. Frey, J. Mancilla, A. Guerrero, Y. Repetto & J. Ferreira, (1995) Effects and mode of action of 1,4-naphthoquinones isolated from *Calceolaria sessilis* on tumoral cells and *Trypanosoma* parasites. *Comp Biochem Physiol C Pharmacol Toxicol Endocrinol* **112**: 119-128.
- Morello, J.A. & M. Bohnhoff, (1989) Serovars and serum resistance of *Neisseria gonorrhoeae* from disseminated and uncomplicated infections. *J Infect Dis* **160**: 1012-1017.
- Mourad, A., R.L. Sweet, N. Sugg & J. Schachter, (1980) Relative resistance to erythromycin in *Chlamydia trachomatis*. *Antimicrob Agents Chemother* **18**: 696-698.
- Muller, A., D. Gunther, V. Brinkmann, R. Hurwitz, T.F. Meyer & T. Rudel, (2000) Targeting of the pro-apoptotic VDAC-like porin (PorB) of *Neisseria gonorrhoeae* to mitochondria of infected cells. *EMBO J* **19**: 5332-5343.
- Muller, A., J. Rassow, J. Grimm, N. Machuy, T.F. Meyer & T. Rudel, (2002) VDAC and the bacterial porin PorB of *Neisseria gonorrhoeae* share mitochondrial import pathways. *EMBO J* **21**: 1916-1929.
- Murshid, A., J. Gong & S.K. Calderwood, (2010) Heat shock protein 90 mediates efficient antigen cross presentation through the scavenger receptor expressed by endothelial cells-I. *J Immunol* **185**: 2903-2917.
- Nanagara, R., F. Li, A. Beutler, A. Hudson & H.R. Schumacher, Jr., (1995) Alteration of *Chlamydia trachomatis* biologic behavior in synovial membranes. Suppression of surface antigen production in reactive arthritis and Reiter's syndrome. *Arthritis Rheum* **38**: 1410-1417.
- Neff, L., S. Daher, P. Muzzin, U. Spenato, F. Gulacar, C. Gabay & S. Bas, (2007) Molecular characterization and subcellular localization of macrophage infectivity potentiator, a *Chlamydia trachomatis* lipoprotein. *J Bacteriol* **189**: 4739-4748.
- Neisser, A., (1879) Über eine der Gonorrhoe eigenthümliche Micrococcusform. *Centralblatt für medizinische Wissenschaft* **17**: 497-500.
- Nichols, B.A., P.Y. Setzer, F. Pang & C.R. Dawson, (1985) New view of the surface projections of *Chlamydia trachomatis*. *J Bacteriol* **164**: 344-349.
- Nicholson, T.L., L. Olinger, K. Chong, G. Schoolnik & R.S. Stephens, (2003) Global stage-specific gene regulation during the developmental cycle of *Chlamydia trachomatis*. *J Bacteriol* **185**: 3179-3189.
- Nickens, K.P., J.D. Wikstrom, O.S. Shirihai, S.R. Patierno & S. Ceryak, (2013) A bioenergetic profile of non-transformed fibroblasts uncovers a link between death-resistance and enhanced spare respiratory capacity. *Mitochondrion* **13**: 662-667.
- Norville, I.H., K. O'Shea, M. Sarkar-Tyson, S. Zheng, R.W. Titball, G. Varani & N.J. Harmer, (2011) The structure of a *Burkholderia pseudomallei* immunophilin-inhibitor complex reveals new approaches to antimicrobial development. *Biochem J* **437**: 413-422.
- Ohnishi, M., D. Golparian, K. Shimuta, T. Saika, S. Hoshina, K. Iwasaku, S. Nakayama, J. Kitawaki & M. Unemo, (2011a) Is *Neisseria gonorrhoeae* initiating a future era of untreatable gonorrhea?: detailed characterization of the first strain with high-level resistance to ceftriaxone. *Antimicrob Agents Chemother* **55**: 3538-3545.
- Ohnishi, M., M. Unemo, D. Golparian, K. Shimuta, T. Saika, S. Hoshina, K. Iwasaku, S.I. Nakayama & J. Kitawaki, (2011b) O3-S4.01 The new superbug *Neisseria gonorrhoeae* makes gonorrhoea untreatable?—first high-level ceftriaxone resistance worldwide and public health importance. *Sex Transm Infect* **87**.

- Omsland, A., J. Sager, V. Nair, D.E. Sturdevant & T. Hackstadt, (2012) Developmental stage-specific metabolic and transcriptional activity of *Chlamydia trachomatis* in an axenic medium. *PNAS* **109**: 19781-19785.
- Ovcinnikov, N.M. & V.V. Delektorskij, (1971) Electron microscope studies of gonococci in the urethral secretions of patients with gonorrhoea. *Br J Vener Dis* **47**: 419-439.
- Pal, D. & P. Chakrabarti, (1999) Cis peptide bonds in proteins: residues involved, their conformations, interactions and locations. *J Mol Biol* **294**: 271-288.
- Papadogeorgakis, H., T.E. Pittaras, J. Papaparaskevas, V. Pitiriga, A. Katsambas & A. Tsakris, (2010) *Chlamydia trachomatis* serovar distribution and *Neisseria gonorrhoeae* coinfection in male patients with urethritis in Greece. *J Clin Microbiol* **48**: 2231-2234.
- Parker, N., P.G. Crichton, A.J. Vidal-Puig & M.D. Brand, (2009) Uncoupling protein-1 (UCP1) contributes to the basal proton conductance of brown adipose tissue mitochondria. *J Bioenerg Biomembr* **41**: 335-342.
- Parker, N., A. Vidal-Puig & M.D. Brand, (2008) Stimulation of mitochondrial proton conductance by hydroxynonenal requires a high membrane potential. *Biosci Rep* **28**: 83-88.
- Parks, K.S., P.B. Dixon, C.M. Richey & E.W. Hook, 3rd, (1997) Spontaneous clearance of *Chlamydia trachomatis* infection in untreated patients. *Sex Transm Dis* **24**: 229-235.
- Peeling, R.W., J. Peeling & R.C. Brunham, (1989) High-resolution ³¹P nuclear magnetic resonance study of *Chlamydia trachomatis*: induction of ATPase activity in elementary bodies. *Infect Immun* **57**: 3338-3344.
- Pereira, P.J., M.C. Vega, E. Gonzalez-Rey, R. Fernandez-Carazo, S. Macedo-Ribeiro, F.X. Gomis-Ruth, A. Gonzalez & M. Coll, (2002) *Trypanosoma cruzi* macrophage infectivity potentiator has a rotamase core and a highly exposed alpha-helix. *EMBO Rep* **3**: 88-94.
- Pfleger, J., M. He & M. Abdellatif, (2015) Mitochondrial complex II is a source of the reserve respiratory capacity that is regulated by metabolic sensors and promotes cell survival. *Cell Death Dis* **6**.
- Piel, J., (2004) Metabolites from symbiotic bacteria. *Nat Prod Rep* **21**: 519-538.
- Piel, J., (2006) Bacterial symbionts: prospects for the sustainable production of invertebrate-derived pharmaceuticals. *Curr Med Chem* **13**: 39-50.
- Pieretti, S., J.R. Haanstra, M. Mazet, R. Perozzo, C. Bergamini, F. Prati, R. Fato, G. Lenaz, G. Capranico, R. Brun, B.M. Bakker, P.A. Michels, L. Scapozza, M.L. Bolognesi & A. Cavalli, (2013) Naphthoquinone derivatives exert their antitrypanosomal activity via a multi-target mechanism. *PLoS Negl Trop Dis* **7**: e2012.
- Pils, S., D.T. Gerrard, A. Meyer & C.R. Hauck, (2008) CEACAM3: an innate immune receptor directed against human-restricted bacterial pathogens. *Int J Med Microbiol* **298**: 553-560.
- Poole, R.K. & B.A. Haddock, (1975) Dibromothymoquinone - Inhibitor of Aerobic Electron-Transport at Level of Ubiquinone in *Escherichia Coli*. *Febs Letters* **52**: 13-16.
- Porat, N., M.A. Apicella & M.S. Blake, (1995) *Neisseria gonorrhoeae* utilizes and enhances the biosynthesis of the asialoglycoprotein receptor expressed on the surface of the hepatic HepG2 cell line. *Infect Immun* **63**: 1498-1506.
- Rahfeld, J.U., K.P. Rucknagel, B. Schelbert, B. Ludwig, J. Hacker, K. Mann & G. Fischer, (1994) Confirmation of the existence of a third family among peptidyl-prolyl cis/trans isomerases. Amino acid sequence and recombinant production of parvulin. *FEBS Lett* **352**: 180-184.
- Rajalingam, K., H. Al-Younes, A. Muller, T.F. Meyer, A.J. Szczepek & T. Rudel, (2001) Epithelial cells infected with *Chlamydophila pneumoniae* (*Chlamydia pneumoniae*) are resistant to apoptosis. *Infect Immun* **69**: 7880-7888.
- Ram, S., M. Cullinane, A.M. Blom, S. Gulati, D.P. McQuillen, R. Boden, B.G. Monks, C. O'Connell, C. Elkins, M.K. Pangburn, B. Dahlback & P.A. Rice, (2001) C4bp binding to porin mediates stable serum resistance of *Neisseria gonorrhoeae*. *Int Immunopharmacol* **1**: 423-432.
- Ram, S., F.G. Mackinnon, S. Gulati, D.P. McQuillen, U. Vogel, M. Frosch, C. Elkins, H.K. Guttormsen, L.M. Wetzler, M. Oppermann, M.K. Pangburn & P.A. Rice, (1999) The contrasting mechanisms of serum resistance of *Neisseria gonorrhoeae* and group B *Neisseria meningitidis*. *Mol Immunol* **36**: 915-928.

- Ramirez-Ortiz, Z.G., W.F. Pendergraft, 3rd, A. Prasad, M.H. Byrne, T. Iram, C.J. Blanchette, A.D. Luster, N. Hacohen, J. El Khoury & T.K. Means, (2013) The scavenger receptor SCARF1 mediates the clearance of apoptotic cells and prevents autoimmunity. *Nat Immunol* **14**: 917-926.
- Ramsey, K.H., H. Schneider, A.S. Cross, J.W. Boslego, D.L. Hoover, T.L. Staley, R.A. Kushner & C.D. Deal, (1995) Inflammatory cytokines produced in response to experimental human gonorrhoea. *J Infect Dis* **172**: 186-191.
- Raulston, J.E., C.H. Davis, T.R. Paul, J.D. Hobbs & P.B. Wyrick, (2002) Surface accessibility of the 70-kilodalton *Chlamydia trachomatis* heat shock protein following reduction of outer membrane protein disulfide bonds. *Infect Immun* **70**: 535-543.
- Rechner, C., C. Kühlewein, A. Müller, H. Schild & T. Rudel, (2007) Host glycoprotein Gp96 and scavenger receptor SREC interact with PorB of disseminating *Neisseria gonorrhoeae* in an epithelial invasion pathway. *Cell Host Microbe* **2**: 393-403.
- Reglier-Poupet, H., C. Frehel, I. Dubail, J.L. Beretti, P. Berche, A. Charbit & C. Raynaud, (2003) Maturation of lipoproteins by type II signal peptidase is required for phagosomal escape of *Listeria monocytogenes*. *J Biol Chem* **278**: 49469-49477.
- Rego, A.C., S. Vesce & D.G. Nicholls, (2001) The mechanism of mitochondrial membrane potential retention following release of cytochrome c in apoptotic GT1-7 neural cells. *Cell Death Differ* **8**: 995-1003.
- Reimer, A., A. Blohm, T. Quack, C.G. Grevelding, V. Kozjak-Pavlovic, T. Rudel, U. Hentschel & U.R. Abdelmohsen, (2015) Inhibitory activities of the marine streptomycete-derived compound SF2446A2 against *Chlamydia trachomatis* and *Schistosoma mansoni*. *J Antibiot* **68**: 674-679.
- Reimer, A., F. Seufert, M. Weiwad, J. Ebert, N.M. Bzdyl, C.M. Kahler, M. Sarkar-Tyson, U. Holzgrabe, T. Rudel & V. Kozjak-Pavlovic, (2016) Inhibitors of macrophage infectivity potentiator-like PPIases affect neisserial and chlamydial pathogenicity. *Int J Antimicrob Agents* **48**: 401-408.
- Reitzer, L.J., B.M. Wice & D. Kennell, (1979) Evidence that glutamine, not sugar, is the major energy source for cultured HeLa cells. *J Biol Chem* **254**: 2669-2676.
- Rejman Lipinski, A., J. Heymann, C. Meissner, A. Karlas, V. Brinkmann, T.F. Meyer & D. Heuer, (2009) Rab6 and Rab11 regulate *Chlamydia trachomatis* development and golgin-84-dependent Golgi fragmentation. *PLoS Pathog* **5**: e1000615.
- Resnikoff, S., D. Pascolini, D. Etya'ale, I. Kocur, R. Pararajasegaram, G.P. Pokharel & S.P. Mariotti, (2004) Global data on visual impairment in the year 2002. *Bull World Health Organ* **82**: 844-851.
- Riboldi-Tunncliffe, A., B. König, S. Jessen, M.S. Weiss, J. Rahfeld, J. Hacker, G. Fischer & R. Hilgenfeld, (2001) Crystal structure of Mip, a prolyl isomerase from *Legionella pneumophila*. *Nat Struct Biol* **8**: 779-783.
- Rice, P.A., M.S. Blake & K.A. Joiner, (1987) Mechanisms of stable serum resistance of *Neisseria gonorrhoeae*. *Antonie Van Leeuwenhoek* **53**: 565-574.
- Richards, T.S., A.E. Knowlton & S.S. Grieshaber, (2013) *Chlamydia trachomatis* homotypic inclusion fusion is promoted by host microtubule trafficking. *BMC Microbiol* **13**: 185.
- Richardson, C.J., S.S. Schalm & J. Blenis, (2004) PI3-kinase and TOR: PIKTORing cell growth. *Semin Cell Dev Biol* **15**: 147-159.
- Rosignol, R., R. Gilkerson, R. Aggeler, K. Yamagata, S.J. Remington & R.A. Capaldi, (2004) Energy substrate modulates mitochondrial structure and oxidative capacity in cancer cells. *Cancer Res* **64**: 985-993.
- Rotman, E. & H.S. Seifert, (2014) The genetics of *Neisseria* species. *Annu Rev Genet* **48**: 405-431.
- Rudel, T., A. Schmid, R. Benz, H.A. Kolb, F. Lang & T.F. Meyer, (1996) Modulation of *Neisseria* porin (PorB) by cytosolic ATP/GTP of target cells: parallels between pathogen accommodation and mitochondrial endosymbiosis. *Cell* **85**: 391-402.
- Sabers, C.J., M.M. Martin, G.J. Brunn, J.M. Williams, F.J. Dumont, G. Wiederrecht & R.T. Abraham, (1995) Isolation of a protein target of the FKBP12-rapamycin complex in mammalian cells. *J Biol Chem* **270**: 815-822.
- Santo-Domingo, J. & N. Demaurex, (2012) Perspectives on: SGP symposium on mitochondrial physiology and medicine: the renaissance of mitochondrial pH. *J Gen Physiol* **139**: 415-423.

- Schmelzle, T. & M.N. Hall, (2000) TOR, a central controller of cell growth. *Cell* **103**: 253-262.
- Schmitter, T., F. Agerer, L. Peterson, P. Munzner & C.R. Hauck, (2004) Granulocyte CEACAM3 is a phagocytic receptor of the innate immune system that mediates recognition and elimination of human-specific pathogens. *J Exp Med* **199**: 35-46.
- Schwoppe, C., H.H. Winkler & H.E. Neuhaus, (2002) Properties of the glucose-6-phosphate transporter from *Chlamydia pneumoniae* (HPTcp) and the glucose-6-phosphate sensor from *Escherichia coli* (UhpC). *J Bacteriol* **184**: 2108-2115.
- Scidmore, M.A., D.D. Rockey, E.R. Fischer, R.A. Heinzen & T. Hackstadt, (1996) Vesicular interactions of the *Chlamydia trachomatis* inclusion are determined by chlamydial early protein synthesis rather than route of entry. *Infect Immun* **64**: 5366-5372.
- Seib, K.L., M.P. Simons, H.J. Wu, A.G. McEwan, W.M. Nauseef, M.A. Apicella & M.P. Jennings, (2005) Investigation of oxidative stress defenses of *Neisseria gonorrhoeae* by using a human polymorphonuclear leukocyte survival assay. *Infect Immun* **73**: 5269-5272.
- Sena, L.A. & N.S. Chandel, (2012) Physiological roles of mitochondrial reactive oxygen species. *Mol Cell* **48**: 158-167.
- Shemer-Avni, Y., D. Wallach & I. Sarov, (1988) Inhibition of *Chlamydia trachomatis* growth by recombinant tumor necrosis factor. *Infect Immun* **56**: 2503-2506.
- Shibata, M., J. Ishii, H. Koizumi, N. Shibata, N. Dohmae, K. Takio, H. Adachi, M. Tsujimoto & H. Arai, (2004) Type F scavenger receptor SREC-I interacts with advillin, a member of the gelsolin/villin family, and induces neurite-like outgrowth. *J Biol Chem* **279**: 40084-40090.
- Siekierka, J.J., S.H. Hung, M. Poe, C.S. Lin & N.H. Sigal, (1989) A cytosolic binding protein for the immunosuppressant FK506 has peptidyl-prolyl isomerase activity but is distinct from cyclophilin. *Nature* **341**: 755-757.
- Simons, M.P., W.M. Nauseef & M.A. Apicella, (2005) Interactions of *Neisseria gonorrhoeae* with adherent polymorphonuclear leukocytes. *Infect Immun* **73**: 1971-1977.
- Simons, M.P., W.M. Nauseef, T.S. Griffith & M.A. Apicella, (2006) *Neisseria gonorrhoeae* delays the onset of apoptosis in polymorphonuclear leukocytes. *Cell Microbiol* **8**: 1780-1790.
- Sipkema, D., R. Osinga, W. Schatton, D. Mendola, J. Tramper & R.H. Wijffels, (2005) Large-scale production of pharmaceuticals by marine sponges: sea, cell, or synthesis? *Biotechnol Bioeng* **90**: 201-222.
- Somani, J., V.B. Bhullar, K.A. Workowski, C.E. Farshy & C.M. Black, (2000) Multiple drug-resistant *Chlamydia trachomatis* associated with clinical treatment failure. *J Infect Dis* **181**: 1421-1427.
- Sprenger, J., (2010) Faktoren von *Neisseria gonorrhoeae* für die disseminierende Infektion von Epithelzellen, Diploma Thesis, Julius-Maximilians-Universität Würzburg.
- Stephens, D.S., B. Greenwood & P. Brandtzaeg, (2007) Epidemic meningitis, meningococcaemia, and *Neisseria meningitidis*. *Lancet* **369**: 2196-2210.
- Stephens, R.S., S. Kalman, C. Lammel, J. Fan, R. Marathe, L. Aravind, W. Mitchell, L. Olinger, R.L. Tatusov, Q. Zhao, E.V. Koonin & R.W. Davis, (1998) Genome sequence of an obligate intracellular pathogen of humans: *Chlamydia trachomatis*. *Science* **282**: 754-759.
- Stevenson, D.E. & R.D. Hurst, (2007) Polyphenolic phytochemicals-just antioxidants or much more? *Cell Mol Life Sci* **64**: 2900-2916.
- Stewart, D.E., A. Sarkar & J.E. Wampler, (1990) Occurrence and role of cis peptide bonds in protein structures. *J Mol Biol* **214**: 253-260.
- Strahl, H. & L.W. Hamoen, (2010) Membrane potential is important for bacterial cell division. *P Natl Acad Sci USA* **107**: 12281-12286.
- Su, H., L. Raymond, D.D. Rockey, E. Fischer, T. Hackstadt & H.D. Caldwell, (1996) A recombinant *Chlamydia trachomatis* major outer membrane protein binds to heparan sulfate receptors on epithelial cells. *P Natl Acad Sci USA* **93**: 11143-11148.
- Su, H., N.G. Watkins, Y.X. Zhang & H.D. Caldwell, (1990) *Chlamydia trachomatis*-host cell interactions: role of the chlamydial major outer membrane protein as an adhesin. *Infect Immun* **58**: 1017-1025.
- Suzuki, S., A. Kubo, H. Shinano & K. Takama, (1992) Inhibition of the electron transport system in *Staphylococcus aureus* by trimethylamine-N-oxide. *Microbios* **71**: 145-148.

- Takahashi, N., T. Hayano & M. Suzuki, (1989) Peptidyl-prolyl cis-trans isomerase is the cyclosporin A-binding protein cyclophilin. *Nature* **337**: 473-475.
- Takeda, U., T. Okada, M. Takagi, S. Gomi, J. Itoh, M. Sezaki, M. Ito, S. Miyadoh & T. Shomura, (1988) SF2446, new benzo[a]naphthacene quinone antibiotics. I. Taxonomy and fermentation of the producing strain, isolation and characterization of antibiotics. *J Antibiot (Tokyo)* **41**: 417-424.
- Tamura, Y., J. Osuga, H. Adachi, R. Tozawa, Y. Takanezawa, K. Ohashi, N. Yahagi, M. Sekiya, H. Okazaki, S. Tomita, Y. Iizuka, H. Koizumi, T. Inaba, H. Yagyu, N. Kamada, H. Suzuki, H. Shimano, T. Kadowaki, M. Tsujimoto, H. Arai, N. Yamada & S. Ishibashi, (2004) Scavenger receptor expressed by endothelial cells I (SREC-I) mediates the uptake of acetylated low density lipoproteins by macrophages stimulated with lipopolysaccharide. *J Biol Chem* **279**: 30938-30944.
- Tan, G.M., H.J. Lim, T.C. Yeow, E. Movahed, C.Y. Looi, R. Gupta, B.P. Arulanandam, S. Abu Bakar, N.S. Sabet, L.Y. Chang & W.F. Wong, (2016) Temporal proteomic profiling of *Chlamydia trachomatis*-infected HeLa-229 human cervical epithelial cells. *Proteomics* **16**: 1347-1360.
- Thalmann, J., K. Janik, M. May, K. Sommer, J. Ebeling, F. Hofmann, H. Genth & A. Klos, (2010) Actin re-organization induced by *Chlamydia trachomatis* serovar D-evidence for a critical role of the effector protein CT166 targeting Rac. *PLoS One* **5**: e9887.
- Thomas, T.R., Kavlekar, D. P., LokaBharathi, P. A., (2010) Marine Drugs from Sponge-Microbe Association-A Review. *Mar Drugs* **8**: 1417-1468.
- Thomas, T.R.A., D.P. Kavlekar & P.A. LokaBharathi, (2010) Marine Drugs from Sponge-Microbe Association-A Review. *Mar Drugs* **8**: 1417-1468.
- Thomson, N.R., M.T. Holden, C. Carder, N. Lennard, S.J. Lockey, P. Marsh, P. Skipp, C.D. O'Connor, I. Goodhead, H. Norbertzack, B. Harris, D. Ormond, R. Rance, M.A. Quail, J. Parkhill, R.S. Stephens & I.N. Clarke, (2008) *Chlamydia trachomatis*: genome sequence analysis of lymphogranuloma venereum isolates. *Genome Res* **18**: 161-171.
- Tipples, G. & G. McClarty, (1993) The obligate intracellular bacterium *Chlamydia trachomatis* is auxotrophic for three of the four ribonucleoside triphosphates. *Mol Microbiol* **8**: 1105-1114.
- Tjaden, J., H.H. Winkler, C. Schwoppe, M. Van Der Laan, T. Mohlmann & H.E. Neuhaus, (1999) Two nucleotide transport proteins in *Chlamydia trachomatis*, one for net nucleoside triphosphate uptake and the other for transport of energy. *J Bacteriol* **181**: 1196-1202.
- Tobiason, D.M. & H.S. Seifert, (2006) The obligate human pathogen, *Neisseria gonorrhoeae*, is polyploid. *PLoS Biol* **4**: e185.
- Touriño, S., D. Lizárraga, A. Carreras, C. Matito Sánchez, V. Ugartondo, M. Mitjans, J.J. Centelles, M.P. Vinardell, L. Juliá, M. Cascante & J.L. Torres, (2008) Antioxidant/prooxidant effects of bioactive polyphenolics. *EJEAFChe* **7**: 3348-3352.
- Tseng, H.J., Y. Srikhanta, A.G. McEwan & M.P. Jennings, (2001) Accumulation of manganese in *Neisseria gonorrhoeae* correlates with resistance to oxidative killing by superoxide anion and is independent of superoxide dismutase activity. *Mol Microbiol* **40**: 1175-1186.
- Unal, C., K.F. Schwedhelm, A. Thiele, M. Weiwad, K. Schweimer, F. Frese, G. Fischer, J. Hacker, C. Faber & M. Steinert, (2011) Collagen IV-derived peptide binds hydrophobic cavity of *Legionella pneumophila* Mip and interferes with bacterial epithelial transmigration. *Cell Microbiol* **13**: 1558-1572.
- Unal, C.M. & M. Steinert, (2014) Microbial peptidyl-prolyl cis/trans isomerases (PPlases): virulence factors and potential alternative drug targets. *Microbiol Mol Biol Rev* **78**: 544-571.
- Unemo, M., C. Del Rio & W.M. Shafer, (2016) Antimicrobial Resistance Expressed by *Neisseria gonorrhoeae*: A Major Global Public Health Problem in the 21st Century. *Microbiol Spectr* **4**.
- Unemo, M., D. Golparian, R. Nicholas, M. Ohnishi, A. Gallay & P. Sednaoui, (2012) High-level cefixime- and ceftriaxone-resistant *Neisseria gonorrhoeae* in France: novel penA mosaic allele in a successful international clone causes treatment failure. *Antimicrob Agents Chemother* **56**: 1273-1280.
- Valsecchi, F., C. Monge, M. Forkink, A.J. de Groof, G. Benard, R. Rossignol, H.G. Swarts, S.E. van Emst-de Vries, R.J. Rodenburg, M.A. Calvaruso, L.G. Nijtmans, B. Heeman, P. Roestenberg, B. Wieringa, J.A. Smeitink, W.J. Koopman & P.H. Willems, (2012) Metabolic consequences of

- NDUFS4 gene deletion in immortalized mouse embryonic fibroblasts. *Biochim Biophys Acta* **1817**: 1925-1936.
- van Putten, J.P., T.D. Duensing & J. Carlson, (1998) Gonococcal invasion of epithelial cells driven by P.IA, a bacterial ion channel with GTP binding properties. *J Exp Med* **188**: 941-952.
- van Putten, J.P. & S.M. Paul, (1995) Binding of syndecan-like cell surface proteoglycan receptors is required for *Neisseria gonorrhoeae* entry into human mucosal cells. *EMBO J* **14**: 2144-2154.
- Vasilescu, J., X. Guo & J. Kast, (2004) Identification of protein-protein interactions using in vivo cross-linking and mass spectrometry. *Proteomics* **4**: 3845-3854.
- Verlinde, C.L.M., V. Hannaert, C. Blonski, M. Willson, J.J. Perie, L.A. Fothergill-Gilmore, F.R. Opperdoes, M.H. Gelb, W.G.J. Hol & P.A.M. Michels, (2001) Glycolysis as a target for the design of new anti-trypanosome drugs. *Drug Resist Updat* **4**: 50-65.
- Virji, M., K. Makepeace, D.J. Ferguson & S.M. Watt, (1996) Carcinoembryonic antigens (CD66) on epithelial cells and neutrophils are receptors for Opa proteins of pathogenic *Neisseriae*. *Mol Microbiol* **22**: 941-950.
- Voges, M., V. Bachmann, R. Kammerer, U. Gophna & C.R. Hauck, (2010) CEACAM1 recognition by bacterial pathogens is species-specific. *BMC Microbiol* **10**: 117.
- Waage, A., A. Halstensen, R. Shalaby, P. Brandtzaeg, P. Kierulf & T. Espevik, (1989) Local production of tumor necrosis factor alpha, interleukin 1, and interleukin 6 in meningococcal meningitis. Relation to the inflammatory response. *J Exp Med* **170**: 1859-1867.
- Wagner, C., A.S. Khan, T. Kamphausen, B. Schmausser, C. Unal, U. Lorenz, G. Fischer, J. Hacker & M. Steinert, (2007) Collagen binding protein Mip enables *Legionella pneumophila* to transmigrate through a barrier of NCI-H292 lung epithelial cells and extracellular matrix. *Cell Microbiol* **9**: 450-462.
- Wang, G.Y., (2006) Diversity and biotechnological potential of the sponge-associated microbial consortia. *J Ind Microbiol Biot* **33**: 545-551.
- Wang, S.K., D.L. Patton & C.C. Kuo, (1992) Effects of ascorbic acid on *Chlamydia trachomatis* infection and on erythromycin treatment in primary cultures of human amniotic cells. *J Clin Microbiol* **30**: 2551-2554.
- Wang, S.P., J.T. Grayston, E.R. Alexander & K.K. Holmes, (1975) Simplified microimmunofluorescence test with trachoma-lymphogranuloma venereum (*Chlamydia trachomatis*) antigens for use as a screening test for antibody. *J Clin Microbiol* **1**: 250-255.
- Wang, S.P., Grayston, J. T., (1971) Classification of TRIC and related strains with microimmunofluorescence. In: Nichols, R. L. (ed.): Trachoma and related disorders caused by chlamydial agents. Excerpta Medica, Amsterdam. 305-321.
- Wang, S.P., C.C. Kuo, R.C. Barnes, R.S. Stephens & J.T. Grayston, (1985) Immunotyping of *Chlamydia trachomatis* with monoclonal antibodies. *J Infect Dis* **152**: 791-800.
- Wang, Y., S. Kahane, L.T. Cutcliffe, R.J. Skilton, P.R. Lambden & I.N. Clarke, (2011) Development of a transformation system for *Chlamydia trachomatis*: restoration of glycogen biosynthesis by acquisition of a plasmid shuttle vector. *PLoS Pathog* **7**: e1002258.
- WHO, (2012) Global action plan to control the spread and impact of antimicrobial resistance in *Neisseria gonorrhoeae*. Geneva, WHO.
- WHO, (2016a) WHO Guidelines For The Treatment of *Chlamydia trachomatis*. WHO Document Production Services, Geneva, Switzerland.
- WHO, (2016b) WHO Guidelines For The Treatment of *Neisseria gonorrhoeae*. WHO Document Production Services, Geneva, Switzerland.
- Williams, J.N., P.J. Skipp, H.E. Humphries, M. Christodoulides, C.D. O'Connor & J.E. Heckels, (2007) Proteomic analysis of outer membranes and vesicles from wild-type serogroup B *Neisseria meningitidis* and a lipopolysaccharide-deficient mutant. *Infect Immun* **75**: 1364-1372.
- Wintermeyer, E., B. Ludwig, M. Steinert, B. Schmidt, G. Fischer & J. Hacker, (1995) Influence of site specifically altered Mip proteins on intracellular survival of *Legionella pneumophila* in eukaryotic cells. *Infect Immun* **63**: 4576-4583.
- Wiznerowicz, M. & D. Trono, (2003) Conditional suppression of cellular genes: lentivirus vector-mediated drug-inducible RNA interference. *J Virol* **77**: 8957-8961.

- Wright, H.R., A. Turner & H.R. Taylor, (2007) Trachoma and poverty: unnecessary blindness further disadvantages the poorest people in the poorest countries. *Clin Exp Optom* **90**: 422-428.
- Wu, M., A. Neilson, A.L. Swift, R. Moran, J. Tamagnine, D. Parslow, S. Armistead, K. Lemire, J. Orrell, J. Teich, S. Chomicz & D.A. Ferrick, (2007) Multiparameter metabolic analysis reveals a close link between attenuated mitochondrial bioenergetic function and enhanced glycolysis dependency in human tumor cells. *Am J Physiol Cell Physiol* **292**: C125-136.
- Yong, E.C., E.Y. Chi & C.C. Kuo, (1987) Differential antimicrobial activity of human mononuclear phagocytes against the human biovars of *Chlamydia trachomatis*. *J Immunol* **139**: 1297-1302.
- Yong, E.C., S.J. Klebanoff & C.C. Kuo, (1982) Toxic effect of human polymorphonuclear leukocytes on *Chlamydia trachomatis*. *Infect Immun* **37**: 422-426.
- Zaura, E., B.J. Keijser, S.M. Huse & W. Crielaard, (2009) Defining the healthy "core microbiome" of oral microbial communities. *BMC Microbiol* **9**: 259.
- Zeth, K., V. Kozjak-Pavlovic, M. Faulstich, M. Fraunholz, R. Hurwitz, O. Kepp & T. Rudel, (2013) Structure and function of the PorB porin from disseminating *Neisseria gonorrhoeae*. *Biochem J* **449**: 631-642.
- Zhang, H., P.N. Tay, W. Cao, W. Li & J. Lu, (2002) Integrin-nucleated Toll-like receptor (TLR) dimerization reveals subcellular targeting of TLRs and distinct mechanisms of TLR4 activation and signaling. *FEBS Lett* **532**: 171-176.
- Zhang, J.P. & R.S. Stephens, (1992) Mechanism of *C. trachomatis* attachment to eukaryotic host cells. *Cell* **69**: 861-869.
- Zhou, Z., E. Hartwig & H.R. Horvitz, (2001) CED-1 is a transmembrane receptor that mediates cell corpse engulfment in *C. elegans*. *Cell* **104**: 43-56.

6 APPENDIX

6.1 Abbreviations

μ	micro
<i>A. castellanii</i>	<i>Acanthamoeba castellanii</i>
ABs	aberrant RBs
AcLDL	acetylated low-density lipoprotein
ADP	adenosine diphosphate
AHT	anhydrotetracycline
ANT	the adenine nucleotide translocase
APS	ammonium persulfate
ATP	adenosine triphosphate
<i>B. pseudomallei</i>	<i>Burkholderia pseudomallei</i>
BpML1	macrophage infectivity potentiator of <i>B. pseudomallei</i>
BSA	bovine serum albumin
<i>C. trachomatis</i>	<i>Chlamydia trachomatis</i>
CCCP	carbonyl cyanide m-chloro phenyl hydrazone
cDNA	complementary DNA
CEACAM	human carcinoembryonic antigen-related cell adhesion molecules
cfu	colony forming unit
cHSP60	chlamydial HSP60
CNBr	cyanogen bromide
Co-IP	Co-immunoprecipitation
C-terminal	carboxy-terminal
CTP	cytidine triphosphate
Ctr-MIP	macrophage infectivity potentiator of <i>C. trachomatis</i>
DAPI	4',6-diamidino-2-phenylindole
DC	denaturing condition
DGI	disseminated gonococcal infection
dH ₂ O	distilled H ₂ O
DMEM	Dulbecco's modified Eagle medium
DMSO	dimethyl sulfoxide
DNA	deoxyribonucleic acid
dNTP	desoxynucleosid triphosphate
DUS	DNA uptake sequence
<i>E. coli</i>	<i>Escherichia coli</i>
EBs	elementary bodies
ECAR	extracellular acidification rate
ECL	enhanced chemiluminescence
EDTA	ethylenediaminetetraacetic acid
EGF	epidermal growth factor
EtOH	ethanol
FADH ₂	reduced form of flavin adenine dinucleotide
FCCP	carbonyl cyanide-4-(trifluoromethoxy)phenylhydrazone
FCS	fetal calf serum
FKBP	FK506-binding protein
F ₀ F ₁ -ATP synthase	F ₀ F ₁ -ATPase
G-6-P	glucose-6-phosphate

GC	gonococcus
gDNA	genomic DNA
GFP	green fluorescent protein
GTP	guanosine triphosphate
h	hour(s)
H ₂ DCF-DA	2,7-dichlorodihydrofluorescein diacetate
Hepes	4-(2-hydroxyethyl)-1-piperazineethanesulfonic acid
HIV	human immunodeficiency virus
HRP	horseradish peroxidase
HSP	heat shock protein
HSPG	heparan sulphate proteoglycans
IC ₅₀	half maximal inhibitory concentration
Ig	immunoglobulin
IMM	inner mitochondrial membrane
IMS	intermembrane space between IMM and OMM
IPTG	Isopropyl- β -D-thiogalactopyranosid
kb	kilobase
K _D	binding constant
kDa	kilodalton
<i>L. pneumophila</i>	<i>Legionella pneumophila</i>
LB	lysogeny broth
LGV	lympho-granuloma venereum
LOS	lipooligosaccharide
LPDI	low phosphate-dependent invasion
Lp-MIP	macrophage infectivity potentiator of <i>L. pneumophila</i>
LPS	lipopolisaccharides
M	molar
min	minutes
MIP	macrophage infectivity potentiator
MOI	multiplicity of infection
mTOR	mammalian target of rapamycin
<i>N. gonorrhoeae</i>	<i>Neisseria gonorrhoeae</i>
NADPH	nicotinamide adenine dinucleotide phosphate
NC	native condition
NETs	neutrophil extracellular traps
Ng-MIP	macrophage infectivity potentiator of <i>N. gonorrhoeae</i>
NLRs	NOD-like receptors
Nm-MIP	macrophage infectivity potentiator of <i>N. meningitidis</i>
NQO	4-nitroquinoline 1-oxide
N-terminal	amino-terminal
OCR	oxygen consumption rate
OD ₅₅₀	optical density measured at a wavelength of 550 nm
OMM	outer mitochondrial membrane
Omp	outer membrane protein
Opa	opacity-associated
OXPPOS	oxidative phosphorylation
PAGE	polyacrylamide gel electrophoresis
PBS	phosphate buffered saline

PCR	polymerase chain reaction
PD	pull-down
PFA	paraformaldehyde
PI	propidium iodide
PI3K	phosphoinositide 3-kinase
PMN	polymorphonuclear leukocyte
PMSF	phenylmethanesulfonyl fluoride
p-NPPC	p-nitrophenol phosphorylcholine
PPlase	peptidyl prolyl <i>cis-trans</i> isomerase
PPM	proteose peptone medium
qRT-PCR	quantitative real-time PCR
RBs	reticulate bodies
rCtr-MIP	recombinant Ctr-MIP
RNA	ribonucleic acid
ROS	reactive oxygen species
Rp	rapamycin
rpm	revolutions per minute
RT	room temperature
RU	resonance units
<i>S. aureus</i>	<i>Staphylococcus aureus</i>
<i>S. mansoni</i>	<i>Schistosoma mansoni</i>
SD	standard deviation
SDS	sodium dodecyl sulphate
sec	secondes
shRNA	short hairpin RNA
SPR	surface plasmon resonance
SREC-I	scavenger receptor expressed on endothelial cells 1
STI	Sexually transmitted infection
T3SS	type III secretion system
TBS	Tris buffered saline
TCA	trichloroacetic acid
TCA cycle	tricarboxylic acid cycle
TEM	transmission electron microscopy
TEMED	tetramethylethylenediamine
TLRs	toll-like receptors
TMRM	Tetramethylrhodamine, methyl ester
TNF- α	tumor necrosis factor- α
Tris	tris(hydroxymethyl)aminomethane
Trolox	6-hydroxy-2,5,7,8-tetramethylchroman-2-carboxylic acid
TSB	Tryptone Soya Broth
UTP	uridine triphosphate
UV	ultra violet
v/v	volume per volume
w/v	weight per volume
WHO	World Health Organization
$\Delta\psi$	mitochondrial membrane potential

6.2 Publications and presentations

Publications

- Abdelmohsen, U.R., C. Cheng, **A. Reimer**, V. Kozjak-Pavlovic, A.K. Ibrahim, T. Rudel, U. Hentschel, R. Edrada-Ebel & S.A. Ahmed, (2015) Antichlamydial sterol from the Red Sea sponge *Callispongia* aff. *implexa*. *Planta Med* **81**: 382-387.
- Cheng, C., E.M. Othman, **A. Reimer**, M. Grune, V. Kozjak-Pavlovic, H. Stopper, U. Hentschel & U.R. Abdelmohsen, (2016) Ageloline A, new antioxidant and antichlamydial quinolone from the marine sponge-derived bacterium *Streptomyces* sp SBT345. *Tetrahedron Letters* **57**: 2786-2789.
- Chowdhury, S., **A. Reimer**, M. Sharan, V. Kozjak-Pavlovic, A. Eulalio, B. Prusty, M. Fraunholz, K. Karunakaran & T. Rudel, (2016) Chlamydia trachomatis Prevents Mitochondrial Fragmentation By The miR-30c-P53-Drp1 Axis. *J. Cell Biol.* (under revision)
- Reimer, A.**, A. Blohm, T. Quack, C.G. Grevelding, V. Kozjak-Pavlovic, T. Rudel, U. Hentschel & U.R. Abdelmohsen, (2015) Inhibitory activities of the marine streptomycete-derived compound SF2446A2 against *Chlamydia trachomatis* and *Schistosoma mansoni*. *J Antibiot* **68**: 674-679.
- Reimer, A.**, F. Seufert, M. Weiwad, J. Ebert, N.M. Bzdyl, C.M. Kahler, M. Sarkar-Tyson, U. Holzgrabe, T. Rudel & V. Kozjak-Pavlovic, (2016) Inhibitors of macrophage infectivity potentiator-like PPlases affect neisserial and chlamydial pathogenicity. *Int J Antimicrob Agents* **48**: 401-408.

Talks and poster presentations

- Reimer, A.**, T. Rudel, & V. Kozjak-Pavlovic, (2014) Analysis of the interaction between neisserial porin and endothelial receptor. 8th Jointed Ph.D. Students Meeting of the SFB 630, SFB 766 and FOR 854, Würzburg. (talk)
- Reimer, A.**, V. Kozjak-Pavlovic, U. Abdelmohsen, U. Hentschel-Humeida, U. Holzgrabe, G. Bringmann & T. Rudel, (2015) Search for inhibitors against *Neisseria gonorrhoeae* and *Chlamydia trachomatis*. Best of SFB 630 - and Future Perspectives, Würzburg. (poster)
- Reimer, A.**, F. Seufert, M. Weiwad, U. Holzgrabe, T. Rudel & V. Kozjak-Pavlovic, (2016) Inhibitors of macrophage infectivity potentiator-like PPlases affect chlamydial pathogenicity. German Chlamydia Workshop, Freiburg. (poster)

6.3 Danksagung

Ganz herzlich möchte ich mich an dieser Stelle bei allen bedanken, die zur Entstehung meiner Arbeit beigetragen haben.

Herrn Prof. Dr. Thomas Rudel danke ich für die Möglichkeit meine Doktorarbeit am Lehrstuhl für Mikrobiologie anfertigen zu dürfen, aber auch für die gute Betreuung und die konstruktiven Denkanstöße.

Besonders möchte ich mich bei meiner Betreuerin PD Dr. Vera Kozjak-Pavlovic für die großartige Betreuung, all die Hilfe, Unterstützung und für die hervorragenden Ideen bedanken. Vielen Dank, dass Du stets Zeit für mich gefunden hast!

Bei Herrn Prof. Dr. Georg Krohne möchte ich mich herzlich bedanken für die Übernahme des Zweitgutachtens. Außerdem bedanke ich mich bei der gesamten EM-Arbeitsgruppe für die Unterstützung bei der Elektronenmikroskopie.

Weiterhin bedanke ich mich bei meinen Kooperationspartnern für die gute Zusammenarbeit und Unterstützung (Dr. Ursula Eilers, Dr. Christina Schüle-Völk, Prof. Dr. Thomas Müller, Dr. Matthias Weiwad, Prof. Dr. Almut Schulze, Dr. Jessica Flöter, Sudha Janaki Raman, Dr. Eman Maher Othman und Prof. Dr. Helga Stopper), und die Bereitstellung von interessanten Compounds (Prof. Dr. Ulrike Holzgrabe, Florian Seufert, Prof. Dr. Ute Hentschel, Dr. Usama Ramadan Abdelmohsen, Prof. Dr. Gerhard Bringmann, Raina Seupel).

Ganz herzlich möchte ich mich beim gesamten Lehrstuhl für Mikrobiologie für die nette Arbeitsatmosphäre und Hilfsbereitschaft bedanken. Besonderen Dank an Sebastian, unter anderem für die Hilfe an der Operetta, Annette für die Diskussion von Ergebnissen, Michaela und Yibo für das Beibringen der Neisserien-Methoden, Lisa und Christine für die herzliche Aufnahme am Lehrstuhl und Roy für die großartigen Fluoreszenzbilder und das Diskutieren von Kinofilmen.

Ebenso danke ich Allen, die zusammen mit mir in C237 gearbeitet haben, für die tolle Arbeitsstimmung. Aber besonders danke ich Elke Maier für ihre alltägliche Unterstützung, Hilfe, Geduld und die gute Laune!

Besonders danke ich meinen Kollegen/-innen Dani, Kathrin, Jessica und Max, aus denen Freunde und Leidensgenossen wurden. Nicht nur möchte ich Danke sagen für die

Hilfe im Labor, sondern vor allem auch für die moralische und seelische Unterstützung in den Kaffeepausen und beim Herumalbern zwischen den Inkubationszeiten. Vielen, vielen Dank für die großartige gemeinsame Doktorzeit!

Franzi, meiner Curlysister, danke ich für die Schulter, an die ich mich jederzeit anlehnen konnte, für den Beistand an den Tiefpunkten des Laboralltags, für die Aufmunterung und die Problemlösungen! Danke, dass du an meiner Seite warst!

Meinen Eltern und auch meiner Schwester Tatjana danke ich dafür, dass ihr immer an mich geglaubt habt, mich in meinem Vorhaben unterstützt und mir Rückhalt gegeben habt.

Abschließend, möchte ich mich bei meinem Ehemann André bedanken für die großartige Unterstützung, all die Hilfe und Geduld, die tägliche Motivation, Aufmunterung und Liebe. Danke für einfach Alles!

6.4 Selbstständigkeitserklärung

Hiermit erkläre ich an Eides statt, die Dissertation: „**Search for novel antimicrobials against *Neisseria gonorrhoeae* and *Chlamydia trachomatis***“, eigenständig, d. h. insbesondere selbstständig und ohne Hilfe eines kommerziellen Promotionsberaters, angefertigt und keine anderen, als die von mir angegebenen Quellen und Hilfsmittel verwendet zu haben.

Ich erkläre außerdem, dass die Dissertation weder in gleicher noch in ähnlicher Form bereits in einem anderen Prüfungsverfahren vorgelegen hat.

Würzburg, den 24.01.2017